



City Research Online

City, University of London Institutional Repository

Citation: Eberendu, I. (1985). Plane frame stability analysis based on the inelastic zone method. (Unpublished Doctoral thesis, The City University)

This is the accepted version of the paper.

This version of the publication may differ from the final published version.

Permanent repository link: <https://openaccess.city.ac.uk/id/eprint/34906/>

Link to published version:

Copyright: City Research Online aims to make research outputs of City, University of London available to a wider audience. Copyright and Moral Rights remain with the author(s) and/or copyright holders. URLs from City Research Online may be freely distributed and linked to.

Reuse: Copies of full items can be used for personal research or study, educational, or not-for-profit purposes without prior permission or charge. Provided that the authors, title and full bibliographic details are credited, a hyperlink and/or URL is given for the original metadata page and the content is not changed in any way.

PLANE FRAME STABILITY ANALYSIS

BASED ON

THE INELASTIC ZONE METHOD

BY

IKECHI EBERENDU, M.Sc., C.Eng., M.I.Struct.E.

THESIS SUBMITTED FOR THE DEGREE

OF

DOCTOR OF PHILOSOPHY

**The City University
Department Of Civil Engineering
London**

July, 1985

CONTENTS

ACKNOWLEDGEMENTS	7
ABSTRACT	8
NOTATION	9
CHAPTER 1	
INTRODUCTION	13
1.1 Historical Note	13
1.2 Plane Frame Stability Analysis	13
1.3 Plane Frame Classifications	16
1.4 Existing Methods Of Metal Plane Frame Stability Analysis	17
1.5 Existing Methods Of Metal Plane Frame Design	31
1.5.1 Frame Design Based On The Strengths Of The Individual Members	32
1.5.2 Frame Design Based On The Strength Of The Entire Frame	35
1.6 Need For A New Method Of Plane Frame Stability Analysis	36
1.7 Scope	37
CHAPTER 2	
MOMENT-CURVATURE-AXIAL FORCE RELATIONSHIPS FOR A CROSS-SECTION	40
2.1 Introduction	40
2.2 Assumptions	41
2.3 Stress Distribution Diagrams	43
2.4 The Moment-Curvature-Axial Force Relationships For A Cross- Section Subjected To The Elastic Stress Distribution	45
2.5 The Moment-Curvature-Axial Force Relationships For A Rectangular Cross-Section Subjected To The Primary Yield Stress Distribution	47

2.6	The Moment-Curvature-Axial Force Relationships For A Rectangular Cross-Section Subjected To The Secondary Yield Stress Distribution	50
2.7	The Moment-Curvature-Axial Force Relationships For An I-Shaped Cross-Section Subjected To The Primary Yield Stress Distribution	52
2.7.1	Partial Yielding Of Top Flange	52
2.7.2	Full Yielding Of Top Flange And Partial Yielding Of Web	54
2.8	The Moment-Curvature-Axial Force Relationships For An I-Shaped Cross-Section Subjected To The Secondary Yield Stress Distribution	57
2.8.1	Full Yielding Of Flange And Partial Yielding Of Web At Both Ends Of Cross-Section	58
2.8.2	Full Yielding Of Top Flange And Partial Yielding Of Bottom Flange And Full Or Partial Yielding Of Web	61
2.9	Notes On The Use Of The Formulae Presented In This Chapter	63
2.10	Applications Of The Formulae Presented In This Chapter	63
 CHAPTER 3		
TANGENT FLEXIBILITY COEFFICIENTS FOR INELASTIC BEAM-COLUMNS		69
3.1	Introduction	69
3.2	Assumptions	69
3.3	Basic Principles	72
3.4	Flexibility Coefficients For An Elastic Beam-Column	81
3.5	Flexibility Coefficients For An Inelastic Beam-Column	85
3.5.1	Derivation Of The Flexibility Coefficients	85
3.5.2	Formulae For The Flexibility Coefficients For The Beam-Column Bent In Double Curvature	96

3.5.3	Formulae For The Flexibility Coefficients For The Beam-Column Bent In Single Curvature	101
3.6	Flexibility Coefficients For An Initially-Curved Beam-Column	102
3.7	Notes On The Use Of The Formulae Presented In This Chapter	106
3.8	Applications Of The Formulae Presented In This Chapter	108

CHAPTER 4

	PLANE FRAME STABILITY ANALYSIS	110
4.1	Introduction	110
4.2	Load Simulation	110
4.3	Geometry Simulation	111
4.4	Tangent Stiffness Matrix For A Beam-Column	112
4.4.1	Beam-Column Rigidly-Connected To A Plane Frame At Both Ends	113
4.4.2	Beam-Column Rigidly-Connected To A Plane Frame At One End And Pinned At The Other End	115
4.4.3	Beam-Column Pinned To A Plane Frame At Both Ends	115
4.4.4	Examples	116
4.5	The Transformation Matrices For Beam-Column End Forces And Displacements	117
4.6	Nodal Forces And Displacements	119
4.7	The Stable Equilibrium Path	122
4.8	Attainment Of The Ultimate Yield Moment Of A Cross-Section At An End Of A Beam-Column	123
4.9	Failure Conditions	124
4.10	Flow Chart	124

CHAPTER 5

COMPARISON OF EXISTING THEORETICAL AND EXPERIMENTAL RESULTS	127
5.1 Introduction	127
5.2 Theoretical Results	127
5.2.1 Frame Analysed By Andreaus And D'Asdia	128
5.2.2 Frame Designed By Majid And Anderson	135
5.2.3 Frame Designed By Horne And Majid	140
5.2.4 Frame Designed By Horne And Majid	146
5.2.5 Frame Designed By Anderson	152
5.3 Experimental Results	158
5.3.1 Portal Frames Tested By Yen, Lu And Driscoll, Jr.	158
5.3.2 Pitched-Roof Portal Frame Tested By Majid	164
5.4 Summary Of Frame Failure Load Parameters	168

CHAPTER 6

EXPERIMENTS	169
6.1 Introduction	169
6.2 Frame Geometry And Loads	170
6.3 Material Properties	174
6.4 Instrumentation For Frame Testing	177
6.5 Frame Testing Procedure	180
6.6 Frame Test Results	182
6.7 Remarks	191

CHAPTER 7

DESIGN RECOMMENDATIONS FOR METAL PLANE FRAMES	196
7.1 Introduction	196
7.2 General Procedures For Plane Frame Design	196

7.2.1	Design Objectives	197
7.2.2	Means Of Achieving The Design Objectives	198
7.2.3	Initial Estimates Of Member Section Sizes	201
7.2.4	Steps Of Analysis	202
7.3	Use Of The Inelastic Zone Method For Plane Frame Design	204
7.4	Limiting Moment Method For Plane Frame Design	204
7.5	Design Examples	206
CHAPTER 8		
CONCLUSION		
		226
APPENDICES		
Appendix 1	Formulae For The Moment-Curvature-Axial Force Relationships For A Rectangular Cross-Section Of An Elastic-Perfectly-Plastic Material.	230
Appendix 2	Formulae For The Moment-Curvature-Axial Force Relationships For An I-Shaped Cross-Section Of An Elastic-Perfectly-Plastic Material.	232
Appendix 3	Newton's Method Of Successive Approximations For Solving An Equation Of One Unknown	237
Appendix 4	Formulae For Solving 2, 3 And 4 Simultaneous Equations	238
Appendix 5	A Parametric Study Of The Proposed Deflection Curve For An Inelastic Zone Of A Beam-Column	242
Appendix 6	Conversion Table	268
REFERENCES		
		269

ACKNOWLEDGEMENTS

I gratefully acknowledge Dr. K.S. Virdi for supervising the work described in this thesis and for his advice during my experimental investigations. I am grateful to Dr. C.D'Mello and to Dr. F.Brant for their assistance in taking readings during the tests. I am also grateful to [REDACTED] for assembling the equipments and assisting me during all stages of the tests.

I gratefully appreciate the advice given to me by the Computer Unit Advisory Staff about my use of the City University's computers and word-processors.

I sincerely thank my wife, [REDACTED], for her unrelenting encouragement for this research and my son, [REDACTED] and my daughters, [REDACTED] and [REDACTED] for their help during the period of this research and all members of my family in Nigeria for taking charge of Home affairs during the period of my studies in the United Kingdom.

ABSTRACT

A new method of structural stability analysis which accounts for the spread of inelasticity along structural members is presented in this thesis. This method is called the **inelastic zone method** and is employed here to investigate the behaviour of metal plane frames loaded to failure. For a given loading on a plane frame, the inelastic zones which may be present along the frame members are identified without a finite discretization of the members and their cross-sections. Account is taken of any initial member curvature in determining the tangent force-displacement relationships for the members. A bilinear stress-strain relationship for the material is adopted. The equation for the deflection curve for an inelastic zone which is similar to that for the deflection curve for an elastic beam-column is assumed, the main difference being that this assumed equation contains additional terms for satisfying curvature boundary conditions. The accuracy of this equation is examined in a Parametric Study. In this thesis, rectangular and I-shaped cross-sections have been considered for the frame members. The tangent force-displacement relationships so determined at a given load level are used to analyse the plane frame using the stiffness method of structural analysis in which account is taken of the changes of geometry of the frame. By repeating this procedure for increasing loads, the stable equilibrium path for the frame can be traced.

Experiments were conducted on two portal frames built-up from mild steel members having rolled I-shaped cross-sections. This was aimed at building a model with realistic geometrical imperfections and residual stresses. The results obtained are compared with those predicted by the proposed method and good agreement is obtained for ultimate loads, deflections and spread of plasticity.

Frame failure loads obtained by theoretical methods and experiments reported in the literature are compared with those obtained by the inelastic zone method. Good agreement is obtained while the inelastic zone method is shown to give lower-bound values of frame failure loads.

Recommendations for the design of metal plane frames are also given. In addition, a new, simplified method of plane frame design which avoids the computation of frame failure loads and member effective lengths but considers an estimated ultimate strength of each member cross-section based on the results obtained from a non-linear, elastic analysis of the frame subjected to the working loads is presented. This method is called the **limiting moment method** and can be applied to all types of plane frame under general loadings. Examples which illustrate the application of this method to frame design are given.

NOTATION**DESCRIPTION**

E	Young's modulus of elasticity
σ	stress at a point
ϵ	strain at a point
A_s	ultimate strain/yield strain
B_s	ultimate stress/yield stress
E_s	slope of tangent to the strain-hardening curve on the material stress-strain diagram
C_s	E_s/E [= $(B_s-1)/(A_s-1)$]
H	depth of cross-section
B	width of rectangular cross-section or width of flange of I-shaped cross-section
T	thickness of flange of I-shaped cross-section
t	thickness of web of I-shaped cross-section or metric tonne when applied to a force
n	depth from edge to neutral axis of cross-section
a	depth of elastic core of cross-section
a_1	depth of inelastic zone from edge of cross-section for ultimate stress distribution diagram
I_z	second moment of area of cross-section about its z-axis
A	area of cross-section
Z_1	elastic modulus of cross-section
ψ	curvature of cross-section
θ	end rotation of zone or member
L	length of member
B_i	length of zone i of member
L_0	original length of member
u_0	initial central deflection of member

k_0	π/L_0
γ	flexibility coefficient for an elastic or inelastic zone
α	flexibility coefficient for a beam-column
k	stiffness coefficient for a beam-column
Δ	displacement along the y-axis of a member
δ	displacement along the x-axis of a member
x	longitudinal axis of member
X	longitudinal axis of frame
y	transverse axis of member
Y	transverse axis of frame
z	out-of-plane axis perpendicular to x- and y- axes
Z	out-of-plane axis perpendicular to X- and Y- axes
ϕ	slope of member
λ	load parameter (or factor)
P	axial force
P_s	squash load for cross-section ($= \sigma_y/A$)
P_E	Euler buckling load for member ($= \pi^2 EI_z/L^2$)
M_i	bending moment at point i along beam-column
M_p	full plastic moment of cross-section
C_p	squash load ratio ($= P/P_s$)
C_e	Euler buckling load ratio ($= P/P_E$)
C_0	amplification factor for axial load effect [$= 1/(1-C_e)$]
R_i	bending moment ratio ($= M_i/M_{y1}$)
R_a	intermediate yield moment ratio ($= M_{y2}/M_{y1}$)
R_b	ultimate yield moment ratio ($= M_{y3}/M_{y1}$)
Σ	summation



support fixed in three directions



pinned support or joint



simple support



rolling support



plastic hinge without considering inelastic zones



inelastic zone along a member



plastic hinge and inelastic zones

Suffix

i	integer for point, end, zone or member
y	yield
u	ultimate
e	elastic
f	failure
y1	first yield
y2	intermediate yield
y3	ultimate yield
lw	limiting under working loads
sh	strain-hardening

Equations, Figures and Tables are numbered as follows:

(i,j)

where i is the Chapter and j is the Equation, Figure or Table number.

Also, Sections and Sub-Sections of chapters are numbered as follows:

(i,j) and (i,j,k)

where i is the Chapter, j is the Section and k is the Sub-Section.

Equations in an Appendix are numbered as follows:

(A_i,j)

where A_i is the Appendix i and j is the Equation number.

In the main, metric units of measurement are adopted in this thesis. However, imperial units of measurement have also been used where necessary (for example, in experiments and in frame stability analyses by other authors). For purposes of conversion from one unit to another, a Conversion Table is given in Appendix 6.

Other notations are described wherever they occur in this thesis.

CHAPTER 1

INTRODUCTION

1.1 Historical Note

Structural stability theory originated from the early classic works of Euler (1) on the stability of metal columns. Lagrange, Considere, Engeser, von Karman and Shanley were among other early investigators of this subject (2,3,4,52). In 1759, Euler established that a **bifurcation of equilibrium paths** and **elastic buckling** occur when an initially-straight, prismatic, column has a critical compressive axial load. In 1770, Lagrange confirmed this theory for slender columns of different end conditions. In 1889, Considere and Engesser introduced the double modulus and tangent modulus theories respectively for **inelastic buckling**. In 1910, von Karman presented a stability analysis of an eccentrically-loaded column. In 1947, Shanley proved that the tangent modulus theory is more correct than the double modulus theory. Today, numerous works are available on the stability of columns and other structural elements such as beams, plates, shells and frames.

In this thesis, the inelastic stability of metal plane frames which form parts of metal space (or three-dimensional) frameworks will be considered.

1.2 Plane Frame Stability Analysis

As the costs of labour and materials increase, the overall cost of constructing an engineering structure (such as a building or a bridge) increases. Any efforts to reduce this cost must allow for a reduction of the total quantity of materials employed in the construction of the structure. For a framed structure, this could lead to the use of

slender members. Where the framed structure is tall, instability due to the build-up of large axial forces in the predominantly-axially-loaded members (such as columns) and to the development of large bending moments in the predominantly-transversely-loaded members (such as beams) could arise at loads much lower than the anticipated frame failure loads. The option of increasing the sizes of members to avoid these problems may, in turn, lead to uneconomic designs. Considerations for the introduction of some form of bracing against sideways movements may often provide a feasible and economic solution to the problem. Nevertheless, in a practical design environment, the actual financial constraints associated with the design of the structure may, indeed, dictate the best line of action to take.

Notwithstanding economic considerations in structural design, a structure must fulfil its basic functions with ample margins of safety against collapse and undue deflections. These aspects of structural behaviour, indeed, underly the need for all frame stability analyses and imply that frame failure loads must be determined before levels of safety can be established.

A realistic determination of the failure load of a structure should include all structural elements of the structure. For example, in the case of a steel-framed building, the contributions of the steel space frames and all concrete slabs and concrete or brick walls to the strength of the structure should be allowed for. It is possible to obtain an estimate of the failure load of such a built-up structure by employing experimental techniques. These would involve building several models of the structure and subjecting each model to different combinations of load to failure. Such procedures would not only lead

to much expense but also may not necessarily reflect the actual conditions to be found in the real structure when built. Nevertheless, such procedures may be inevitable in the absence of adequate analytical techniques. On the other hand, a stability analysis of the structure incorporating the different structural elements of the structure and accounting for general loadings would be very expensive and prohibitive as a routine design procedure particularly where several trial designs are required before a satisfactory design is achieved.

In some framed structures (such as steel-framed, tall buildings), plane frames can be identified which are constrained to displace significantly within their own planes and negligibly out-of-plane under the actions of the general loadings on the structure by judiciously introducing out-of-plane restraints such as shear walls, floor beams and diagonal bracings for these plane frames. Also, these frames generally have members of I-shapes which have low torsional and minor-axis bending stiffnesses when compared with their major axis bending stiffnesses and their members may have rigid, semi-rigid or simple connections with the out-of-plane restraints. Such frames, in general, represent the weak links in the make-up of the space frame for the structure and also lend themselves easily to elastic or inelastic stability analysis. Thus, if a space frame consists of a number of plane frames, the least failure load obtained from stability analyses of all the plane frames, each subjected to its range of total design loads, will give a good indication of the failure load for the space frame. This approach is, where permissible, a more economical and practical procedure for estimating the strength or adequacy of the space frame than any attempt to treat the entire structure as one unit for analytical purposes.

The existence of plane frames in structures, taken in isolation, is not sufficient to warrant a stability analysis for design. Other factors which make this necessary for frame design include the uncertainties associated with frame behaviour and design. The main areas of uncertainty are the true types, nature, distribution, combinations, frequency and magnitudes of the applied loads and the true nature and behaviour of the connections and foundations. Also, plane frames are customarily required to sustain their working loads under purely elastic conditions (5) and the maximum specified joint displacements are customarily required not to be exceeded under elastic conditions (5). However, in view of the foregoing factors which affect true frame behaviour, no guarantee can be given in practical design that these requirements can be met. Thus, the specified working loads may induce inelastic conditions in the frame and the expected factor of safety may not be attained.

A rational, practical, economic and realistic design of a framed structure which consists of a series of inter-connected plane frames should, therefore, be based on stability analyses of the plane frames. ✓

1.3 Plane Frame Classifications

Numerous configurations of plane frame are possible. In general, a **rectangular** plane frame (that is one that has only vertical and horizontal members) which has no member discontinuity at any joint or in any storey is often classified as a **regular** frame (40). Such a frame may not necessarily have a vertical axis of symmetry. Any plane frame that is not regular is often classified as an **irregular** frame. A frame may be **braced** or **unbraced** against sidesway depending on the presence

or absence of adequate external or internal in-plane restraints at all the beam levels or within all stories using diagonal bracings. Varying degrees of elastic and inelastic restraints are also possible and partial restraints may be applied at selected beam levels. Unbraced rectangular plane frames are also classified as **sway** frames (46).

1.4 Existing Methods Of Metal Plane Frame Stability Analysis

A plane frame which fails under elastic conditions is said to fail by **elastic instability** (7). This type of failure is characteristic of plane frames having perfect members primarily subjected to axial forces. For these frames, therefore, the applied loads do not induce significant joint displacements and member bending moments at any stage of loading before failure. At failure, however, a bifurcation of equilibrium paths becomes possible resulting in unstable behaviour and the corresponding failure loads are described as the **buckling** or the **elastic critical loads**. Fully-braced frames loaded by concentrated loads at the joints and regular frames whose columns only are axially-loaded are examples of frames that can fail by elastic instability.

When, at least, one cross-section of one member of a plane frame is strained into the inelastic domain due to any combination of primary effects (such as axial forces, bending moments and material non-linearity) and secondary effects (such as initial imperfections, eccentric loadings at connections and support deformations), then failure by **inelastic instability** can result. The degree of inelasticity present in any loaded frame at any stage up to failure depends entirely on the contributions of these effects to the overall performance of the frame. A plane frame subjected to loadings at the joints and also along its members is an example of a frame that can fail by inelastic

instability.

Techniques of stability analysis which attempt to describe the above behaviour patterns for loaded plane frames are available. These techniques range from simple, manual, analytical methods aiming to provide reasonable solutions with the minimum of computational effort to more rigorous, computer-based methods aiming to provide more accurate results but at the expense of much computational effort.

The **slope-deflection method**, used in conjunction with **stability functions** (14), is widely adopted in the determination of the elastic critical loads of plane frames (4,7,8,9,10,11,12,13). In this method, the axial shortenings of members are ignored and only two degrees of freedom (rotational and translational) are considered at each node. Non-linear effects due to member axial forces are accounted for through the use of stability functions which modify the member flexural stiffnesses calculated on the assumption of zero axial force. The **zero-determinant** concept for the resulting stiffness matrix of the entire frame is employed to establish the elastic critical loads of the plane frames. The classical **integration technique** has also been used for this purpose (15) but to relatively simple frames.

The **stiffness method** (11,16,17), which is an extension of the slope deflection method that includes the axial deformations of members, is the most widely adopted method of structural analysis when using a computer and is also employed for the determination of the elastic critical loads for plane frames.

In considering inelastic effects in a plane frame, two main concepts of behaviour are available, the **concentrated inelasticity** and the **distributed inelasticity concepts** (18).

The **concentrated inelasticity** concept is also described as a **plastic hinge** concept because it is mainly applicable to structural steel members and frames since these are ductile and exhibit definite plastic behaviour before strain-hardening. Basically, this concept, pioneered by Baker (84) and later extended by Horne and Heyman (19), ignores the gradual spread of inelastic zones along the frame members as the applied loads on the frame are gradually increased and assumes all inelastic effects to be concentrated at each member end cross-section where the resulting bending moment becomes equal to the **ultimate moment of resistance (also called the full-plastic moment)** of the cross-section. Thus, an abrupt transition from elastic stress distribution into a fully-plastic stress distribution at such an end cross-section occurs while the entire length of each member of the frame remains elastic at all stages of loading up to failure (20,21,22,23). A **plastic hinge** is said to form at a cross-section which attains its full-plastic moment so that no additional bending moment can be attracted to that cross-section and this is accounted for in modifying the flexural properties of the relevant members at the relevant stage of loading.

The concentrated inelasticity concept is employed in a plane frame stability analysis through two basic methods, the **rigid-plastic** and the **elastic-plastic methods**. These methods may, however, lead to widely different results.

The **rigid-plastic method** adopts the rigid-plastic stress-strain and moment-curvature relationships for the member cross-sections for the determination of the failure load of a plane frame (19,24,25,26,27,28,29). In this method, the failure of a plane frame by the formation of a sufficient number of plastic hinges at various locations to transform the frame into a **mechanism** is assumed to precede failure

due to the build-up of axial forces in the frame members. In addition to the mechanism condition, the yield condition (in which the maximum bending moment at a cross-section is not greater than the full-plastic moment of the cross-section) and the equilibrium condition (in which the resulting bending moment distribution is in equilibrium with the applied loads) must be satisfied. The mechanism condition gives an upper-bound value of the frame failure load while the yield and equilibrium conditions give a lower-bound value of the frame failure load. The satisfaction of these three conditions is the fundamental requirement of the uniqueness theorem of plastic collapse (28). Also, no joint displacements are assumed to exist until a mechanism has been formed and plastic failure occurs. A first-order, rigid-plastic method ignores axial force effects while a second-order, rigid-plastic method includes axial force effects in the computations. The stability analysis is carried out by selecting a number of trial mechanisms for a plane frame, setting up and solving the virtual work equations of balancing the external work done by the applied loads and the internal work done by the full-plastic moments on the assumed plastic hinges. The correct mechanism is taken to be that which corresponds to the least frame failure load obtained. Extensions of this method to include the strain-hardening property of structural steel can be made using Horne's rigid-plastic-rigid stress-strain relationships (30) in which Horne assumed strain-locking to take place at the start of strain-hardening. However, Medland (30) and Horne and Medland (31) modified this idealization to a rigid-plastic-strain-hardening idealization. In either case, additional terms are introduced in the basic work equation to allow for the effects of strain-hardening. The general procedure adopted requires a knowledge

of the bending moment diagram for the frame under the given set of loads so that the plastic hinge length, associated with each plastic hinge, can be determined. This length is taken to be the sum of the lengths between the ends of the relevant members meeting at the plastic hinge position and the points of intersection of the tangent drawn to the bending moment diagram at those ends with the longitudinal axes of the members. This approach is, therefore, semi-graphical and time-consuming particularly when applied to multi-storey, multi-bay frames.

The results obtained by applying the rigid-plastic method can be improved by employing either the shakedown theorem (22) or the Merchant-Rankine formula (32) or its modification by Wood (32). The shakedown theorem leads to the computation of a collapse load which generally lies between the first yield load and the rigid-plastic collapse load for the frame as the frame, subjected to variable repeated loading, shakes down due to either alternating plasticity or incremental collapse (22,33,34,35). For the majority of plane frames designed in practice, however, variable repeated loading is not employed and the designs are based on statically-applied loadings. On the other hand, the Merchant-Rankine formula is based on statically-applied loads and is, therefore, more employed in practice than the shakedown theorem. The Merchant-Rankine formula leads to a frame failure load which is lower than both the rigid-plastic collapse load and the elastic critical load for the frame and is expressed as follows:

$$1/P_f = 1/P_e + k/P_p \quad (1.1)$$

where P_f = frame failure load,

P_e = frame elastic critical load,

P_p = frame rigid-plastic collapse load and

k = unity or Wood's modification factor of 0.9 introduced to

account for strain-hardening and composite action.

The apparent simplicity of the Merchant-Rankine formula which is related to the Rankine formula for struts, has attracted the attention of many investigators. Majid (36) concluded that it is reasonable. Davies (22) concluded that it is inadequate for tall frames where instability problems are significant. Moses (37) demonstrated that it is unsuitable for inelastic frame buckling. Ariaratnam (21) pointed out that it has no theoretical basis and that one reason for its rejection lies in the fact that it does not allow for imperfections as allowed for in columns. Anderson and Lok (32,38) pointed out that it is a useful alternative in the absence of adequate computer software and recommended its use for realistic, regular, plane frames with their bay widths not less than their storey heights.

Modifications to the **linear interaction formula** represented by Eqn. (1.1) have been proposed by Anderson and Lok and by Scholz in the form of curves. By making use of the deteriorated elastic critical load for a plane frame obtained for each formation of a plastic hinge up to failure, Anderson and Lok (38) derived a **fitting curve** represented by the following formula:

$$\lambda/\lambda_p = (1 - 0.4 * \lambda_p / \lambda_c) [1 - (\lambda/\lambda_c)^2] \quad (1.2)$$

where λ = frame failure load factor,

λ_p = frame load factor for plastic collapse load and

λ_c = frame load factor for lowest elastic critical load.

This curve ignores strain-hardening and composite action. Scholz, on the other hand, developed a **multi-curve interaction method** (85,86,87) which depends not only on the plastic collapse and the elastic critical loads but also on the slenderness ratio of a member, a limiting

slenderness ratio for the member and a reduction factor which lies between 0.4 and unity. This method can be applied to either the entire frame or to a limited sub-frame made up of some columns and beams within a chosen storey. In the latter procedure, several sub-frames are tried and the least failure load obtained is taken to be the failure load for the entire frame. Scholz's method also does not consider strain-hardening and composite action.

In practice, however, the Merchant-Rankine formula or any of its modifications has limited application as it gives conservative results only when specific conditions are satisfied. By requiring separate computations for the plastic collapse load and the elastic critical load (each requiring a different loading arrangement), the application of these formulae to frame design can be time-consuming. The most obvious limitation of these formulae is that they cannot be applied to irregular frames subjected to general loadings and in which significant non-linear effects are present.

The second-order **elastic-plastic method**, on the other hand, adopts ✓ elastic-plastic stress-strain relationships for the member cross-sections for plane frame stability analysis. The mechanism concept of ✓ the rigid-plastic method is dropped and joint displacements and member ✓ end forces are calculated for each formation of a plastic hinge using the standard stiffness method. Thus, the **step-by-step formation of** ✓ **plastic hinges** is followed until the frame fails. However, the first-order method ignores axial force effects on member stiffness whereas the second-order method includes these effects. Thus, the first-order method adopts elastic-plastic moment-curvature relationships for the member cross-sections whereas the second-order method adopts elastic-

✓ plastic moment-curvature-axial force relationships for the member cross-sections (3,17,23,36,39,40,41,42,43,44,45,46,47). Consequently, the second-order method gives the more realistic results which are reasonably close to, but generally higher than, those obtained experimentally or by means of more rigorous methods. Strain-hardening is allowed for by employing an elastic-plastic-strain-hardening material stress-strain idealization (27). Each analysis for the formation of a plastic hinge gives a point on the **stable equilibrium path (or load-deflection curve)** for the frame. By performing several such analyses, each time checking the positive-definiteness of the determinant of the frame tangent stiffness matrix or testing for loss of convergence, the entire stable equilibrium path can be traced and the failure load parameter (usually for proportional loading) evaluated. Thus, at failure, the number of plastic hinges present in the frame depends largely on the manner in which non-linear effects due to the axial forces are included in the analysis.

✓ The **distributed inelasticity concept** attempts to describe the true behaviour of structural materials and is, therefore, generally applicable to all structural materials. This concept accounts for ✓ simple and complex distributions of stress on member cross-sections, ✓ spread of inelastic zones along frame members and primary and secondary effects in structures. It is employed in plane frame stability analysis ✓ through the use of **numerical integration methods** involving finite subdivisions of frame members and their cross-sections. The accuracy of these numerical integration methods can be increased by increasing the number of sub-divisions.

An early attempt to employ the distributed inelasticity concept to metal plane frame stability analysis was made by Lu in investigating the

behaviour of a steel, pin-based, regular, unbraced portal frame having a uniformly distributed load on the beam and equal, concentrated loads on the columns (7,48,49,50,51). Chwalla had earlier obtained the failure load of a similar portal frame without the concentrated column loads by assuming failure by elastic instability and employing the **classical integration technique** (3,7,52). Chwalla's method, therefore, gave an upper-bound to the true frame failure load whereas Lu's method established a lower-bound to the true frame failure load.

In Lu's method, the frame members are sub-divided into finite segments and the cross-section at the end of each segment is further sub-divided into finite sub-elements. Then, assuming axial force effects in the beam to be negligible, the moment-curvature curve for the beam and the moment-curvature-axial force curves for the columns are derived using a numerical integration technique. The moment-rotation curve for the beam and the moment-rotation-axial force curve for the columns are next determined for a chosen set of the applied loads by a numerical integration technique. The length of each segment along a member is made equal to a constant (say four) times the radius of gyration of the member cross-section. These curves are plotted on the same set of axes and the moment and rotation for their point of intersection give the moment and rotation at the knee of the portal frame assumed effectively braced against sidesway. Then, the bending moment distribution diagram for the entire frame is drawn. However, a sidesway mode of failure is assumed. Therefore, an analysis of the frame in a sidesway configuration becomes necessary. This is accomplished by first employing the bending moment diagram for the beam to determine the yielding zones along the beam and employing the moment-

curvature curve for the beam to derive the effective flexural stiffness and carry-over factors for the beam (after ignoring the yielding zones) by **column analogy** (29). Then, the flexural stiffness factor for each column is derived assuming elastic behaviour and employing stability-type functions. By applying an arbitrary sidesway and equal, arbitrary bending moments to the tops of the columns and using the above factors, a bending moment distribution for the entire frame in a sidesway configuration is established using standard **moment distribution procedure**. The column shear forces can now be determined. The sum of these shear forces must be positive if the frame is stable under the applied loads. If this is the case, the above procedure is repeated for increased applied loads. The loads corresponding to a zero or negative value of the sum of the column shear forces represent the failure loads for the frame at which inelastic instability of the frame occurs.

Lu's method is cumbersome to apply to tall, regular and irregular plane frames. However, it formed a basis for the numerical integration methods of plane frame stability analysis in current usage.

In the numerical integration methods, each frame member is subdivided into a number of elements (or segments) and the cross-section at the end of each element is sub-divided into a number of sub-elements prior to analysis. These sub-divisions are, therefore, employed for the frame loaded from the elastic domain (for which exact methods of analysis involving no sub-divisions are available) into the inelastic domain. The loads on the frame are applied at the nodal points. At each load level, the force and moment equilibrium equations for the determination of the moment-curvature-axial force relationships for the cross-section at each nodal point are set up and used to derive expressions for the moment-rotation-axial force relationships for each

element along the frame member in terms of the unknown nodal forces and displacements. Then, the imposition of the conditions of compatibility of nodal displacements and equilibrium of nodal forces gives sufficient simultaneous equations which are solved iteratively to determine the nodal forces and displacements. Two main methods are employed here namely, the **finite difference** and the **finite element methods**. Some basic differences, however, exist between these two methods.

In the finite difference method, finite difference forms of the equations for curvatures and rotations are used and these are based on a curve whose slope at a point equidistant from two nodes can be represented by the relative displacement of the nodes divided by the distance between the nodes. In the finite element method, however, expressions for curvatures and rotations are derived by assuming a curve (or displacement function) for each element, notably a cubic curve for an element subjected to combined bending moment and axial force (that is a beam-column) and a straight-line for an element subjected only to an axial force (for example, a triangulated truss member). Moreover, in the finite difference method, the relevant equations are usually expressed in forms which lead firstly to the determination of one displacement at each node (notably transverse to the member) from which all other unknown quantities can be determined whereas in the finite element method, the element tangent stiffnesses are determined and employed in obtaining all nodal displacements from which the nodal forces can be determined. In each method, the end of elastic behaviour (or the onset of inelastic behaviour) and the inelastic zones that may be present along the frame member at a given load level are not identified. Interest is focussed on the determination of the load-

deflection curve for the frame and each analysis for the given set of loads gives a point on this curve. By increasing the applied loads and repeating the relevant procedure, the entire load-deflection curve for the frame can be traced. Examples of application of the finite difference method are given in References 36, 55 and 56. In References 36 and 55, Moses also derived the moment-curvature relationships for an I-shaped cross-section by analytical means by ignoring the contributions of the axial force. Examples of application of the finite element method are given in References 57, 58 and 59. Seniwigse (57) showed the use of a **bilinear (elastic-strain-hardened)** stress-strain relationship for the steel. Kang and Scordelis (58) also showed the use of a similar bilinear representation of the stress-strain relationship for steel. Zanaty and Murray (59) confined all plastic effects to 10% of the relevant member length from the relevant end of the member, thus assuming the central 80% of a member length to remain always elastic. The use of a bilinear material stress-strain idealization for time-independent, inelastic behaviour is also demonstrated by Smith and Sidebottom (60) and by Erbatur (88).

Recently, Andreaus and D'Asdia (61) presented an extension of the elastic-plastic method which also employs the distributed inelasticity concept. Basically, the well-known **force method** (11,62), instead of the stiffness method, is employed to establish the load steps for plastic hinge formation. Then, the influence of **spread of yielding zones** is allowed for by adopting smaller intermediate load steps and specifying a convenient number of sub-divisions for a member length and solving the non-linear force and moment equilibrium equations either numerically or by means of generated linear yield domains for the corresponding reduced depth of the elastic core of the cross-section at each specified

location. With these, the reduced axial and flexural properties of the cross-section, and hence of the entire member, are derived. The influence of geometrical non-linearities is accounted for by applying fictitious forces, derived by multiplying the difference between the linear elastic and the non-linear stiffness matrices for a member by the corresponding current end displacement vectors, at the relevant joint of the frame. The non-linear stiffness is derived by employing stability functions for the case when the effect of yielding zones is ignored and by employing a numerical integration technique for including this effect. Being based on the force method, however, this method cannot be easily applied to frames in which the degree of statical indeterminacy is large (for example, tall, irregular frames).

The typical equilibrium paths obtainable from the plastic hinge methods of frame stability analysis and a true equilibrium path obtainable from an experiment are given in Reference 3 and shown in Fig. 1.1 and the existing methods of plane frame stability analysis described above are summarized in Table 1.1. The typical equilibrium path obtainable from a numerical integration technique is not given in Fig. 1.1 mainly because of the variable nature of the ensuing results but can lie between the true curve and that obtainable from the second-order elastic-plastic method if very large member and cross-sectional sub-divisions are employed.

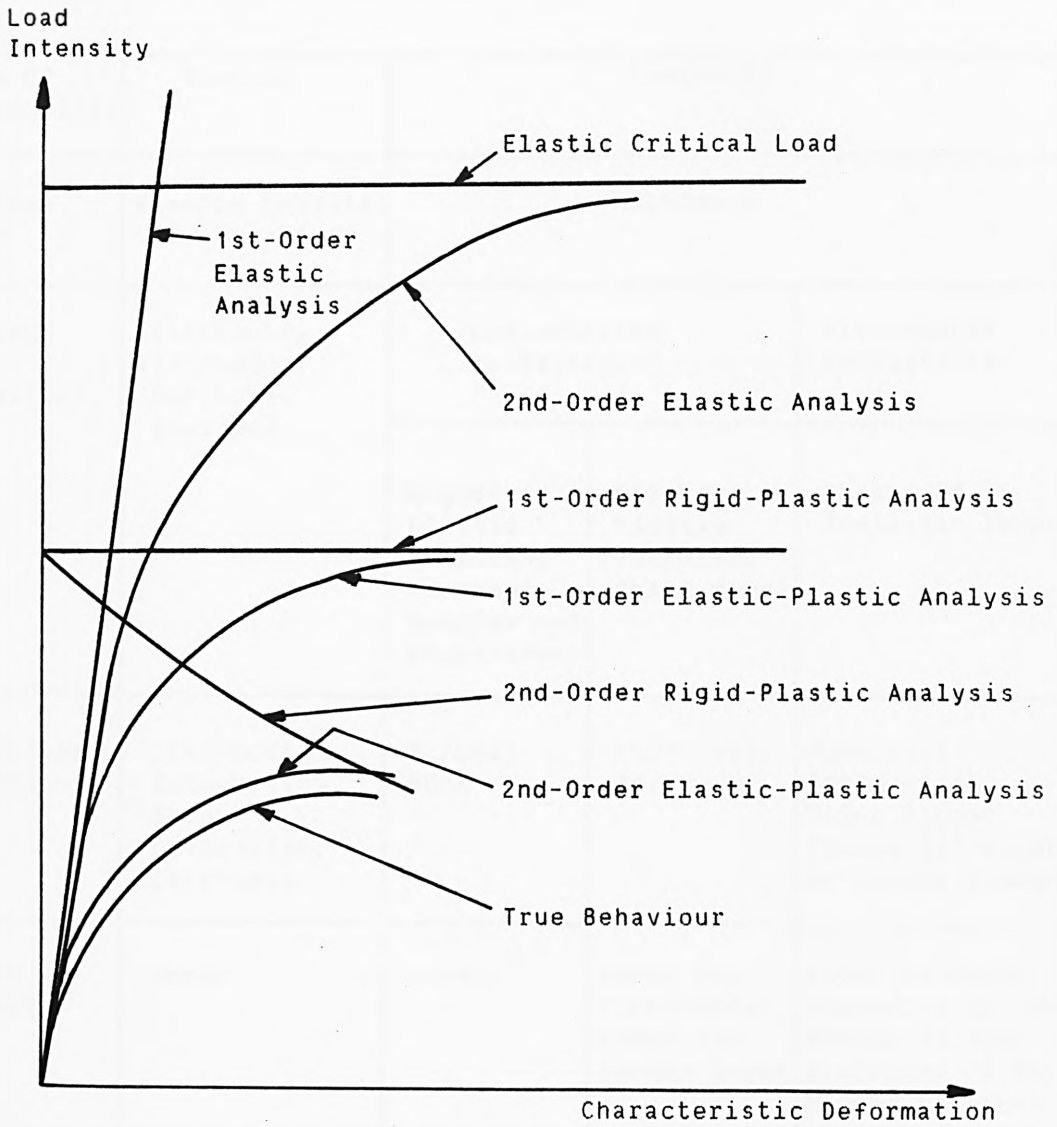


Fig. 1.1 Typical Equilibrium Paths For Metal Plane Frames (3)

Table 1.1 Summary Of Existing Methods Of Metal Plane Frame Stability Analysis

Mode Of Instability	Elastic	Inelastic		
Failure Load	Elastic Critical (Or Buckling)	Ultimate		
Concept Of Behaviour	Elasticity (Including Merchant-Rankine)	Concentrated Inelasticity		Distributed Inelasticity
		Rigid-Plastic (Including Merchant-Rankine And Shake-down)	Elastic-Plastic (Including Shake-down)	Spread Of Inelastic Zones
Analytical Techniques	Classical Integration, Slope Deflection, Stiffness	Virtual Work	Stiffness, Force	Numerical Integration Using Either Finite Differences Or Finite Elements
Bound Of Result	Upper	Upper	Upper For First-Order, Lower For Second-Order	Lower Or Upper Depending On The Number Of Sub-Divisions Of Each Member Or Cross-Section

1.5 Existing Methods Of Metal Plane Frame Design

The existence of several methods of metal plane frame stability analysis and the different levels of accuracy which they give present great difficulty of choice for a frame designer particularly with regard to achieving specified frame design objectives. The outcome is that varying standards of frame design are achieved in practice. Nevertheless, these methods provide the essential ingredients for

selecting feasible member section sizes, connections and foundations for plane frames in practice.

This thesis is mainly concerned with the stability analysis of metal plane frames. Attention will, therefore, be confined to the selection of suitable member section sizes for plane frames in all design considerations.

In general, a plane frame design requires a number of trial analyses of the frame in which member section sizes are revised for each analysis before the most feasible set of member section sizes can be selected. The method of analysis adopted for the design, therefore, must have a profound bearing on the achievement of any specified design objectives.

Metal frame design can be sub-divided into two broad classifications, namely:

- (i) design based on the strengths of the individual members and
- (ii) design based on the strength of the entire frame.

These classifications will now be briefly described.

1.5.1 Frame Design Based On The Strengths Of The Individual Members

A frame design based on the strengths of the individual members assumes that these strengths can be accurately determined. Also, while limitations are imposed on the permissible slenderness of each frame member, the design generally results in limiting the maximum stresses on member cross-sections to specified values.

There are two basic methods of design here, the **working-stress** and the **limit-state design methods**. In the working-stress method, the working loads are employed in the computations. Furthermore, the specified permissible stresses are lower than the material yield

stresses, elastic stress-distribution for each cross-section is assumed, only elastic analysis of the frame is, therefore, adopted and each member cross-section is adjudged to be adequate if the condition represented by the following interaction equation is satisfied:

$$f_a / F_a + f_b / F_b \leq 1.0 \quad (1.3)$$

where f_a is applied axial stress,

F_a is permissible axial stress (for bending moment absent),

f_b is applied bending stress and

F_b is permissible bending stress (for axial force absent).

In the limit-state method, an elastic analysis of the frame subjected to factored working loads (based on a load factor greater than unity) is employed and an arbitrary re-distribution of the resulting bending moments is carried out to allow for plastic behaviour. The interaction equation (1.3) is also employed but the strength of each cross-section is based on a fully-plastic stress distribution instead of an elastic stress distribution. In each method, limitations are imposed on deflections for satisfying serviceability criteria under working loads and analysis for joint displacements and member end bending moments is often based on linear elastic (and seldom on non-linear elastic or inelastic) behaviour. This approach is considered to be adequate for practical purposes. On the other hand, the employment of inelastic analysis in this regard runs counter to the simplicity of this method of frame design.

Although the results of several studies of isolated beam-column behaviour are available (2,3,63,64,65,66,67,68,69,70,71,72), these are based on assumed boundary conditions (notably pinned, fixed or elastically-restrained) often unrelated to the actual conditions present

in frames. From these studies, however, the concept of **effective length** for a beam-column is evolved which is widely adopted in the simplified working-stress and limit-state design methods briefly described above. The effective length of a compression member relates the ultimate axial load for the member to the **Euler load** (calculated for pinned ends) for the member. Guidelines, in the form of formulae and nomograms, are usually recommended (74,75,76) for computing approximate values of these effective lengths in design codes of practice and structural steel design publications. Chen (73) emphasized the need for a better knowledge of end restraints for columns which form parts of frames. By employing a **substitute frame approach**, Wood also produced charts for computing the effective lengths of columns in braced frames (77). The computation of effective lengths based only on the elastic flexural stiffness of a frame column and its adjoining members and ignoring the actual loads on the frame has been pointed out by Moy and Downs (78) to be inadequate for accounting for instability effects. For example, in the context of overall frame failure rather than isolated column failure, the effective length of each column in the portal frame shown in Fig. 1.2 should vary with the applied loads, P, Q and R whereas this length is usually taken to be constant when failure is based on isolated

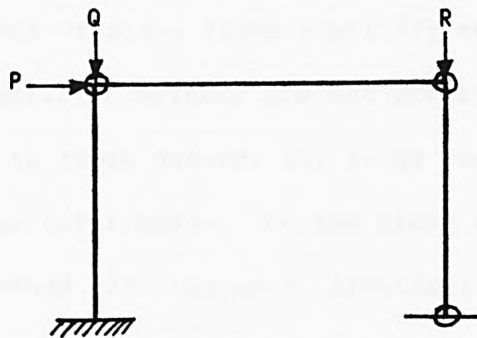


Fig. 1.2

column behaviour. Moy and Downs, therefore, advocated the avoidance of the effective length approach to frame design and proposed that the permissible axial load in the interaction equation should be the buckling load for a pin-ended column while the permissible bending moment should be the full-plastic moment of the cross-section divided by a factor given by

$$\beta = 1.2 + A_F/30 \quad (1.4)$$

where A_F is an elastic amplification factor defined as the elastic second-order moment divided by the elastic first-order moment. This proposal appears reasonable but cannot overcome all the problems of the effective length approach since it is based on a non-representative frame column.

It is evident from the foregoing remarks that a realistic computation of the ultimate strengths for the members of regular and irregular frames should include not only elastic considerations but also any inelastic effects in the members and their adjoining members arising from all material, geometric and loading effects. Thus, the design of plane frames on the basis of the ultimate strengths of their members cannot always guarantee to produce a safe or economic design.

1.5.2 Frame Design Based On The Strength Of The Entire Frame

Of the methods of plane frame stability analysis described above, the numerical integration methods are not practical or economic tools for design owing to their demands for large computer time and storage even for regular portal frames. On the other hand, the second-order elastic-plastic method is the most practical method for achieving specified frame design objectives. However, because it is strictly applicable to structural steel frames, its application to other metal

frames is approximate since these frames do not exhibit the same degree of ductility as structural steel. Also, considerations of economy often make the rigid-plastic method, Merchant-Rankine formula (or any of its modifications) and **optimum design** methods (which also employ the concentrated inelasticity concept of structural behaviour) to be employed in practical plane frame design. In an optimum design method, a function (such as weight, cross-sectional area or second moment of area) is optimized using a linear or non-linear programming method (79,80,81). These methods, however, cannot have the versatility and the accuracy of the second-order elastic-plastic method.

Therefore, before using any method of frame stability analysis for plane frame design, its economic advantages should be weighed against its analytical disadvantages.

1.6 Need For A New Method Of Plane Frame Stability Analysis

It has been shown that although rigorous numerical integration methods employing the more correct distributed inelasticity concept of structural behaviour are available for plane frame stability analysis, practical and economic considerations make it necessary to frequently employ simplified techniques for frame design. Some of these techniques do not require the determination of frame failure loads. Instead, they rely on the strengths of the individual frame members assuming known boundary conditions for these members. However, no accurate assessment of the boundary conditions for a plane frame member, taken in isolation, can be made (73). Therefore, plane frames designed by these techniques can be either over-designed (in which case the objective of economy is not maintained) or under-designed (in which case the objective of

ultimate strength or serviceability is not maintained). The treatment of a plane frame as one unit in analysis must, therefore, remain the most effective and most correct method of assessing both safety and economy in frame design, a view also supported by Horne and Merchant (6). Some other techniques rely on the determination of the failure load of the entire frame by adopting the concentrated inelasticity concept of structural behaviour. Of these methods, the second-order elastic-plastic method remains the most versatile and the most reliable method.

Despite the versatility of the second-order elastic-plastic method, a practical and economic method of adopting the distributed inelasticity concept is necessary not only for structural steel frames but also for other metal plane frameworks. It is essential for such a method to have a level of accuracy which compares favourably with experimental and existing theoretical techniques and to be applicable to all types of metal plane frame under general loadings.

1.7 Scope

The main aim of the work described in this thesis is to develop a practical and economic method for including the effect of spread of inelasticity in members of a plane frame on its strength and stability. A method is proposed here which avoids the finite discretization of plane frame members and their cross-sections but identifies the lengths and locations of **distinct zones of inelasticity** that may be present in a plane frame member at any stage of loading up to failure. This method adopts a simplified, **bilinear stress-strain relationship** for a metal while the special case of elastic-perfectly-plastic stress-strain relationship is limited to structural steel. Various combinations of

elastic and inelastic zones for each frame member under any combination of axial force and end bending moments are considered. By also accounting for the initial curvature of the member, the tangent force-displacement relationships for the member are derived. This method is, therefore, appropriately called the **inelastic zone method**.

In Chapter 2, exact formulae for computing the moment-curvature-axial force relationships for rectangular and I-shaped cross-sections frequently used for metal plane frame design are presented. In each case, the **spread of inelasticity** within the cross-section is accounted for. Other cross-sections of arbitrary shape are not considered here because these shapes are not usually employed for metal plane frame design.

In Chapter 3, the proposed inelastic zone method is employed to derive beam-column tangent flexibility coefficients in forms which are directly suitable for plane frame stability analysis by any of the standard techniques of structural analysis.

Chapter 4 is concerned with the use of the tangent flexibility coefficients derived in Chapter 3 in performing stability analyses of plane frames by the stiffness method of structural analysis.

Published theoretical and experimental results are compared with those obtained by the proposed inelastic zone method in Chapter 5.

Chapter 6 describes tests on two portal frames built from a rolled steel section and includes comparison of test results with the theory developed in the earlier chapters.

Recommendations for plane frame design, in general, and the use of the inelastic zone method, in particular, are given in Chapter 7. Also, a new simplified method for plane frame design which avoids the

computation of frame failure loads and the use of the member effective length concept is presented in this thesis. This method limits bending moments, calculated using working loads, to estimated values based on the specified ultimate strengths of the member cross-sections and is called the **limiting moment method**.

Conclusions drawn from the work described in this thesis and some suggestions for extending the application of the inelastic zone method to other areas of structural stability are given in Chapter 8.

CHAPTER 2

MOMENT-CURVATURE-AXIAL FORCE RELATIONSHIPS FOR A CROSS-SECTION

2.1 Introduction

The response of a beam-column to a given combination of axial force and end bending moments up to failure depends, among other things, on the moment-curvature-axial force ($M-\psi-P$) relationships for each cross-section and, consequently, on the moment-rotation-axial force ($M-\theta-P$) relationships for the entire beam-column. The $M-\psi-P$ relationships for cross-sections are considered in this chapter while the $M-\theta-P$ relationships for a beam-column are considered in Chapter 3.

The $M-\psi-P$ relationships for a cross-section are governed by the material stress-strain ($\sigma-\epsilon$) relationships and also by the magnitudes of the initial (or residual) stresses present in the section. These generally give rise to non-linear or irregular stress distribution diagrams for the cross-section. Closed-form solutions of the resulting force and moment equilibrium equations ($P = \int_A \sigma \cdot dA$ and $M_z = \int_A \sigma y \cdot dA$ where y is the distance of the point considered from the centroid of the cross-section) are difficult to obtain or even may be non-existent. Hence, recourse to numerical integration techniques (66,82), involving sub-divisions of the cross-section into elemental areas and the use of constant stress over each elemental area, has to be made, albeit at the expense of much computer time and storage. While the accuracy obtained by using numerical integration techniques increases with increasing the number of elemental areas employed, reasonable results can, however, be obtained even for very complicated shapes of cross-section. Alternatively, numerical quadrature formulae can be used speeding up the

integration process considerably (83).

By linearizing the material stress-strain relationships and also employing simple shapes of cross-section, closed-form solutions of the governing equilibrium equations can be obtained leading to direct formulae which avoid the discretization of the cross-sections. Thus, it becomes possible to achieve significant economy in the computations.

In this chapter, new formulae for the M - ψ - P relationships are developed for rectangular and doubly-symmetric I-shaped cross-sections for the general case of elastic-strain-hardened materials. Simplified formulae (some of which are well-known) derived from the formulae for the general case for the particular case of elastic-perfectly-plastic materials are given in Appendices 1 and 2 for rectangular and I-shaped cross-sections respectively. Rectangular cross-sections are considered because they are simple and aid understanding of the principles involved. Doubly-symmetric I-shaped cross-sections bent about their major axes of bending are considered because they are the most commonly-adopted cross-sections for metal plane frame members. Thus, the formulae presented in this chapter and in Appendices 1 and 2 directly serve as practical design aids for metal plane frames and also highlight the importance of shape of cross-section in structural stability analysis and design.

2.2 Assumptions

The following assumptions are made in this chapter:

1. The cross-section is subjected to a uniaxial bending moment and an axial force.
2. The effects of shear stresses are negligible.

3. The strain distribution for the cross-section is linear.
 This implies that plane sections before bending remain plane after bending (Euler-Bernoulli's Theorem).
4. The stress-strain (σ - ϵ) diagram for the material is the same in tension as it is in compression.
5. A bilinear idealization is used to represent the actual stress-strain relationship for the material.

This is widely adopted in metal stability studies. Fig. 2.1(a) shows the bilinear, elastic-perfectly-plastic stress-strain idealization often adopted for structural steel. Fig. 2.1(b) shows the bilinear, elastic-strain-hardened stress-strain idealization adopted for structural steel and many other metals and alloys.

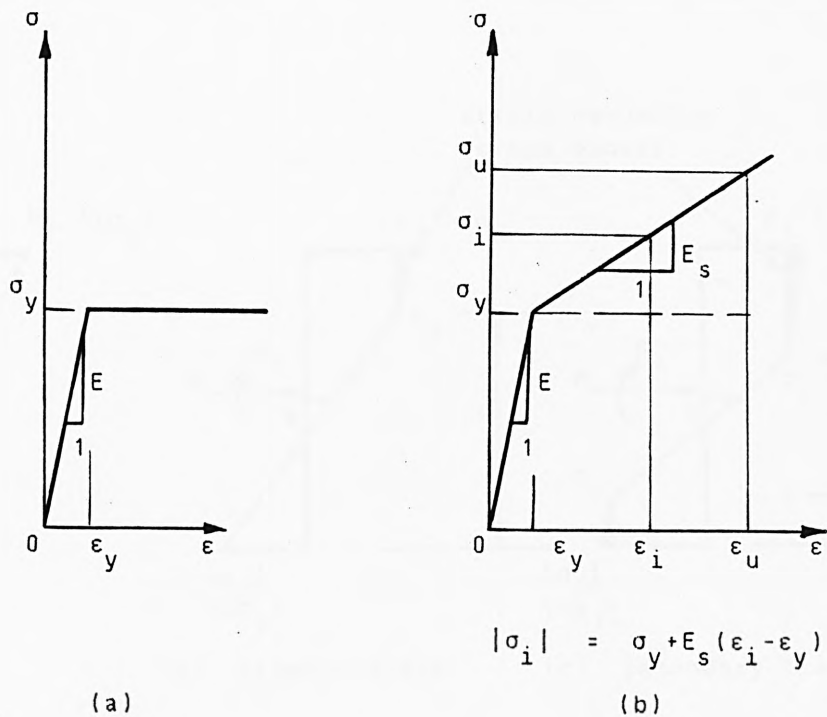


Fig. 2.1 Bilinear Stress-Strain Idealizations For Metals And Alloys

6. Residual stresses are not included in the analysis.

The effects of residual stress patterns can be indirectly allowed for by modifications to the bilinear stress-strain idealizations of Fig. 2.1; for example, by reducing the value of yield stress or ignoring strain-hardening. This latter approach was found by Wood (77), Galambos (3) and El-Zanaty and Murray (59) to compensate for the effects of residual stresses reasonably without the need to engage in more elaborate analysis.

2.3 Stress Distribution Diagrams

The stress distribution diagrams often employed in inelastic stability analysis for a cross-section are shown in Fig. 2.2. The use of these diagrams in the inelastic zone method will now be described.

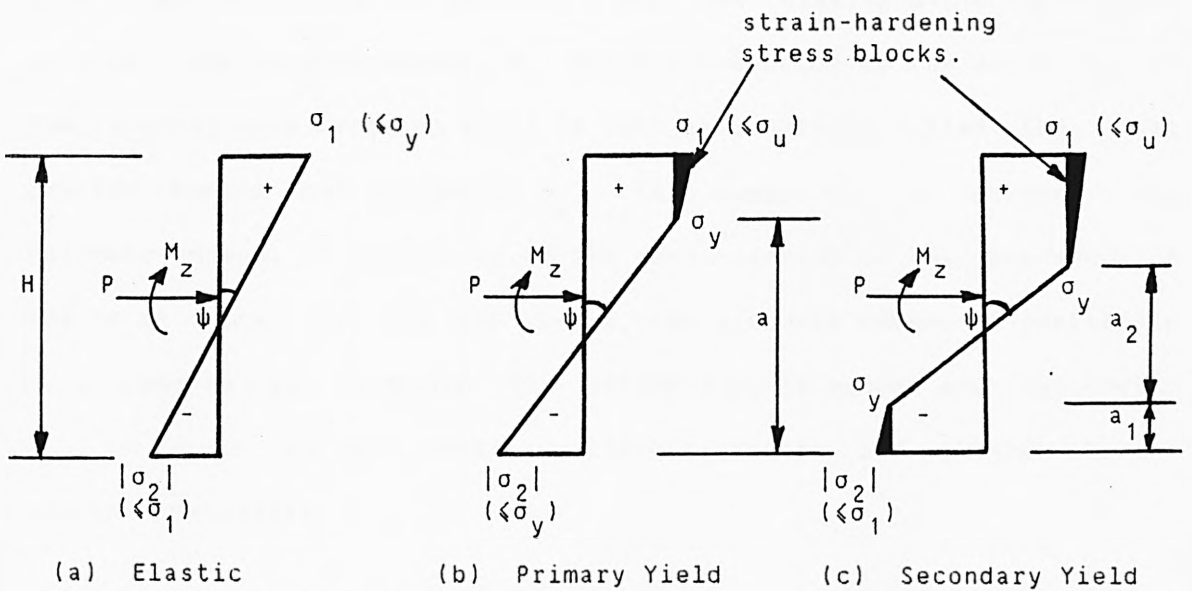


Fig. 2.2 Relevant Stress Distribution Diagrams

Fig. 2.2(a) shows the elastic stress distribution diagram in which the absolute value of the top fibre stress, σ_1 , is greater than that of the bottom fibre stress, σ_2 , owing to the presence of the axial force, P . The bending moment, M_z , which corresponds to the first attainment of the yield stress at the top of the cross-section (i.e. $|\sigma_1| = \sigma_y$) is here called the **first yield moment** and designated M_{y1} .

Fig. 2.2(b) shows the primary yield stress distribution diagram for the elastic-perfectly-plastic material together with a stress block due to strain-hardening for the case of the inelastic zones spreading from the top of the cross-section. The bending moment, M_z , which corresponds to the first attainment of the yield stress at the bottom of the cross-section (i.e. $|\sigma_2| = \sigma_y$) is here called the **intermediate yield moment** and designated M_{y2} .

Fig. 2.2(c) shows the secondary yield stress distribution diagram for an elastic-perfectly-plastic material together with stress blocks due to strain-hardening for the case of inelastic zones spreading from both ends of the cross-section. For the elastic-perfectly-plastic material, the bending moment, M_z , which corresponds to the depth, a_2 , of the elastic core becoming equal to zero is generally called the **full plastic moment** and designated M_p . This moment is, in essence, the ultimate moment of resistance of the cross-section in the presence of the axial force, P . In this thesis, the ultimate moment of resistance of a cross-section is called its **ultimate yield moment** and designated M_{y3} in order to suit elastic-perfectly-plastic and elastic-strain-hardened materials.

2.4 The Moment-Curvature-Axial Force Relationships For A Cross-Section Subjected To The Elastic Stress Distribution

Fig. 2.3 shows a rectangular cross-section and an I-shaped cross-section. In each case, the axis of bending is the z-axis. The formulae developed for I-shaped cross-sections may also be applied to cellular sections with two or more webs and with additional flange plates provided all plate elements of the cross-section are symmetrically-located about the y-axis. The value of the web thickness, t , is then taken to be the sum of the different web thicknesses while the value of the flange thickness, T , is taken to be the sum of the original flange and the additional flange thicknesses.

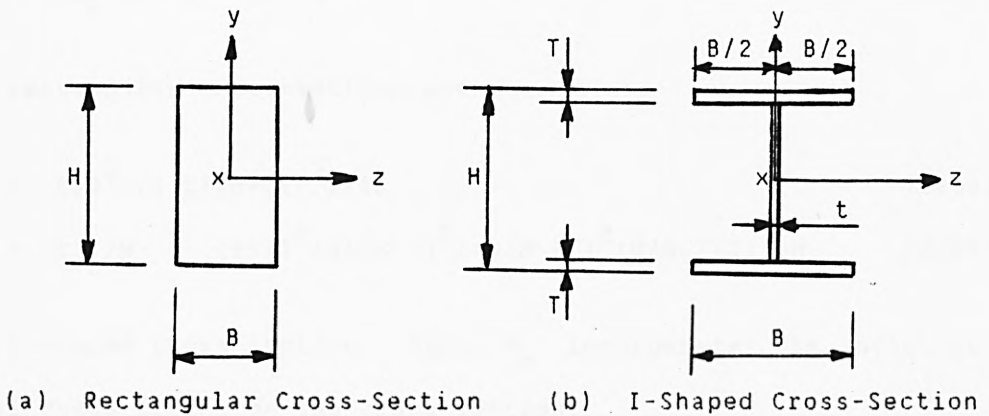


Fig. 2.3 Rectangular And I-Shaped Cross-Sections

Fig. 2.4 shows the relevant strain and stress distribution diagrams.

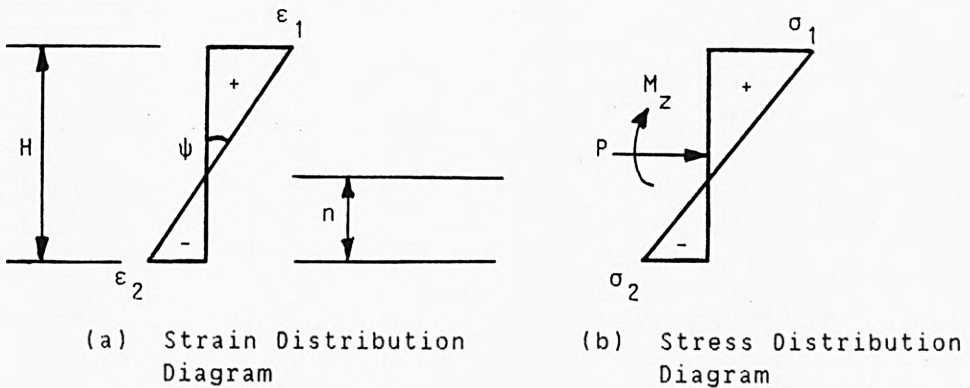


Fig. 2.4 Strain And Stress Distribution Diagrams

The M- ψ -P relationships are determined from the equilibrium of bending moments and longitudinal forces as follows:

$$P = A(\sigma_1 + \sigma_2)/2 \quad (2.1)$$

$$\psi = M_z / (EI_z) = (\sigma_1 - \sigma_2) / (EH) = (\epsilon_1 - \epsilon_2) / H \quad (2.2)$$

$$M_z = (\sigma_1 - P/A)Z_1 \quad (2.3)$$

where the stress and strain intensities, σ_2 and ϵ_2 , retain their negative signs as shown in Fig. 2.4 and where the second moment of area, I_z , and the elastic modulus, Z_1 , of the cross-section are given by

$$I_z = BH^3/12 \quad (2.4a)$$

$$Z_1 = 2I_z/H = BH^2/6 \quad (2.4b)$$

for the rectangular cross-section and

$$I_z = [BH^3 - (B-t)(H-2T)^3]/12 \quad (2.5a)$$

$$Z_1 = 2I_z/H = [BT(T^2/3 + (H-T)^2) + t(H-2T)^2(H/6 - T/3)]/H \quad (2.5b)$$

for the I-shaped cross-section. Also, M_z incorporates the influence of the axial force acting on the cross-section.

The first yield moment, M_{y1} , is determined from Eqn. (2.3) by replacing σ_1 by σ_y thus:

$$M_{y1} = (\sigma_y - P/A)Z_1 \quad (2.6)$$

2.5 The Moment-Curvature-Axial Force Relationships For A Rectangular Cross-Section Subjected To The Primary Yield Stress Distribution

Fig. 2.5 shows the relevant strain and stress distribution diagrams including strain-hardening.

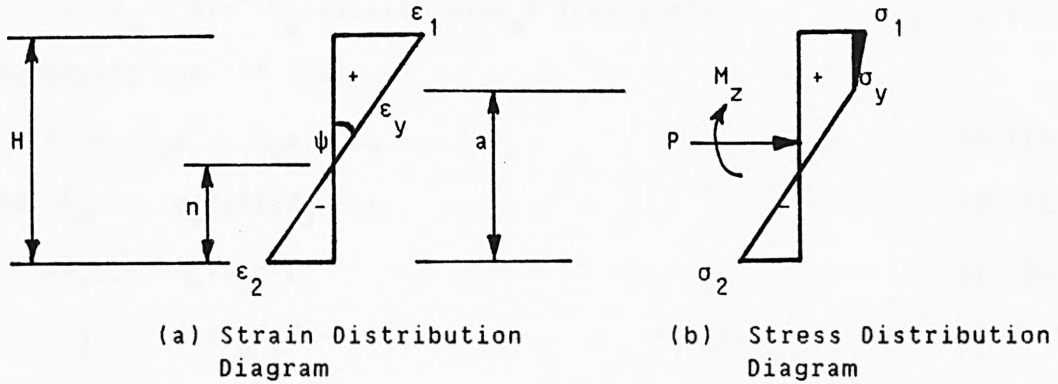


Fig. 2.5

With the notations of Fig. 2.5, the following expressions for strains, stresses and curvature are readily obtained:

$$\epsilon_1 = \epsilon_y (H-n)/(a-n) \quad (2.7a)$$

$$\epsilon_2 = -\epsilon_y n/(a-n) \quad (2.7b)$$

$$\sigma_1 = \sigma_y [1+C_s (H-a)/(a-n)] \quad (2.7c)$$

$$\sigma_2 = -\sigma_y n/(a-n) \quad (2.7d)$$

$$\psi = (\epsilon_y - \epsilon_2)/a = \epsilon_y/(a-n) \quad (2.7e)$$

Considering the equilibrium of longitudinal forces,

$$P = P_s - aB(\sigma_y - \sigma_2)/2 + \psi_1 \quad (2.8a)$$

where $P_s = \sigma_y A \quad (2.8b)$

$$A = BH \quad (2.8c)$$

$$\begin{aligned} \psi_1 &= (\sigma_1 - \sigma_y)(H-a)B/2 \\ &= \sigma_y B C_s (H-a)^2/[2(a-n)] \end{aligned} \quad (2.8d)$$

Taking moments about the centroid of the cross-section,

$$M_z = aB(\sigma_y - \sigma_2)(H/2 - a/3)/2 + \psi_2 \quad (2.9a)$$

where $\psi_2 = \psi_1(H/6 - a/3) \quad (2.9b)$

The ϕ terms are the contributions of the strain-hardening stress block.

Substitution of Eqns. (2.7d) and (2.8d) into Eqn. (2.8a) gives

$$\begin{aligned}
 P &= P_s - \sigma_y a B [1+n/(a-n)]/2 + \sigma_y B C_s (H-a)^2/[2(a-n)] \\
 &= P_s + \sigma_y B [C_s (H-a)^2 - a^2]/[2(a-n)] \\
 &= P_s + \sigma_y B [a^2(C_s - 1) - a(2C_s H) + C_s H^2]/[2(a-n)] \quad (2.10a)
 \end{aligned}$$

Re-arranging Eqn. (2.10a),

$$n = C_1 a^2 + C_2 a + C_3 \quad (2.10b)$$

$$\text{where } C_0 = \sigma_y B/[2(P_s - P)] \quad (2.10c)$$

$$C_1 = C_0(C_s - 1) \quad (2.10d)$$

$$C_2 = 1 - 2C_0 C_s H \quad (2.10e)$$

$$C_3 = C_0 C_s H^2 \quad (2.10f)$$

Substitution of Eqns. (2.7d) and (2.9b) into Eqn. (2.9a) gives

$$\begin{aligned}
 M_z &= \sigma_y a B [1+n/(a-n)] [H/2 - a/3]/2 \\
 &\quad + \sigma_y B C_s [(H^2 - 2aH + a^2)/(a-n)] [H/6 + a/3]/2 \\
 &= \sigma_y B [a^2(3H - 2a) + C_s (H^2 - 2aH + a^2)(H + 2a)]/[12(a-n)] \\
 &= \sigma_y B [a^3(2(C_s - 1)) + a^2(3H(1 - C_s)) + C_s H^3]/[12(a-n)] \quad (2.11)
 \end{aligned}$$

Substitution of Eqn. (2.10b) into Eqn. (2.11) gives

$$12M_z(a - C_1 a^2 - C_2 a - C_3)/(\sigma_y B) = a^3[2(C_s - 1)] + a^2[3H(1 - C_s)] + C_s H^3 \quad (2.12)$$

Re-arranging Eqn. (2.12),

$$D_1 a^3 + D_2 a^2 + D_3 a + D_4 = 0 \quad (2.13a)$$

$$\text{where } D_1 = 2(C_s - 1) \quad (2.13b)$$

$$D_2 = 3H(1 - C_s) + 12C_1 M_z/(\sigma_y B) \quad (2.13c)$$

$$D_3 = 12(C_2 - 1)M_z/(\sigma_y B) \quad (2.13d)$$

$$D_4 = C_s H^3 + 12C_3 M_z/(\sigma_y B) \quad (2.13e)$$

A detailed derivation of the equations for determining the depths of the neutral axis and the elastic core has been given above. In subsequent sections of this chapter, the equations for these depths,

based on the procedures adopted in this section, will be given without derivations.

Determination Of Curvature

The depth, a , of the elastic core is determined from Eqn. (2.13a) for given values of the axial force, P , and bending moment, M_z , by using Newton's method (see Appendix 3) or any other suitable method. Substitution of the resulting value of a into Eqn. (2.10b) gives the depth, n , to the neutral axis of the cross-section. Then, substitution of these values of a and n into Eqn. (2.7e) gives the value of the curvature, ψ .

Determination Of The Intermediate Yield Moment

In this case, $\sigma_2 = -\sigma_y$ and, therefore, $n = a/2$. Substitution of this value of n into Eqn. (2.10b) gives

$$a = [(0.5 - C_2) - \{(C_2 - 0.5)^2 - 4C_1C_3\}^{0.5}] / (2C_1) \quad (2.14)$$

Thus, M_{y2} is determined by substitution of Eqn. (2.14) and $n = a/2$ into Eqn. (2.11).

2.6 The Moment-Curvature-Axial Force Relationships For A Rectangular Cross-Section Subjected To The Secondary Yield Stress Distribution

Fig. 2.6 shows the relevant strain and stress distribution diagrams including strain-hardening.

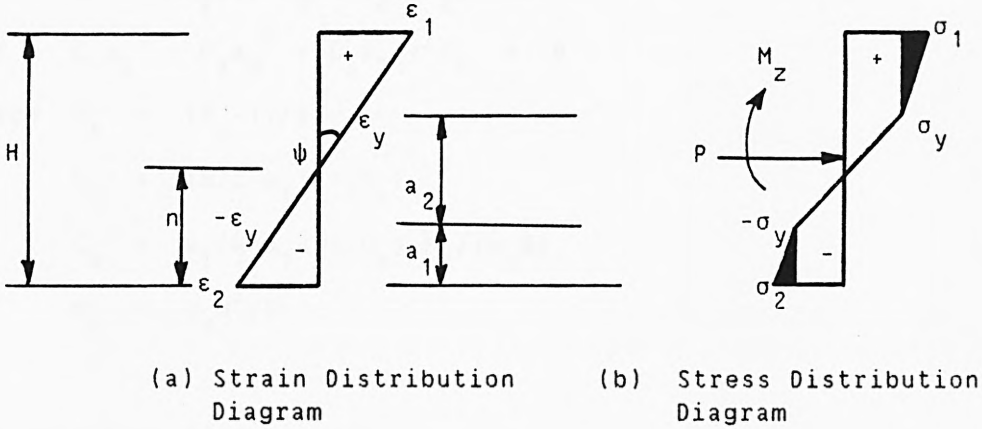


Fig. 2.6

With the notations of Fig. 2.6,

$$\epsilon_1 = \epsilon_y [2(H-a_1)/a_2 - 1] \quad (2.15a)$$

$$\epsilon_2 = -\epsilon_y [1 + 2a_1/a_2] \quad (2.15b)$$

$$\sigma_1 = \sigma_y [1 + 2C_s (H-a_1-a_2)/a_2] \quad (2.15c)$$

$$\sigma_2 = -\sigma_y [1 + 2C_s a_1/a_2] \quad (2.15d)$$

$$\psi = 2\epsilon_y/a_2 = 2\sigma_y/(Ea_2) \quad (2.15e)$$

$$n = a_1 + a_2/2 \quad (2.15f)$$

Considering the equilibrium of longitudinal forces,

$$P = P_s - \sigma_y B(2a_1+a_2) + \varphi_1 - \varphi_2 \quad (2.16a)$$

where $\varphi_1 = \sigma_y B C_s (H-a_1-a_2)^2/a_2$ (2.16b)

and $\varphi_2 = \sigma_y B C_s a_1^2/a_2$ (2.16c)

Considering moment equilibrium about the centroid of the cross-section,

$$M_z = \sigma_y B [a_2 (H/2 - a_1 - a_2/3) + a_1 (H - a_1)] + \varphi_3 + \varphi_4 \quad (2.17a)$$

where $\varphi_3 = \varphi_1 [H/6 + (a_1 + a_2)/3]$ (2.17b)

and $\varphi_4 = \varphi_2 [H/2 - a_1/3]$ (2.17c)

The ψ terms are the contributions of the strain-hardening stress blocks.

Following the procedure adopted in Section 2.5, the relevant formulae are as follows:

$$a_1 = \frac{P_s - P + \sigma_y B \{ C_s (H - a_2)^2 / a_2 - a_2 \}}{2 \sigma_y B \{ 1 + C_s (H - a_2) / a_2 \}} \quad (2.18)$$

$$\text{and } C_1 a_2^3 + C_2 a_2^2 + C_3 a_2 + C_4 = 0 \quad (2.19a)$$

$$\text{where } C_1 = (C_s - 1) / 3 \quad (2.19b)$$

$$C_2 = (H/2 - a_1)(1 - C_s) \quad (2.19c)$$

$$C_3 = a_1(H - a_1)(1 - C_s) - M_z / (\sigma_y B) \quad (2.19d)$$

$$C_4 = C_s H^3 / 6 \quad (2.19e)$$

Determination Of Curvature

Eqns. (2.18) and (2.19a) are solved by iteration. Firstly, a trial value is assumed for a_2 . This value is substituted into Eqn. (2.18) to determine a value for a_1 . This value of a_1 is substituted into Eqn. (2.19a) and the resulting cubic equation is solved by Newton's or similar method to determine a revised value for a_2 . This revised value for a_2 is substituted oncemore into Eqn. (2.18) and the whole process is repeated until successive values of a_1 and a_2 satisfy a convergence criterion. Then the accepted value for a_2 is substituted into Eqn. (2.15e) to determine the curvature, ψ .

Determination Of The Ultimate Yield Moment

The maximum strain, ϵ_1 , is set equal to the specified ultimate strain, ϵ_u . Then, from Eqn. (2.15a),

$$\epsilon_1 = \epsilon_u = \epsilon_y \{ 2(H - a_1) - a_2 \} / a_2 = A_s \epsilon_y \quad (2.20a)$$

$$\text{i.e. } a_1 = H - a_2(1 + A_s) / 2 \quad (2.20b)$$

From Eqns. (2.18) and (2.20b),

$$D_1 a_2^2 + D_2 a_2 + D_3 = 0 \quad (2.21a)$$

$$\text{where } D_1 = \sigma_y B A_s (C_s - 1) \quad (2.21b)$$

$$D_2 = P_s [1 - C_s (1 + A_s)] + P \quad (2.21c)$$

$$D_3 = H P_s C_s \quad (2.21d)$$

$$\text{from which } a_2 = [-D_2 - \{D_2^2 - 4D_1 D_3\}^{0.5}] / (2D_1) \quad (2.21e)$$

M_{y3} is determined from Eqn. (2.19a) by substituting Eqns. (2.20b) and (2.21e) into Eqn. (2.19a) and setting M_z equal to M_{y3} .

2.7 The Moment-Curvature-Axial Force Relationships For An I-Shaped Cross-Section Subjected To The Primary Yield Stress Distribution

The relevant strain and stress distribution diagrams are the same as those of Fig. 2.5. Two cases are required to be considered in this section, namely:

1. Partial yielding of top flange and
2. Full yielding of top flange and partial yielding of web.

In each case, Eqns. (2.7) are applicable and the procedures adopted in Section 2.5 for the rectangular cross-section are also applicable.

2.7.1 Partial Yielding Of Top Flange

Consideration of equilibrium of longitudinal forces gives

$$P = P_s - (\sigma_y - \sigma_2) [B\{T(2a-T) + (a-T-H)^2\} + t(H-2T)(2a-H)] / (2a) + \varphi_1 \quad (2.22a)$$

$$\text{where } \varphi_1 = \sigma_y B C_s [(H-a)^2 / (a-n)] / 2 \quad (2.22b)$$

$$P_s = \sigma_y A \quad (2.22c)$$

$$A = 2BT + t(H-2T) \quad (2.22d)$$

Consideration of moment equilibrium about the centroid of the cross-section gives

$$M_z = (\sigma_y - \sigma_2) \{ BT \{ T(H/2 - T/3) + (a - T)(H - T) \} + \{ t(H - 2T)^3 - B(a - H + T)^2(2a + H - 4T) \} / 6 \} / (2a) + \psi_2 \quad (2.23a)$$

$$\text{where } \psi_2 = \psi_1 [H/6 + a/3] \quad (2.23b)$$

The ψ terms are the contributions of the strain-hardening stress block.

Determination Of Curvature

The relevant formulae for the depth, n , to the neutral axis and the depth, a , of the elastic core are given by the following equations:

$$n = C_1 a^2 + C_2 a + C_3 \quad (2.24a)$$

$$\text{and } D_1 a^3 + D_2 a^2 + D_3 a + D_4 = 0 \quad (2.24b)$$

$$\text{where } C_0 = \sigma_y / [2(P_s - P)] \quad (2.24c)$$

$$C_1 = C_0 B (C_s - 1) \quad (2.24d)$$

$$C_2 = 1 + 2C_0 [BH(1 - C_s) - A] \quad (2.24e)$$

$$C_3 = C_0 H [BH(C_s - 1) + A] \quad (2.24f)$$

$$D_1 = 2(C_s - 1) \quad (2.24g)$$

$$D_2 = 8T - H(5 + 4C_s) + 12C_1 M_z / (\sigma_y B) \quad (2.24h)$$

$$D_3 = 4[3M_z(C_s - 1) / (\sigma_y B) + (H - T)(4T - H)] \quad (2.24i)$$

$$D_4 = 12C_3 M_z / (\sigma_y B) + T^2(4T - 3H) + t(H - 2T)^3 / B - (H - T)^2(H - 4T) + C_s H^3 \quad (2.24j)$$

The value of a obtained by solving Eqn. (2.24b) is substituted into Eqn. (2.24a) to obtain n from which ψ is determined from Eqn. (2.7e).

Determination Of The Intermediate Yield Moment

The corresponding depth, a , of the elastic core is determined by substituting $n = a/2$ (since $\sigma_2 = -\sigma_y$) into Eqn. (2.24a) and solving the resulting quadratic equation. If this value of a is within the limits

$$(H - T) < a < H$$

then its substitution and the substitution of $\sigma_2 = -\sigma_y$ into Eqn. (2.23a) gives the correct value for M_{y2} . Otherwise, it becomes necessary to consider the case of partial web yielding in the top of the cross-section.

2.7.2' Full Yielding Of Top Flange And Partial Yielding Of Web

The strain and stress distribution diagrams required in this section are given in Fig. 2.7 which is the same as Fig. 2.5 showing additional strain and stress intensities for the top flange/web connection.

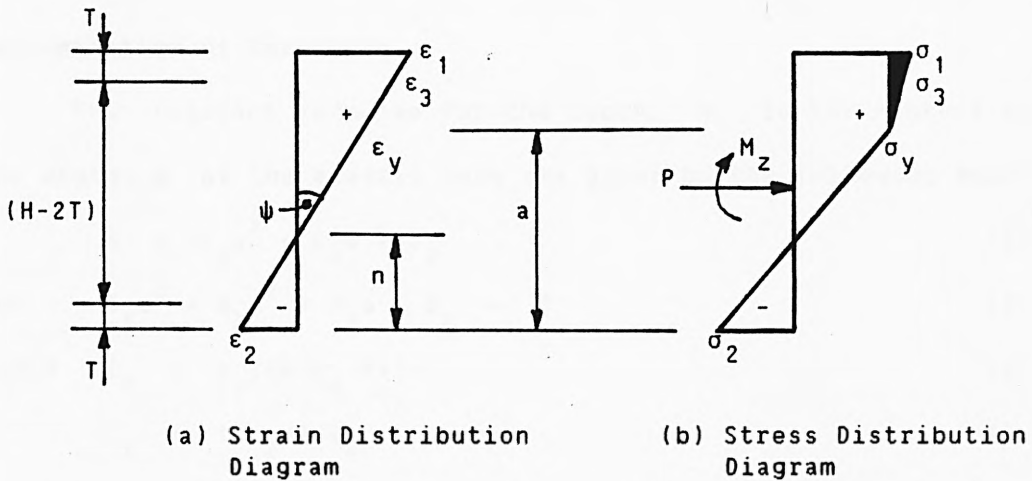


Fig. 2.7

The additional strain and stress intensities are as follows:

$$\epsilon_3 = \epsilon_y (H-n-T)/(a-n) \quad (2.25a)$$

$$\sigma_3 = \sigma_y [1 + C_s (H-T-a)/(a-n)] \quad (2.25b)$$

Consideration of equilibrium of longitudinal forces gives

$$P = P_s - (\sigma_y - \sigma_2) [T(B-t)(2a-T) + a^2 t] / (2a) + \phi_1 + \phi_2 \quad (2.26a)$$

$$\begin{aligned} \text{where } \phi_1 &= t(\sigma_3 - \sigma_y)(H-T-a)/2 \\ &= \sigma_y C_s t (H-T-a)^2 / [2(a-n)] \end{aligned} \quad (2.26b)$$

$$\begin{aligned} \text{and } \psi &= BT(\sigma_1 + \sigma_3 - 2\sigma_y)/2 \\ &= \sigma_y BTC_s [(2H-T) - 2a]/[2(a-n)] \end{aligned} \quad (2.26c)$$

Consideration of moment equilibrium about the centroid of the cross-section gives

$$\begin{aligned} M_z &= (\sigma_y - \sigma_2) [BT\{T(H/2 - T/3) + (a-T)(H-T)\} \\ &\quad + t(a-T)^2(H/2 - a/3 - 2T/3)] / (2a) + \psi_3 + \psi_4 \end{aligned} \quad (2.27a)$$

$$\text{where } \psi_3 = \psi_1 [(H/6 - 2T/3) + a/3] \quad (2.27b)$$

$$\text{and } \psi_4 = \psi_2 [H/2 - T/3 \{(3H - 2T - 3a)/(2H - T - 2a)\}] \quad (2.27c)$$

The ψ terms are the contributions of the strain-hardening stress block.

Determination Of Curvature

The relevant formulae for the depth, n , to the neutral axis and the depth, a , of the elastic core are given by the following equations:

$$n = C_1 a^2 + C_2 a + C_3 \quad (2.28a)$$

$$\text{and } D_1 a^3 + D_2 a^2 + D_3 a + D_4 = 0 \quad (2.28b)$$

$$\text{where } C_0 = \sigma_y / [2(P_s - P)] \quad (2.28c)$$

$$C_1 = t(C_s - 1)C_0 \quad (2.28d)$$

$$C_2 = 1 - C_0 [2\{T[B(1 + C_s) - t] + tC_s(H - T)\}] \quad (2.28e)$$

$$C_3 = C_0 [T^2(B - t) + tC_s(H - T)^2 + BTC_s(2H - T)] \quad (2.28f)$$

$$D_1 = t(C_s - 1)/3 \quad (2.28g)$$

$$D_2 = tH(1 - C_s)/2 + 2C_1 M_z / \sigma_y \quad (2.28h)$$

$$\begin{aligned} D_3 &= (H - T)[T(B - t) + C_s\{t(H/6 + T/3) - BT\}] \\ &\quad + 2M_z(C_2 - 1)/\sigma_y \end{aligned} \quad (2.28i)$$

$$\begin{aligned} D_4 &= T^2(H/2 - 2T/3)(t - B) + 2C_3 M_z / \sigma_y \\ &\quad + C_s [t(H - T)^2(H/6 - 2T/3) + BT\{H(2H - T)/2 - T(3H - 2T)/3\}] \end{aligned} \quad (2.28j)$$

The value of a obtained by solving Eqn. (2.28b) is substituted into Eqn. (2.28a) to obtain n from which ψ is determined from Eqn. (2.7e).

Determination Of The Intermediate Yield Moment

The depth, a , of the elastic core corresponding to the intermediate yield moment is determined by substituting $n = a/2$ (since $\sigma_2 = -\sigma_y$) into Eqn. (2.28a) and solving the resulting quadratic equation. If this value of a is within the limits

$$T \leq a \leq (H-T) \quad (2.28k)$$

then its substitution and the substitution of $\sigma_2 = -\sigma_y$ into Eqn. (2.27a) gives the correct value for M_{y2} . The limiting axial forces for the cross-section for application of these formulae are defined as follows:

For $a = (H-T)$ and $\sigma_1 = \sigma_u$, the limiting axial force is given by

$$P_{11} = P_s - \sigma_y [2(B-t)(2T-H)(H-T) + B(H-T)^2 + H(H-2T)(B-T)] / (H-T) + P_{s1} \quad (2.28l)$$

For $a = T$ and $\sigma_1 = \sigma_u$, the limiting axial force is given by

$$P_{12} = P_s - \sigma_y BT + P_{s2} \quad (2.28m)$$

where P_{s1} and P_{s2} are the contributions of the strain-hardening stress blocks given by

$$\begin{aligned} P_{s1} &= BT(\sigma_u - \sigma_y) / 2 \\ &= \sigma_y BT(B_s - 1) / 2 \end{aligned} \quad (2.28n)$$

$$\begin{aligned} P_{s2} &= BT[(\sigma_u - \sigma_y) + (H-2T)(\sigma_u - \sigma_y) / H] / 2 \\ &\quad + t(H-2T)[(H-2T)(\sigma_u - \sigma_y) / H] / 2 \\ &= (\sigma_u - \sigma_y) [2BT(H-T) + t(H-2T)^2] / (2H) \\ &= \sigma_y (B_s - 1) [2BT(H-T) + t(H-2T)^2] / (2H) \end{aligned} \quad (2.28p)$$

2.8 The Moment-Curvature-Axial Force Relationships For An I-Shaped Cross-Section Subjected To The Secondary Yield Stress Distribution

The strain and stress distribution diagrams required in this Section are given in Fig. 2.8 which is the same as Fig. 2.5 showing additional strain and stress intensities for the flange/web connections.

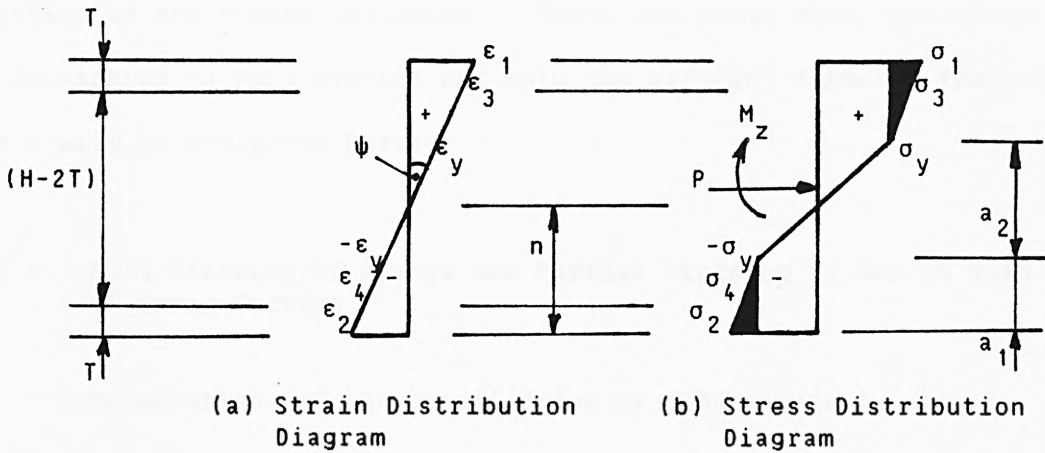


Fig. 2.8

The additional strain and stress intensities are as follows:

$$\epsilon_3 = \epsilon_y \left[\frac{2(H-a_1)-T}{a_2} - 1 \right] \quad (2.29a)$$

$$\epsilon_4 = -\epsilon_y \left[1 + \frac{2(a_1-T)}{a_2} \right] \quad (2.29b)$$

$$\sigma_3 = \sigma_y \left[1 + 2C_s \left\{ \frac{(H-a_1)-T}{a_2} - 1 \right\} \right] \quad (2.29c)$$

$$\sigma_4 = -\sigma_y \left[1 + 2C_s \left(\frac{a_1-T}{a_2} \right) \right] \quad (2.29d)$$

Four cases are possible in this section, namely:

1. Partial yielding of both flanges,
2. Full yielding of flange and partial yielding of web at the top of the cross-section and partial yielding of bottom flange,
3. Full yielding of flange and partial yielding of web at both ends of the cross-section and

4. Full yielding of top flange and partial yielding of bottom flange and full or partial yielding of web.

The M- ψ -P relationships for the cross-section for cases 1 and 2 can be approximately determined from those for cases 1 and 2 respectively in Section 2.7 by setting a_1 equal to zero. This approximate approach is quite reasonable since a_1 is mostly a small fraction of the flange thickness. These two cases will, therefore, not be considered in this section and only the relevant formulae for cases 3 and 4 will be presented here.

2.8.1 Full Yielding Of Flange And Partial Yielding Of Web At Both Ends Of Cross-Section

Consideration of the equilibrium of longitudinal forces, with reference to Fig. 2.8, gives

$$P = P_s - \sigma_y [2BT + t\{2(a_1 - T) + a_2\}] + \psi_1 + \psi_2 - \psi_3 - \psi_4 \quad (2.30a)$$

$$\text{where } \psi_1 = \sigma_y C_s t [H - T - a_1 - a_2]^2 / a_2 \quad (2.30b)$$

$$\begin{aligned} \psi_2 &= BT(\sigma_3 + \sigma_1 - 2\sigma_y) \\ &= \sigma_y BTC_s [2(H - a_1 - a_2) - T] / a_2 \end{aligned} \quad (2.30c)$$

$$\begin{aligned} \psi_3 &= (\sigma_4 - \sigma_y)(a_1 - T)t/2 \\ &= \sigma_y t C_s (a_1 - T)^2 / a_2 \end{aligned} \quad (2.30d)$$

$$\begin{aligned} \psi_4 &= BT(\sigma_2 - \sigma_4 - 2\sigma_y) \\ &= \sigma_y BTC_s (2a_1 - T) / a_2 \end{aligned} \quad (2.30e)$$

Consideration of moment equilibrium about the centroid of the cross-section gives

$$\begin{aligned} M_z &= \sigma_y [BT(H - T) + t\{(a_1 - T)(H - T - a_1) + a_2(H/2 - a_1 - a_2/3)\}] \\ &\quad + \psi_5 + \psi_6 + \psi_7 + \psi_8 \end{aligned} \quad (2.31a)$$

$$\begin{aligned} \text{where } \varphi_5 &= \varphi_1 [H/2 - T - (H - T - a_1 - a_2)/3] \\ &= \sigma_y C_s t (Q_9 - a_2)^2 (Q_{10} + a_2/3) / a_2 \end{aligned} \quad (2.31b)$$

$$\begin{aligned} \varphi_6 &= \varphi_2 [H/2 - T/3 \{ [2(\sigma_3 - \sigma_y) + (\sigma_1 - \sigma_y)] / [\sigma_3 + \sigma_1 - 2\sigma_y] \}] \\ &= \sigma_y C_s BT (Q_{11} - 2a_2) [H/2 - T/3 \{ (Q_{12} - 3a_2) / (Q_{11} - 2a_2) \}] / a_2 \end{aligned} \quad (2.31c)$$

$$\begin{aligned} \varphi_7 &= \varphi_3 [H/2 - T - (a_1 - T)/3] \\ &= \sigma_y C_s t Q_{13} / a_2 \end{aligned} \quad (2.31d)$$

$$\begin{aligned} \varphi_8 &= \varphi_4 [H/2 - T/3 \{ (3a_1 - 2T) / (2a_1 - T) \}] \\ &= \sigma_y C_s BT Q_{14} / a_2 \end{aligned} \quad (2.31e)$$

$$Q_9 = H - T - a_1 \quad (2.31f)$$

$$Q_{10} = [H/2 - 2T + a_1] / 3 \quad (2.31g)$$

$$Q_{11} = 2(H - a_1) - T \quad (2.31h)$$

$$Q_{12} = 3(H - a_1) - 2T \quad (2.31i)$$

$$Q_{13} = (a_1 - T)^2 (H/2 - 2T/3 - a_1/3) \quad (2.31j)$$

$$Q_{14} = H(2a_1 - T) / 2 - T(3a_1 - 2T) / 3 \quad (2.31k)$$

The relevant formulae for the depths a_1 and a_2 in Fig. 2.8 are given by

$$a_1 = \frac{P - P_s + \sigma_y [2BT + t(a_2 - 2T)] - \sigma_y C_s [t\{(H - T - a_2)^2 - T^2\} + 2BT(H - a_2)] / a_2}{2\sigma_y [C_s \{t(2T - H + a_2) - 2BT\} / a_2 - t]} \quad (2.32a)$$

$$C_1 a_2^3 + C_2 a_2^2 + C_3 a_2 + C_4 = 0 \quad (2.32b)$$

$$\text{where } C_1 = t(C_s - 1) / 3 \quad (2.32c)$$

$$C_2 = t[H/2 - a_1 + C_s(Q_{10} - 2Q_9/3)] \quad (2.32d)$$

$$\begin{aligned} C_3 &= t[(a_1 - T)(H - T - a_1) + C_s(Q_9^2/3 - 2Q_9Q_{10})] \\ &\quad + BT(H - T)(1 - C_s) - M_z / \sigma_y \end{aligned} \quad (2.32e)$$

$$C_4 = C_s [t(Q_{13} + Q_9^2 Q_{10}) + BT(HQ_{11} / 2 - TQ_{12} / 3 + Q_{14})] \quad (2.32f)$$

Determination Of Curvature

Eqns. (2.32a) and (2.32b) are solved by iteration. The procedure is similar to that described in Section 2.6. The resulting value for a_2 is substituted into Eqn. (2.15e) to determine the curvature, ψ .

Determination Of The Ultimate Yield Moment

The maximum strain, ϵ_1 , is set equal to the specified ultimate strain, ϵ_u . Then the depth, a_1 , is given by:

$$a_1 = H - a_2(1+A_s)/2 \quad (2.33)$$

The depth, a_2 , of the elastic core is determined from the following equation:

$$D_1 a_2^2 + D_2 a_2 + D_3 = 0 \quad (2.34a)$$

$$\text{where } D_1 = \sigma_y t A_s (1-C_s) \quad (2.34b)$$

$$D_2 = 2\sigma_y [tH(C_s - 1) - \{T(B-t) + C_s [t(H-T) + BT]\}] + P_s [1 + C_s (1 + A_s)] - P \quad (2.34c)$$

$$D_3 = -P_s H C_s \quad (2.34d)$$

$$\text{from which } a_2 = [-D_2 + \{D_2^2 - 4D_1 D_3\}^{0.5}] / (2D_1) \quad (2.34e)$$

Substitution of Eqns. (2.33) and (2.34e) into Eqn. (2.31a) gives M_2 which now is equal to M_{y3} .

The formulae derived in this section are valid within the following limits:

$$a_1 > T \quad (2.35a)$$

$$(a_1 + a_2) < (H - T) \quad (2.35b)$$

If condition (2.35b) is not satisfied, the axial force is very low and the approximate approach for case 1 in Section 2.8 is adopted. The limiting axial force and bending moment for the application of these formulae are defined as follows:

For $a_1 = T$ and $\sigma_1 = \sigma_u$, the limiting axial force is given by

$$P_{13} = P_s - \sigma_y BT - \sigma_y a_2 t + P_{s3} \quad (2.36a)$$

and the corresponding limiting bending moment is given by

$$M_{13} = \sigma_y BT(H-T) + \sigma_y a_2 t(H/2-T-a_2/3) + M_{s3} \quad (2.36b)$$

where P_{s3} and M_{s3} are the contributions of the strain-hardening stress blocks given by

$$\begin{aligned} P_{s3} &= BT[(\sigma_u - \sigma_y) + (\sigma_u - \sigma_y)(H-2T-a_2)/(H-T-a_2)]/2 \\ &\quad + t(H-2T-a_2)(H-2T-a_2)(\sigma_u - \sigma_y)/[2(H-T-a_2)] \\ &\quad - [|\sigma_2| - \sigma_y]BT/2 \\ &= [BT((\sigma_u - \sigma_y)(2H-3T-2a_2)/(H-T-a_2) - (|\sigma_2| - \sigma_y))] \\ &\quad + t(\sigma_u - \sigma_y)(H-2T-a_2)^2/(H-T-a_2)]/2 \end{aligned} \quad (2.36c)$$

$$\begin{aligned} M_{s3} &= BT(\sigma_u - \sigma_y)[1 + (H-2T-a_2)/\{2(H-T-a_2)\}][H/2-T/2] \\ &\quad + t(\sigma_u - \sigma_y)(H-2T-a_2)^2/\{2(H-T-a_2)\}[H/2-T-(H-2T-a_2)/3] \\ &\quad + BT[|\sigma_2| - \sigma_y][H/2-T/3]/2 \end{aligned} \quad (2.36d)$$

and where a_2 is determined by setting $\sigma_1 = \sigma_u$ and $a_1 = T$ in Eqn. (2.15c) to obtain

$$a_2 = 2C_s(H-T)/(B_s + 2C_s - 1) \quad (2.36e)$$

and σ_2 is determined by employing this value of a_2 and $a_1 = T$ in Eqn. (2.15d) to obtain

$$\sigma_2 = -\sigma_y[1 + 2C_s T/a_2] \quad (2.36f)$$

2.8.2 Full Yielding Of Top Flange And Partial Yielding Of Bottom Flange And Full Or Partial Yielding Of Web

Fig. 2.9 shows the relevant stress distribution diagrams. In each case, a_1 is less than the flange thickness, T . The determination of the relevant formulae for the $M-\psi-P$ relationships for the cross-section using these stress distribution diagrams is cumbersome. It can be seen,

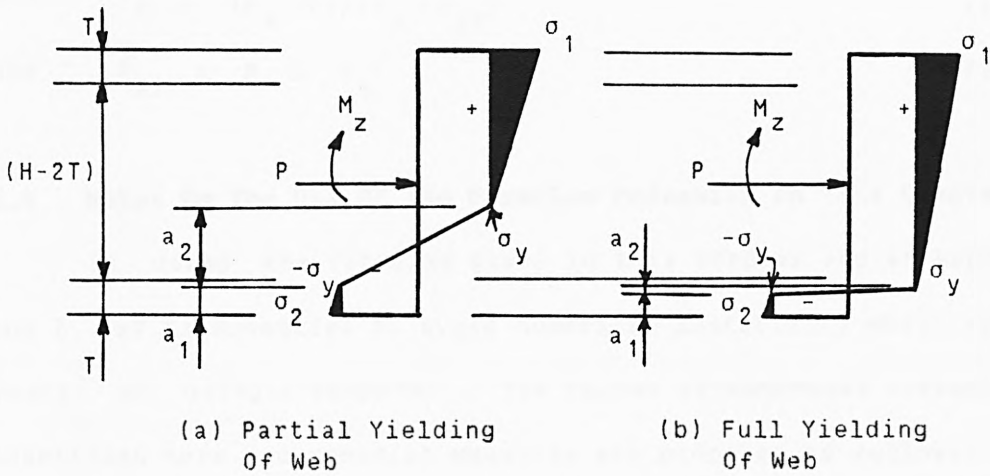


Fig. 2.9

however, that most of the cross-section has yielded and that the elastic portion of the cross-section is very small indeed. Thus, the ultimate yield moment, M_{y3} , of the cross-section is determined approximately by linear interpolation as follows:

In the limit when the triangular stress block due to strain-hardening extends from its maximum value at the top of the cross-section to zero at the bottom of the cross-section, the depth, a_1 , and the ultimate yield moment, M_{y3} , of the cross-section vanish and the corresponding axial force becomes equal to the squash load modified by strain-hardening as follows:

$$\begin{aligned}
 P_s' &= P_s [1 + (\sigma_u - \sigma_y) / (2\sigma_y)] \\
 &= P_s [(\sigma_u + \sigma_y) / (2\sigma_y)] \\
 &= P_s (B_s + 1) / 2
 \end{aligned}
 \tag{2.37a}$$

where P_s' is the modified squash load of the cross-section. An approximate value for M_{y3} can be obtained by interpolating between the case of $a_1 = T$ (as given in Section 2.8.1) and $a_1 = 0$ as follows:

$$M_{y3} = M_{13} R_c
 \tag{2.37b}$$

where $R_c = (P_s' - P) / (P_s' - P_{13})$ (2.37c)

and $P_{13} \leq P \leq P_s'$ (2.37d)

2.9 Notes On The Use Of The Formulae Presented In This Chapter

In using the formulae given in this chapter and in Appendices 1 and 2, it is essential to avoid numerical instability which arises as a result of using a computer. The causes of numerical instability are identified here and remedial measures are proposed as follows:

1. At the attainment of the ultimate yield moment of a cross-section, the depth of the elastic core becomes very small for the elastic-strain-hardened material and zero for the elastic-perfectly-plastic material leading to excessively-large and infinite curvatures respectively. These levels of curvatures must be avoided by computing curvatures using a specified, very low, non-zero, positive value for the depth of the elastic core (say 1mm to 10mm depending on the desired level of accuracy). However, if such a selected value is found to cause numerical instability, then a slightly higher value than that value should be tried.

2. These formulae are not applicable to the case of a zero value for the axial force. Thus, a minimum, non-zero, positive value for this force (say 1.0kN) must be specified.

2.10 Applications Of The Formulae Presented In This Chapter

The first illustration of the formulae derived above involves the determination of the moment-curvature-axial force relationships for an I-shaped cross-section having the following dimensions:

$$H = 310.4 \text{ mm}$$

$$B = 125.2 \text{ mm}$$

$$T = 14.0 \text{ mm}$$

$$t = 8.9 \text{ mm}$$

The material is structural mild steel having the following properties:

$$E = 210.0 \text{ kN/mm}^2$$

$$\sigma_y = 0.25 \text{ kN/mm}^2$$

Allowance for strain-hardening is made by adopting the following values for the strain-hardening constants:

$$A_s = 40.0$$

$$B_s = 1.1$$

Also, the squash load ratios employed are 0.001, 0.2, 0.4 and 0.6.

The second illustration of the formulae derived above involves the determination of moment-curvature-axial force relationships for a rectangular cross-section having the following dimensions:

$$H = 310.4 \text{ mm}$$

$$B = 29.0 \text{ mm}$$

The depth of the cross-section was chosen to match that of the I-shaped cross-section and the width of the cross-section was chosen to give an ultimate yield moment close to that for the I-shaped cross-section in order to highlight the importance of shape of cross-section in inelastic behaviour. All procedures and material properties are the same as those employed for the I-shaped cross-section.

Results

The yield moment ratios and moment-curvature-axial force relationships are given in Table 2.1 and Fig. 2.10 respectively for the I-shaped cross-section and in Table 2.2 and Fig. 2.11 respectively for the rectangular cross-section. It can be seen from these results that

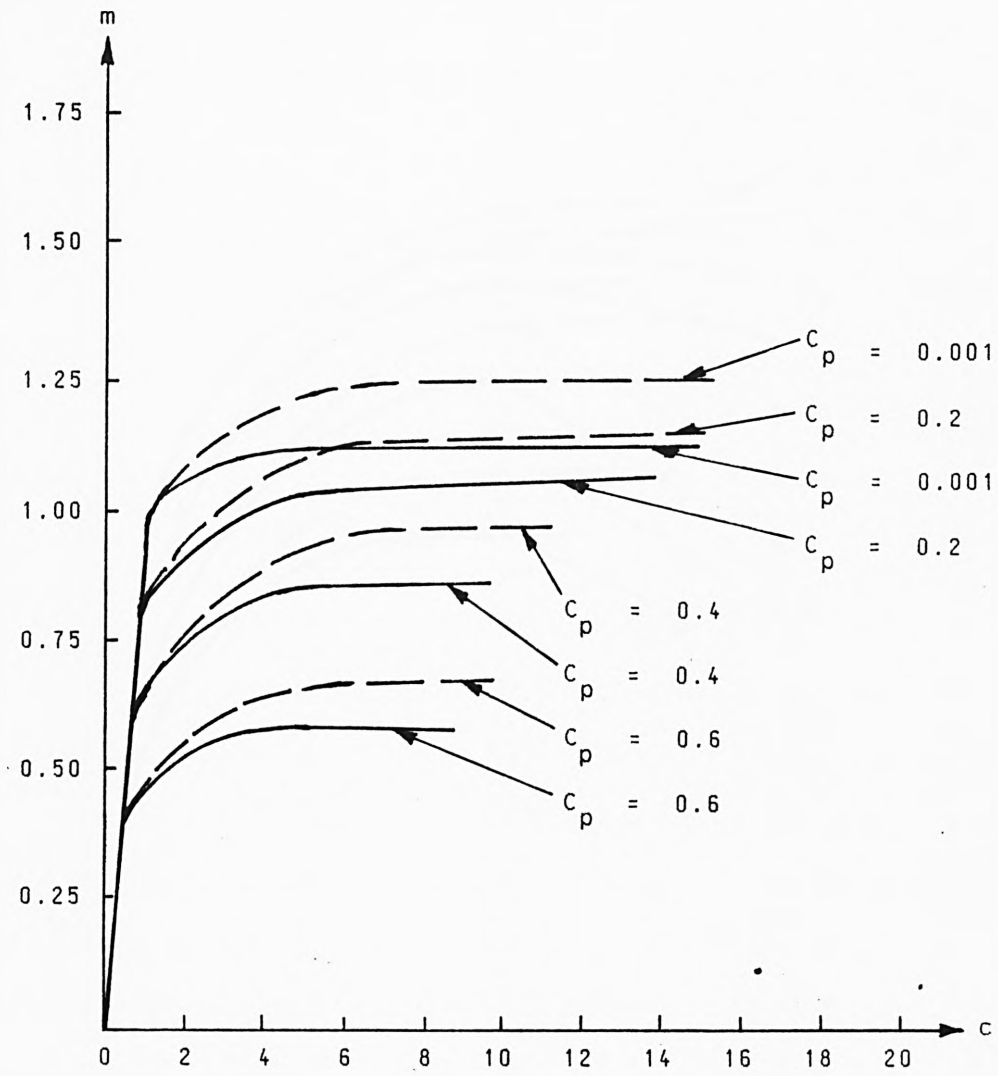
the increasing axial compressive force causes reductions in the values of the yield moments while strain-hardening has the beneficial effect of increasing the values of the intermediate and ultimate yield moments for the cross-section. Also, it can be deduced from Tables 2.1 and 2.2 that these cross-sections have reasonably close ultimate yield moments but widely different first yield moments for the same values of the axial force due mainly to their different ultimate yield moment ratios which, in turn, depend on the shape and dimensions of each cross-section. It follows, therefore, that the correct yield moment ratios for cross-sections should be adopted in inelastic analysis of structures in order to determine the end of elastic behaviour and the onset of inelastic behaviour. This can only be accomplished by accounting for the true shape of cross-section of a member in the analysis.

Table 2.1 Yield Moment Ratios For The I-Shaped Cross-Section

C_p	P (kN)	M_{y1} ($\times 10^6$) (kN.mm)	Yield Moment Ratios			
			Elastic-Perfectly-Plastic Material		Elastic-Strain-Hardened Material	
			R_a	R_b	R_a	R_b
0.001	1.51	0.151	1.002	1.155	1.002	1.254
0.2	300.95	0.121	1.283	1.358	1.285	1.469
0.4	601.90	0.091	1.379	1.474	1.465	1.659
0.6	902.85	0.060	1.381	1.477	1.594	1.743

Table 2.2 Yield Moment Ratios For The Rectangular Cross-Section

			Yield Moment Ratios			
			Elastic-Perfectly-Plastic Material		Elastic-Strain-Hardened Material	
C_p	P (kN)	M_{y1} ($\times 10^6$) (kN.mm)	R_a	R_b	R_a	R_b
0.001	2.25	0.116	1.002	1.502	1.002	1.600
0.2	450.08	0.093	1.400	1.800	1.400	1.915
0.4	900.16	0.070	1.800	2.100	1.801	2.271
0.6	1350.24	0.047	2.120	2.400	2.206	2.712



$$m = M/[M_{y1}]_{p0}$$

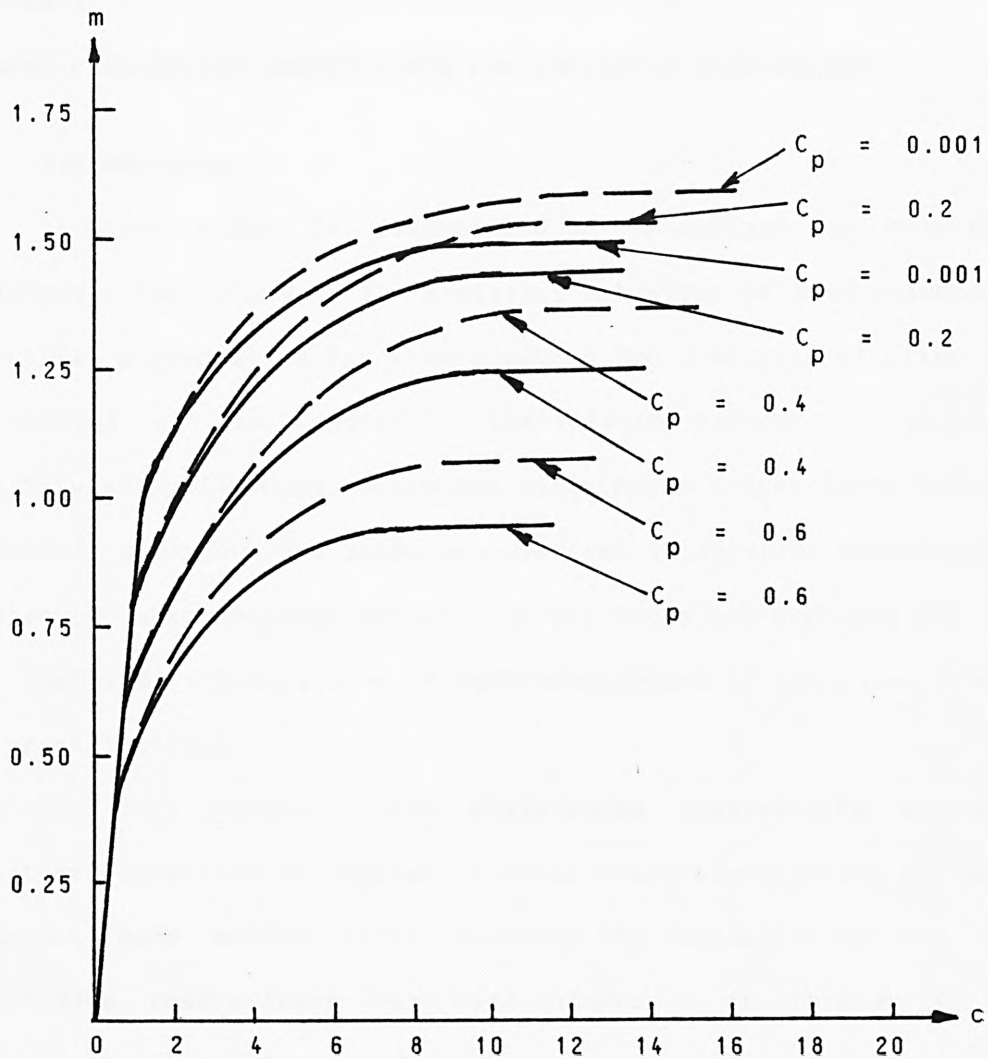
$$c = \psi/\psi_{y1}$$

where $[M_{y1}]_{p0}$ is the first yield moment for $C_p = 0.001$

————— denotes curve for elastic-perfectly-plastic material

- - - - - denotes curve for elastic-strain-hardened material

Fig. 2.10 M- ψ -P Relationships For The I-Shaped Cross-Section



$$m = M/[M_{y1}]_{p0}$$

$$c = \psi/\psi_{y1}$$

where $[M_{y1}]_{p0}$ is the first yield moment for $C_p = 0.001$

————— denotes curve for elastic-perfectly-plastic material

- - - - - denotes curve for elastic-strain-hardened material

Fig. 2.11 M- ψ -P Relationships For The Rectangular Cross-Section

CHAPTER 3

TANGENT FLEXIBILITY COEFFICIENTS FOR INELASTIC BEAM-COLUMNS

3.1 Introduction

A plane frame is essentially an assemblage of beam-columns. Therefore, the study of the inelastic behaviour of beam-columns is an essential prerequisite for investigating the stability of plane frames. As pointed out in Chapter 1, the existing methods of plane frame stability analysis which employ the distributed inelasticity concept of structural behaviour are based on numerical integration techniques, the accuracy of which depends not only on the technique employed but also on the number of sub-divisions of each beam-column of the plane frame and its cross-sections.

In this chapter, the **distributed inelasticity concept** of structural behaviour is applied to metal beam-columns using the proposed **inelastic zone method**. This involves the derivation of the **tangent flexibility coefficients** for beam-columns. In Chapter 4, these coefficients will be employed in obtaining the **tangent stiffness coefficients** for beam-columns for use in the stability analysis of plane frames by the stiffness method.

3.2 Assumptions

In addition to the assumptions made in Chapter 2, the following assumptions are now made:

1. The beam-column can be represented entirely by its centre-line for analytical purposes.

This is valid for structural members that can be classified as shallow members (that is, the ratio of the

length of a member to its depth is greater than, say, six).

2. The beam-column is adequately restrained against lateral-torsional buckling and local buckling of the plate elements of its cross-section in the case of an I-shaped cross-section.

This implies that out-of-plane displacements for the beam-column are not allowed or are negligible. The restraints required to justify this assumption are, however, not included in the analysis.

3. The bending moments are applied about one principal axis of the cross-section of the beam-column.

This implies that the beam-column is constrained to displace in the plane of the frame.

4. The influence of shear deformations is small and, therefore, neglected.

This permits the use of the ordinary theory of bending.

5. Directions of applied loads do not change on account of nodal displacements and rotations.

6. The beam-column loads are concentrated at the ends of the beam-column and lie in the plane of the frame.

Thus, uniformly-distributed loads on the beam-column are replaced by their statical, concentrated equivalents.

7. There is no gross distortion or deformation of the cross-

sectional dimensions of the beam-column at any load level.

8. The maximum bending moments occur at the ends of the beam-column resulting in the beam-column bending in either single or double curvature. Accordingly, the inelastic zones start from one end or both ends of the beam-column and spread inwards along the beam-column.

Thus, for a beam-column bent in single curvature and likely to have its maximum bending moment along its length, a node should be inserted at its mid-span or at its likely position of maximum bending moment.

9. The beam-column is prismatic throughout its length.

However, a non-prismatic beam-column can be simulated as a number of equivalent prismatic beam-columns for analysis.

10. Axial deformations due to curvature (known as "bowing") are too small in comparison with the beam-column length and are, therefore, neglected.

11. The displacements are small so that the curvature at a cross-section can be represented by the second derivative of the displacement, y , of the cross-section located at a distance, x , from the end of the beam-column as follows:

$$\psi = d^2y/d^2x \quad (3.1)$$

This is a reasonable assumption widely adopted in structural analysis.

12. Forces acting in the directions of the positive member axes and anti-clockwise moments and rotations are of positive signs.

3.3 Basic Principles

Under elastic conditions, the cross-sections of a beam-column experience the **elastic stress-distribution diagram** shown in Fig. 2.2a. As inelastic conditions set in due to increases in either the applied end moments or the applied axial load, the absolute value of the bending moment at an end cross-section becomes greater than the first yield moment, M_{y1} , of the cross-section. A **plastic or strain-hardened zone** appears along the beam-column and co-exists with the **elastic zone** in the remainder of the beam-column. Further increases of the absolute value of the bending moment at this end or increases in the applied axial load cause the plastic or strain-hardened zone to spread inwards into the beam-column. The portion of the beam-column over which this plastic or strain-hardened zone has spread experiences the **primary yield stress distribution diagram** (Fig. 2.2b) for its cross-sections while the remaining portion of the beam-column retains the elastic stress distribution diagram for its cross-sections. These portions of the beam-column are classified as the **inelastic and elastic zones** respectively. The actual stress intensities vary from cross-section to cross-section following the bending moment distribution along the beam-column.

As the absolute value of the end bending moment becomes greater than the intermediate yield moment, M_{y2} , of the cross-section, the plastic or strain-hardened zone spreads further inwards into the beam-column causing further reductions of the length of the elastic zone and,

now, giving rise to an inelastic zone along the beam-column containing the **secondary yield stress distribution diagram** (Fig. 2.2c) for its cross-sections. Thus, when a beam-column is loaded by a given combination of axial force and end bending moments, up to failure, various combinations of elastic and inelastic zones can be present in the beam-column for each load combination. The maximum number of such zone combination types is the square of the number of the distinct stress distribution diagrams (that is, nine using the three stress distribution diagrams of Fig. 2.2). It is also evident that the absolute value of the bending moment at each **zone intersection point** must be equal to either M_{y1} or M_{y2} and that the absolute value of the maximum bending moment at an end of a beam-column must not be greater than the ultimate yield moment, M_{y3} , of the cross-section.

The various possible zone combination types are given in Tables 3.1 (types 1 to 9 inclusive) and 3.2 (types 10 to 18 inclusive) for beam-columns bent in double curvature and single curvature respectively.

From Tables 3.1 and 3.2, it can be seen that the depth of the elastic core for the elastic zone is constant and equal to the depth of the cross-section whereas that of an inelastic zone is variable and diminishes as the bending moment increases in value within the zone. This leads to a constant flexural rigidity for the elastic zone and a variable flexural rigidity for an inelastic zone as evidenced by the slopes of the $M-\psi-P$ graphs of Figs. 2.10 and 2.11. Indeed, as the depth of the elastic core tends to zero, the curvature of the cross-section tends to infinity. Thus, the presence of an inelastic zone in a beam-column causes reductions in the flexural stiffness of the beam-column culminating in zero flexural stiffness at failure. On the other hand, the flexural stiffness of an inelastic beam-column depends largely on

Table 3.1 Zone Combination Types For A Beam-Column Bent In Double Curvature

Type	Zone Combination And Bending Moment Diagrams	Remarks
1		$0 \leq M_1 \leq M_{y1}$ $0 \leq M_2 \leq M_{y1}$
2		$M_{y1} < M_1 \leq M_{y2}$ $0 < M_3 \leq M_{y1}$ $ M_2 = M_{y1} = R_2 M_1 $
3		$0 < M_1 \leq M_{y1}$ $M_{y1} < M_3 \leq M_{y2}$ $ M_2 = M_{y1} = R_2 M_3 $
4		$M_{y2} < M_1 \leq M_{y3}$ $0 < M_4 \leq M_{y1}$ $ M_2 = M_{y2} = R_2 M_1 $ $ M_3 = M_{y1} = R_3 M_1 $
5		$0 < M_1 \leq M_{y1}$ $M_{y2} < M_4 \leq M_{y3}$ $ M_2 = M_{y1} = R_2 M_4 $ $ M_3 = M_{y2} = R_3 M_4 $

Table 3.1 (Continued)

Type	Zone Combination And Bending Moment Diagrams	Remarks
6		$M_{y1} < M_1 \leq M_{y2}$ $M_{y1} < M_4 \leq M_{y2}$ $ M_2 = M_{y1} = R_2 M_1 $ $ M_3 = M_{y1} = R_3 M_4 $
7		$M_{y2} < M_1 \leq M_{y3}$ $M_{y1} < M_5 \leq M_{y2}$ $ M_2 = M_{y2} = R_2 M_1 $ $ M_3 = M_{y1} = R_3 M_1 $ $ M_4 = M_{y1} = R_4 M_5 $
8		$M_{y1} < M_1 \leq M_{y2}$ $M_{y2} < M_5 \leq M_{y3}$ $ M_2 = M_{y1} = R_2 M_1 $ $ M_3 = M_{y1} = R_3 M_5 $ $ M_4 = M_{y2} = R_4 M_5 $
9		$M_{y2} < M_1 \leq M_{y3}$ $M_{y2} < M_6 \leq M_{y3}$ $ M_2 = M_{y2} = R_2 M_1 $ $ M_3 = M_{y1} = R_3 M_1 $ $ M_4 = M_{y1} = R_4 M_6 $ $ M_5 = M_{y2} = R_5 M_6 $

Table 3.2 Zone Combination Types For A Beam-Column Bent In Single Curvature

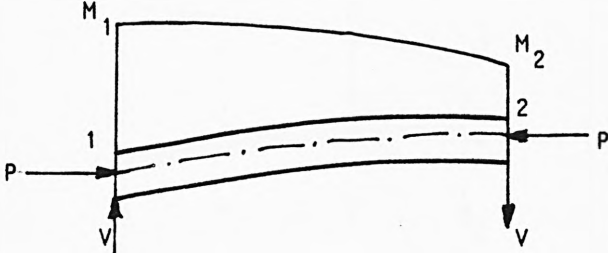
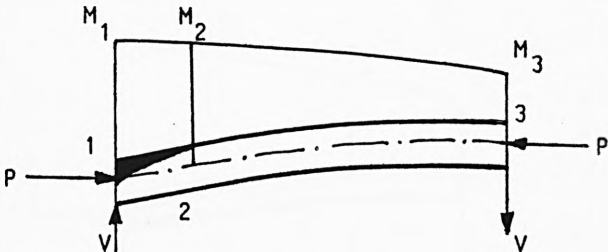
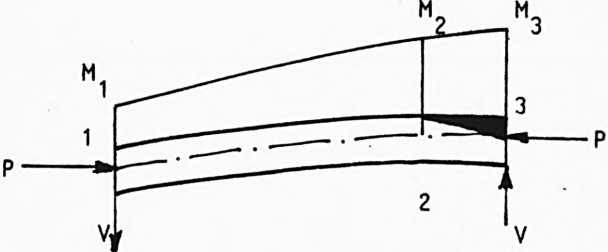
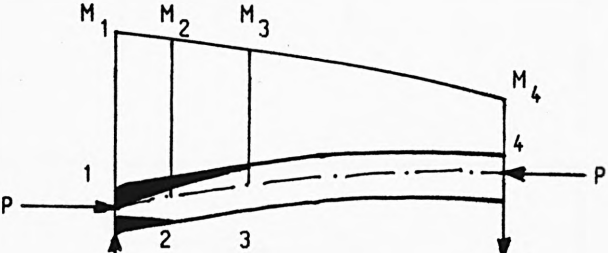
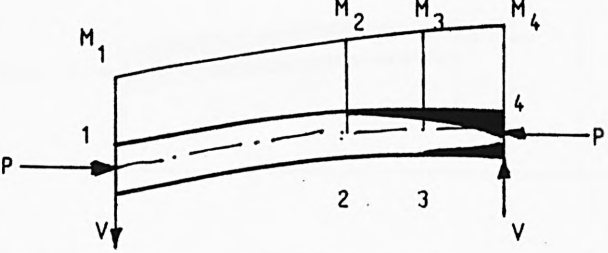
Type	Zone Combination And Bending Moment Diagrams	Remarks
10		<p>Similar to zone combination type 1 with the sign of M_2 reversed.</p>
11		<p>Similar to zone combination type 2 with the sign of M_3 reversed.</p>
12		<p>Similar to zone combination type 3 with the signs of M_2 and M_3 reversed.</p>
13		<p>Similar to zone combination type 4 with the sign of M_4 reversed.</p>
14		<p>Similar to zone combination type 5 with the signs of M_2, M_3 and M_4 reversed.</p>

Table 3.2 (Continued)

Type	Zone Combination And Bending Moment Diagrams	Remarks
15		$M_{y1} < M_1 \leq M_{y2}$ $M_{y1} < M_4 \leq M_{y2}$ $ M_2 = M_1 + G_2 (M_4 - M_1)$ $ M_3 = M_1 + G_3 (M_4 - M_1)$ $0 < G_2 < G_3 < 1.0$
16		$M_{y2} < M_1 \leq M_{y3}$ $M_{y1} < M_4 \leq M_{y2}$ $M_2 = M_1 + G_2 (M_4 - M_1)$ $M_3 = M_{y2} \text{ for } M_4 < M_{y2} \text{ or}$ $M_3 = M_1 + G_3 (M_4 - M_1)$ $0 < G_2 < G_3 < 1.0$
17		$M_{y1} \leq M_1 < M_{y2}$ $M_{y2} < M_4 \leq M_{y3}$ $M_2 = M_{y2} \text{ for } M_1 < M_{y2} \text{ or}$ $M_2 = M_1 + G_2 (M_4 - M_1)$ $M_3 = M_1 + G_3 (M_4 - M_1)$ $0 < G_2 < G_3 < 1.0$
18		$M_{y2} < M_1 \leq M_{y3}$ $M_{y2} < M_4 \leq M_{y3}$ $M_2 = M_1 + G_2 (M_4 - M_1)$ $M_3 = M_1 + G_3 (M_4 - M_1)$ $0 < G_2 < G_3 < 1.0$

the elastic core remaining in the beam-column at each load level. It is, therefore, essential to determine the **moment-rotation-axial force relationships** for a beam-column at all load levels up to failure.

The moment-rotation-axial force (M- θ -P) relationships for an inelastic beam-column are derived by employing the exact expression for the deflection curve for an elastic beam-column to represent the deflection curve for the elastic zone and a similar expression, which additionally satisfies the curvature boundary conditions, for an inelastic zone. In this way, approximations to the deflected shape are confined to the inelastic zones thus minimizing error in analysis. The use of a curve similar to that for the elastic zone for an inelastic zone simplifies the computations. Using these curves, rotation compatibility at each zone intersection point is satisfied in order to obtain a sufficient number of equations for determining the deflections of the zone intersection points in terms of, among other things, the lengths of the zones. Equilibrium of shear forces is satisfied at each zone intersection point in order to obtain the lengths of the zones in terms of, among other things, the deflections of the zone intersection points. The solution of the relevant equations is obtained by iteration. In general, the number of necessary equations increases with the number of inelastic zones along the beam-column and the complexity of the computations increases accordingly. As soon as the lengths of the zones and the deflections of the zone intersection points become known, all other quantities concerning the beam-column behaviour (for example, the end rotations) become known. Hence, by employing various values of the end bending moments and the axial force, the M- θ -P relationships for the beam-column can be derived. The above procedures can be applied to a prismatic beam-column that is straight or that has a

slight initially-curved profile.

The M- θ -P relationships so determined are used to derive the tangent flexibility (or influence) coefficient, defined as the displacement of an end of a beam-column due to a unit value of the corresponding force at either end of the beam-column. This is accomplished by writing the known limiting bending moment at each zone intersection point in terms of the absolute value of the bending moment at the end of the beam-column at which the corresponding inelastic zone started spreading and arranging the equations for the end rotations of the beam-column such that each end rotation is equated to the sum of the rotation due to the relative end displacements and the product of each end bending moment and a coefficient which becomes the flexibility coefficient for that end. For an analysis by the stiffness method, these flexibility coefficients must be employed in obtaining the tangent stiffness coefficients for each beam-column. This is accomplished by re-arranging the resulting equations such that the end bending moments and shear forces are written in terms of the remaining quantities. Furthermore, the tangent axial stiffness of each beam-column must be included in the analysis since three degrees of freedom are required at each node of a plane frame. This is accomplished by employing the full area of the cross-section for the elastic zone and a reduced area of cross-section, based on the remaining **elastic core**, for the inelastic zones in computing the tangent axial flexibility coefficient for the entire beam-column and inverting this coefficient to obtain its tangent axial stiffness coefficient.

In general, the resulting tangent stiffness matrix for the inelastic beam-column is asymmetric owing to the presence and

distribution of inelastic zones in the beam-column whereas that of an elastic beam-column is symmetric.

The principle of superposition of separate load effects is not employed in determining these tangent stiffnesses for the inelastic beam-column since the length of each zone must depend on the total shear force distribution along the beam-column. Consequently, although incremental loading is used in the analysis, the total joint displacements and member forces are calculated for each set of total loads on the frame by initially assuming elastic behaviour and then searching for the presence of inelastic zones. By considering several loadings on the frame, the stable equilibrium path for the frame can be traced. Failure results when the frame stiffness vanishes. This is detected when a solution of the governing equations cannot be obtained within a reasonable number of iterations. The corresponding load on the frame is, therefore, greater than the failure load of the frame and the failure load is taken to lie between this load and the previous load at which a convergent solution of the governing equations was obtained.

Based on the above principle of the inelastic zone method, the relevant tangent flexibility coefficients will now be derived for the various zone combination types for a beam-column, beginning with the elastic beam-column as presented in Section 3.4. Zone Combination Type 1 shown in Table 3.1 is chosen for this purpose. A general procedure for deriving the relevant coefficients for an inelastic beam-column, showing all steps of analysis, is outlined in Section 3.5. Zone Combination Type 6 shown in Table 3.1 is chosen for this purpose. Based on this general procedure, the relevant formulae for the tangent flexibility coefficients for the remaining zone combination types given in Tables 3.1 and 3.2 are presented in Section 3.5.

The derivation of the tangent stiffness coefficients for a beam-column from these tangent flexibility coefficients is given in Chapter 4 where the stiffness method is employed for the stability analysis of plane frames.

3.4 Flexibility Coefficients For An Elastic Beam-Column

Fig. 3.1 shows zone combination type 1 which is an elastic beam-column bent in double curvature.

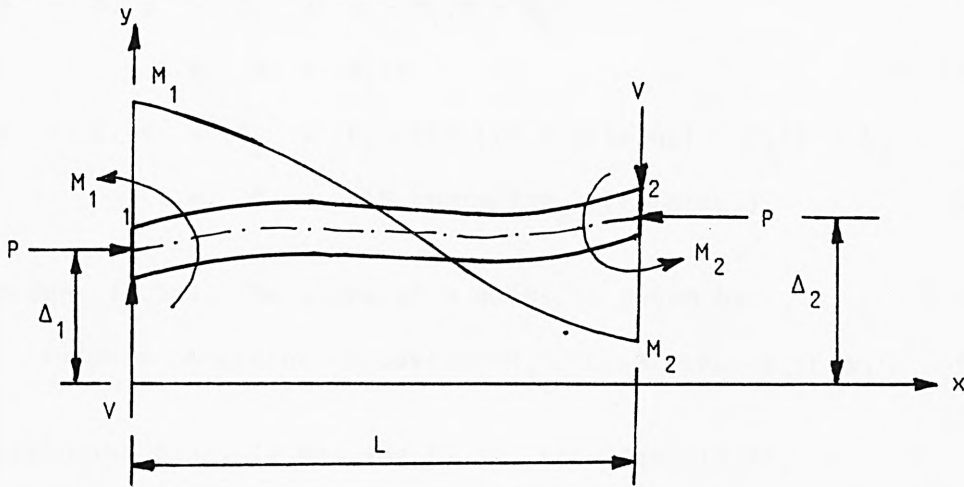


Fig. 3.1 Zone Combination Type 1

The shear force, V and the bending moment, M_x , at a point whose distance from the y -axis is x are given by

$$V = [M_1 + M_2 + P(\Delta_2 - \Delta_1)]/L \quad (3.2)$$

$$\begin{aligned} M_x &= M_1 - V \cdot x + P(y - \Delta_1) \\ &= M_1(1 - x/L) - M_2(x/L) + P[y - \Delta_1 - (\Delta_2 - \Delta_1)x/L] \end{aligned} \quad (3.3)$$

The curvature at any point is given by

$$y'' = d^2y/dx^2 = -M_x/(EI_z) \quad (3.4a)$$

$$\text{i.e. } y'' = [-M_1(1 - x/L) + M_2(x/L) - P\{y - \Delta_1(1 - x/L) - \Delta_2(x/L)\}]/(EI_z) \quad (3.4b)$$

$$\text{i.e. } y'' + Py/(EI_z) = [-M_1(1-x/L) + M_2(x/L) + P\{\Delta_1(1-x/L) + \Delta_2(x/L)\}]/(EI_z) \quad (3.4c)$$

The solution of this second-order differential equation is given by

$$y = A\cos(nx) + B\sin(nx) - M_1(1-x/L)/P + M_2(x/L)/P + \Delta_1(1-x/L) + \Delta_2(x/L) \quad (3.5a)$$

$$\text{where } n = [P/(EI_z)]^{1/2} \quad (3.5b)$$

and A and B are arbitrary constants determined by satisfying deflection boundary conditions thus:

$$\text{at } x = 0, y = \Delta_1 = A - M_1/P + \Delta_1 \quad (3.6a)$$

$$\text{i.e. } A = M_1/P \quad (3.6b)$$

$$\text{at } x = L, y = \Delta_2 = M_1\cos(nL)/P + B\sin(nL) + M_2/P + \Delta_2 \quad (3.7a)$$

$$\text{i.e. } B = -[M_1\cos(nL) + M_2]/[P\sin(nL)] \quad (3.7b)$$

From Eqn. (3.5a), the slope at a point is given by:

$$y' = dy/dx = -A\sin(nx) + B\cos(nx) + M_1/(PL) + M_2/(PL) - \Delta_1/L + \Delta_2/L \quad (3.8)$$

Substituting Eqns. (3.6b) and (3.7b) into Eqn. (3.8),

$$\begin{aligned} y' &= -M_1n\sin(nx)/P - n\cos(nx)[M_2 + M_1\cos(nL)]/[P\sin(nL)] \\ &\quad + M_1/(PL) + M_2/(PL) - \Delta_1/L + \Delta_2/L \\ &= M_1\{[1/L - n(\sin(nx) + \cos(nL)\cos(nx))/\sin(nL)]\}/P \\ &\quad + M_2\{[1/L - n\cos(nx)/\sin(nL)]\}/P - \Delta_1/L + \Delta_2/L \end{aligned} \quad (3.9a)$$

$$\begin{aligned} \text{at } x = 0, y' = \theta_1 &= M_1\{[1/L - n\cos(nL)/\sin(nL)]\}/P \\ &\quad + M_2\{[1/L - n/\sin(nL)]\}/P \\ &\quad + \Delta_1[-1/L] + \Delta_2[1/L] \\ &= M_1\alpha_{11} + M_2\alpha_{12} + (\Delta_2 - \Delta_1)/L \end{aligned} \quad (3.9b)$$

$$\begin{aligned} \text{at } x = L, y' = \theta_2 &= M_1\{[1/L - n(\sin(nL) + \cos^2(nL))/\sin(nL)]\}/P \\ &\quad + M_2\{[1/L - n\cos(nL)/\sin(nL)]\}/P \\ &\quad + \Delta_1[-1/L] + \Delta_2[1/L] \\ &= M_1\alpha_{21} + M_2\alpha_{22} + (\Delta_2 - \Delta_1)/L \end{aligned} \quad (3.9c)$$

$$\text{where } \alpha_{11} = [1/L - n/\tan(nL)]/P \quad (3.9d)$$

$$\alpha_{12} = [1/L - n/\sin(nL)]/P \quad (3.9e)$$

$$\begin{aligned} \alpha_{21} &= [1/L - n(\sin^2(nL) + \cos^2(nL))/\sin(nL)]/P \\ &= [1/L - n/\sin(nL)]/P \end{aligned} \quad (3.9f)$$

$$\alpha_{22} = [1/L - n/\tan(nL)]/P \quad (3.9g)$$

These coefficients are the flexural flexibility coefficients for the elastic beam-column. It can be seen that they are entirely independent of the values of the end bending moments. In other words, they are constant for the given value of the axial force and for all values of end bending moments less than, or equal to, the first yield moment of the cross-section. The axial flexibility coefficient for the beam-column is given by

$$\alpha_a = L/(AE) \quad (3.9h)$$

Also, it can be observed that

$$\alpha_{11} = \alpha_{22} \quad (3.10a)$$

$$\alpha_{12} = \alpha_{21} \quad (3.10b)$$

The Deflection Curve

The deflected shape of the elastic beam-column is given by Eqn. (3.5a). This equation can be written as

$$y = y_c + y_d \quad (3.11a)$$

where y_c is the deflection component due to curvature and is given by

$$y_c = A\cos(nx) + B\sin(nx) - M_1(1-x/L)/P + M_2(x/L)/P \quad (3.11b)$$

and y_d is the deflection component due to end displacements and is given by

$$y_d = \Delta_1(1-x/L) + \Delta_2(x/L) \quad (3.11c)$$

Also, the variation of slope along the beam-column is given by Eqn. (3.8) which can be written as

$$y' = y'_c + y'_d \quad (3.12a)$$

$$\begin{aligned} \text{where } y'_c = & M_1 \left[\frac{1}{L} - n \frac{\sin(nx) + \cos(nx)/\tan(nL)}{\sin(nL)} \right] / P \\ & + M_2 \left[\frac{1}{L} - n \cos(nx) / \sin(nL) \right] / P \end{aligned} \quad (3.12b)$$

$$\text{and } y'_d = (\Delta_2 - \Delta_1) / L \quad (3.12c)$$

The subscripts c and d represent "due to curvature" and "due to end displacements" respectively.

These deflection and rotation components are shown in Fig. 3.2 where the original, undeformed, straight length, 1^0-2^0 , is transformed, after deformation, to the curved profile $1-M-N-2$.

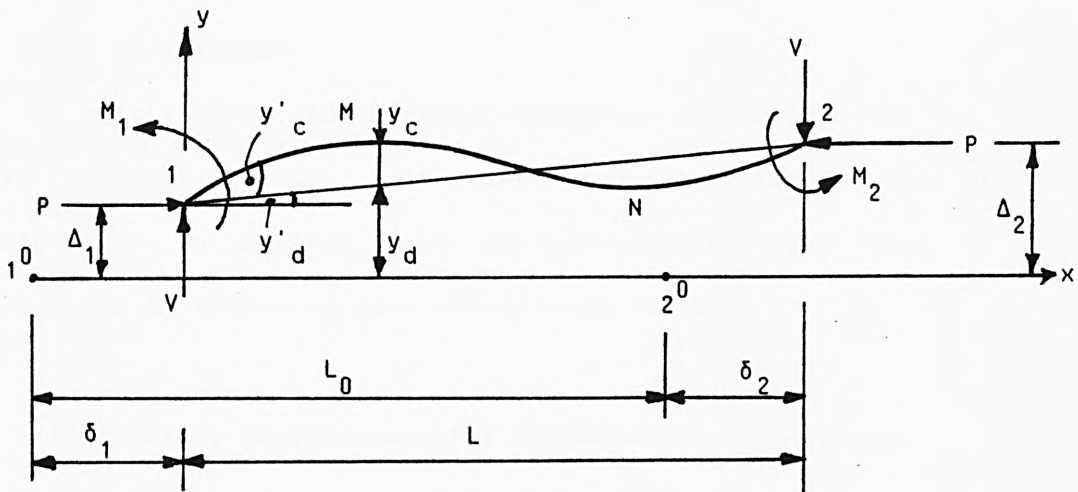


Fig. 3.2

This transformation is due to a

- (a) net displacement, $(\delta_2 - \delta_1)$, along the x-axis,
- (b) displacement, Δ_1 , along the y-axis,
- (c) rigid-body rotation, $[(\Delta_2 - \Delta_1) / L]$, and a
- (d) rotation due to curvature caused by the end bending moments, M_1 and M_2 .

So far, only an axial compressive force has been considered. For an axial tensile force, a negative value is assigned to P in Eqns. (3.2) to (3.4) inclusive. The well-known solution of the resulting second-order differential equation is given by

$$y = A \cosh(nx) + B \sinh(nx) - M_1[(1-x/L)/P] + M_2[(x/L)/P] + \Delta_1(1-x/L) + \Delta_2(x/L) \quad (3.13)$$

where P has a negative sign and hyperbolic functions replace their trigonometric equivalents in Eqn. (3.5a). Hence, from Eqn. (3.8), it follows that

$$y' = A n \sinh(nx) + B n \cosh(nx) - M_1/(PL) + M_2/(PL) - \Delta_1/L + \Delta_2/L \quad (3.14)$$

Note the positive sign for $A n \sinh(nx)$ in Eqn. (3.14) and the negative sign for $A n \sinh(nx)$ in Eqn.(3.8). All other quantities are obtained as for axial compression.

In what follows, the relevant equations are derived for the case of axial compression only. The relevant equations for the case of axial tension can be derived from the equations for the case of axial compression by employing Eqns. (3.13) and (3.14).

3.5 Flexibility Coefficients For An Inelastic Beam-Column

The flexibility coefficients derived in this section apply to a straight beam-column. Those for an initially-curved beam-column are derived in Section 3.6.

3.5.1 Derivation Of The Flexibility Coefficients

Fig. 3.3 shows zone combination type 6 which has inelastic zones spreading from both ends of the beam-column as also shown in Table 3.1. The three zones and four points which define the boundaries of the zones are numbered sequentially from the left-hand end of the beam-column.

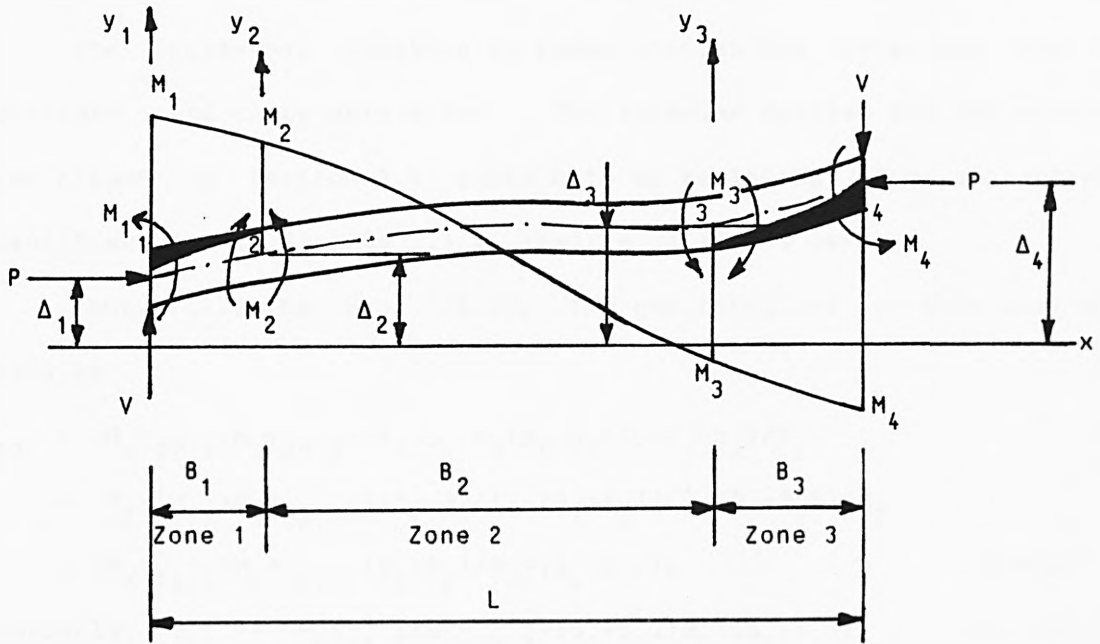


Fig. 3.3 Zone Combination Type 6

Also, the length of a typical zone, m , is denoted as B_m and the total displacement of a zone intersection point, i , from the x -axis of the beam-column is denoted as Δ_i whereas the displacement of the zone intersection point due to curvature is denoted as D_i (see Fig. 3.4). Zones 1 and 3 are the inelastic zones while zone 2 is the elastic zone.

In order to simplify the computations, the approach adopted in Section 3.4 for the elastic beam-column will be adopted here by taking the origin of co-ordinates for each zone at its left-hand end as shown in Fig. 3.3. Also, following the numbering system adopted, the identification number for a zone is the same as the number for the left-hand end of the zone. Thus, the flexural flexibility coefficients for the zone, m , are written as

$$\gamma_{mm,m'} \quad \gamma_{m,m+1,m'} \quad \gamma_{m+1,m,m'} \quad \text{and} \quad \gamma_{m+1,m+1,m'}$$

The constant shear force in this zone is given by

$$V = [M_2 + M_3 - P\{D_2 + D_3 + B_1(\Delta_4 - \Delta_1)/L - (B_1 + B_2)(\Delta_4 - \Delta_1)/L\}]/B_2 \quad (3.16a)$$

where $V = [M_1 + M_4 + P(\Delta_4 - \Delta_1)]/L \quad (3.16b)$

Thus, the length of the zone is given by

$$B_2 = [M_2 + M_3 - P(D_2 + D_3)]/[(M_1 + M_4)/L] \quad (3.16c)$$

and is, therefore, independent of the end displacements, Δ_1 and Δ_4 , of the beam-column.

The Inelastic Zone 1

Since the exact equation for the deflection curve of an inelastic beam-column is unknown, as pointed out in Chapter 1, an approximate equation, based on Eqn. (3.5a) for an elastic beam-column, is proposed here for this zone as follows:

$$y = A\cos(m_1x) + B\sin(q_1x) - M_1[(1-x/B_1)/P] - M_2(x/B_1)/P + \Delta_1(1-x/B_1) + \Delta_2(x/B_1) \quad (3.17)$$

where the arbitrary constants, A and B, satisfy the deflection conditions and m_1 and q_1 satisfy the curvature conditions at the ends of the zone.

The validity and limitations of Eqn. (3.17) are established in a Parametric Study given in Appendix 5. This Study shows that Eqn. (3.17) is accurate for the ratio, $C_1 = m_1/q_1 = 1.0$ and that any error increases as C_1 increases above unity and diminishes as the rotation, $(\Delta_2 - \Delta_1)/B_1$, increases. This Study also shows that Eqn. (3.17) is a reasonable representation of the unknown deflection curve for an inelastic zone of a beam-column since it requires the deflections of all zone intersection points along the beam-column to be taken into account in all computations of tangent flexibility coefficients for the beam-column.

The Arbitrary Constants, m_1 And q_1

Let ψ_i be curvature at point i . For the elastic zone 2, we have

$$\psi_i = -M_i / (EI_z) \quad (3.18a)$$

$$\text{and } n = \sqrt{[P / (EI_z)]} \quad (3.18b)$$

Eqn. (3.18b) can be written as

$$n = \sqrt{[M_i / (EI_z)](P/M_i)} = \sqrt{[|\psi_i| P / M_i]} \quad (3.18c)$$

Based on this analogy, the values of m_1 and q_1 are given by:

$$m_1 = \sqrt{(|\psi_1| P / M_1)} \text{ for the left-hand end 1} \quad (3.19a)$$

$$q_1 = \sqrt{(|\psi_2| P / M_2)} \text{ for the right-hand end 2} \quad (3.19b)$$

The Arbitrary Constants, A And B

Following Eqns. (3.6b) and (3.7b),

$$A = M_1 / P \quad (3.20a)$$

$$\text{and } B = -[M_1 \cos(m_1 B_1) - M_2] / [P \sin(q_1 B_1)] \quad (3.20b)$$

Tangent Flexural Flexibility Coefficients For Zone 1

Following Eqns. (3.9), (3.15) and (3.16), the end rotations for this zone are

$$\theta_1 = \theta_{12} = M_1 \gamma_{11,1} - M_2 \gamma_{12,1} + D_2 / B_1 + (\Delta_4 - \Delta_1) / L \quad (3.21a)$$

$$\theta_{21} = M_1 \gamma_{21,1} - M_2 \gamma_{22,1} + D_2 / B_1 + (\Delta_4 - \Delta_1) / L \quad (3.21b)$$

and its length is

$$B_1 = [M_1 - M_2 + P D_2] / [(M_1 + M_4) / L] \quad (3.21c)$$

where its tangent flexural flexibility coefficients are given by

$$\gamma_{11,1} = [1 / B_1 - q_1 \cos(m_1 B_1) / \sin(q_1 B_1)] / P \quad (3.21d)$$

$$\gamma_{12,1} = [1 / B_1 - q_1 / \sin(q_1 B_1)] / P \quad (3.21e)$$

$$\gamma_{21,1} = [1 / B_1 - m_1 \sin(m_1 B_1) - q_1 \cos(m_1 B_1) / \tan(q_1 B_1)] / P \quad (3.21f)$$

$$\gamma_{22,1} = [1 / B_1 - q_1 / \tan(q_1 B_1)] / P \quad (3.21g)$$

where $r = \text{number of zones} + 1 = \text{node identification number for the right-hand end of the beam-column.}$

The Inelastic Zone 3

From Eqns.(3.22), the end rotations for this zone are given by

$$\theta_{34} = -M_3\gamma_{33,3} + M_4\gamma_{34,3} + D_3/B_3 + (\Delta_4 - \Delta_1)/L \quad (3.23a)$$

$$\theta_4 = \theta_{43} = -M_3\gamma_{43,3} + M_4\gamma_{44,3} + D_3/B_3 + (\Delta_4 - \Delta_1)/L \quad (3.23b)$$

Also, the length of the zone is given by

$$B_3 = [-M_3 + M_4 + PD_3] / [(M_1 + M_4)/L] \quad (3.23c)$$

or can simply be obtained from

$$B_3 = L - B_1 - B_2 \quad (3.23d)$$

The Deflection Components, D_2 And D_3 (Fig. 3.4)

Rotation compatibility at point 2 demands that

$$\theta_{23} - \theta_{21} = 0 \quad (3.24)$$

Hence, substitution of Eqns.(3.15a) and (3.21b) into Eqn.(3.24) gives

$$-M_1\gamma_{21,1} + M_2(\gamma_{22,1} + \gamma_{22,2}) + M_3\gamma_{23,2} - D_2(1/B_1 + 1/B_2) - D_3/B_2 = 0 \quad (3.25)$$

Similarly, rotation compatibility at point 3 demands that

$$\theta_{34} - \theta_{32} = 0 \quad (3.26)$$

Hence, substitution of Eqns.(3.15b) and (3.23a) into Eqn.(3.26) gives

$$M_2\gamma_{32,2} + M_3(\gamma_{33,2} + \gamma_{33,3}) - M_4\gamma_{34,3} - D_2/B_2 - D_3(1/B_2 + 1/B_3) = 0 \quad (3.27)$$

Let

$$C_2 = 1/B_1 + 1/B_2 \quad (3.28a)$$

$$C_3 = 1/B_2 + 1/B_3 \quad (3.28b)$$

$$E_2 = \gamma_{22,1} + \gamma_{22,2} \quad (3.28c)$$

$$E_3 = \gamma_{33,2} + \gamma_{33,3} \quad (3.28d)$$

This means that for a typical zone intersection point, m,

$$C_m = 1/B_{m-1} + 1/B_m \quad (3.29a)$$

$$\text{and } E_m = \gamma_{mm,m-1} + \gamma_{mm,m} \quad (3.29b)$$

Substitution of Eqns. (3.28) into Eqns. (3.25) and (3.27) and re-arranging the resulting equations in matrix form gives

$$\begin{bmatrix} C_2 & 1/B_2 \\ 1/B_2 & C_3 \end{bmatrix} \begin{Bmatrix} D_2 \\ D_3 \end{Bmatrix} = \begin{Bmatrix} F_2 \\ F_3 \end{Bmatrix} \quad (3.30a)$$

$$\text{where } F_2 = -M_1 \gamma_{21,1} + M_2 E_2 + M_3 \gamma_{23,2} \quad (3.30b)$$

$$F_3 = M_2 \gamma_{32,2} + M_3 E_3 - M_4 \gamma_{34,3} \quad (3.30c)$$

A solution of Eqn. (3.30a) in general terms is required so that the contribution of the bending moment at each end of each zone to the deflection of each zone intersection point and, hence, to the end rotations of the beam-column, can be explicitly determined. This makes the re-arrangement of the equations for the end rotations in terms of only the end moments and displacements, as required by Eqns. (3.9b) and (3.9c), possible and, therefore, leads to the determination of the flexural flexibility coefficients for the beam-column. In Appendix 4, general solutions of 2, 3 and 4 simultaneous equations are presented. These can be used for computing the required deflection components due to curvature for the zone intersection points for the various types of zone combination given in Tables 3.1 and 3.2.

Using the formulae given in Appendix 4 for the general solution of two simultaneous equations, the general solution of Eqn.(3.30a) is given by

$$\begin{aligned}
D_2 &= [Q_{11}F_2 + Q_{12}F_3]/C_2 \\
&= [M_1(-Q_{11}\gamma_{21,1}) + M_2(Q_{11}E_2 + Q_{12}\gamma_{32,2}) + M_3(Q_{11}\gamma_{23,2} + Q_{12}E_3) \\
&\quad + M_4(-Q_{12}\gamma_{34,3})]/C_2 \quad (3.31a)
\end{aligned}$$

$$\begin{aligned}
D_3 &= [Q_{21}F_2 + F_3]/F_{22} \\
&= [M_1(-Q_{21}\gamma_{21,1}) + M_2(Q_{21}E_2 + \gamma_{32,2}) + M_3(Q_{21}\gamma_{23,2} + E_3) \\
&\quad + M_4(-\gamma_{34,3})]/F_{22} \quad (3.31b)
\end{aligned}$$

The Flexibility Coefficients For The Beam-Column

As for the elastic beam-column, the end rotations for this beam-column are required in terms of its end bending moments and displacements as follows:

$$\theta_1 = M_1\alpha_{11} + M_4\alpha_{14} + (\Delta_4 - \Delta_1)/L \quad (3.32a)$$

$$\theta_4 = M_1\alpha_{41} + M_4\alpha_{44} + (\Delta_4 - \Delta_1)/L \quad (3.32b)$$

where the α coefficients are the tangent flexural flexibility coefficients for the beam-column.

Substitution of Eqn. (3.31a) into Eqn. (3.21a) gives

$$\begin{aligned}
\theta_1 &= M_1[\gamma_{11,1} - Q_{11}\gamma_{21,1}/(B_1C_2)] + M_2[-\gamma_{12,1} + (Q_{11}E_2 + Q_{12}\gamma_{32,2})/(B_1C_2)] \\
&\quad + M_3[(Q_{11}\gamma_{23,2} + Q_{12}E_3)/(B_1C_2)] + M_4[-Q_{12}\gamma_{34,3}/(B_1C_2)] \quad (3.33a)
\end{aligned}$$

Also, substitution of Eqn. (3.31b) into Eqn. (3.23b) gives

$$\begin{aligned}
\theta_4 &= M_1[-Q_{21}\gamma_{21,1}/(B_3F_{22})] + M_2[(Q_{21}E_2 + \gamma_{32,2})/(B_3F_{22})] \\
&\quad + M_3[-\gamma_{43,3} + (Q_{21}\gamma_{23,2} + E_3)/(B_3F_{22})] \\
&\quad + M_4[\gamma_{44,3} - \gamma_{34,3}/(B_3F_{22})] \quad (3.33b)
\end{aligned}$$

The next step is to eliminate M_2 and M_3 from Eqns. (3.33a) and (3.33b). This is accomplished by writing M_2 in terms of M_1 (as shown in Table 3.1) as it is associated with the inelastic zone spreading from end 1 which is brought about by M_1 being greater than the first yield moment, M_{y1} . Similarly, M_3 is written in terms of M_4 as follows:

$$M_2 = R_2 M_1 \quad (3.34a)$$

$$M_3 = R_3 M_4 \quad (3.34b)$$

where the coefficients R_2 and R_3 are related to the zone intersection points 2 and 3 respectively and are known since the bending moments are known. Substitution of Eqns. (3.34) into Eqns. (3.33) gives

$$\begin{aligned} \theta_1 = & M_1 [\gamma_{11,1} - R_2 \gamma_{12,1} + \{-Q_{11} \gamma_{21,1} + R_2 (Q_{11} E_2 + Q_{12} \gamma_{32,2})\} / (B_1 C_2)] \\ & + M_4 \{ [R_3 (Q_{11} \gamma_{23,2} + Q_{12} E_3) - Q_{12} \gamma_{34,3}] / (B_1 C_2) \} \\ & + (\Delta_4 - \Delta_1) / L \end{aligned} \quad (3.35a)$$

$$\begin{aligned} \theta_4 = & M_1 \{ [-Q_{21} \gamma_{21,1} + R_2 (Q_{21} E_2 + \gamma_{32,2})\} / (B_3 F_{22}) \} \\ & + M_4 \{ [\gamma_{44,3} - R_3 \gamma_{43,3} + \{R_3 (Q_{21} \gamma_{23,2} + E_3) - \gamma_{34,3}\} / (B_3 F_{22}) \} \\ & + (\Delta_4 - \Delta_1) / L \end{aligned} \quad (3.35b)$$

Comparing Eqns. (3.35) with Eqns. (3.32), the required tangent flexural flexibility coefficients for the beam-column are given by

$$\alpha_{11} = \gamma_{11,1} - R_2 \gamma_{12,1} + \{-Q_{11} \gamma_{21,1} + R_2 (Q_{11} E_2 + Q_{12} \gamma_{32,2})\} / (B_1 C_2) \quad (3.36a)$$

$$\alpha_{14} = \{R_3 (Q_{11} \gamma_{23,2} + Q_{12} E_3) - Q_{12} \gamma_{34,3}\} / (B_1 C_2) \quad (3.36b)$$

$$\alpha_{41} = \{-Q_{21} \gamma_{21,1} + R_2 (Q_{21} E_2 + \gamma_{32,2})\} / (B_3 F_{22}) \quad (3.36c)$$

$$\alpha_{44} = \gamma_{44,3} - R_3 \gamma_{43,3} + \{R_3 (Q_{21} \gamma_{23,2} + E_3) - \gamma_{34,3}\} / (B_3 F_{22}) \quad (3.36d)$$

It is also necessary to compute the tangent axial flexibility coefficient for the beam-column. This is accomplished by computing the average tangent axial flexibility coefficient for each zone based on the remaining elastic core for the zone and summing these as follows:

$$\alpha_a = [B_1/A_{12} + B_2/A_{23} + B_3/A_{34}] / E \quad (3.37a)$$

where $A_{m,m+1}$ = Average cross-sectional area for the elastic core for zone m .

$$= (A_m + A_{m+1}) / 2 \quad (3.37b)$$

A_m = Cross-sectional area of the elastic core at point m .

In general terms, therefore, the tangent axial flexibility coefficient for an inelastic beam-column is given by

$$\alpha_a = \sum_1^n [B_m / A_{m,m+1}] / E \quad (3.38)$$

where m is the zone number and n is the number of zones along the beam-column.

Iteration Scheme

Solutions of the various equations presented so far are obtained by iteration using suitable starting values for the deflection components due to curvature and modifying these values at the end of each cycle of iteration until a specified convergence criterion is satisfied. The convergence criterion adopted here is

$$|(f_c - f_p) / f_p| < \xi \quad (3.39)$$

where f_c = current value of a function

f_p = previous value of the function

ξ = 0.0001 to 0.0002 (3.40)

A general iteration scheme for the computations is given below.

1. For the given beam-column and the combination of axial force and end bending moments, determine the type of zone combination and calculate the curvatures at the ends of all zones using the formulae presented in Chapter 2.
2. Compute the cross-sectional areas of the elastic core at the ends of all zones.
3. Compute m_m and q_m for each zone, m , from Eqns. (3.22d) and (3.22e).

4. Assume starting values for the displacement components of the zone intersection points due to curvature.
5. Compute the length of each zone from Eqn. (3.22c).
6. Compute the flexibility coefficients for each zone from Eqns. (3.22f), (3.22g), (3.22h) and (3.22i).
7. Obtain revised values for the displacement components of the zone intersection points due to curvature by solving the relevant equations (for example, Eqn. (3.30a) for Zone Combination Type 6).
8. Check for convergence. If this is not satisfied, use displacement component values obtained at Step 7 as starting values and go back to Step 5, repeating the process until the convergence criterion is satisfied. Then go to Step 9.
9. Compute the tangent flexibility coefficients for the beam-column using the appropriate formulae (for example, formulae given by Eqns. (3.36) for Zone Combination Type 6).

3.5.2 Formulae For The Flexibility Coefficients For The Beam-Column Bent In Double Curvature

Based on the general procedure presented in Section 3.5.1, the relevant formulae for the remaining zone combination types given in Table 3.1 will now be given. The notations adopted here are the same as those adopted in Section 3.5.1. Also, since Eqn. (3.38) is generally employed for determining the tangent axial flexibility coefficient for an inelastic beam-column, this coefficient will not be repeated in this section.

Formulae For Zone Combination Types 2 And 3

The formulae given here are for Zone Combination Type 2. The tangent flexural flexibility coefficients for Zone Combination Type 3, which is a mirror-image of Zone Combination Type 2, are derived from those given here by inter-changing the end node numbers for Zone Combination Type 2.

The deflection component of the zone intersection point, 2, due to curvature is given by

$$D_2 = [-M_1 \gamma_{21,1} + M_2 E_2 + M_3 \gamma_{23,2}] / C_2 \quad (3.41a)$$

from which the required flexural flexibility coefficients for both zone combination types are as follows:

$$(\alpha_{11})_2 = (\alpha_{33})_3 = \gamma_{11,1} - \gamma_{21,1} / (B_1 C_2) + R_2 \{ E_2 / (B_1 C_2) - \gamma_{12,1} \} \quad (3.41b)$$

$$(\alpha_{13})_2 = (\alpha_{31})_3 = \gamma_{23,2} / (B_1 C_2) \quad (3.41c)$$

$$(\alpha_{31})_2 = (\alpha_{13})_3 = \gamma_{21,1} / (B_2 C_2) + R_2 \{ \gamma_{32,2} - E_2 / (B_2 C_2) \} \quad (3.41d)$$

$$(\alpha_{33})_2 = (\alpha_{11})_3 = \gamma_{33,2} - \gamma_{23,2} / (B_2 C_2) \quad (3.41e)$$

where $(\alpha_{ij})_k$ is the tangent flexural flexibility coefficient, α_{ij} , for zone combination type k.

Formulae For Zone Combination Types 4 And 5

The formulae given here are for Zone Combination Type 4. The tangent flexural flexibility coefficients for Zone Combination Type 5, which is a mirror-image of Zone Combination Type 4, are derived from those given here by inter-changing the end node numbers for Zone Combination Type 4.

The relevant matrix equation for determining the deflection components at the zone intersection points 2 and 3 due to curvature is

given by

$$\begin{bmatrix} C_2 & -1/B_2 \\ -1/B_2 & C_3 \end{bmatrix} \begin{Bmatrix} D_2 \\ D_3 \end{Bmatrix} = \begin{Bmatrix} F_2 \\ F_3 \end{Bmatrix} \quad (3.42a)$$

$$\text{where } F_2 = -M_1\gamma_{21,1} + M_2E_2 - M_3\gamma_{23,2} \quad (3.42b)$$

$$F_3 = -M_2\gamma_{32,2} + M_3E_3 + M_4\gamma_{34,3}$$

From Appendix 4, the general solution of Eqn. (3.42a) is given by

$$\begin{Bmatrix} D_2 \\ D_3 \end{Bmatrix} = \begin{Bmatrix} (Q_{11}F_2 + Q_{12}F_3)/A_{11} \\ (Q_{12}F_2 + F_3)/F_{22} \end{Bmatrix} \quad (3.42c)$$

from which the required flexural flexibility coefficients for both zone combination types are as follows:

$$(\alpha_{11})_4 = (\alpha_{44})_5 = \gamma_{11,1} - R_2\gamma_{12,1} + [-Q_{11}\gamma_{21,1} + R_2\{Q_{11}E_3 - Q_{12}\gamma_{32,2}\} + R_3\{-Q_{11}\gamma_{23,2} + Q_{12}E_3\}]/(B_1C_2) \quad (3.42d)$$

$$(\alpha_{14})_4 = (\alpha_{41})_5 = Q_{12}\gamma_{34,3}/(B_1C_2) \quad (3.42e)$$

$$(\alpha_{41})_4 = (\alpha_{14})_5 = R_3\gamma_{43,3} - [-Q_{21}\gamma_{21,1} + R_2\{Q_{21}E_2 - \gamma_{32,2}\} + R_3\{-Q_{21}\gamma_{23,2} + E_4\}]/(B_3F_{22}) \quad (3.42f)$$

$$(\alpha_{44})_4 = (\alpha_{11})_5 = \gamma_{44,3} - \gamma_{34,3}/(B_3F_{22}) \quad (3.42g)$$

Formulae For Zone Combination Types 7 And 8

The formulae given here are for Zone Combination Type 7. The tangent flexural flexibility coefficients for Zone Combination Type 8, which is a mirror-image of Zone Combination Type 7, are derived from those given here by inter-changing the end node numbers for Zone

Combination Type 7.

The relevant matrix equation for determining the deflection components at the zone intersection points 2, 3 and 4 due to curvature is given by

$$\begin{bmatrix} C_2 & -1/B_2 & 0 \\ -1/B_2 & C_3 & 1/B_3 \\ 0 & 1/B_3 & C_4 \end{bmatrix} \begin{Bmatrix} D_2 \\ D_3 \\ D_4 \end{Bmatrix} = \begin{Bmatrix} F_2 \\ F_3 \\ F_4 \end{Bmatrix} \quad (3.43a)$$

$$\text{where } \begin{Bmatrix} F_2 \\ F_3 \\ F_4 \end{Bmatrix} = \begin{Bmatrix} -M_1\gamma_{21,1} + M_2E_2 - M_3\gamma_{23,2} \\ -M_2\gamma_{32,2} + M_3E_3 + M_4\gamma_{34,3} \\ M_3\gamma_{43,3} + M_4E_4 - M_5\gamma_{45,4} \end{Bmatrix} \quad (3.43b)$$

From Appendix 4, the general solution of Eqn. (3.43a) is given by

$$\begin{Bmatrix} D_2 \\ D_3 \\ D_4 \end{Bmatrix} = \begin{Bmatrix} (Q_{11}F_2 + Q_{12}F_3 + Q_{13}F_4)/A_{11} \\ (Q_{21}F_2 + Q_{22}F_3 + Q_{23}F_4)/F_{22} \\ (Q_{31}F_2 + Q_{32}F_3 + F_4)/F_{33} \end{Bmatrix} \quad (3.43c)$$

from which the required flexural flexibility coefficients for both zone combination types are as follows:

$$(\alpha_{11})_7 = (\alpha_{55})_8 = \gamma_{11,1} - R_2\gamma_{12,1} + \{-Q_{11}\gamma_{21,1} + R_2(Q_{11}E_2 - Q_{12}\gamma_{32,2}) + R_3(-Q_{11}\gamma_{23,2} + Q_{12}E_3 + Q_{13}\gamma_{43,3})\}/(B_1C_2) \quad (3.43d)$$

$$(\alpha_{15})_7 = (\alpha_{51})_8 = [R_4(Q_{12}\gamma_{34,3} + Q_{13}E_4) - Q_{13}\gamma_{45,4}]/(B_1C_2) \quad (3.43e)$$

$$(\alpha_{51})_7 = (\alpha_{15})_8 = [-Q_{31}\gamma_{21,1} + R_2(Q_{31}E_2 - Q_{32}\gamma_{32,2}) + R_3(-Q_{31}\gamma_{23,2} + Q_{32}E_3 + \gamma_{43,3})]/(B_4F_{33}) \quad (3.43f)$$

$$(\alpha_{55})_7 = (\alpha_{11})_8 = -R_4\gamma_{54,4} + \gamma_{55,4} + \{R_4(Q_{32}\gamma_{34,3} + E_4) - \gamma_{45,4}\}/(B_4F_{33}) \quad (3.43g)$$

Formulae For Zone Combination Type 9

The relevant matrix equation for determining the deflection component at the zone intersection points 2, 3, 4 and 5 due to curvature is given by

$$\begin{bmatrix} C_2 & -1/B_2 & 0 & 0 \\ -1/B_2 & C_3 & 1/B_3 & 0 \\ 0 & 1/B_3 & C_4 & -1/B_4 \\ 0 & 0 & -1/B_4 & C_5 \end{bmatrix} \begin{Bmatrix} D_2 \\ D_3 \\ D_4 \\ D_5 \end{Bmatrix} = \begin{Bmatrix} F_2 \\ F_3 \\ F_4 \\ F_5 \end{Bmatrix} \quad (3.44a)$$

where

$$\begin{Bmatrix} F_2 \\ F_3 \\ F_4 \\ F_5 \end{Bmatrix} = \begin{Bmatrix} -M_1\gamma_{21,1} + M_2E_2 - M_3\gamma_{23,2} \\ -M_2\gamma_{32,2} + M_3E_3 + M_4\gamma_{34,3} \\ M_3\gamma_{43,3} + M_4E_4 - M_5\gamma_{45,4} \\ -M_4\gamma_{54,4} + M_5E_5 - M_6\gamma_{56,5} \end{Bmatrix} \quad (3.44b)$$

From Appendix 4, the general solution of Eqn. (3.44a) is given by

$$\begin{Bmatrix} D_2 \\ D_3 \\ D_4 \\ D_5 \end{Bmatrix} = \begin{Bmatrix} (Q_{11}F_2 + Q_{12}F_3 + Q_{13}F_4 + Q_{14}F_5)/A_{11} \\ (Q_{21}F_2 + Q_{22}F_3 + Q_{23}F_4 + Q_{24}F_5)/F_{22} \\ (Q_{31}F_2 + Q_{32}F_3 + Q_{33}F_4 + Q_{34}F_5)/F_{33} \\ (Q_{41}F_2 + Q_{42}F_3 + Q_{43}F_4 + F_5)/F_{44} \end{Bmatrix} \quad (3.44c)$$

from which the required flexural flexibility coefficients are:

$$\alpha_{11} = \gamma_{11,1} - R_2\gamma_{12,1} + \{-Q_{11}\gamma_{21,1} + R_2(Q_{11}E_2 - Q_{12}\gamma_{32,2}) + R_3(-Q_{11}\gamma_{23,2} + Q_{12}E_3 + Q_{13}\gamma_{43,3})\}/(B_1C_2) \quad (3.44d)$$

$$\alpha_{16} = [R_4(Q_{12}\gamma_{34,3} + Q_{13}E_4 - Q_{14}\gamma_{54,4}) + R_5(-Q_{13}\gamma_{45,4} + Q_{14}E_5) - Q_{14}\gamma_{56,5}]/(B_1C_2) \quad (3.44e)$$

$$\alpha_{61} = [-Q_{41}\gamma_{21,1} + R_2(Q_{41}E_2 - Q_{42}\gamma_{32,2}) + R_3(-Q_{41}\gamma_{23,2} + Q_{42}E_3 + Q_{43}\gamma_{43,3})]/(B_5F_{44}) \quad (3.44f)$$

$$\alpha_{66} = \frac{-R_5 \gamma_{65,5} + \gamma_{66,5} + \{R_4 (Q_{42} \gamma_{34,3} + Q_{43} E_4 - \gamma_{54,4}) + R_5 (-Q_{43} \gamma_{45,4} + E_5) - \gamma_{56,5}\}}{(8 F_{44})} \quad (3.44g)$$

3.5.3 Formulae For The Flexibility Coefficients For The Beam-Column Bent In Single Curvature

The formulae presented here follow the same general procedure adopted in Section 3.5.2 for the beam-column bent in double curvature. The maximum number of zones along the beam-column is three since no point of contraflexure exists along the beam-column. Consequently, the full range of computations is less here than for the beam-column bent in double curvature.

Formulae For Zone Combination Types 10, 11, 12, 13 And 14

Zone combination types 10, 11, 12, 13 and 14 are similar to, and have the same formulae for the flexibility coefficients as, zone combination types 1, 2, 3, 4 and 5 respectively but the sign of the bending moment at the right-hand end of each zone combination type here must be reversed.

Formulae For Zone Combination Types 15, 16, 17 And 18

These zone combination types have inelastic zones throughout their lengths which are brought about by the simultaneous actions of both end bending moments. Since the maximum number of possible zones for a beam-column bent in single curvature is three, only three inelastic zones are necessary to describe these beam-columns. Thus, the bending moments, M_2 and M_3 , at the zone intersection points 2 and 3 are written in terms of both end bending moments thus:

$$M_2 = |M_1| + G_2(|M_4| - |M_1|) \quad (3.45a)$$

$$M_3 = |M_1| + G_3(|M_4| - |M_1|) \quad (3.45b)$$

where G_2 and G_3 are arbitrarily-chosen, positive factors satisfying the condition

$$0 < G_2 < G_3 < 1.0 \quad (3.45c)$$

Following the general procedure adopted for Zone Combination Types 4 and 5, the relevant flexural flexibility coefficients for these zone combination types are obtained as follows:

$$\alpha_{11} = \frac{\gamma_{11,1} - (1-G_2)\gamma_{12,1} + \{-Q_{11}\gamma_{21,1} + (1-G_2)(Q_{11}E_2 - Q_{12}\gamma_{32,2} + (1-G_3)(-Q_{11}\gamma_{23,2} + Q_{12}E_3)\}}{(B_1C_2)} \quad (3.46a)$$

$$\alpha_{14} = \frac{G_2\gamma_{12,1} + \{Q_{12}\gamma_{34,3} - G_2(Q_{11}E_2 - Q_{12}\gamma_{32,2} - G_3(-Q_{11}\gamma_{23,2} + Q_{12}E_3)\}}{(B_1C_2)} \quad (3.46b)$$

$$\alpha_{41} = \frac{(1-G_3)\gamma_{43,3} - \{-Q_{21}\gamma_{21,1} + (1-G_2)(Q_{21}E_2 - \gamma_{32,2}) + (1-G_3)(-Q_{21}\gamma_{23,2} + E_3)\}}{(B_3F_{22})} \quad (3.46c)$$

$$\alpha_{44} = \frac{-G_3\gamma_{43,3} + \gamma_{44,3} + \{-\gamma_{34,3} + G_2(Q_{21}E_2 - \gamma_{32,2}) + G_3(-Q_{21}\gamma_{23,2} + E_3)\}}{(B_3F_{22})} \quad (3.46d)$$

3.6 Flexibility Coefficients For An Initially-Curved Beam-Column

All the formulae presented so far in this chapter are applicable to an initially-straight member. In practice, however, members may possess initially-curved profiles due to manufacturing processes, fabrication or construction methods. It is, therefore, essential to investigate the responses of such curved members to applied loads. As before, attention is concentrated on the derivation of the flexibility coefficients for the beam-column.

A sinusoidal representation of the initial curved profile of a beam-column is widely adopted in the literature on structural stability as a reasonable representation of the true curve and this representation will also be adopted here.

The general form of the equation for the sinusoidal curve of Fig. 3.6 is

$$y_0 = u_0 \sin(k_0 x) \quad (3.47a)$$

where $k_0 = \pi/L_0$ (3.47b)

L_0 is initial straight length of beam-column

and u_0 is the measured or assumed deflection of centre of beam-column.

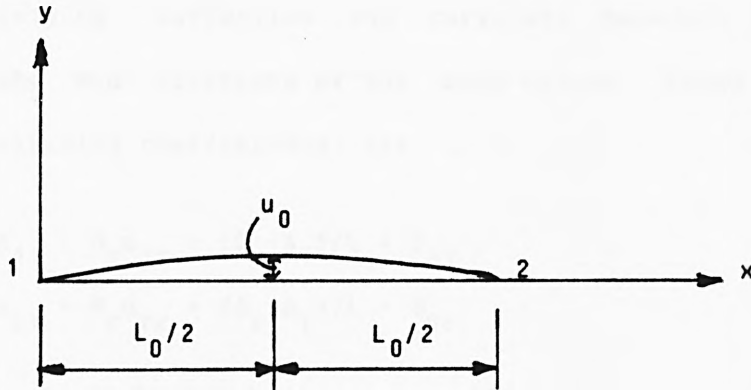


Fig. 3.6 A Sinusoidal Curve For A Beam-Column

Since bending strains are caused by the net curvature of the beam-column, the basic differential equation (3.4a) now includes the initial curvature thus:

$$y'' - y_0'' = -M_x/(EI_z) \quad (3.48a)$$

Following the procedure adopted in Section 3.4 for the elastic beam-column, the solution of Eqn. (3.48a) now becomes

$$y = A \cos(nx) + B \sin(nx) - M_1(1-x/L)/P + M_2(x/L)/P + \Delta_1(1-x/L) + \Delta_2(x/L) + y_0[1/(1-C_e)] \quad (3.48b)$$

$$\text{where } C_e = P/P_E \quad (3.48c)$$

For the inelastic beam-column, therefore, the general expression for the deflection curve given by Eqn. (3.17) for a typical zone, m , is now modified to include the initial deflection thus:

$$y = A\cos(m_m x) + B\sin(q_m x) - M_1(1-x/L)/P + M_r(x/L)/P + \Delta_1(1-x/L) + \Delta_r(x/L) + C_0 u_0 \sin(k_0 x) \quad (3.49a)$$

where r is the identification number for the right end of the beam-column. From Eqn. (3.49a), the slope of the zone, m , now becomes

$$y' = -A m_m \sin(m_m x) + B q_m \cos(q_m x) + M_1/(PL) + M_r/(PL) + (\Delta_r - \Delta_1)/L + C_0 k_0 u_0 \cos(k_0 x) \quad (3.49b)$$

where $C_0 = 1/(1-C_e)$ and the constants A , B , m_m and q_m retain their values satisfying deflection and curvature boundary conditions. Similarly, the end rotations of the beam-column, based on tangent flexural flexibility coefficients, are

$$\theta_1 = M_1 \alpha_{11} + M_r \alpha_{1r} + (\Delta_r - \Delta_1)/L + \theta_{01} \quad (3.50a)$$

$$\theta_r = M_1 \alpha_{r1} + M_r \alpha_{rr} + (\Delta_r - \Delta_1)/L + \theta_{0r} \quad (3.50b)$$

$$\text{where } \theta_{01} = C_0 k_0 u_0 \quad (3.50c)$$

$$\theta_{0r} = -C_0 k_0 u_0 = -\theta_{01} \quad (3.50d)$$

and the tangent flexural flexibility coefficients retain their values for an elastic beam-column. For an inelastic beam-column, however, the equations for determining the deflection components due to curvature at the zone intersection points (for example, Eqn. (3.30a)) remain valid and unchanged since the rotations due to initially-curved profile at each zone intersection point are numerically equal and, therefore, cancel out when the rotation compatibility condition is imposed.

The length of each zone is, however, modified as follows:

Considering a typical zone, m , of a beam-column loaded as shown in Fig.(3.7), the length of this zone now becomes

$$B_m = [M_m - M_{m+1} + P(D_{m+1} - D_m) + P(D_{0,m+1} - D_{0,m})] / V \quad (3.51a)$$

where $V = (M_1 + M_n) / L$ (as before) (3.51b)

and from Eqn.(3.47a),

$$D_{0,m} = C_0 u_0 \sin(k_0 L_m) \quad (3.51c)$$

$$D_{0,m+1} = C_0 u_0 \sin[k_0 (L_m + B_m)] \quad (3.51d)$$

where L_m is the distance from end 1 of the beam-column to the first end, m , of the zone as shown in Fig. 3.7. The bending moment, $P(D_{0,m+1} - D_{0,m})$ is, therefore, an additional term required to account for the influence of initial curvature of the beam-column. This bending moment depends on the lengths of the zones of the beam-column. These lengths can only be determined during the iteration process for calculating the displacements of the zone intersection points. As a first approximation, it is best to ignore the contribution of this bending

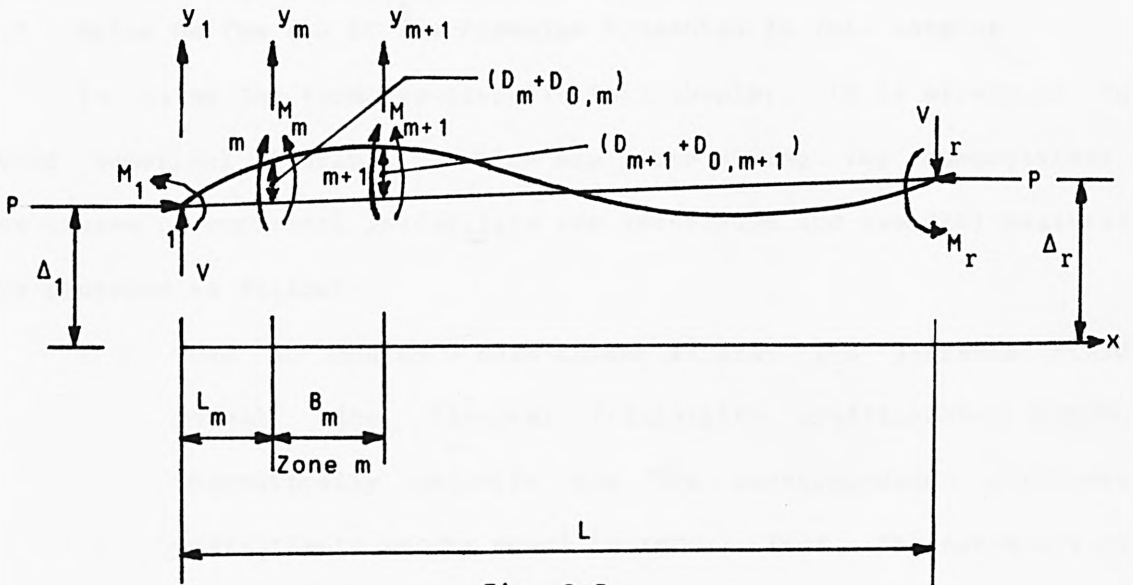


Fig. 3.7

moment in estimating a starting value for iteration for the length of each zone.

Also, the tangent axial flexibility coefficient for the elastic beam-column can be estimated by sub-dividing the original curved length of the beam-column into a few segments (for example, four) and adopting Eqn. (3.38). However, since the initial central deflection of the beam-column is usually very small in comparison with its original length (often taken to lie between $L_0/3000.0$ and $L_0/1000.0$), it is sufficiently accurate to avoid sub-dividing the member and employ its full length, L_0 , in computing the tangent axial flexibility coefficient. Thus, for the inelastic beam-column, the lengths of the inelastic zones, as computed from Eqn. (3.51a), are employed in Eqn. (3.38) in computing its tangent axial flexibility coefficient.

All the formulae for the flexibility coefficients for the beam-column remain unchanged but the values of these coefficients are, of course, altered by the revised values of the lengths of the zones.

3.7 Notes On The Use Of The Formulae Presented In This Chapter

In using the formulae given in this chapter, it is essential to avoid numerical instability which may arise during the computations. The causes of numerical instability are identified and remedial measures are proposed as follows:

1. When an end of a beam-column attains its ultimate yield moment, the flexural flexibility coefficients become theoretically infinite and the corresponding stiffness coefficients become equal to zero. Thus, the curvature of the beam-column at this end becomes infinite as the depth of

the elastic core of the cross-section vanishes. However, as suggested in Section 2.9, excessive or infinite values of curvatures must be avoided. An indirect approach is to compute the flexibility coefficients for the beam-column using the chosen minimum value for the depth of elastic core of the cross-section and then to multiply the coefficients by a sufficiently large, positive number (not less than 10^6) in order to render this end very flexible so that the corresponding flexural stiffness coefficients tend to zero. Thus, a plastic hinge is considered to form at this end.

2. As the limiting axial force, P_{13} [see Eqns. (2.36a) and (A2.9a)] for the cross-section of a beam-column is exceeded, its intermediate yield moment, M_{y2} , approaches, or may exceed, its ultimate yield moment, M_{y3} , giving rise to a zero or negative value for the length of the corresponding inelastic zone bounded by M_{y2} and M_{y3} . This situation must be avoided either by ignoring M_{y2} in the computations so that the inelastic zone is bounded by the first yield moment, M_{y1} , and the ultimate yield moment, M_{y3} or by assigning a very small, positive value (say 5.0mm) to the length of the inelastic zone bounded by M_{y2} and M_{y3} .
3. An infinite curvature of a cross-section can give rise to an infinite deflection of a zone intersection point. Thus, in addition to limiting the curvature of a cross-section which attains a plastic hinge to a finite value (as suggested in Section 2.9), the deflection of a zone intersection point

adjacent to a plastic hinge must be limited to a finite value (for example, one-quarter of the length of the beam-column).

3.8 Applications Of The Formulae Presented In This Chapter

The applications of the formulae for the tangent flexibility coefficients for inelastic beam-columns presented in this chapter are illustrated in this section using a beam-column loaded as Zone Combination Type 8 (see Table 3.1). The cross-sections considered are the I-shaped and rectangular cross-sections considered in Section 2.10. The material properties considered are also those utilized in Section 2.10. In each case, the following data are adopted:

$$L = 5000.0\text{mm}$$

$$P = 0.2P_s$$

$$M_1 = M_{y2}$$

$$M_5 = (M_{y2} + M_{y3})/2$$

The appropriate first yield moment and yield moment ratios are given in Tables 2.1 and 2.2 for the I-shaped and rectangular cross-sections respectively.

The tangent flexural flexibility coefficients are given in the following form:

$$\alpha_{ij} = L/(EI_z\phi_{ij}) \quad (3.52)$$

where ϕ_{ij} is a flexural flexibility factor. Also, the tangent axial flexibility coefficient is given in the following form:

$$\alpha_a = \phi_a L/(AE) \quad (3.53)$$

where ϕ_a is an axial flexibility factor.

Results

The results obtained are summarized in Table 3.3 for the beam-column of I-shaped cross-section and in Table 3.4 for the beam-column of rectangular cross-section. These results show that for the given load combinations the length of the elastic zone is of the order of 75% of the length of the beam-column of I-shaped cross-section and 65% of the length of the beam-column of rectangular cross-section even in the absence of a plastic hinge.

The tangent stiffness coefficients derived from these tangent flexibility coefficients will be given in Sub-Section 4.4.4.

Table 3.3 Results For The Beam-Column Of I-Shaped Cross-Section

Material	B_1 (mm)	B_2 (mm)	B_3 (mm)	B_4 (mm)	ψ_{11}	ψ_{15}	ψ_{51}	ψ_{55}	ψ_a
Elastic-Perfectly-Plastic	555	3812	558	75	3.42	-8.06	-8.57	2.78	1.09
Elastic-Strain-Hardened	546	3725	549	180	3.47	-8.11	-8.98	2.92	1.11

Table 3.4 Results For The Beam-Column Of Rectangular Cross-Section

Material	B_1 (mm)	B_2 (mm)	B_3 (mm)	B_4 (mm)	ψ_{11}	ψ_{15}	ψ_{51}	ψ_{55}	ψ_a
Elastic-Perfectly-Plastic	685	3269	689	357	3.75	-9.13	-10.7	3.21	1.06
Elastic-Strain-Hardened	670	3205	672	453	3.81	-9.19	-11.2	3.35	1.06

CHAPTER 4

PLANE FRAME STABILITY ANALYSIS

4.1 Introduction

In Chapter 3, the tangent flexibility coefficients for a beam-column were evaluated for any load level up to failure. These coefficients lend themselves easily to plane frame stability analysis by any of the standard methods of structural analysis. In this chapter, the stiffness method of structural analysis is employed in plane frame stability analysis. Thus, it will be necessary to derive the tangent stiffness coefficients for a beam-column from these tangent flexibility coefficients.

The stability analysis presented here not only gives the stable equilibrium path and failure load of a plane frame but also gives the locations and lengths of all inelastic zones that may be present in the frame at any load level. The analysis can be applied not only to plane frames but also to single-span and multi-span beam-columns.

4.2 Load Simulation

For elastic analysis of a plane frame, the loads on the frame may be either concentrated at nodal points of the frame or distributed along the members or any combination of these loads. However, for a stability analysis of a plane frame as developed in this thesis, all loads must be applied at the nodal points of the frame. Thus, distributed loads need to be simulated by their statically-equivalent concentrated loads placed at the nodal points of the frame. This approach is necessary because fixed-end moments cannot be easily evaluated for distributed loads when inelastic zones are present along a beam-column.

For a stability analysis, loading may be proportional or non-proportional. For proportional loading, a load parameter (or factor) is assigned to all loads on the frame. The value of this load parameter is increased as the total load on the frame is increased. A non-proportional loading has a constant part and a variable part and the load parameter is assigned to all the variable parts of the loads on the frame. In either case, however, the analysis of the frame is for the total loads on the frame at any load level up to failure.

4.3 Geometry Simulation

A plane frame is discretized into a number of beam-columns for stability analysis by introducing nodes at various locations on the frame. Initially, nodes are introduced at points of intersection of the members of the frame and also at the supports. Then, certain factors may make it necessary to introduce additional nodes along the members of the frame. These factors are

1. Nature of bending of member,
2. Type of loads on the frame and
3. Behaviour of a structural member.

For a member bent in double curvature, no additional node is required along its length since its maximum bending moments occur at its ends while a point of contraflexure (that is a point of zero bending moment) occurs along its length. However, for a member bent in single curvature, the possibility exists for the bending moment at, or near, its mid-span to be larger than its end bending moment. In order to employ the formulations and assumptions of Chapter 3, therefore, a node must be inserted at its mid-span or the likely position of maximum

bending moment near its mid-span.

A node must also be inserted at the location of each concentrated load required for a stability analysis so that there is no load along the span of each beam-column in accordance with the assumptions made in Chapter 3.

It is sometimes necessary to investigate the behaviour of a particular member within a framework. Perhaps, the bending moments, deflections and rotations at various locations are of interest. These can be monitored by inserting nodes along such a member. However, closely-spaced nodes must be avoided so that the length of an inelastic zone does not tend to zero thus causing numerical instability in the computations.

Supports may be fully fixed, pinned or elastically-restrained. Also, the connections between the members of the frame may be rigid or pinned but it is essential that the frame, or any part of it, does not become a mechanism. Member cross-sectional dimensions, material properties and lengths must be given. However, the members required to restrain the frame against lateral-torsional buckling are not required to be specified as they do not form part of the analysis.

4.4 Tangent Stiffness Matrix For A Beam-Column

Three types of beam-column are considered here namely:

1. Beam-column rigidly-connected to a plane frame at both ends,
2. Beam-column rigidly-connected to a plane frame at one end and pinned to the frame at the other end and
3. Beam-column pinned to a plane frame at both ends.

In each case, the general case of a beam-column having an initially-curved profile will be considered here.

4.4.1 Beam-Column Rigidly-Connected To A Plane Frame At Both Ends

The end rotations of a beam-column bent in double curvature are given by Eqns. (3.50) as follows:

$$\theta_1 = M_1 \alpha_{11} + M_r \alpha_{1r} + (\Delta_r - \Delta_1)/L + \theta_{01} \quad (4.1a)$$

$$\theta_r = M_1 \alpha_{r1} + M_r \alpha_{rr} + (\Delta_r - \Delta_1)/L + \theta_{0r} \quad (4.1b)$$

For simplicity in the present derivation, the end node number, r, given in Eqns. (4.1) is replaced by 2. Thus, the matrix form of the revised Eqns. (4.1) becomes

$$\begin{bmatrix} \alpha_{11} & \alpha_{12} \\ \alpha_{21} & \alpha_{22} \end{bmatrix} \begin{Bmatrix} M_1 \\ M_2 \end{Bmatrix} = \begin{Bmatrix} \theta_1 - \theta_{01} - (\Delta_2 - \Delta_1)/L \\ \theta_2 - \theta_{02} - (\Delta_2 - \Delta_1)/L \end{Bmatrix} \quad (4.2)$$

From Appendix 4, the general solution of Eqn. (4.2) is obtained and simplified as follows:

$$\begin{Bmatrix} M_1 \\ M_2 \end{Bmatrix} = \begin{Bmatrix} k_{11}\theta_1 + k_{12}\theta_2 + k_{13}(\Delta_2 - \Delta_1) + M_{01} \\ k_{21}\theta_1 + k_{22}\theta_2 + k_{23}(\Delta_2 - \Delta_1) + M_{02} \end{Bmatrix} \quad (4.3a)$$

$$\text{where } \beta = \alpha_{11}\alpha_{22} - \alpha_{12}\alpha_{21} \quad (4.3b)$$

$$k_{11} = \alpha_{22}/\beta \quad (4.3c)$$

$$k_{12} = -\alpha_{12}/\beta \quad (4.3d)$$

$$k_{13} = (\alpha_{12} - \alpha_{22})/\beta/L = -(k_{11} + k_{12})/L \quad (4.3e)$$

$$M_{01} = k_{13}L\theta_{01} \quad (4.3f)$$

$$k_{21} = -\alpha_{21}/\beta \quad (4.3g)$$

$$k_{22} = \alpha_{11}/\beta \quad (4.3h)$$

$$k_{23} = (\alpha_{21} - \alpha_{11})/\beta/L = -(k_{21} + k_{22})/L \quad (4.3i)$$

$$M_{02} = k_{23}L\theta_{02} \quad (4.3j)$$

In Eqns. (4.3), the rotation coefficients k_{11} , k_{12} , k_{21} and k_{22} are the flexural stiffness coefficients for the beam-column while the displacement coefficients k_{13} and k_{23} are derived from these flexural

stiffness coefficients.

The shear forces at the ends of a beam-column bent in double curvature are given by Eqn. (3.2) as

$$V = V_1 = -V_2 = [M_1 + M_2 + P(\Delta_2 - \Delta_1)]/L \quad (4.4)$$

Substituting Eqn. (4.3a) into Eqn. (4.4) and re-arranging the resulting equation, one obtains

$$V_1 = -V_2 = k_{31}\theta_1 + k_{32}\theta_2 + k_{33}(\Delta_2 - \Delta_1) + V_{01} \quad (4.5a)$$

$$\text{where } k_{31} = (k_{11} + k_{21})/L \quad (4.5b)$$

$$k_{32} = (k_{12} + k_{22})/L \quad (4.5c)$$

$$k_{33} = (k_{13} + k_{23} + P)/L \quad (4.5d)$$

$$V_{01} = k_{13}\theta_{01} + k_{23}\theta_{02} \quad (4.5e)$$

$$V_{02} = -V_{01} \quad (4.5f)$$

Also, the net axial deformation of a beam-column is derived from Fig. (3.2) and Eqn. (3.38) as

$$\delta_1 - \delta_2 = P\alpha_a \quad (4.6a)$$

$$\text{i.e. } P = P_1 = -P_2 = k_a(\delta_1 - \delta_2) \quad (4.6b)$$

where k_a is the axial stiffness coefficient of the beam-column and is given by

$$k_a = 1/\alpha_a \quad (4.6c)$$

Equations (4.3a), (4.5a) and (4.6b) are put into matrix form as follows:

$$\begin{Bmatrix} P_1 \\ V_1 \\ M_1 \end{Bmatrix} = \begin{bmatrix} k_a & 0 & 0 \\ 0 & -k_{33} & k_{31} \\ 0 & -k_{13} & k_{11} \end{bmatrix} \begin{Bmatrix} \delta_1 \\ \Delta_1 \\ \theta_1 \end{Bmatrix} + \begin{bmatrix} -k_a & 0 & 0 \\ 0 & k_{33} & k_{32} \\ 0 & k_{13} & k_{12} \end{bmatrix} \begin{Bmatrix} \delta_2 \\ \Delta_2 \\ \theta_2 \end{Bmatrix} + \begin{Bmatrix} 0 \\ V_{01} \\ M_{01} \end{Bmatrix} \quad (4.7)$$

$$\begin{Bmatrix} P_2 \\ V_2 \\ M_2 \end{Bmatrix} = \begin{bmatrix} -k_a & 0 & 0 \\ 0 & k_{33} & -k_{31} \\ 0 & -k_{23} & k_{21} \end{bmatrix} \begin{Bmatrix} \delta_1 \\ \Delta_1 \\ \theta_1 \end{Bmatrix} + \begin{bmatrix} k_a & 0 & 0 \\ 0 & -k_{33} & -k_{32} \\ 0 & k_{23} & k_{22} \end{bmatrix} \begin{Bmatrix} \delta_2 \\ \Delta_2 \\ \theta_2 \end{Bmatrix} + \begin{Bmatrix} 0 \\ V_{02} \\ M_{02} \end{Bmatrix} \quad (4.8)$$

Equations (4.7) and (4.8) are expressed symbolically as

$$P_1 = s_{11}\delta_1 + s_{12}\delta_2 + P_{01} \quad (4.9)$$

$$P_2 = s_{21}\delta_1 + s_{22}\delta_2 + P_{02} \quad (4.10)$$

where s_{11} , s_{12} , s_{21} and s_{22} are the tangent stiffness matrices for the beam-column.

4.4.2 Beam-Column Rigidly-Connected To A Plane Frame At One End And Pinned At The Other End

Case 1 - One End Of The Beam-Column Pinned

Consider end 1 of the beam-column to be pinned. In this case, M_1 equals zero and the values of the tangent stiffness coefficients are

$$k_a = 1/\alpha_a \quad (4.11a)$$

$$k_{11} = k_{12} = k_{13} = k_{21} = k_{31} = 0 \quad (4.11b)$$

$$k_{22} = 1/\alpha_{22} \quad (4.11c)$$

$$k_{23} = -1/(L\alpha_{22}) \quad (4.11d)$$

$$k_{32} = 1/(L\alpha_{22}) \quad (4.11e)$$

$$k_{33} = [P-1/(L\alpha_{22})]/L \quad (4.11f)$$

The relevant coefficients for end 2 of the beam-column pinned are derived from the above coefficients by inter-changing the end node numbers for the beam-column.

4.4.3 Beam-Column Pinned To A Plane Frame At Both Ends

In this case, the flexural and displacement stiffness coefficients are zero. The axial stiffness coefficient for the initially-curved beam-column is approximated to AE/L_0 for a very small initial central deflection of the beam-column as suggested in Chapter 3 for the beam-column in the elastic state under the axial force and equal to zero at the attainment of either the squash load of the cross-section or the

elastic buckling load of the beam-column.

4.4.4 Examples

The flexural flexibility coefficients given in Tables 3.4 and 3.5 for the beam-columns of I-shaped and rectangular cross-sections respectively considered in Section 2.10 will now be used to obtain the flexural stiffness coefficients for these beam-columns. These stiffness coefficients will be expressed in the following form:

$$k_{ij} = \beta_{ij} EI_z / L$$

where β_{ij} is a flexural stiffness factor. The stiffness factors are given in Tables 4.1 and 4.2.

Table 4.1 Stiffness Factors For The Beam-Column Of I-Shaped Cross-Section

Material	β_{11}	β_{12}	β_{21}	β_{22}
Elastic-Perfectly-Plastic	3.966	1.285	3.221	1.366
Elastic-Strain-Hardened	4.032	1.310	3.389	1.451

Table 4.2 Stiffness Factors For The Beam-Column Of Rectangular Cross-Section

Material	β_{11}	β_{12}	β_{21}	β_{22}
Elastic-Perfectly-Plastic	4.282	1.285	3.660	1.504
Elastic-Strain-Hardened	4.348	1.304	3.824	1.587

4.5 The Transformation Matrices For Beam-Column End Forces And Displacements

A typical beam-column in a plane frame may have any inclination to the horizontal plane. It becomes necessary to transform the individual beam-column end forces and displacements to a global set of axes before conditions of equilibrium and compatibility at nodal points can be written.

Let member 1^0-2^0 of Fig. 4.1 represent the original beam-column inclined at φ degrees to the horizontal plane (the curve $1^0-3^0-2^0$ indicates an initial curved shape of the beam-column) and displaced to the new equilibrium position $1-2$ as a result of the applied loads on the frame.

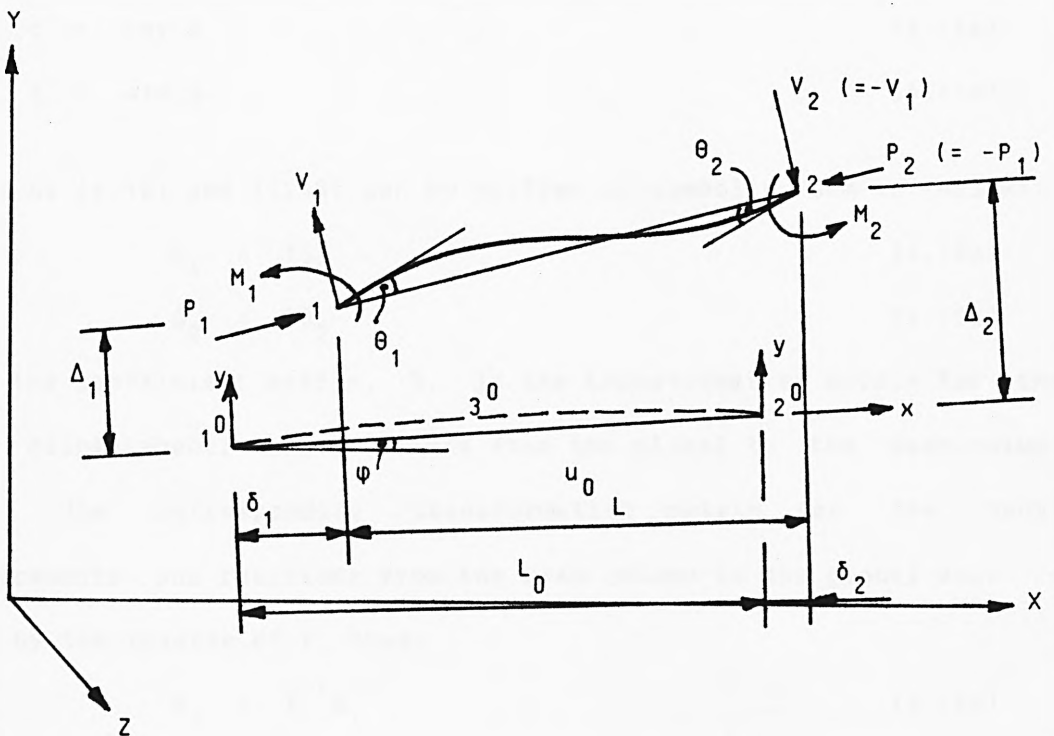


Fig. 4.1

Let the joint displacements along the global frame axes be Δ_{1X} , Δ_{2X} , Δ_{1Y} and Δ_{2Y} and let the joint rotations about the out-of-plane (Z-) axis be θ_{1Z} and θ_{2Z} . These displacements and rotations related to the displacements and rotations referred to the member axes through the following matrix equations:

$$\begin{Bmatrix} \Delta_{1X} \\ \Delta_{1Y} \\ \theta_{1Z} \end{Bmatrix} = \begin{bmatrix} c & -s & 0 \\ s & c & 0 \\ 0 & 0 & 1 \end{bmatrix} \begin{Bmatrix} \delta_1 \\ \Delta_1 \\ \theta_1 \end{Bmatrix} \quad (4.12)$$

$$\begin{Bmatrix} \Delta_{2X} \\ \Delta_{2Y} \\ \theta_{2Z} \end{Bmatrix} = \begin{bmatrix} c & -s & 0 \\ s & c & 0 \\ 0 & 0 & 1 \end{bmatrix} \begin{Bmatrix} \delta_2 \\ \Delta_2 \\ \theta_2 \end{Bmatrix} \quad (4.13)$$

where $c = \cos \varphi$ (4.14a)

and $s = \sin \varphi$ (4.14b)

Equations (4.12) and (4.13) can be written in symbolic form as follows:

$$\Delta_1 = T\delta_1 \quad (4.15a)$$

$$\Delta_2 = T\delta_2 \quad (4.15b)$$

where the coefficient matrix, T , is the transformation matrix for the nodal displacements and rotations from the global to the beam-column axes. The corresponding transformation matrix for the nodal displacements and rotations from the beam-column to the global axes is given by the inverse of T , thus:

$$\delta_1 = T^{-1}\Delta_1 \quad (4.16a)$$

$$\delta_2 = T^{-1}\Delta_2 \quad (4.16b)$$

Owing to the orthogonality of the cartesian co-ordinate axes, T^{-1} is obtained by transposing the elements of T thus:

$$T^{-1} = \begin{bmatrix} c & s & 0 \\ -s & c & 0 \\ 0 & 0 & 1 \end{bmatrix} \quad (4.17)$$

These transformation matrices are also valid for the nodal forces. Thus, if the nodal force vector referred to the global axes is denoted by P while the nodal force vector referred to the beam-column axes is denoted by p , then

$$P_1 = T p_1 \quad (4.18a)$$

$$P_2 = T p_2 \quad (4.18b)$$

Thus, Eqns. (4.9) and (4.10) can be expressed symbolically as

$$P_1 = T s_{11} \delta_1 + T s_{12} \delta_2 + T p_{01} \quad (4.19a)$$

$$P_2 = T s_{21} \delta_1 + T s_{22} \delta_2 + T p_{02} \quad (4.19b)$$

Substitution of Eqns. (4.16) into Eqns. (4.19) gives

$$P_1 = S_{11} \Delta_1 + S_{12} \Delta_2 + T p_{01} \quad (4.20a)$$

$$P_2 = S_{21} \Delta_1 + S_{22} \Delta_2 + T p_{02} \quad (4.20b)$$

where $S_{11} = T s_{11} T^{-1} \quad (4.20c)$

$$S_{12} = T s_{12} T^{-1} \quad (4.20d)$$

$$S_{21} = T s_{21} T^{-1} \quad (4.20e)$$

and $S_{22} = T s_{22} T^{-1} \quad (4.20f)$

4.6 Nodal Forces And Displacements

Let i and j represent any two nodes connected by a beam-column, m , in a plane frame. Then, the compatibility of nodal deformations demands that the same displacement vector, Δ , be assigned to all beam-column ends meeting at nodes i or j . Thus, Δ_i and Δ_j represent the displacement vectors at nodes i and j respectively.

Also, let the external load vector at node i be represented by

$$L_i = \begin{Bmatrix} W_X \\ W_Y \\ M_Z \end{Bmatrix}_i \quad (4.21)$$

where W_X and W_Y are the externally-applied nodal loads in the directions of the global X and Y axes respectively and M_Z is the externally-applied nodal bending moment about the global Z -axis. Similarly, the external load vector at node j is represented by

$$L_j = \begin{Bmatrix} W_X \\ W_Y \\ M_Z \end{Bmatrix}_j \quad (4.22)$$

Then, using subscripts i and j for the subscripts 1 and 2 respectively in Eqns. (4.20), the conditions of equilibrium of forces are applied at nodes i and j , using Eqns. (4.20), (4.21) and (4.22) to obtain the following equations of equilibrium of forces:

$$\Sigma S_{ii} \Delta_i + \Sigma S_{ij} \Delta_j + \Sigma T p_{0i} + L_i = 0 \quad (4.23a)$$

$$\Sigma S_{ji} \Delta_i + \Sigma S_{jj} \Delta_j + \Sigma T p_{0j} + L_j = 0 \quad (4.23b)$$

Eqns. (4.23) are put into matrix form as follows:

$$\begin{bmatrix} \Sigma S_{ii} & \Sigma S_{ij} \\ \Sigma S_{ji} & \Sigma S_{jj} \end{bmatrix} \begin{Bmatrix} \Delta_i \\ \Delta_j \end{Bmatrix} = - \begin{Bmatrix} \Sigma T p_{0i} + L_i \\ \Sigma T p_{0j} + L_j \end{Bmatrix} \quad (4.24)$$

Eqn. (4.24) for a beam-column is expressed in condensed form as

$$S_b \Delta_b = L_b \quad (4.25)$$

where the subscript b refers to the beam-column. For the entire plane frame, therefore, the relevant equilibrium equation is

$$S_f \Delta_f = L_f \quad (4.26)$$

where the subscript f refers to the frame, S_f is the tangent stiffness matrix for the frame, Δ_f is the displacement vector for the frame and L_f is the load vector for the frame with its sign reversed. The matrix, S_f , is assembled from the stiffness matrix, S_b , for each beam-column. The matrix is symmetric for the elastic response and asymmetric for the inelastic response. In general, if any two nodes are not connected by a member, then the corresponding off-diagonal terms of the frame stiffness matrix, S_f , vanish. The frame stiffness matrix, S_f , is a square matrix of order n where n is $3N$ and N is the total number of nodes in the frame.

The nodal displacement vector, Δ_f , is determined from Eqn. (4.26) as

$$\Delta_f = S_f^{-1} L_f \quad (4.27)$$

where S_f^{-1} is the inverse of S_f . It is evident from Eqn. (4.27) that a solution for Δ_f exists only if S_f is positive-definite and, therefore, satisfies the inequality

$$|S_f| > 0 \quad (4.28)$$

It has already been stated that at failure the frame stiffness vanishes. Therefore, the inequality (4.28) expresses a stable condition for the frame and it follows that the onset of instability of the frame is given by the condition

$$|S_f| = 0 \quad (4.29)$$

For the stable frame, therefore, the nodal displacements referred to the beam-column axes are determined by substituting the relevant

nodal displacements from Eqn. (4.27) into Eqns. (4.16) for each beam-column. These are then substituted into Eqns. (4.9) and (4.10) to determine the end force vectors for each beam-column.

4.7 The Stable Equilibrium Path

As stated in Section 4.2, an analysis of a plane frame by the inelastic zone method is for the total loads on the frame. This analysis directly gives a point on the stable equilibrium path for the frame. By incrementing the loading in small amounts, the entire stable equilibrium path for the frame can be traced. At the end of each analysis, the inequality (4.28) is checked and the loads are increased if this inequality is satisfied. In using load increments, however, it is possible to place a total load on the frame which is greater than the failure load of the frame. In this case, the analysis breaks down. It is, therefore, recommended that smaller load increments than those used in the elastic range be used in the inelastic range.

In general, the stable equilibrium path is traced by plotting the load parameter (for proportional loading) or a total joint load (for non-proportional loading) as ordinate against the maximum horizontal (or vertical if this is more critical) joint displacement as abscissa. The failure load corresponds to the point of zero slope. A typical equilibrium path for a plane frame is described in Fig. 4.2.

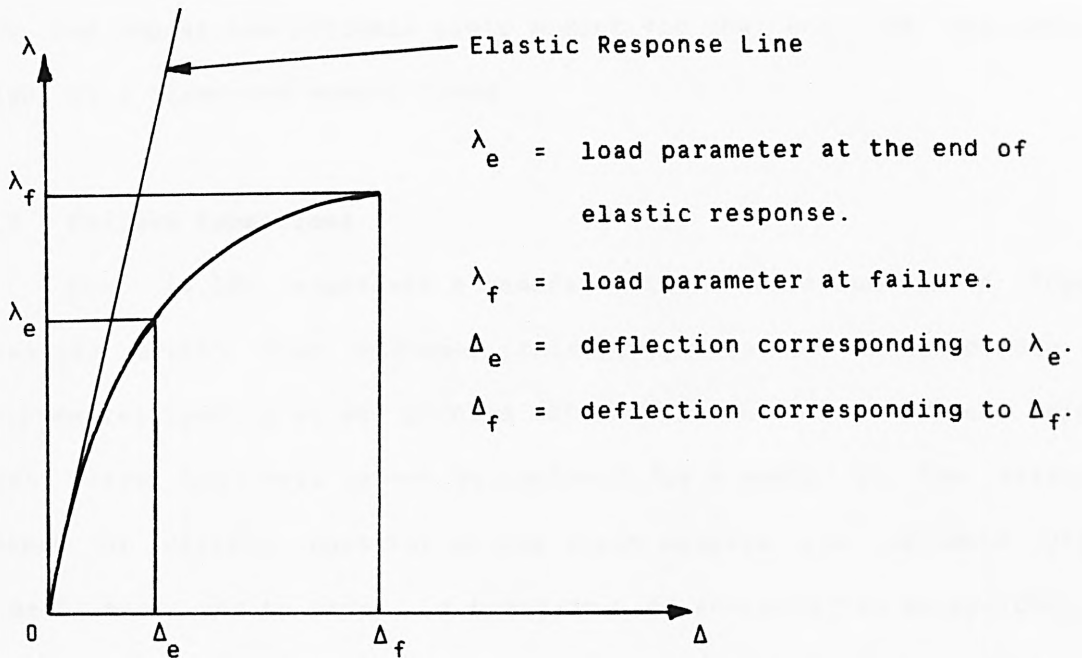


Fig. 4.2 Description Of A Typical Stable Equilibrium Path For A Plane Frame

4.8 Attainment Of The Ultimate Yield Moment Of A Cross-Section At An End Of A Beam-Column

In Section 3.7, a procedure was proposed for monitoring the development of a plastic hinge at an end of a beam-column which attains its ultimate yield moment, M_{y3} . With reference to Eqns. (4.7) and (4.8), the attainment of M_{y3} at end 1 causes the stiffness coefficients K_{11} and K_{12} to vanish while the attainment of M_{y3} at end 2 causes the stiffness coefficients K_{21} and K_{22} to vanish. These coefficients will generally be very small quantities and will not be exactly equal to zero as would be required (since the depth of elastic core is not equal to zero).

Therefore, in order to prevent the bending moment at such an end having zero flexural stiffness from becoming zero during the process of iteration, it is necessary to consider a plastic hinge to form at that

end and impose the ultimate yield moment for that end, of appropriate sign, as a fixed-end moment there.

4.9 Failure Conditions

Eqn. (4.29) expresses a general failure condition for a frame. Analysis breaks down whenever this condition is attained due to incremental loading as was pointed out in Section 4.7. However, since exact zero stiffness cannot be employed for a member in the analysis (depth of elastic core for an end which attains its ultimate yield moment must not be zero), a break-down of analysis can be avoided by terminating analysis as soon as the right-hand side of Eqn. (4.29) or a leading diagonal term in the frame tangent stiffness matrix after a Gaussian elimination process becomes equal to, or less than, a specified small, positive number (say 0.004).

4.10 Flow Chart

A flow chart for plane frame stability analysis by the inelastic zone method is given in Fig. 4.3.

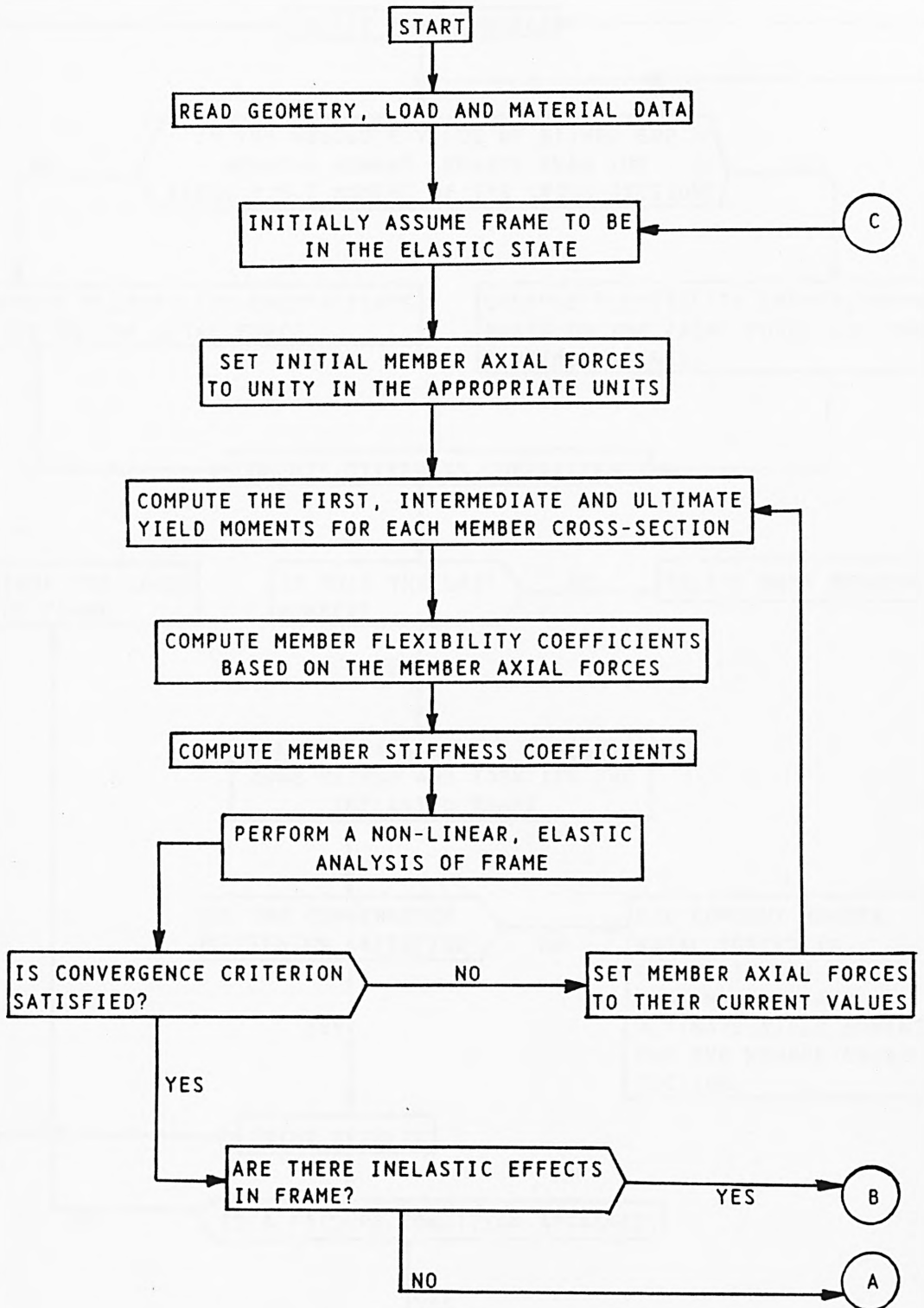


(Fig. 4.3 continued on next page)

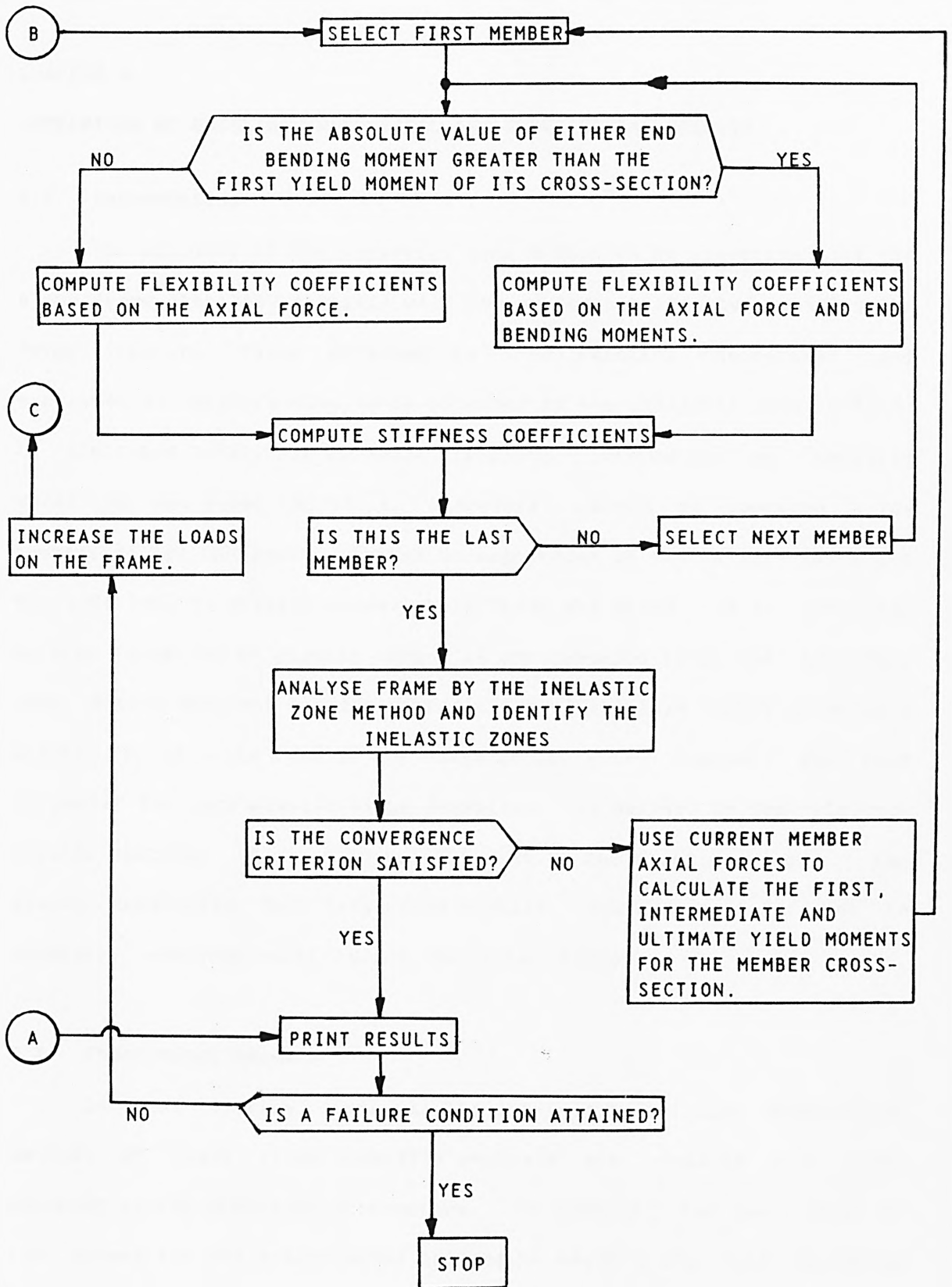


Fig. 4.3 A Flow Chart For Plane Frame Stability Analysis By The Inelastic Zone Method

CHAPTER 5

COMPARISON OF EXISTING THEORETICAL AND EXPERIMENTAL RESULTS

5.1 Introduction

The validity of the inelastic zone method as an effective tool for plane frame stability analysis will now be demonstrated by comparing the frame failure loads obtained by some existing theoretical and experimental methods with those obtained by the inelastic zone method. In published literature on frame stability, information on inelastic zones is not given and these, therefore, cannot be compared. The comparison is, therefore, limited to magnitudes of the failure loads and the locations of plastic hinges where these are given. Also, the step-by-step formation of plastic hinges is not compared since the inelastic zone method does not require a prediction of the load factor at which a plastic hinge would form at any stage of analysis. However, the load parameter for each plastic hinge formation, as derived by the elastic-plastic method, is given in bracket next to the plastic hinge. The frames considered here range from regular, unbraced portal frames to irregular, unbraced multi-storey, multi-bay frames.

5.2 Theoretical Results

In this section, some results obtained by existing theoretical methods of plane frame stability analysis are compared with those obtained by the inelastic zone method. In general, the loads shown on the frames are for proportional loading to which a unit load parameter is assigned. Also, frame member numbers are shown in brackets along the relevant members where these numbers are required in the Tables of member section sizes.

5.2.1 Frame Analysed By Andreaus And D'Asdia (61)

A three-storey, four-bay, regular frame was analysed by Andreaus and D'Asdia based on a modification of the elastic-plastic method to account for finite spread of yielding zones. Fig. 5.1 shows the frame geometry and its working loads. The yielding zones, however, are not given but the frame failure loads and the equilibrium paths for geometrically-linear and non-linear cases are given.

The frame members are of I-shaped cross-sections, the dimensions of which are given in Table 5.1. The material is structural mild steel. The material yield stress is not given but the squash loads for the members are given as follows:

For each column, $P_s = 1460.1 \text{ kN}$

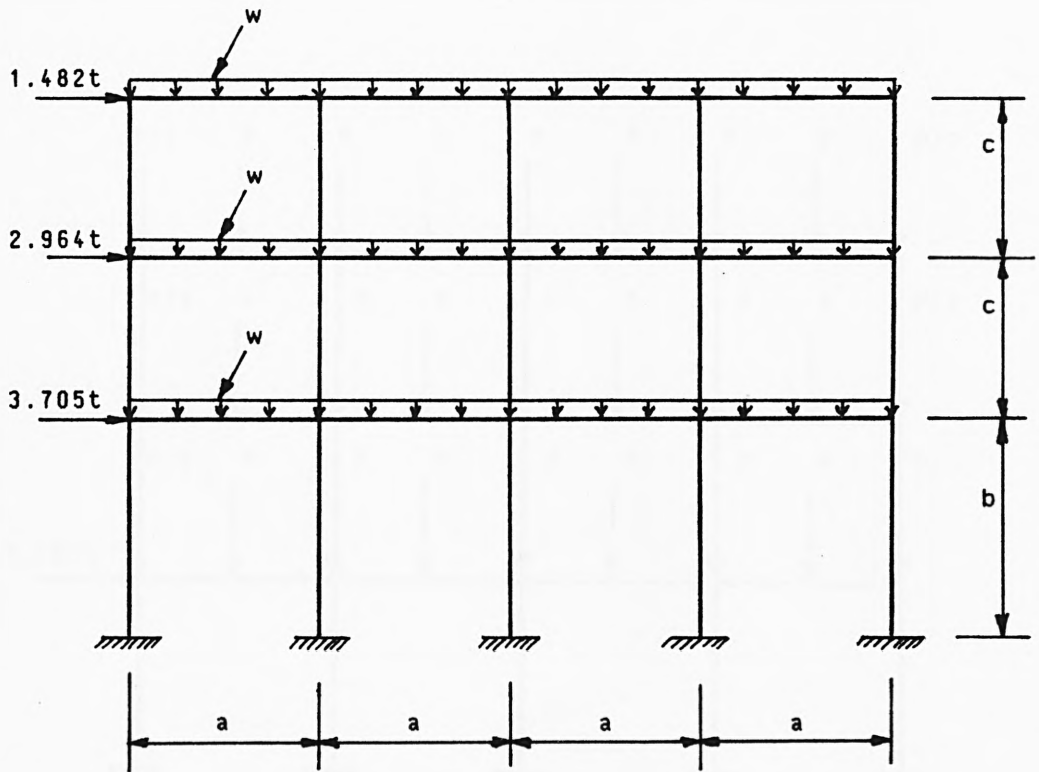
For each beam, $P_s = 1202.9 \text{ kN}$

From these squash loads and the cross-sectional areas given in Table 5.1, the material yield stress for use in the inelastic zone method is calculated to be 0.224 kN/mm^2 . Also, the modulus of elasticity adopted in the inelastic zone method is 207.0 kN/mm^2 .

Two typical load simulations for uniformly-distributed loads on beams, as recommended in Chapter 4 for applying the inelastic zone method, are given in Figs. 5.2 and 5.3 and are employed here for purposes of comparison of results.

Table 5.1 Details Of Member Cross-Sections

Member	Section Size	Section Dimensions (mm)				Cross-Sectional Area (cm^2)
		H	W	T	t	
Column	HEB 180	180.0	180.0	14.0	8.5	65.3
Beam	IPE 300	300.0	150.0	10.7	7.1	53.8



$$w = 2.7 \text{ t/m}$$

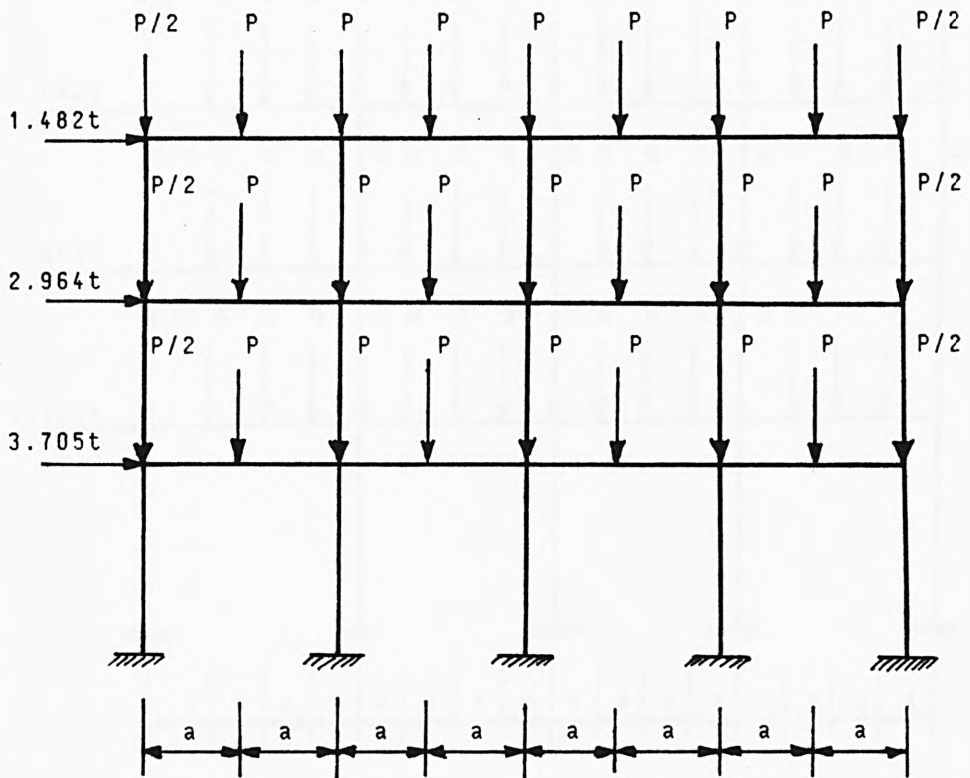
$$L = 3000 \text{ mm}$$

$$a = 6000 \text{ mm}$$

$$b = 4500 \text{ mm}$$

$$c = 3000 \text{ mm}$$

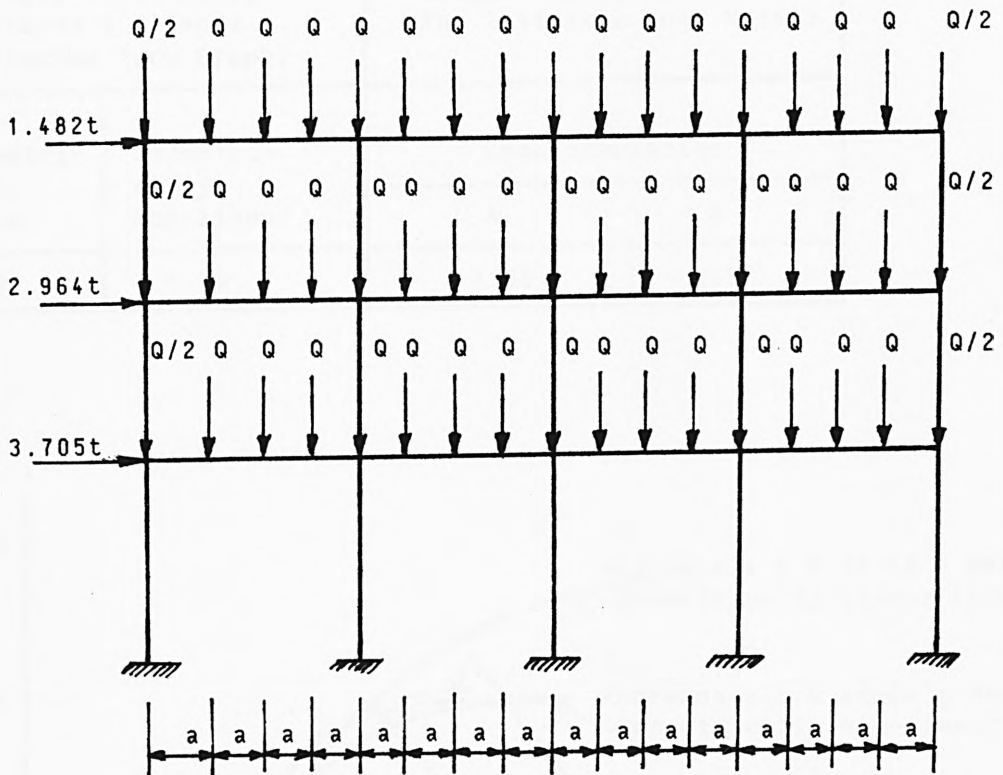
Fig. 5.1 Frame Geometry And Loads



$$P = 8.1t$$

$$a = 3000\text{mm}$$

Fig. 5.2 Load Simulation A



$$Q = 4.05t$$

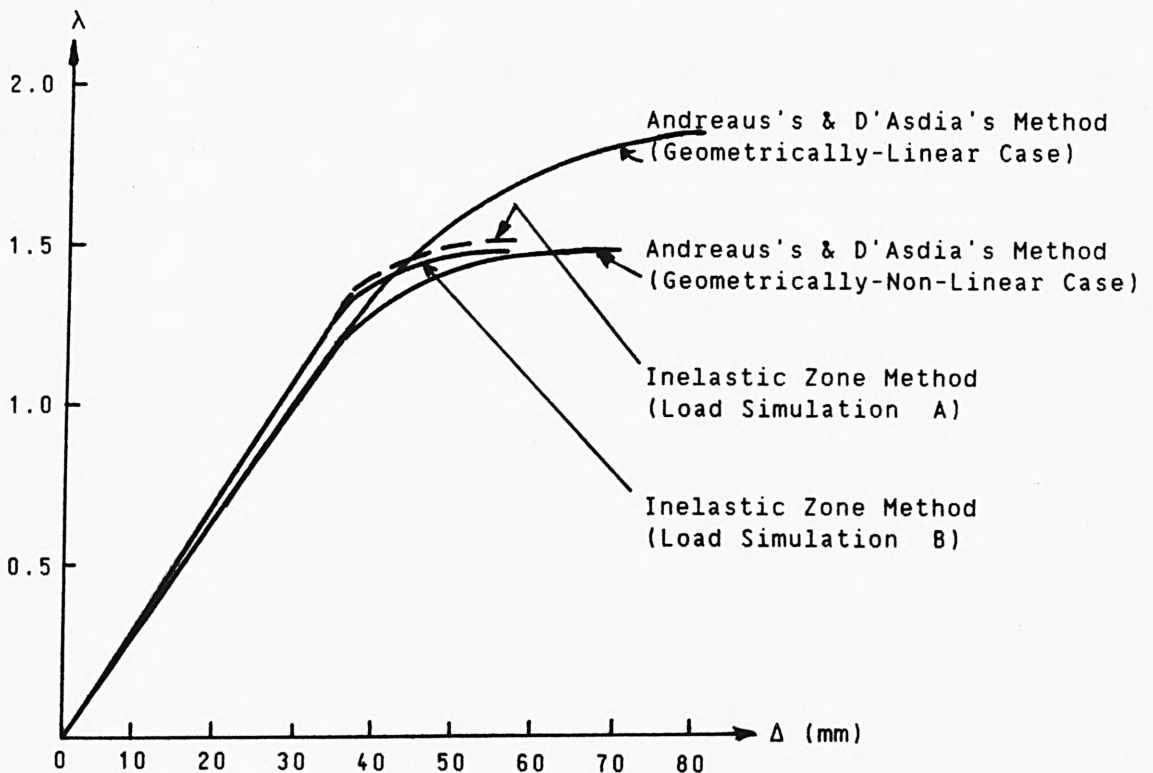
$$a = 1500mm$$

Fig. 5.3 Load Simulation B

Table 5.2 summarizes the frame failure load parameters obtained and Fig. 5.4 shows the equilibrium paths obtained.

Table 5.2 Summary Of Frame Failure Load Parameters

Results Obtained By Andreas & D'Asdia (Extracted From Graph)		Results Obtained By The Inelastic Zone Method	
Geometri- cally Linear	Geometri- cally Non-linear	Load Simulation	
		A	B
1.85	1.50	1.52	1.50



Δ = horizontal deflection of roof beam.

Fig. 5.4 Equilibrium Paths

The above results show that the failure load obtained by the inelastic zone method with load simulation B is equal to that obtained by Andreaus and D'Asdia for the geometrically-non-linear case which more correctly represents the frame behaviour than the geometrically-linear case. Load simulation B is, therefore, better and would give more realistic location of inelastic zones than load simulation A. The inelastic zones near failure for load simulation B are, therefore, given in Fig. 5.5. A load simulation which requires more beam sub-divisions than four would give a slightly lower failure load than load simulation B. However, the failure load obtained by load simulation B is only slightly lower than that produced by load simulation A. Thus, in view of the reduced computer time and storage required for load simulation A, this load simulation can be considered to be adequate for practical and economic design of plane frames.

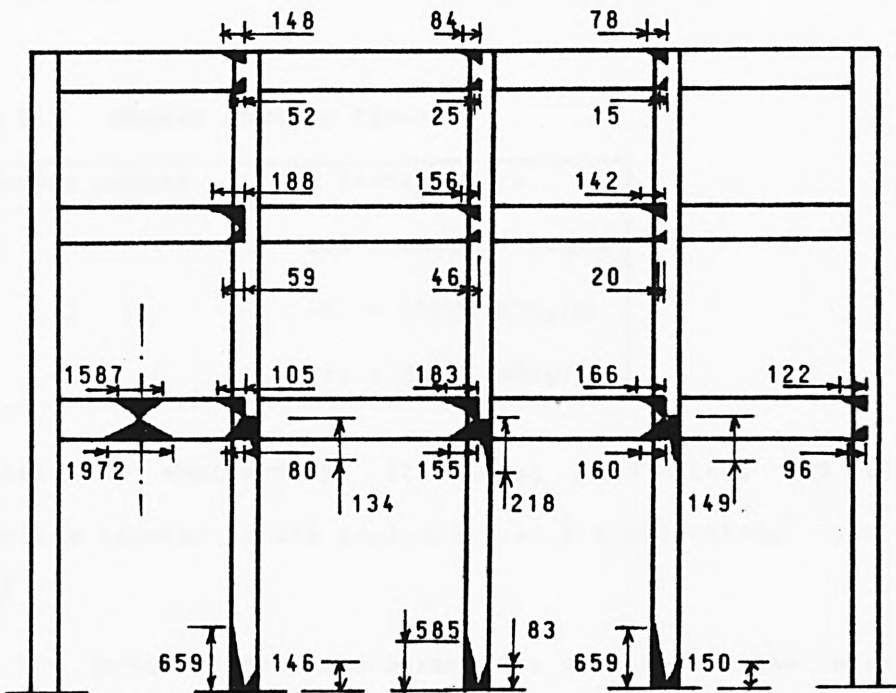


Fig. 5.5 The Inelastic Zones At A Load Parameter Of 1.48 For Load Simulation B

5.2.2 Frame Designed By Majid And Anderson (46)

A four-storey, one-bay, regular frame was designed by Majid and Anderson based on the elastic-plastic method. The frame geometry, working loads and plastic hinges, numbered in their orders of formation, are given in Fig. 5.6. Ten plastic hinges are shown at failure, three in the columns and seven in the beams. The member section sizes are given in Table 5.3.

Table 5.3 Member Section Sizes

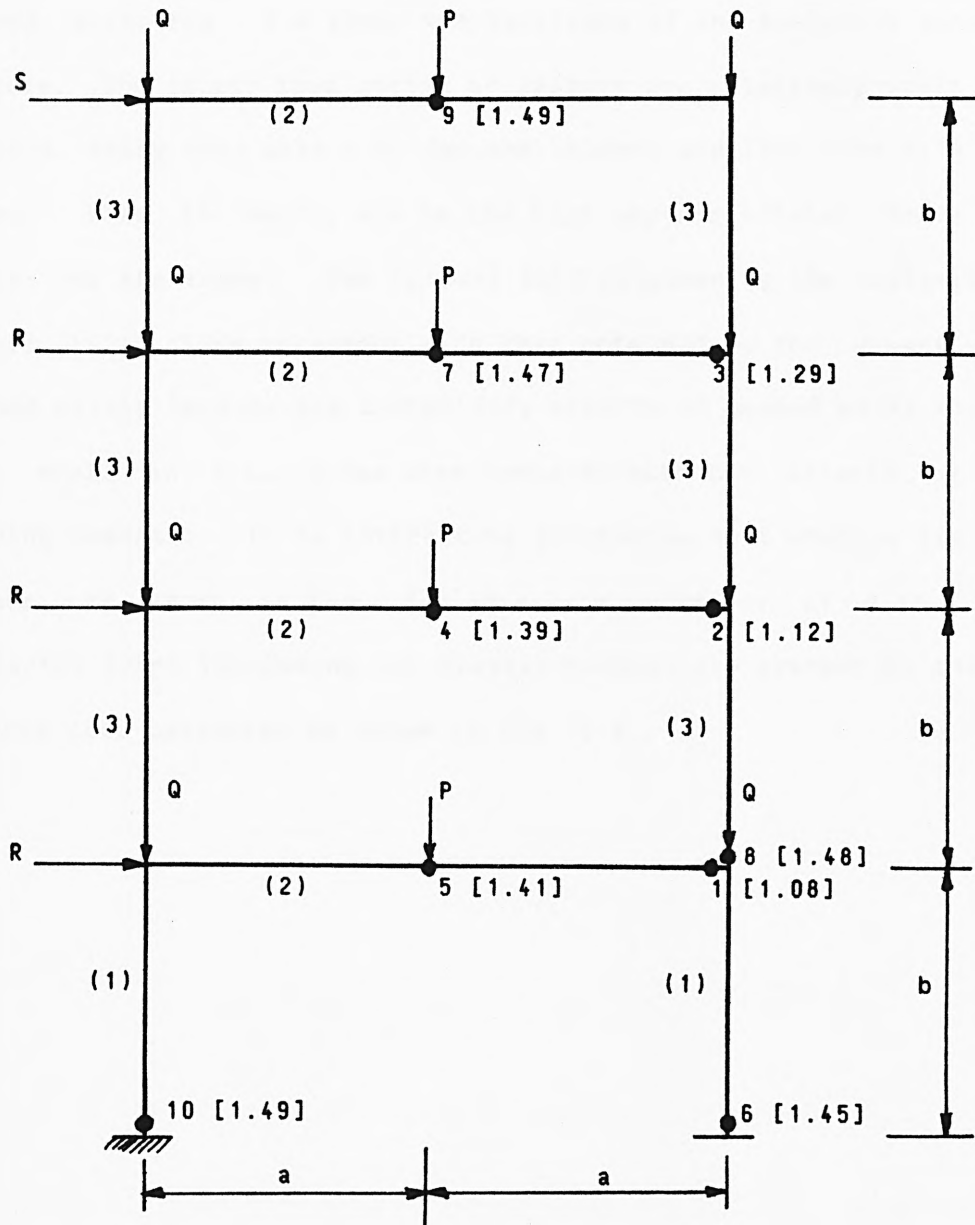
Member Number	Section Size
1	305 x 305UC 118kg/m
2	457 x 152UB 52kg/m
3	254 x 254UC 89kg/m

The material employed is structural mild steel and the material properties adopted in the analysis are $E = 207.0 \text{ kN/mm}^2$ and $\sigma_y = 0.247 \text{ kN/mm}^2$.

The proportional load parameters obtained by the elastic-plastic and inelastic zone methods are summarized in Table 5.4. It can be seen from the results obtained by the inelastic zone method that the working loads cause inelastic effects in the frame.

Table 5.4 Load Parameters

Method Of Analysis	Load Parameter At End Of Elastic Behaviour	Load Parameter At Formation Of First Plastic Hinge	Load Parameter At Failure
Elastic-Plastic	Not Given	1.08	1.49
Inelastic Zone	0.93	1.08	1.48



$$P = 132.0 \text{ kN}$$

$$Q = 64.0 \text{ kN}$$

$$R = 32.0 \text{ kN}$$

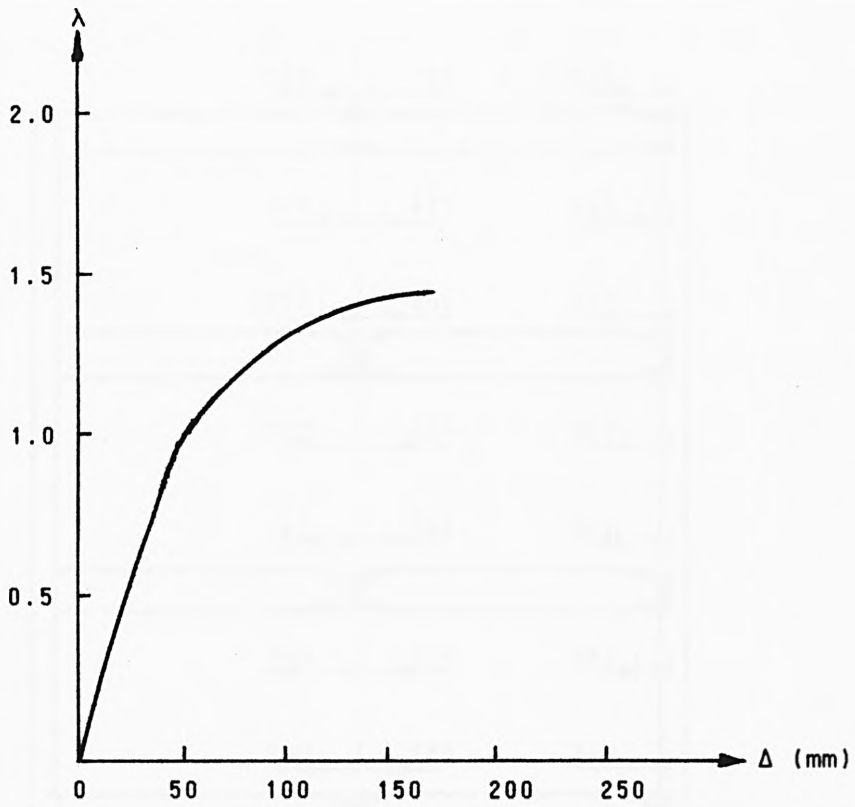
$$S = 16.0 \text{ kN}$$

$$a = 4575 \text{ mm}$$

$$b = 3660 \text{ mm}$$

Fig. 5.6 Frame Geometry And Working Loads

Fig. 5.7 shows the equilibrium path obtained by the inelastic zone method while Fig. 5.8 shows the locations of the inelastic zones near failure. The squash load ratios at failure are relatively small for all members, being less than 0.24 for the columns and less than 0.10 for the beams. This is mostly due to the high bay-width/total frame height ratio for the frame. The failure load obtained by the inelastic zone method is in close agreement with that obtained by the elastic-plastic method mainly because the instability effects of member axial forces are very small in this frame when compared with the effects of member bending moments. It is interesting to observe that whereas six plastic hinges are shown in Fig. 5.6 at a load parameter of 1.45, several inelastic zones (including six plastic hinges) are present in the frame at this load parameter as shown in Fig. 5.8.



Δ = horizontal deflection of roof beam.

Fig. 5.7 Equilibrium Path Obtained By The Inelastic Zone Method

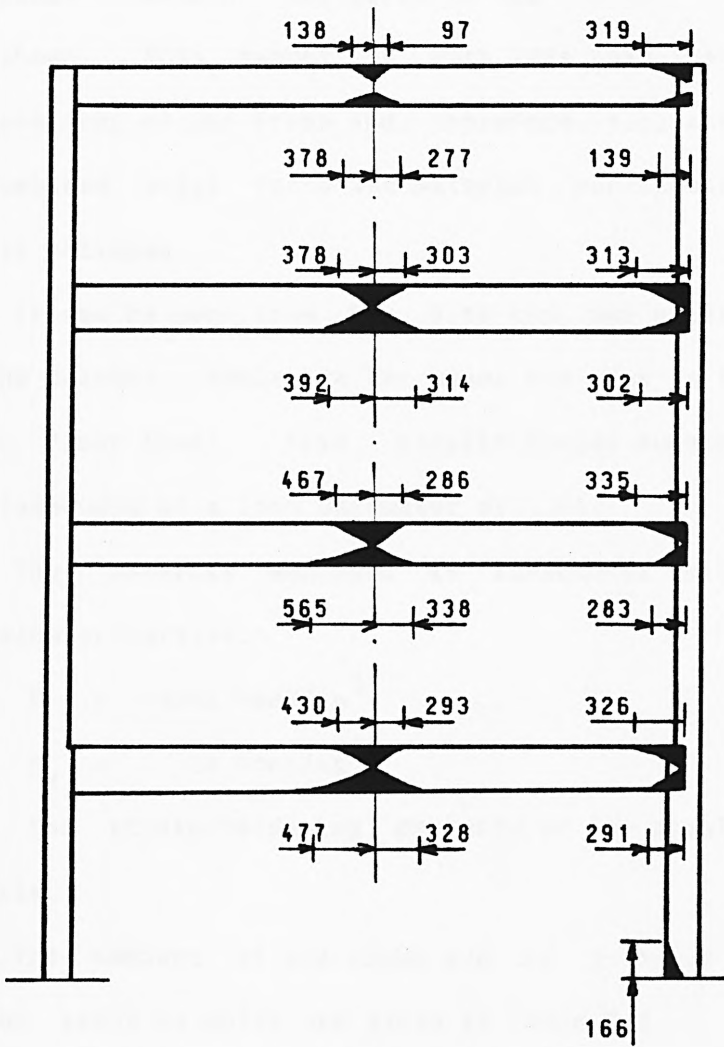


Fig. 5.8 The Inelastic Zones At A Load Parameter Of 1.45

5.2.3 Frame Designed By Horne And Majid (39)

A six-storey, two-bay, irregular frame was designed by Horne and Majid based on the elastic-plastic method. The frame geometry and working loads are given in Fig. 5.9. The plastic hinges and their orders of formation, together with the associated load parameter for each hinge formation, are given in Fig. 5.10. Fourteen plastic hinges are shown. This number is much less than the degree of statical indeterminacy of the frame and, therefore, suggests that instability due to combined axial force and material non-linearity precedes rigid-plastic collapse.

It can be seen from Fig. 5.10 that two plastic hinges are present in the columns, twelve in the beams and none in the members above the fourth floor level. Also, plastic hinges numbered 11,12 and 13 form simultaneously at a load parameter of 1.41.

The material employed is structural mild steel having the following properties:

$$E = 13000 \text{ tonf/in}^2$$

$$\sigma_y = 16 \text{ tonf/in}^2$$

Thus, the strain-hardening property of the steel was ignored in the analysis.

The members of the frame are of I-shaped cross-sections, the section sizes of which are given in Table 5.5.

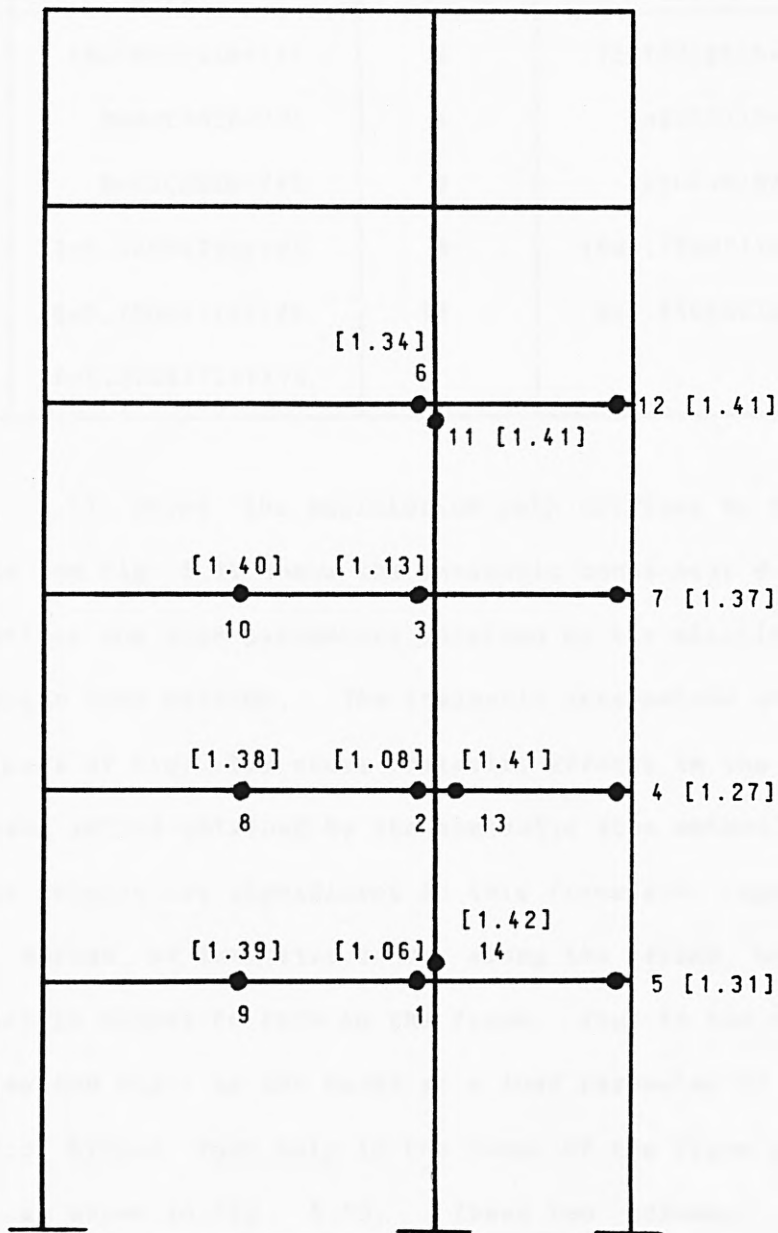


Fig. 5.10 The Plastic Hinges At Failure Obtained By The Elastic-Plastic Method

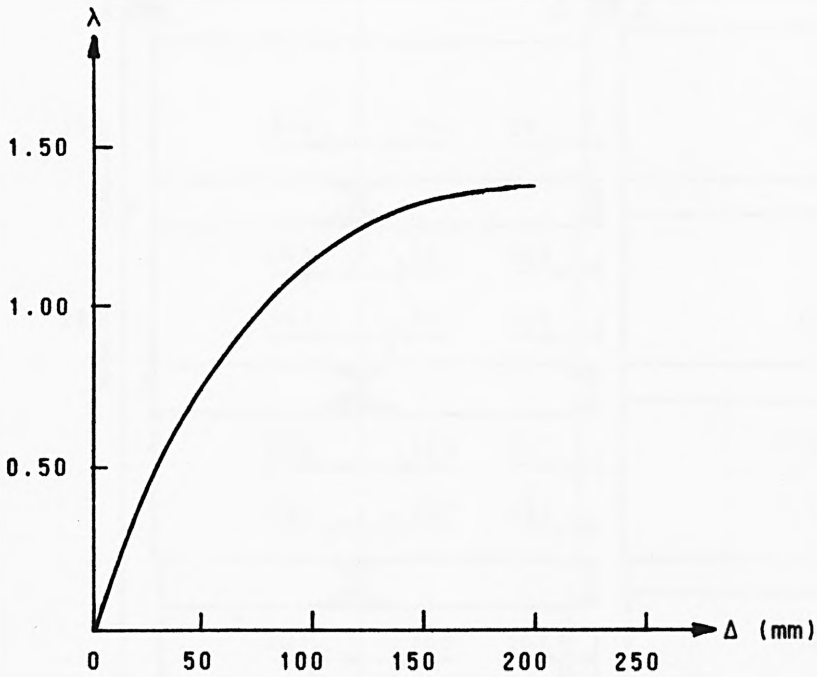
Table 5.5 Member Section Sizes

Member Number	Section Size	Member Number	Section Size
1	10x10UC491bf/ft	2	12x12UC651bf/ft
3	8x8UC401bf/ft	4	8x8UC311bf/ft
5	6x6UC251bf/ft	6	8x8UC351bf/ft
7	12x6.50UB271bf/ft	8	10x5.75UB211bf/ft
9	10x5.75UB211bf/ft	10	8x5.25UB201bf/ft
11	8x5.25UB171bf/ft		

Fig. 5.11 shows the equilibrium path obtained by the inelastic zone method and Fig. 5.12 shows the inelastic zones near failure. Table 5.6 summarizes the load parameters obtained by the elastic-plastic and the inelastic zone methods. The inelastic zone method shows that the working loads of Fig. 5.9 cause inelastic effects in the frame. The squash load ratios obtained by the inelastic zone method confirm that axial force effects are significant in this frame and, together with the extensive spread of inelastic zones along the frame members, cause twelve plastic hinges to form in the frame, four in two columns of the fifth storey and eight in the beams at a load parameter of 1.40 whereas ten plastic hinges form only in the beams of the frame at this load parameter as shown in Fig. 5.10. These two columns, indeed, have relatively high squash load ratios (0.301 for the external column and 0.492 for the internal column). Nevertheless, the failure load parameters obtained by both methods are in close agreement.

Table 5.6 Load Parameters

Method Of Analysis	Load Parameter At End Of Elastic Behaviour	Load Parameter At Formation Of First Plastic Hinge	Load Parameter At Failure
Elastic-Plastic	Not Given	1.06	1.42
Inelastic Zone	0.96	1.02	1.41



Δ = horizontal deflection of roof beam.

Fig. 5.11 Equilibrium Path Obtained By The Inelastic Zone Method

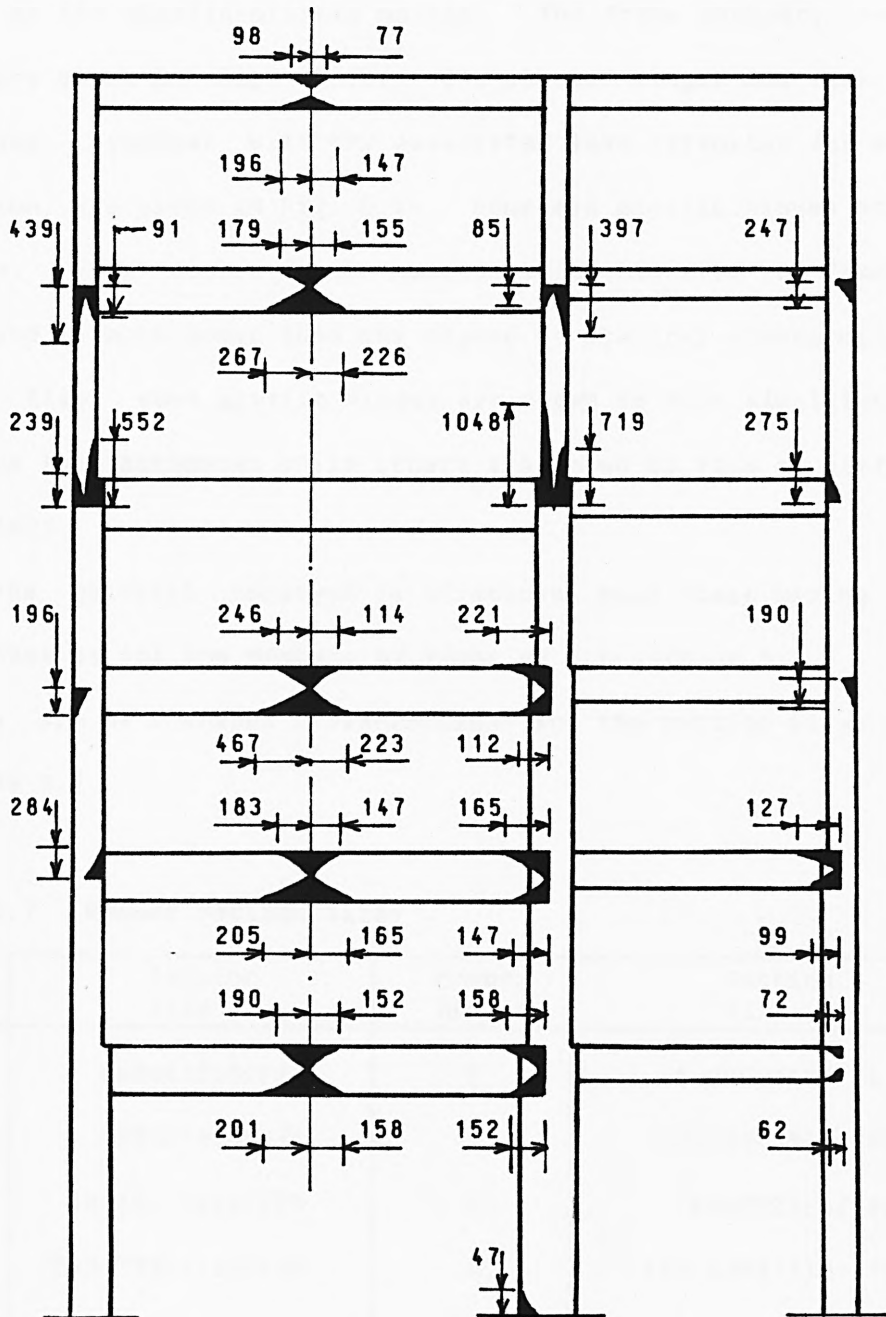


Fig. 5.12 The Inelastic Zones At A Load Parameter Of 1.40

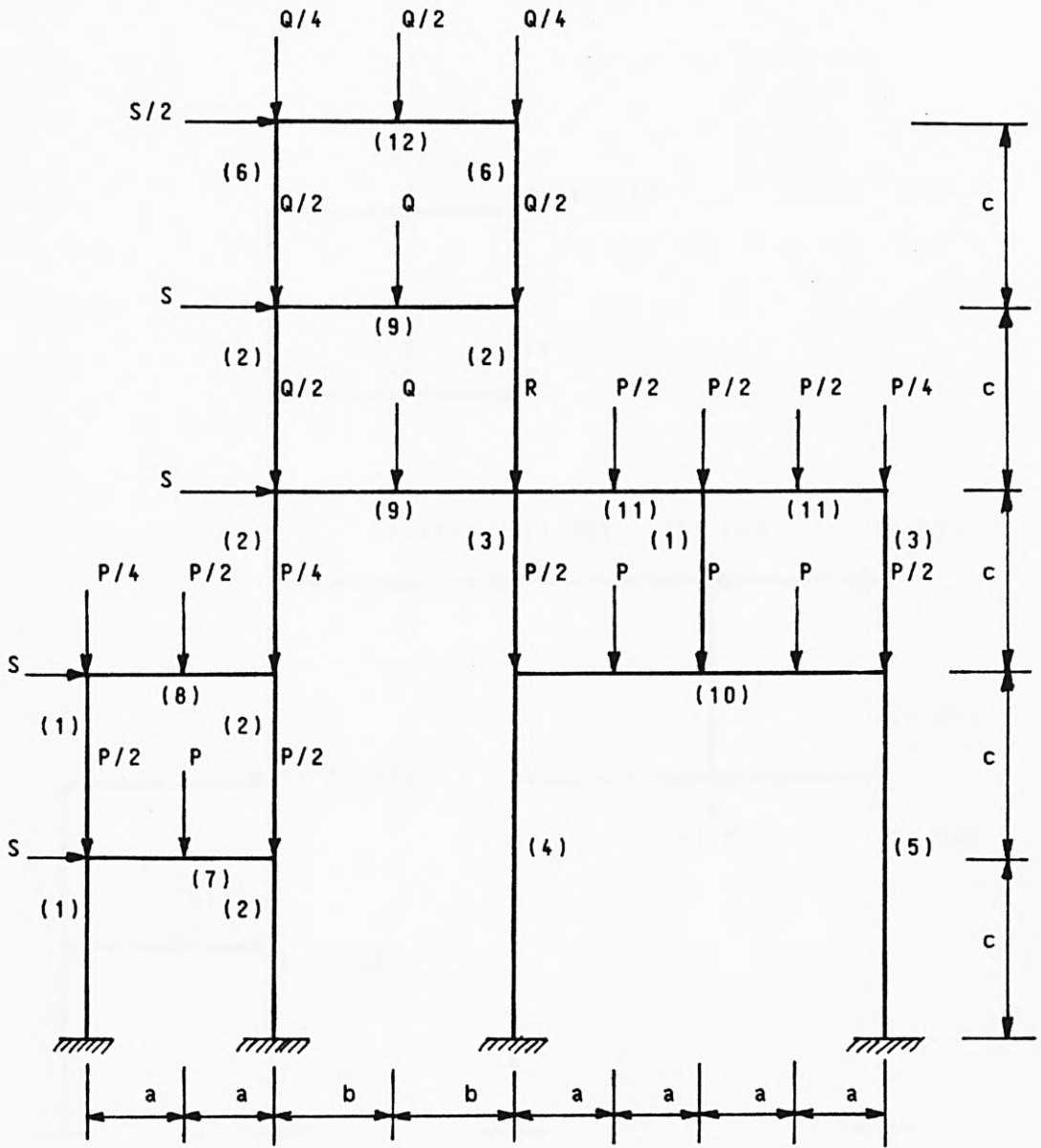
5.2.4 Frame Designed By Horne And Majid (39)

A five-storey, irregular frame was designed by Horne and Majid based on the elastic-plastic method. The frame geometry and working loads are given in Fig. 5.13. The plastic hinges and their orders of formation, together with the associated load parameter for each hinge formation, are given in Fig. 5.14. Fourteen plastic hinges are shown at failure. This number is the same as that shown for the frame in Fig. 5.10 and is much lower than the degree of statical indeterminacy of the frame. Also, some plastic hinges are shown to form simultaneously at the same load parameter while others are shown to form at different load parameters.

The material employed is structural mild steel having the same properties as for the members of frame of sub-section 5.2.3. The frame members are of I-shaped cross-sections and the section sizes are given in Table 5.7.

Table 5.7 Member Section Sizes

Member Number	Section Size	Member Number	Section Size
1	6x6UC201bf/ft	2	8x8UC311bf/ft
3	8x8UC401bf/ft	4	12x12UC651bf/ft
5	10x10UC491bf/ft	6	6x6UC251bf/ft
7	10x5.75UB211bf/ft	8	8x5.25UB171bf/ft
9	12x6.50UB271bf/ft	10	18x7.50UB551bf/ft
11	10x5.75UB251bf/ft	12	8x5.25UB201bf/ft



$$P = 8.4 \text{ tonf}$$

$$Q = 11.2 \text{ tonf}$$

$$R = 7.7 \text{ tonf}$$

$$S = 1.4 \text{ tonf}$$

$$a = 7'-6''$$

$$b = 10'-0''$$

$$c = 12'-0''$$

Fig. 5.13 Frame Geometry And Working Loads

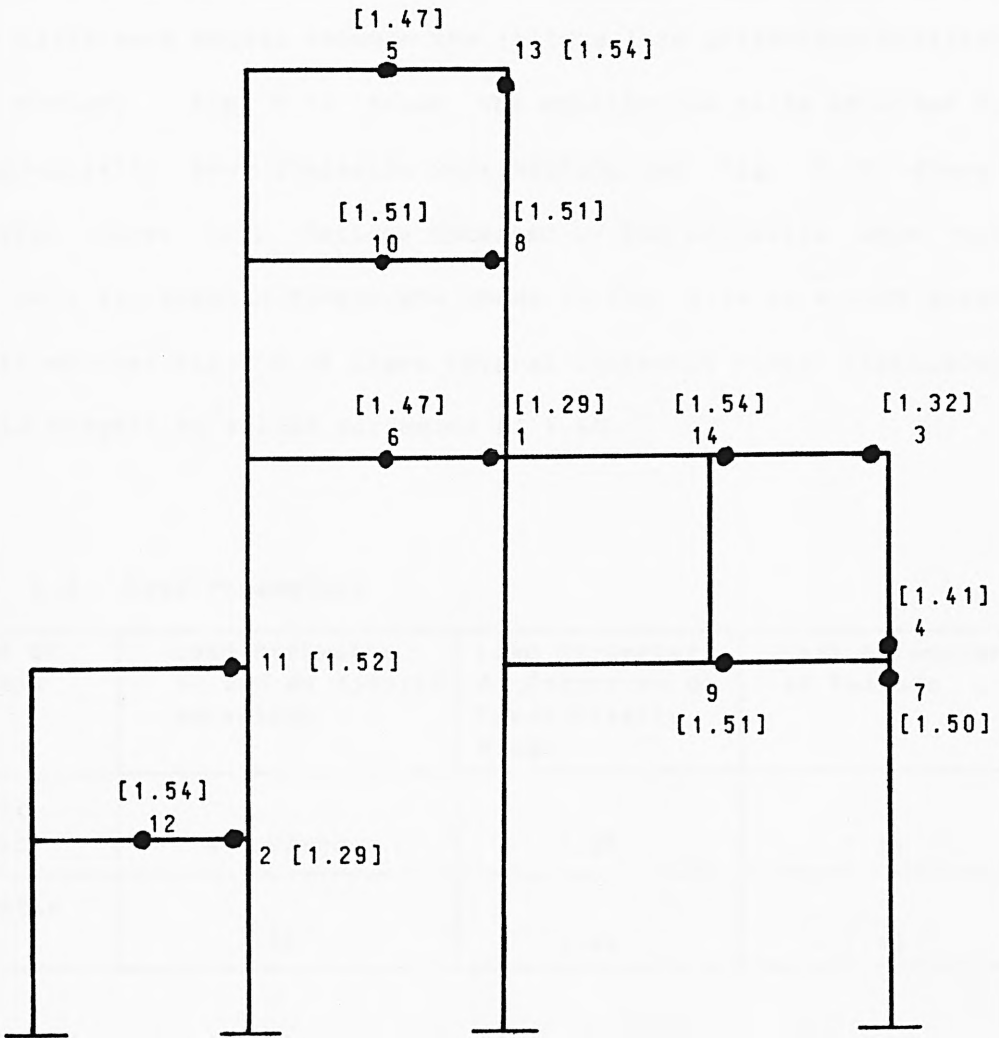
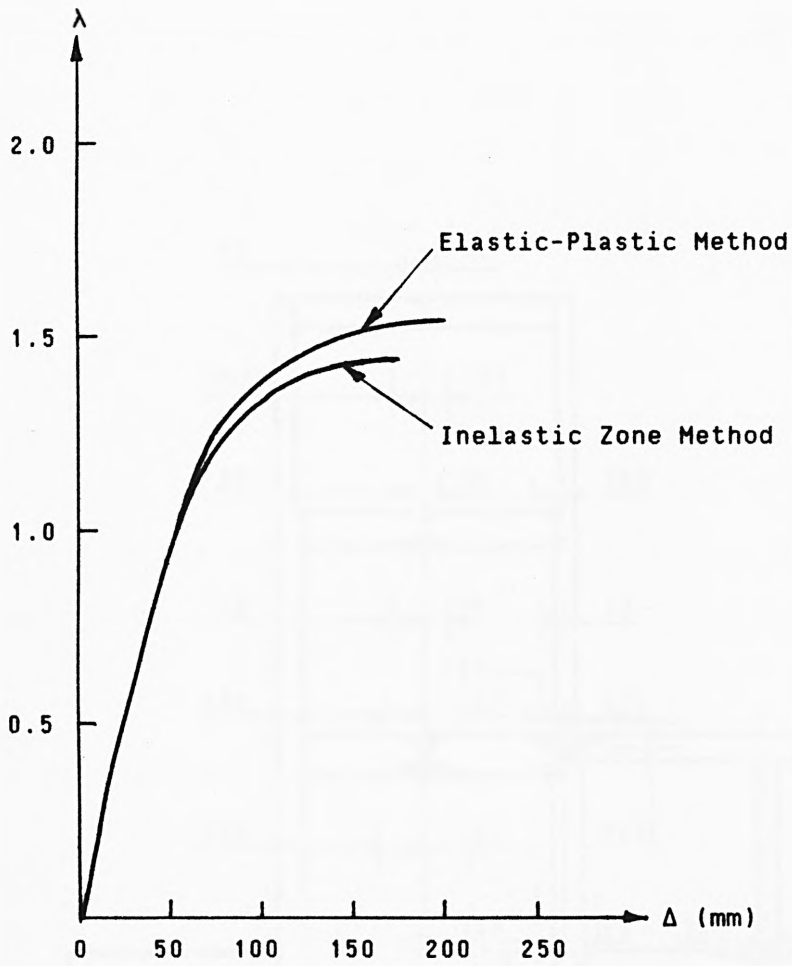


Fig. 5.14 Plastic Hinges At Failure Obtained By The Elastic-Plastic Method

Table 5.8 gives a summary of the load parameters obtained by the elastic-plastic and the inelastic zone methods and shows that the working loads do not cause inelastic effects in the frame although a large difference exists between the failure load parameters obtained by both methods. Fig. 5.15 shows the equilibrium paths obtained by the elastic-plastic and inelastic zone methods and Fig. 5.16 shows the inelastic zones near failure obtained by the inelastic zone method. Also, only six plastic hinges are shown in Fig. 5.14 at a load parameter of 1.47 whereas Fig. 5.16 shows several inelastic zones (including ten plastic hinges) at a load parameter of 1.45.

Table 5.8 Load Parameters

Method Of Analysis	Load Parameter At End Of Elastic Behaviour	Load Parameter At Formation Of First Plastic Hinge	Load Parameter At Failure
Elastic-Plastic	Not Given	1.29	1.54
Inelastic Zone	1.20	1.28	1.46



Δ = horizontal deflection of uppermost roof beam.

Fig. 5.15 Equilibrium Paths Obtained By The Inelastic Zone And Elastic-Plastic Methods

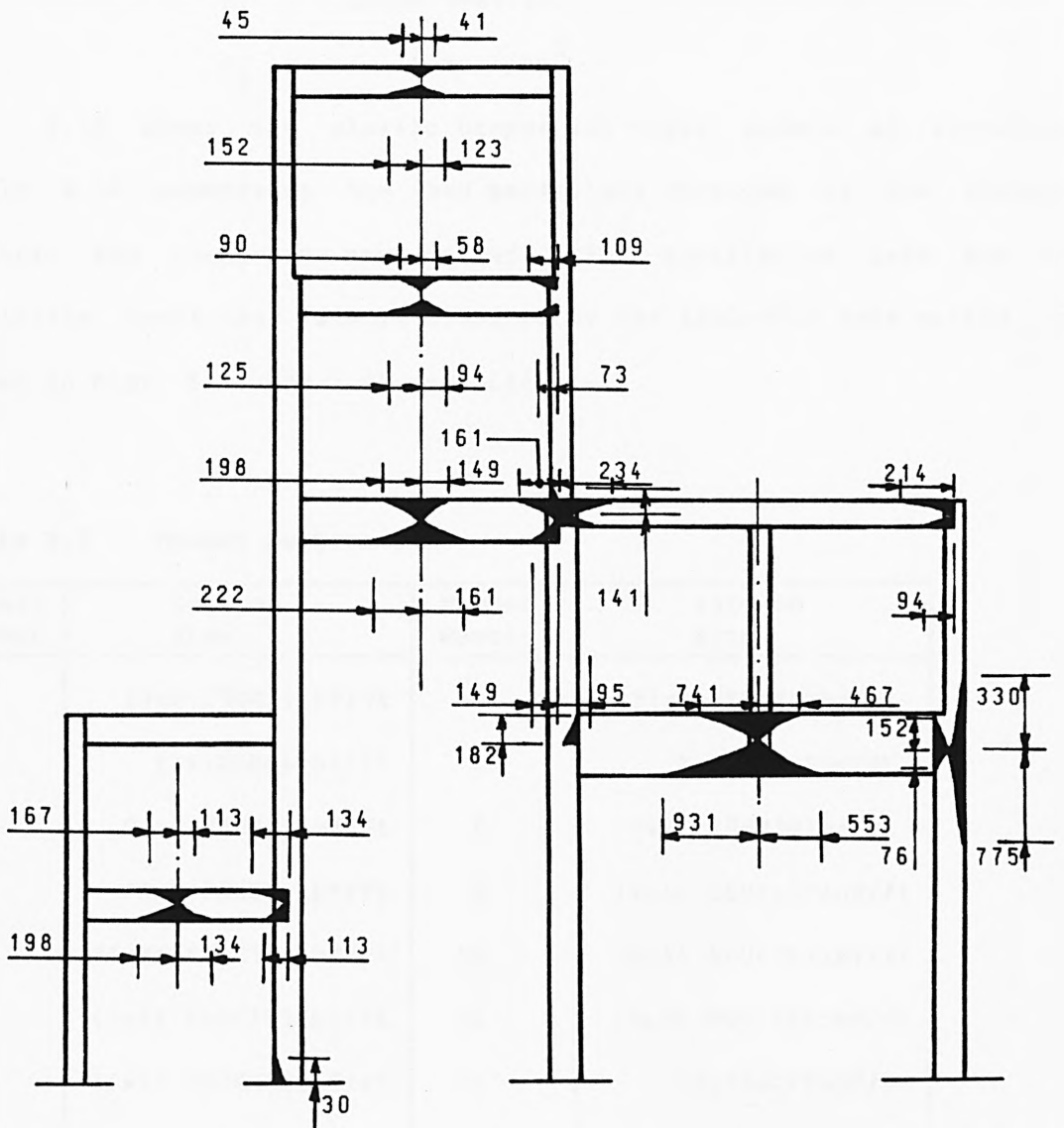


Fig. 5.16 The Inelastic Zones At A Load Parameter Of 1.45

5.2.5 Frame Designed By Anderson (44)

An irregular frame was designed by Anderson based on the elastic-plastic method. The frame geometry and working loads are given in Fig. 5.17. The members have I-shaped cross-sections and the member section sizes are given in Table 5.9. The material is structural mild steel having the following properties:

$$E = 13400 \text{ tonf/in}^2$$

$$\sigma_y = 16 \text{ tonf/in}^2$$

Fig. 5.18 shows the plastic hinges and their orders of formation. Table 5.10 summarizes the load parameters obtained by the elastic-plastic and inelastic zone methods. The equilibrium path and the inelastic zones near failure obtained by the inelastic zone method are shown in Figs. 5.19 and 5.20 respectively.

Table 5.9 Member Section Sizes

Member Number	Section Size	Member Number	Section Size
1	21x8.25UB621bf/ft	2	21x8.25UB551bf/ft
3	27x10UB841bf/ft	4	24x9UB761bf/ft
5	21x8.25UB621bf/ft	6	14x6.75UB301bf/ft
7	18x7.50UB501bf/ft	8	14x14.50UC1191bf/ft
9	14x14.50UC1361bf/ft	10	14x14.50UC1031bf/ft
11	14x14.50UC1031bf/ft	12	14x14.50UC1031bf/ft
13	14x14.50UC1031bf/ft	14	12x12UC791bf/ft
15	12x12UC791bf/ft	16	12x12UC791bf/ft
17	14x14.50UC1361bf/ft		

Member	End	Plastic Moment	Plastic Rotation
1-2	1	1.10	0.00
	2	1.19	0.00
2-3	2	1.19	0.00
	3	1.32	0.00
3-4	3	1.32	0.00
	4	1.36	0.00
4-5	4	1.36	0.00
	5	1.45	0.00
5-6	5	1.45	0.00
	6	1.50	0.00
6-7	6	1.50	0.00
	7	1.51	0.00
7-8	7	1.51	0.00
	8	1.51	0.00
8-9	8	1.51	0.00
	9	1.65	0.00
9-10	9	1.65	0.00
	10	1.69	0.00

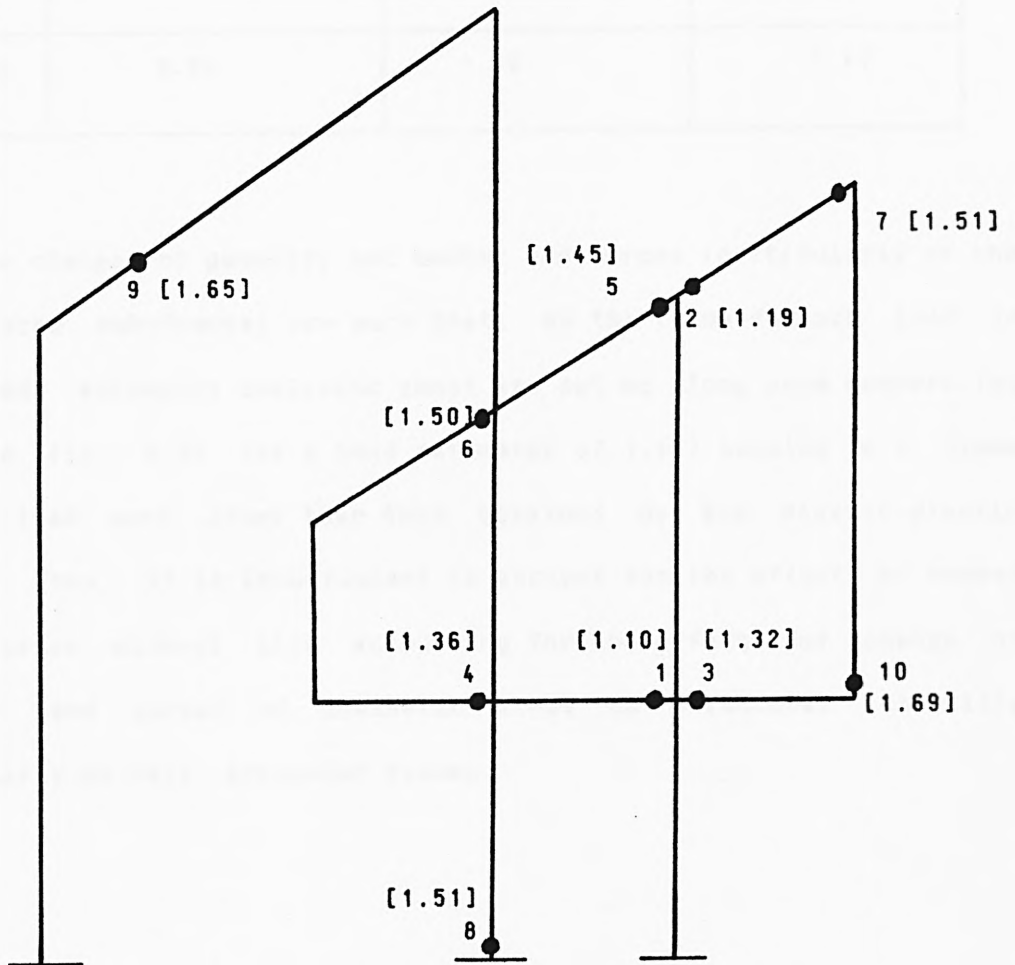
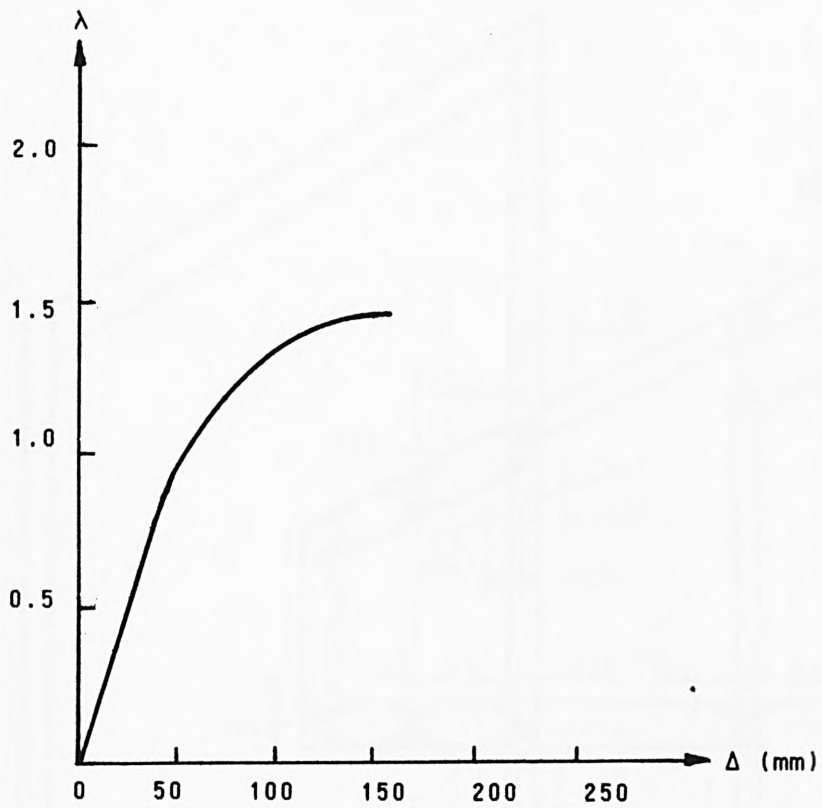


Fig. 5.18 Plastic Hinges Obtained By The Elastic-Plastic Method

Table 5.10 Load Parameters

Method Of Analysis	Load Parameter At End Of Elastic Behaviour	Load Parameter At Formation Of First Plastic Hinge	Load Parameter At Failure
Elastic-Plastic	Not Given	1.10	1.69
Inelastic Zone	0.90	1.10	1.47

The changes of geometry and member end forces (particularly of the cantilevered sub-frames) are such that, as the frame failure load is approached, extensive inelastic zones are set up along some members (as shown in Fig. 5.20 for a load parameter of 1.46) leading to a frame failure load much lower than that obtained by the elastic-plastic method. Thus, it is insufficient to account for the effects of member axial forces without also accounting for the effects of change of geometry and spread of inelastic zones on structural stability particularly of tall, irregular frames.



Δ = vertical deflection of point J (see Fig. 5.17)

Fig. 5.19 Equilibrium Path Obtained By The Inelastic Zone Method

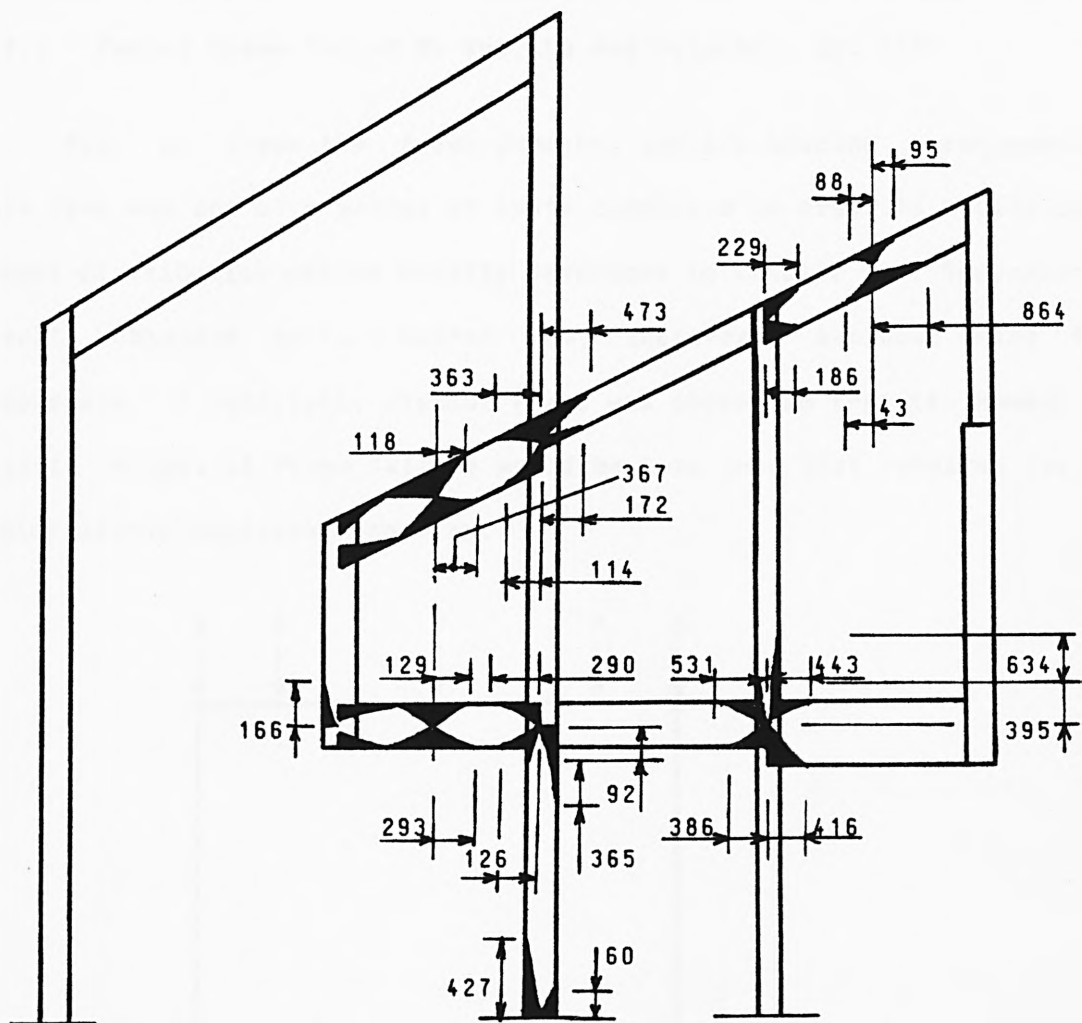


Fig. 5.20 The Inelastic Zones At A Load Parameter Of 1.46

5.3 Experimental Results

In this section, the frame failure loads obtained from a number of reported experiments are compared with those obtained by the proposed inelastic zone method.

5.3.1 Portal Frame Tested By Yen, Lu And Driscoll, Jr. (49)

Fig. 21 shows the frame geometry and its loading arrangements. This test was one of a series of tests conducted in order to verify Lu's moment distribution method briefly described in Chapter 1. Theoretical results obtained by Lu's method are, therefore, included here for comparison. A relatively slender frame was chosen so that the number of plastic hinges at frame failure would be less than that required for a rigid-plastic collapse mechanism.

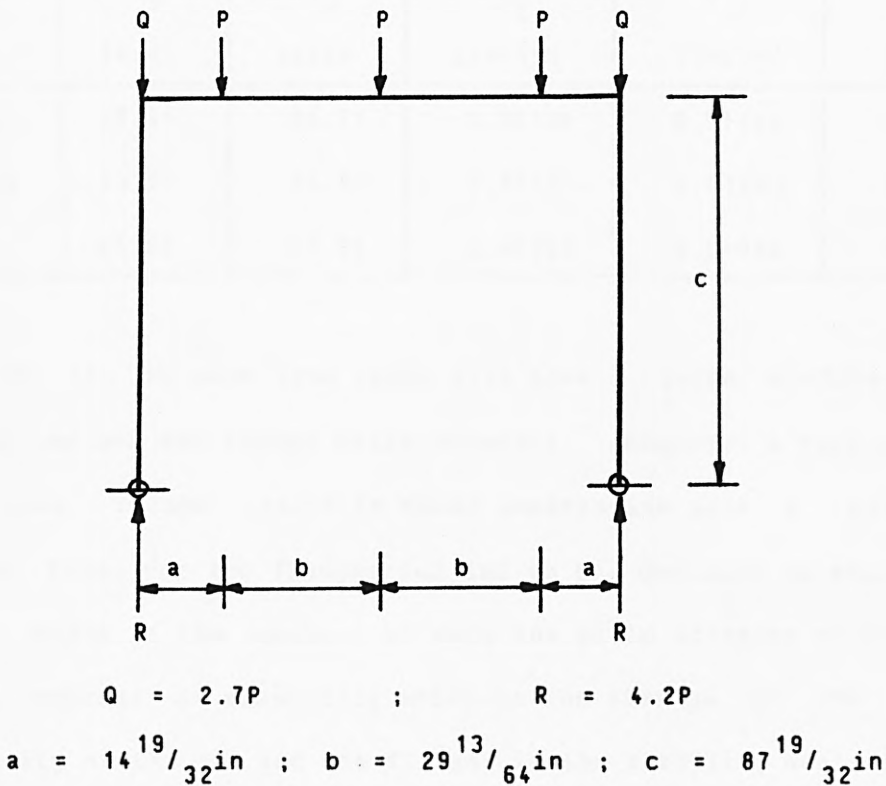


Fig. 5.21 Geometry And Loads For The Test Frame

The frame members were of the same I-shaped cross-section having the following dimensions:

$$H = 2.625 \text{ in}$$

$$B = 1.813 \text{ in}$$

$$T = 0.207 \text{ in}$$

$$t = 0.156 \text{ in}$$

The material was structural steel, the properties of which were obtained by coupon and stub column tests for the stress-strain relationships. The properties obtained by coupon tests are summarized in Table 5.11.

Table 5.11 Summary Of Coupon Test Results

Location	σ_y (ksi)	σ_u (ksi)	ϵ_y (in/in)	ϵ_{sh} (in/in)	E (ksi)
Flange	42.11	54.71	0.00134	0.01336	32047.0
Flange	43.27	54.57	0.00125	0.01403	31592.0
Web	48.28	60.35	0.00167	0.01086	30483.0

It can be seen from Table 5.11 that a large difference exists between the web and flange yield stresses. However, a test on a 6-inch long stub column loaded in axial compression gave a yield stress between those for the flanges and led to the decision to employ a yield stress which is the average of only the yield stresses of the flanges and a modulus of elasticity which is the average of the moduli of elasticity of the web and the flanges in the stability analysis based on Lu's method. Consequently, the properties adopted for analysis were:

(a) $E = 31374.0 \text{ ksi}$

$$\sigma_y = 42.7 \text{ ksi}$$

The strain-hardening properties of the steel were, therefore, ignored in the analysis.

It would, however, be interesting to find out if improved results would be obtained by using average material properties. Thus, in using the inelastic zone method, the following average material properties, obtained by considering all elements of the cross-section, are also employed:

(b) $E = 31374.00 \text{ ksi}$

$$\sigma_y = 44.55 \text{ ksi}$$

Also, in order to estimate the effect of strain-hardening on the behaviour of the frame, the following strain-hardening constants, as defined in Chapter 2, are employed in using the inelastic method:

$$A_s = 40.0$$

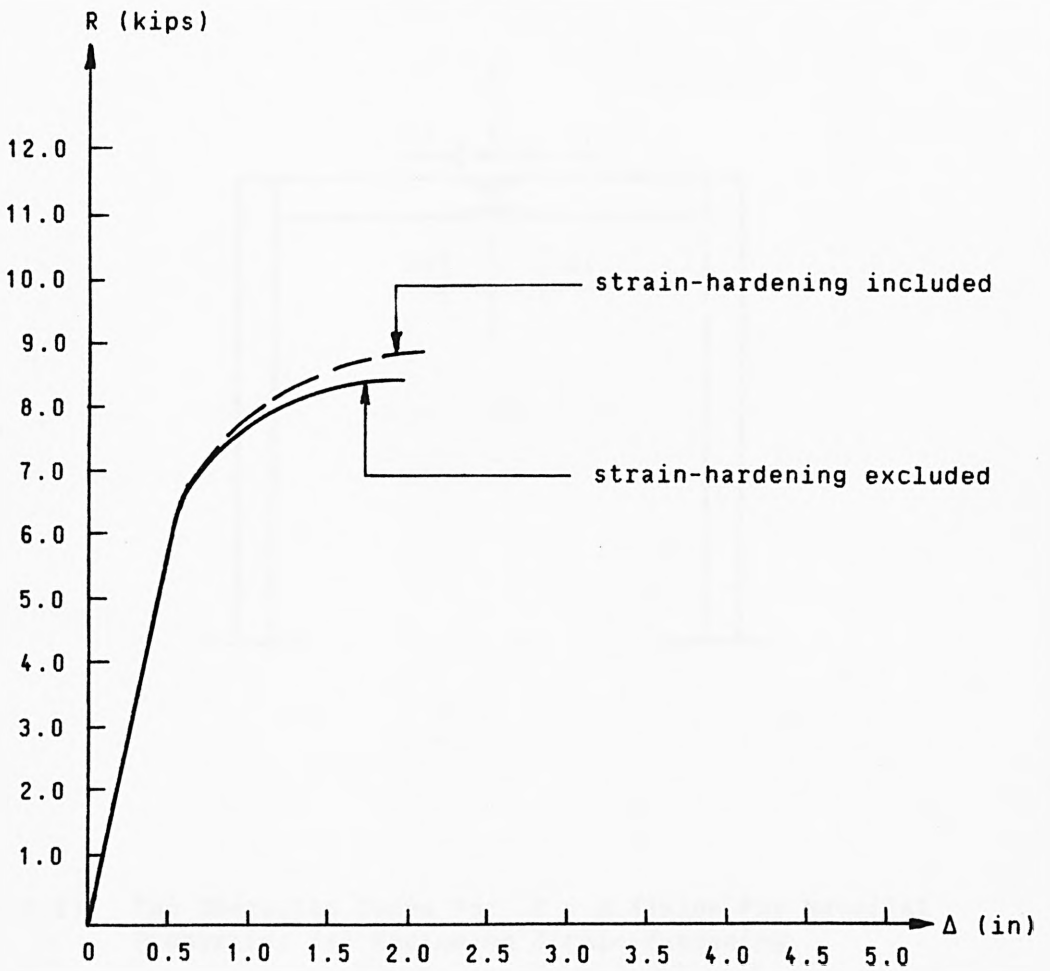
$$B_s = 1.05$$

Fig. 5.22 gives the equilibrium path obtained by the inelastic zone method for the stresses adopted by Yen et al. The inelastic zones present along the frame members were not reported by Yen et al. These zones obtained by the inelastic zone method for a value of the column axial load, R , of 8.31kips are given in Fig. 5.23 for the case excluding strain-hardening. Table 5.12 summarizes the failure loads obtained by Yen et al and by the inelastic zone method. It is evident from Table 5.12 and Fig. 5.23 that the frame has a reserve of strength at a column axial load, R , of 8.31kips although some inelastic zones are present in the frame at this load.

Table 5.12 Values Of The Column Axial Load, R, At Failure

Method	Material Properties	Value Of R At Failure (kips)
Test	Not Applicable	9.16
Lu's Moment Distribution	(a)	8.61
Inelastic Zone (Excluding Strain-Hardening)	(a)	8.50
	(b)	8.81
Inelastic Zone (Including Strain-Hardening)	(a)	8.88
	(b)	9.43

While the failure load given in Table 5.12 by the inelastic zone method for material properties (a) excluding strain-hardening is lower than that obtained by Lu's theory, Table 5.12 shows that results closer to test results are obtained by the proposed inelastic zone method when using average material properties obtained by considering all elements of cross-section and by making some allowance for strain-hardening in the stability analysis of the frame.



Δ = the vertical deflection of centre of beam.

Fig. 5.22 Equilibrium Paths Obtained By The Inelastic Zone Method For Material Properties (a)

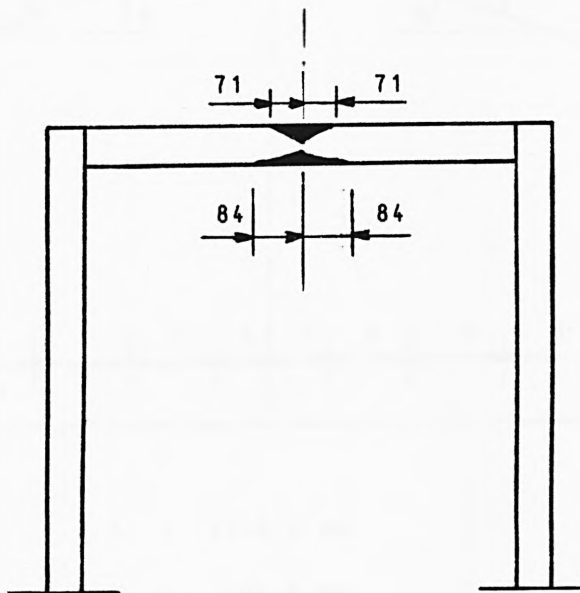
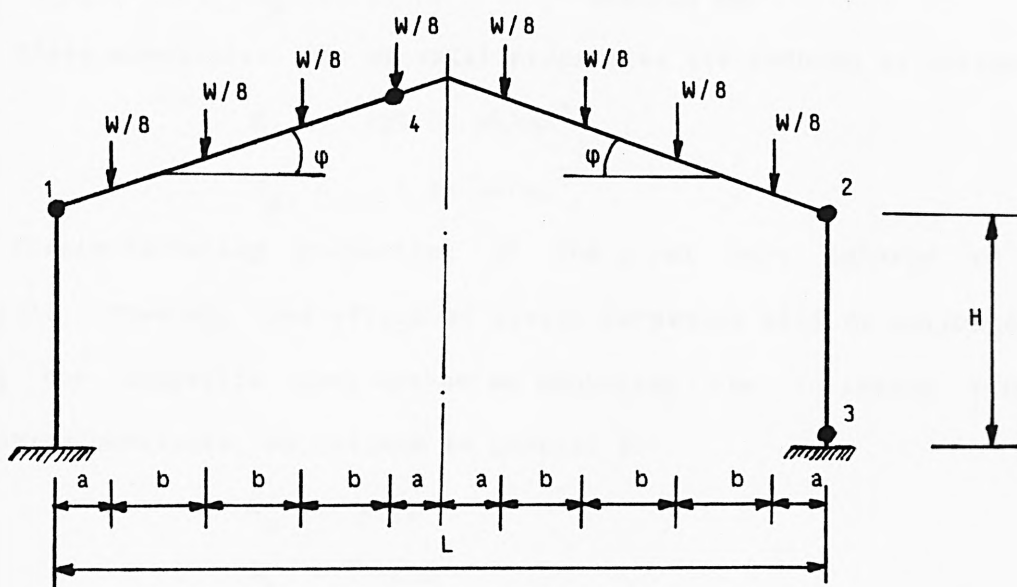


Fig. 5.23 The Inelastic Zones For $R = 8.31$ kips For Material Properties (a) Excluding Strain-Hardening

5.3.2 Pitched-Roof Portal Frame Tested By Majid (43)

The frame geometry and applied loads are given in Fig. 5.24. This frame was also analysed by the elastic-plastic method and the plastic hinges and their orders of formation are also given in Fig. 5.24.



$$L = 1219.0 \text{ mm}$$

$$H = 406.0 \text{ mm}$$

$$\phi = 15^{\circ}$$

$$a = L/16 \text{ mm}$$

$$b = L/8 \text{ mm}$$

Fig. 5.24 Frame Geometry, Loads And Plastic Hinges At Failure

Each frame member had a 13mm x 13mm rectangular cross-section and the material was structural mild steel. No tests were described for determining the material properties. Instead, the following quantities were given for this purpose:

$$M_p \text{ (for zero axial force)} = 153.793 \text{ kN.mm}$$

$$EI_z = 460748.0 \text{ kN.mm}^2$$

The second moment of area and the plastic modulus of the cross-section are computed from the cross-sectional dimensions as

$$I_z = 13^4/12 = 2380.083 \text{ mm}^4$$
$$S_p = 13^3/4 = 549.250 \text{ mm}^3$$

From these quantities, the material properties are deduced as follows:

$$E = 193.59 \text{ kN/mm}^2$$
$$\sigma_y = 0.28 \text{ kN/mm}^2$$

The strain-hardening properties of the steel were ignored in the analysis. However, the effect of strain-hardening will be estimated in using the inelastic zone method by employing the following strain-hardening constants, as defined in Chapter 2:

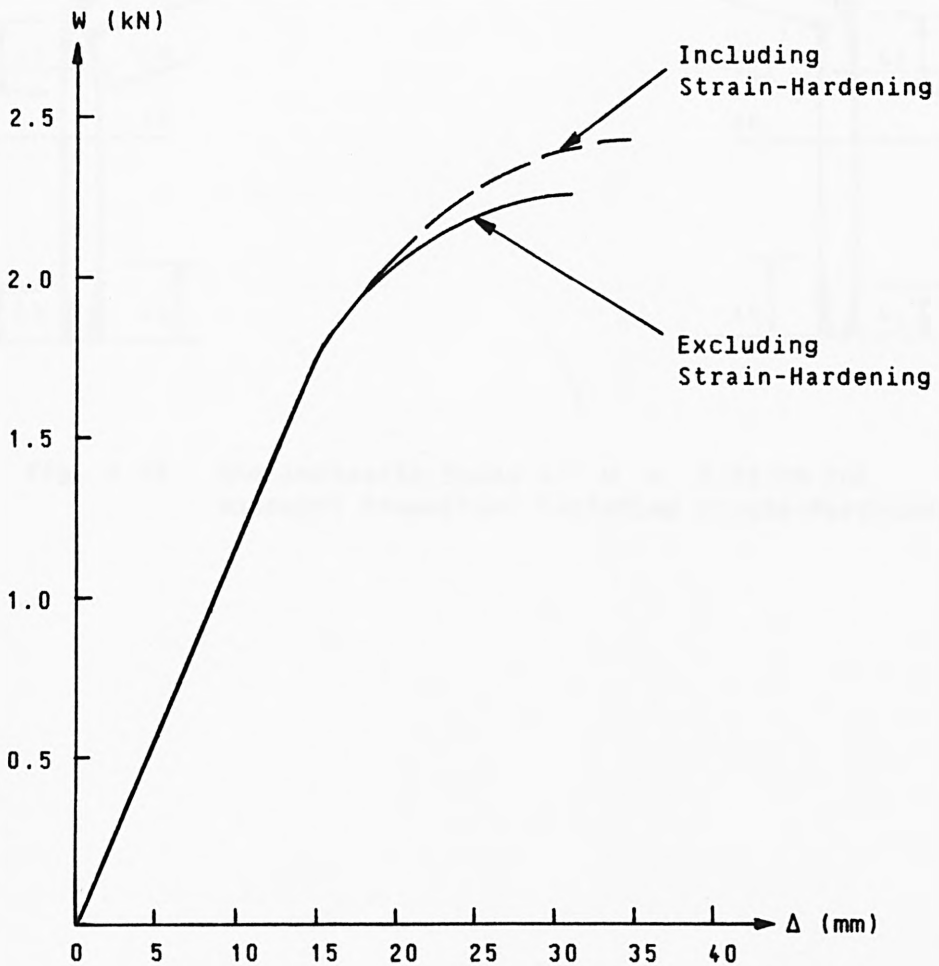
$$A_s = 40.0$$
$$B_s = 1.10$$

The failure loads obtained by the test, the elastic-plastic method and the inelastic zone method, are summarized in Table 5.13. Fig. 5.25 shows the equilibrium paths obtained by the inelastic zone method for the cases including and excluding strain-hardening. The inelastic zones near failure obtained by the inelastic zone method are given in Fig. 5.26.

Majid attributed the difference of 2.5% between the test and analytical results to the strain-hardening property of the steel. However, this difference may also be due to the material properties employed in the analysis and to the adoption of the concentrated inelasticity concept of structural behaviour in the elastic-plastic method. The failure value of W obtained by the inelastic zone method ignoring strain-hardening is lower than that obtained by the elastic-plastic method while the inclusion of some strain-hardening gives a result closer to the test result.

Table 5.13 Values Of The Applied Load, W, At Failure

Method	Value Of W At Failure (kN)
Test	2.469
Elastic-Plastic (Excluding Strain-Hardening)	2.406
Inelastic Zone (Excluding Strain-Hardening)	2.260
Inelastic Zone (Including Strain-Hardening)	2.420



Δ = vertical deflection of the apex of the frame.

Fig. 5.25 Equilibrium Paths Obtained By The Inelastic Zone Method

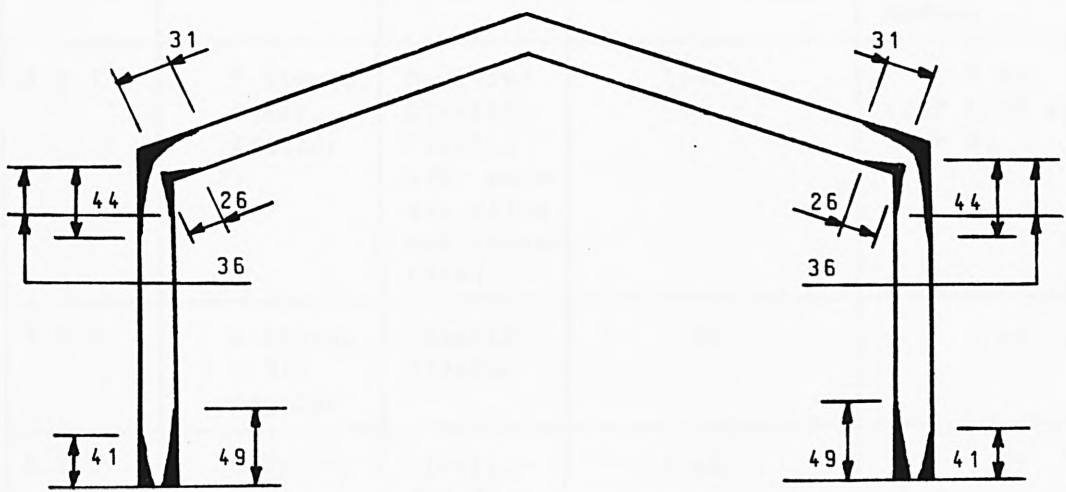


Fig. 5.26 The Inelastic Zones At $W = 2.22$ kN For Material Properties Excluding Strain-Hardening

5.4 Summary Of Frame Failure Load Parameters

Table 5.14 gives a summary of the failure load parameters obtained analytically for the frames considered in this chapter.

Table 5.14 Failure Load Parameters

Section	Type Of Frame	Existing Method Of Analysis	Results Obtained By Using The Existing Method	Results Obtained By Using The Proposed Inelastic Zone Method
5.2.1	3-Storey, 4-Bay, Regular	Modified Elastic-Plastic (for geometrically, non-linear case)	1.50	1.50 (for load simulation B)
5.2.2	4-Storey, 1-Bay, Regular	Elastic-Plastic	1.49	1.48
5.2.3	6-Storey, 2-Bay, Regular	Elastic-Plastic	1.42	1.41
5.2.4	5-Storey, Irregular	Elastic-Plastic	1.54	1.46
5.2.5	Irregular	Elastic-Plastic	1.69	1.47
5.3.1	Regular Portal	Moment-Distribution	8.61 [for unit value of R (see Fig. 5.21)] (Test result = 9.16)	8.50 (excluding strain-hardening)
				8.88 (including strain-hardening)
5.3.2	Pitched-Roof Portal	Elastic-Plastic	2.406 [for unit value of W (see Fig. 5.24)] (Test result = 2.469)	2.26 (excluding strain-hardening)
				2.42 (including strain-hardening)

CHAPTER 6

EXPERIMENTS

6.1 Introduction

The comparisons made in Chapter 5 between the results obtained by the inelastic zone method and some existing theoretical and experimental methods vindicate the inelastic zone method as a viable, theoretical tool for obtaining lower-bound values of frame failure loads. With the exception of the portal frames tested by Yen, Lu and Driscoll (see Section 5.3.1), the remaining frames have storey-height columns of low slenderness ratios and are, therefore, representative of those found in practice. Moreover, the test results given in Section 5.3.2 applied to frames which were braced during the tests against out-of-plane failure occurring before in-plane frame failure as is customarily required for plane frame analysis. The locations of inelastic zones along the frame members for the frames loaded into the inelastic domain were neither reported from the tests nor from the analyses.

In this chapter, experiments on two slender, regular portal frames unbraced both in-plane and out-of-plane and also subjected to both vertical and horizontal concentrated loads are reported. The horizontal load/vertical load ratio adopted was of a magnitude much higher than that commonly found in practice. The objectives for these tests were

1. to determine the distribution of inelastic zones along frame members for frames loaded into the inelastic domain and
2. to compare the results obtained experimentally with those obtained analytically by the inelastic zone method.

6.2 Frame Geometry And Loads

Two portal frames, each loaded as shown in Fig. 6.1, were adopted for the tests. These frames were designated as frames T1 and T2 respectively for distinction. A 127x76x13.36kg/m rolled, mild steel joist was selected for the frame members. The height, h , for frame T1

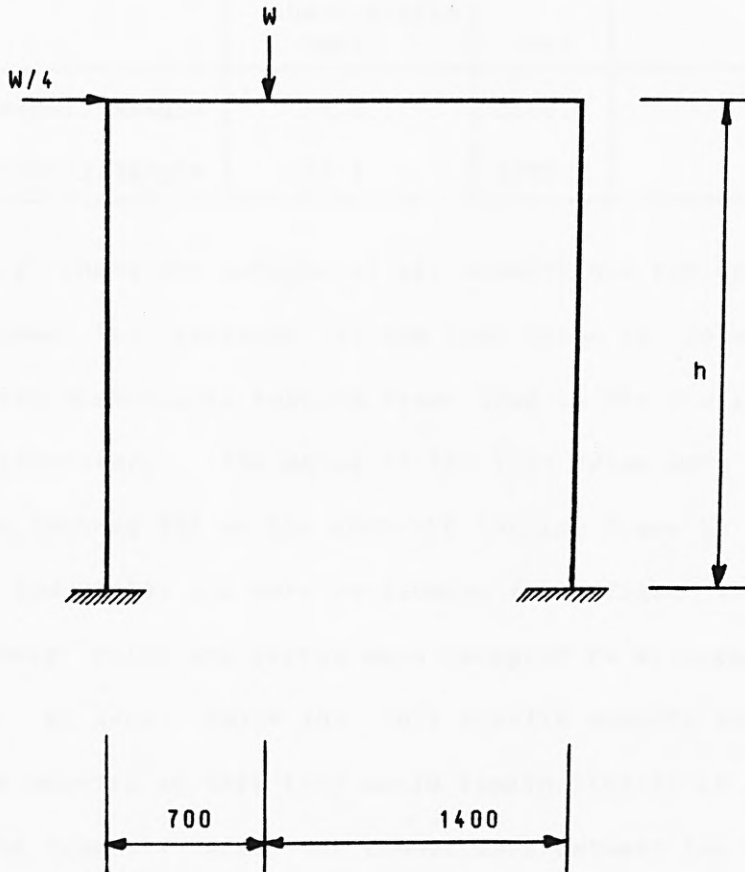


Fig. 6.1 Geometry And Loads For Test Frame

was chosen so as to give an actual height/minor axis radius of gyration ratio of about 145 which can be considered to be high for practical frames. This ratio will hereafter be called an **actual slenderness ratio** in order to distinguish it from a column **slenderness ratio** in which the "effective height" of the column is considered instead of its actual height. The height of frame T2 was taken to be 500mm lower than that of

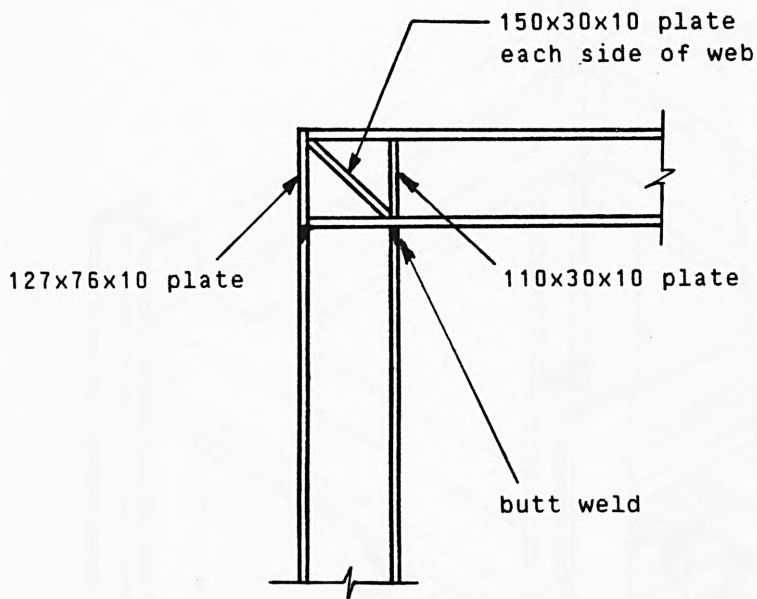
frame T1 so as to give an actual slenderness ratio of about 116.0. Table 6.1 shows the actual slenderness ratios adopted for the columns.

Table 6.1 Actual Slenderness Ratios For Test Frame Columns

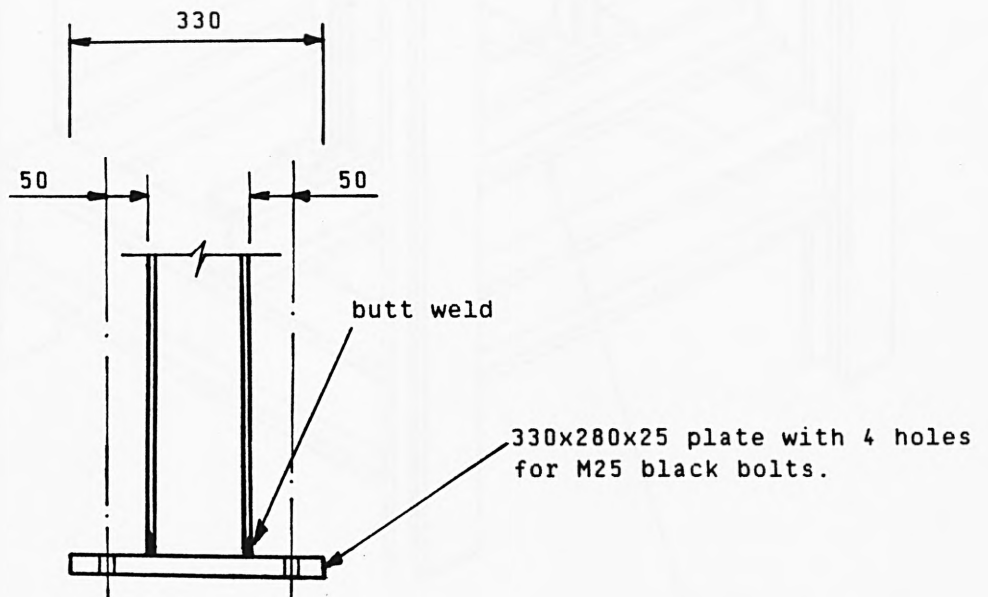
Frame	Column Section Size	Radius Of Gyration About y-axis (mm)	Height h (mm)	Actual Slenderness Ratio
T1	127x76x13.36kg/m	17.2	2500.0	145.35
T2	127x76x13.36kg/m	17.2	2000.0	116.28

Fig. 6.2 shows the details of all connections for one test frame. Fig. 6.3 shows the location of one test frame in relation to the standard three-dimensional testing frame used in the Civil Engineering Structures Laboratory. The bases of the test frame were bolted on to the deep beam (marked B3) of the standard testing frame by means of mild steel bolts and plates and were considered fully fixed for analytical purposes. These bolts and plates were designed to withstand the forces arising from, at least, twice the full plastic moments of the sections for the frame members so that they would remain elastic at all stages of loading of the frames. Also, the connections between the frame members were stiffened by plates in order to ease the force transfer between these members thus avoiding local buckling of the plate elements of the member cross-sections and the setting-up of high stress concentrations.

As shown in Fig. 6.1, the concentrated vertical load on the test frame was offset from the centre of the test frame beam so as to cause sideways of the test frame at any value of the load. Also, the concentrated horizontal load was chosen to be one-quarter of the vertical load so as to give a high horizontal load/vertical load ratio.



(a) Knee Details



(b) Base Details

Note: 6mm fillet welds are used except noted otherwise.

Fig. 6.2 Connection Details For Test Frame

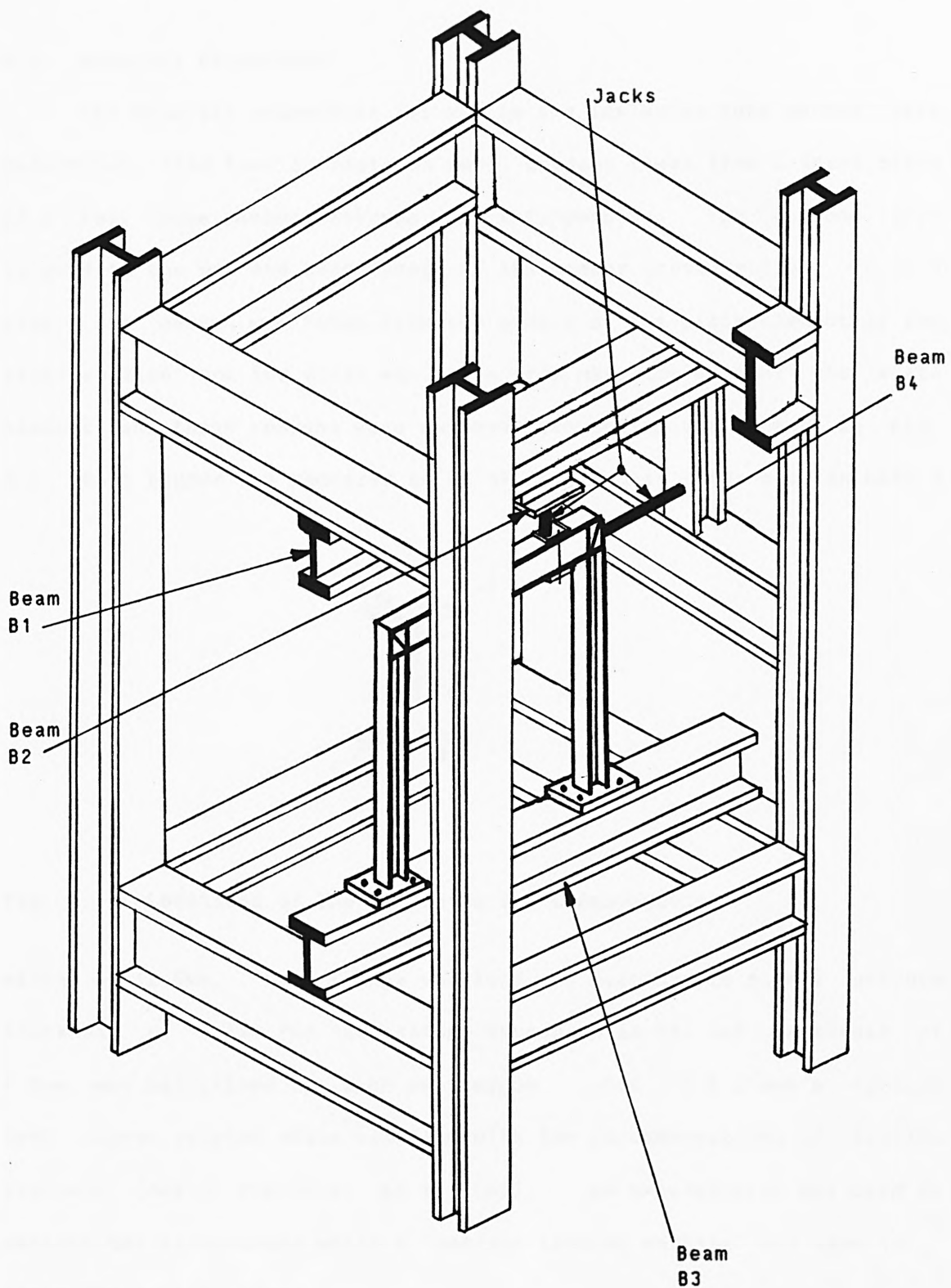


Fig. 6.3 The Test Frame On The Standard Testing Frame

6.3 Material Properties

The material properties for use in the inelastic zone method were determined from tensile tests on small coupons taken from a spare piece of a test frame member reserved for this purpose. Two coupons were taken from the web and each flange of the member cross-section. In each case, one coupon was taken from the centre of the plate element of the cross-section and the other was taken from near the edge of the plate element and these coupons were numbered sequentially as shown in Fig. 6.4. Each coupon was required to be of rectangular cross-section with a

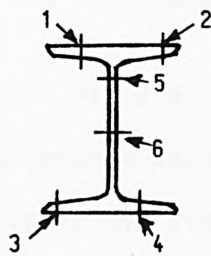


Fig. 6.4 Locations Of The Coupon On The Cross-Section

width of 12.5mm. Each flange outstand was machined to give a uniform thickness of 4.7mm for each flange coupon while the web thickness of 4.5mm was maintained for each web coupon. Fig. 6.5 shows a typical test coupon adopted which complied with the recommendations of British Standard Code of Practice, BS 18 (89). An extensometer was used to measure the elongations while a "Denison testing machine" was used to apply the tensile loads.

The testing of each coupon was commenced by taking readings of the extensometer at no load on the coupon. Then, the loads were applied in small increments of 400.0lbf, each time taking readings of the

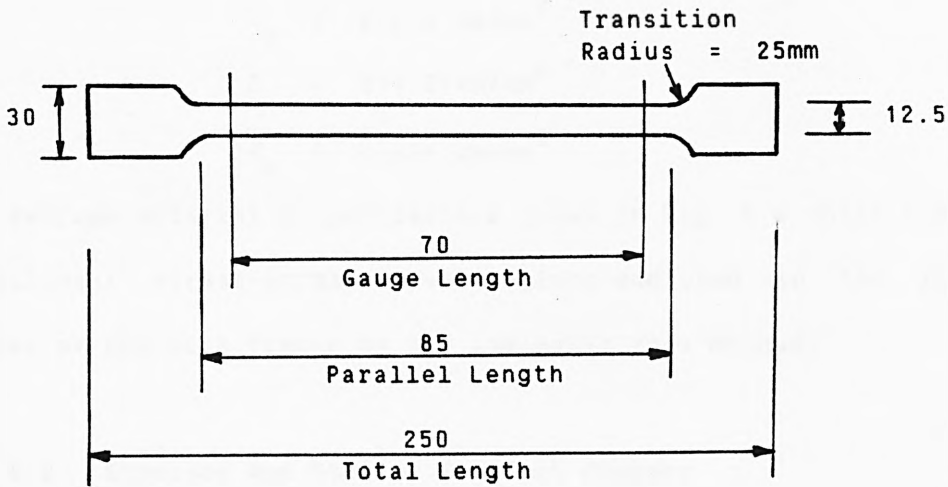


Fig. 6.5 A Typical Test Coupon

extensometer, until a point was reached at which the material exhibited plastic flow when the elongations increased rapidly at the constant load and the material yield stress was attained. When the rate of plastic flow slowed down sufficiently to indicate that the point of equilibrium under the constant load at which strain-hardening would commence was being approached, the extensometer was removed and the "Denison testing machine" was set to full power thus loading the coupon to the point of fracture. This fracture was characterized by a slight reduction of width (the phenomenon of "**necking**") for, and a large total elongation of, each coupon. The resulting stresses and strains for the coupons are given in Table 6.2.

It can be seen from Table 6.2 that the material properties for the cross-section are not constant and are greater for the web than for the flanges. However, these properties are reasonably close together so as to permit the use of average material properties for analysis as is commonly adopted in practical frame design. Thus, the average values of the material properties are as follows:

$$\epsilon_y = 0.00130 \text{ mm/mm}$$

$$\sigma_y = 0.275 \text{ kN/mm}^2$$

$$E = 211.54 \text{ kN/mm}^2$$

$$\sigma_u = 0.459 \text{ kN/mm}^2$$

These average material properties are shown in Fig. 6.6 which also shows the bilinear stress-strain idealizations employed in the stability analyses of the test frames by the inelastic zone method.

Table 6.2 Stresses And Strains For Test Coupons

Coupon Number	Element Of Cross-Section	Yield Stress σ_y (kN/mm ²)	Yield Strain ϵ_y (mm/mm)	Ultimate Stress σ_u (kN/mm ²)
1	Flange	0.259	0.00108	0.441
2	Flange	0.265	0.00115	0.442
3	Flange	0.276	0.00120	0.443
4	Flange	0.270	0.00109	0.443
5	Web	0.285	0.00148	0.491
6	Web	0.293	0.00180	0.491

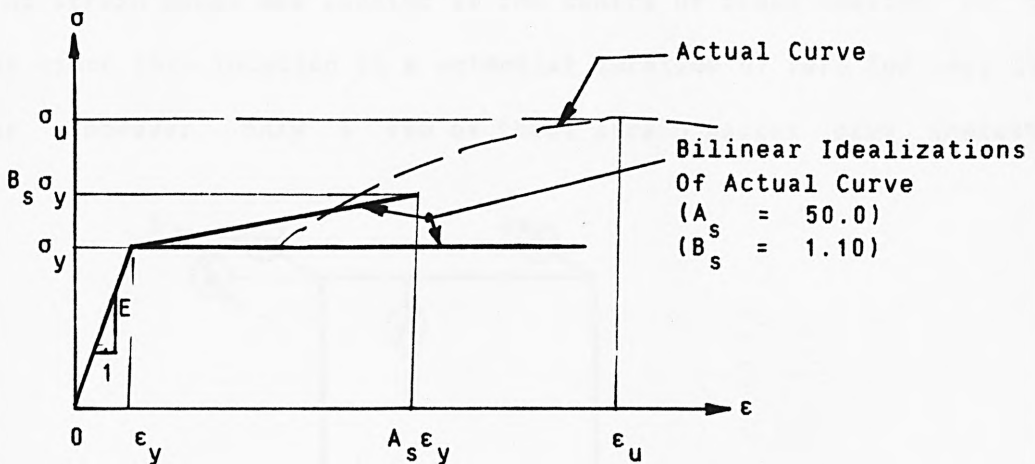


Fig. 6.6 Representative Stress-Strain Diagram For The Mild Steel For The Test Frames

6.4 Instrumentation For Frame Testing

Hydraulic jacks were employed for the application of the loads, dial gauges for the measurement of in-plane and out-of-plane movements and electrical-resistance strain gauges for the measurement of strains.

For each test frame, a 100-kN capacity jack was employed for the vertical load while a 30-kN capacity jack was employed for the horizontal load. A 100mm x 50mm x 6mm thick rectangular plate was placed between the jack and the relevant frame member in order to keep the local bearing stress on the frame member to very low levels within the elastic range.

Also, for each test frame, four dial gauges, numbered and located as shown in Fig. 6.7, were used. Dial gauge 1 measured in-plane horizontal movement of the point of application of the horizontal load, dial gauge 2 measured vertical movement of the point of application of the vertical load and dial gauges 3 and 4 measured out-of-plane horizontal movements of the tops of the two columns.

For test frame T1, 112 strain gauges were employed as shown in Fig. 6.8. A minimum spacing of 50mm was adopted for these strain gauges and no strain gauge was located at the centre of cross-section of the member since this location is a potential location of zero (or very low) stress. However, only a few of these strain gauges gave inelastic

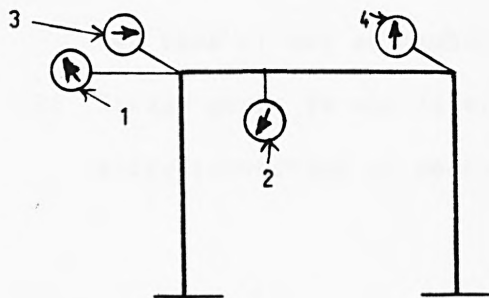
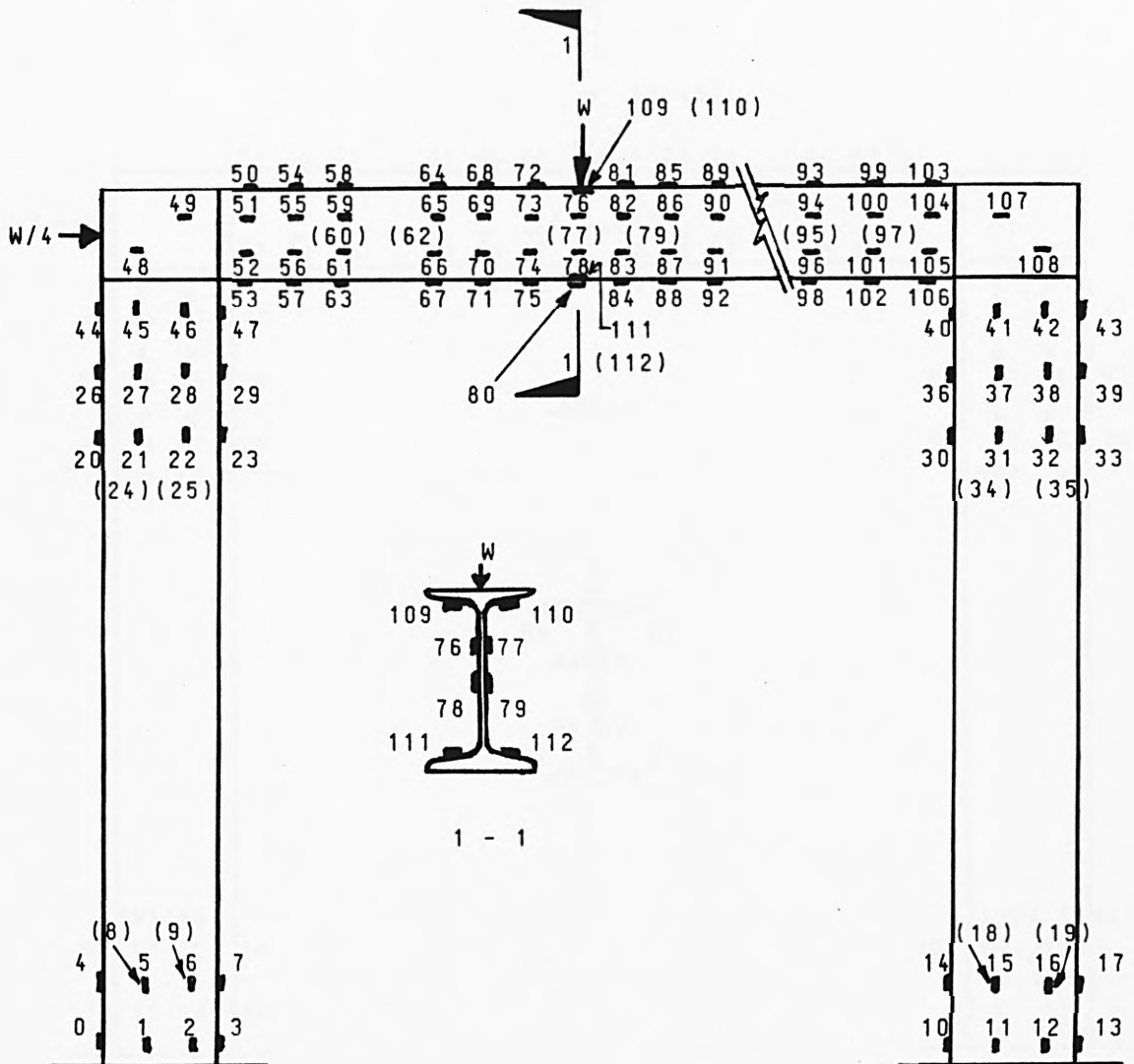
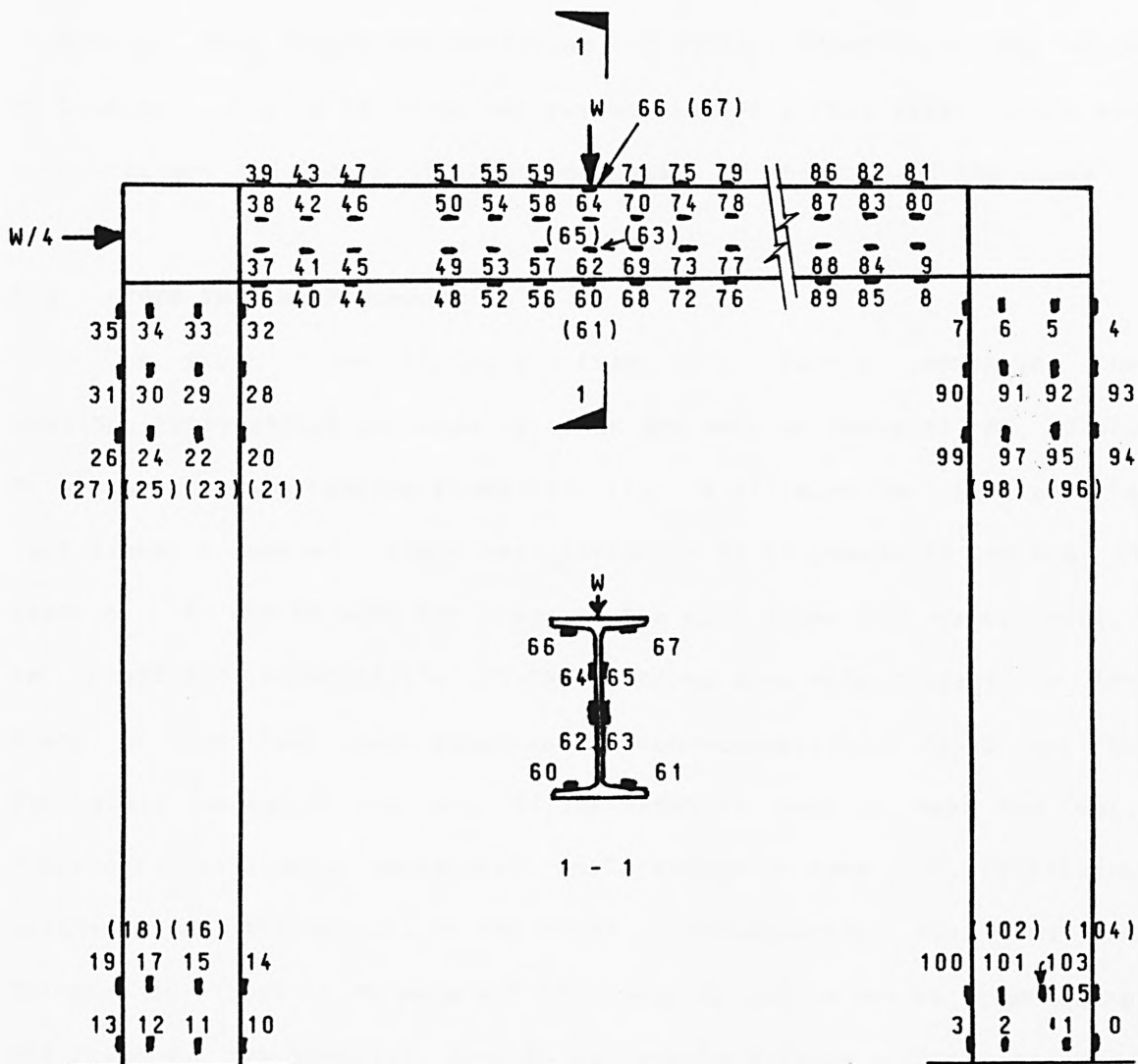


Fig. 6.7 Locations Of Dial Gauges



- Notes: (1) Numbers in brackets are for strain gauges on the far side of web of member.
- (2) Strain gauge 80 was later abandoned in order to allow connection of vertical-load jack to member.

Fig. 6.8 Locations Of Strain Gauges For Test Frame T1



Note: Numbers in brackets are for strain gauges on the far side of web of member.

Fig. 6.9 Locations Of Strain Gauges For Test Frame T2

strains at frame failure. Consequently, for test frame T2, the number of strain gauges was reduced to 100 as shown in Fig. 6.9. All the strain gauges were connected by means of electrical leads to a "Compulog" data logger for measuring the strains directly at any stage of loading. Fig. 6.16 shows the overall view of a test frame, jacks and strain gauges and Fig. 6.17 shows the detail of the knee of the frame.

6.5 Frame Testing Procedure

The first frame tested was frame T1. Before commencing the testing, every effort was made to align the webs of beams B1, B2, B3 and B4 of the standard testing frame (see Fig. 6.3) with the plane of the test frame. However, there was difficulty of alignment of the webs of beams B1, B2 and B3 with the plane of the test frame and, consequently, an inevitable eccentricity of the vertical load with respect to the plane of the test frame remained. This eccentricity could not be accurately measured but was of the order of 2mm to 4mm and was, therefore, initially considered small enough to have no significant influence on the results of the tests. Consequently, the webs and flanges of these beams were not stiffened by plates before commencing the testing. By contrast, beam B4 was easily aligned with the plane of the test frame to give no eccentricity of the applied horizontal load.

The testing of frame T1 commenced by taking initial readings of the dial and strain gauges when no load was applied to the test frame. These readings were recorded. Then, the vertical load was set to 10.0kN while the horizontal load was simultaneously set to 2.5kN in order to maintain the required proportion between these loads. Further readings of the dial and strain gauges were taken and recorded. Vertical load increments of 10.0kN were adopted for strains less than a strain of

0.001mm/mm which is very close to the minimum yield strain of 0.00108mm/mm (see Table 6.2) for the mild steel. After the first attainment of this strain at a strain gauge location, the vertical load increments were reduced to 5kN, then to 4kN and finally to 2kN as the frame failure load was approached. In each case, the horizontal load increment was correspondingly reduced and dial and strain gauge readings were taken and recorded.

The out-of-plane horizontal deflections of the tops of the frame were found to be insignificant until the vertical load reached a value of 56.0kN at which the frame exhibited significant inelastic strains. At this juncture, the larger out-of-plane horizontal deflection was given by dial gauge 4 as 3.73mm. Also, at this load, the "vertical-load" jack had a slight deviation from the vertical plane. This was thought to be due more to the inevitable eccentricity of the vertical load than to the lack of out-of-plane restraints for the tops of the frame since the bottom flange of beam B2 (see Fig. 6.3) was slightly bent by the "vertical-load" jack applying its load non-uniformly on this flange. The frame testing was, therefore, stopped and the frame was unloaded in order to prevent lateral-torsional buckling of the test frame beam and so that beam B2 could be stiffened. The corresponding dial and strain gauge readings at the unloading of the frame were also taken and recorded.

The web and flanges of beam B2 were stiffened on either side of its web by 12.0mm thick rectangular plates at three locations (one at the jack position and each of the other two at 150.0mm away from the jack position). The stiffeners are shown in Fig. 6.18. The frame testing was then commenced by using only three load increments to reach

the value of the vertical load of 56.0kN at which the test frame was unloaded since unloading is elastic even in the inelastic range. At the vertical load of 56.0kN, no further bending of the bottom flange of beam B2 was observed and the vertical-load jack remained vertical indicating the beneficial effect of the stiffening of beam B2 and confirming that the lack of out-of-plane restraints was not detrimental to the stability of the frame at this load. The frame testing continued above this load with the frame remaining stable as long as the maximum out-of-plane horizontal deflection of the knee of the test frame remained lower than the maximum in-plane horizontal deflection of the knee. A critical load was eventually reached at which a large, in-plane horizontal deflection of the knee followed by an uncontrolled out-of-plane horizontal deflection of the top of the test frame column remote from the horizontal load (given by dial gauge 4) occurred and no dial or strain-gauge readings could be taken. This critical load was taken to be the frame failure load and the frame testing was then stopped.

Frame T2 was next tested. The procedure adopted here was similar in many respects to that adopted for frame T1 except that the stiffened beam B2 was now advantageously used from the onset of the testing.

6.6 Frame Test Results

The results obtained from the tests are given in this section. In each case, only strains not less than 0.001mm/mm are tabulated for the last loads at which readings could be taken. The inelastic zones for each frame at these loads are also given. Furthermore, the resulting equilibrium paths for the frames are given and the test results are compared with those obtained by the inelastic zone method. A negative sign is adopted here for a tensile strain.

Results For Test Frame T1

The relevant strain gauge readings are given in Table 6.3. Owing to the non-uniformity of yield stress for the member cross-section and with reference to Table 6.3 and Fig. 6.8, it can be seen that a scattered pattern of inelastic zones results. However, it is clear that zones of elasticity and inelasticity co-exist along the frame members for the frame loaded into the inelastic domain. Thus, from these results, a distribution of inelastic zones near failure showing zones subjected to inelastic strains irrespective of the magnitudes of the strains is given in Fig. 6.10. Fig. 6.11 shows the inelastic zones obtained by the inelastic zone method and Fig. 6.12 shows the equilibrium paths obtained by experiment and by the inelastic zone method.

Table 6.3 Last Recorded Strains Not Less Than 0.001mm/mm For Test Frame T1

Vertical Load, W = 64.0kN					
Strain Gauge Number	Strain ϵ ($\times 10^{-2}$) (mm/mm)	Strain Gauge Number	Strain ϵ ($\times 10^{-2}$) (mm/mm)	Strain Gauge Number	Strain ϵ ($\times 10^{-2}$) (mm/mm)
10	0.298	13	0.494	30	0.114
33	-0.100	39	-0.140	40	0.161
41	0.148	43	-0.116	64	0.105
68	0.125	71	-0.151	72	0.500
73	0.405	74	-0.291	75	-0.617
76	0.413	77	0.387	78	-0.413
79	-0.434	85	0.106	88	-0.140
106	0.125	107	-0.375	110	-1.235
112	-0.145				

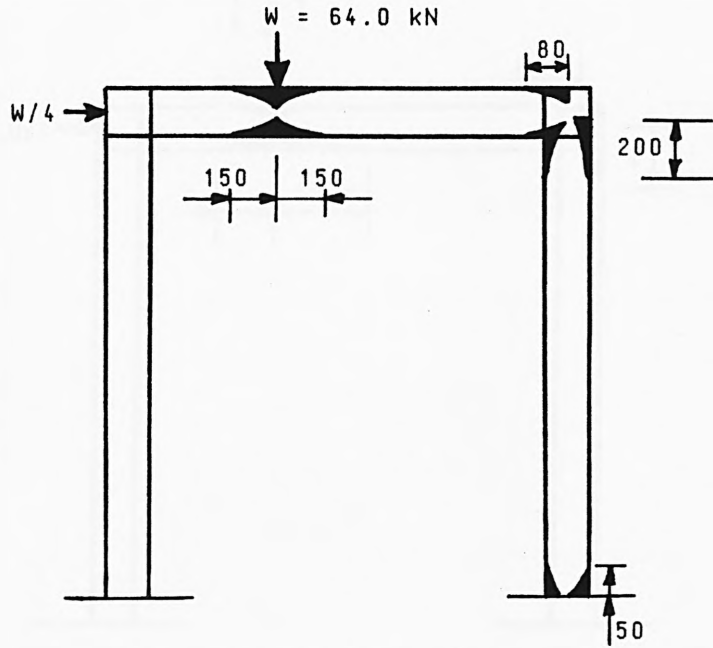
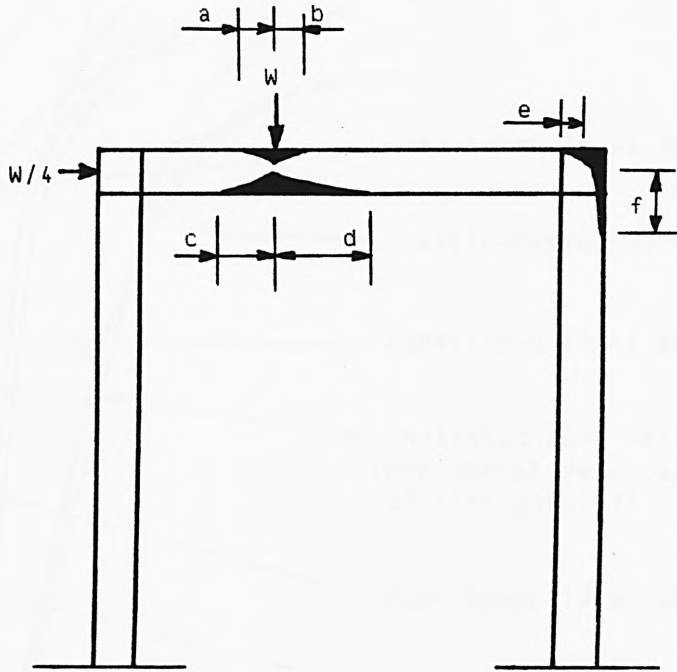


Fig. 6.10 The Inelastic Zones Near Failure Obtained By Experiment For Test Frame T1



For elastic-perfectly-plastic material,

$$a = b = e = f = 0 \quad ; \quad c = 22 \text{ mm} \quad ; \quad d = 27 \text{ mm}$$

For elastic-strain-hardened material,

$$a = 33 \text{ mm} \quad ; \quad b = 42 \text{ mm} \quad ; \quad c = 65 \text{ mm} \quad ; \quad d = 82 \text{ mm} \quad ; \quad e = 26 \text{ mm} \quad ; \quad f = 97 \text{ mm}$$

$$W = 63.0 \text{ kN for elastic-perfectly-plastic material}$$

$$W = 68.0 \text{ kN for elastic-strain-hardened material}$$

Fig. 6.11 The Inelastic Zones Near Failure Obtained By The Inelastic Zone Method For Test Frame T1

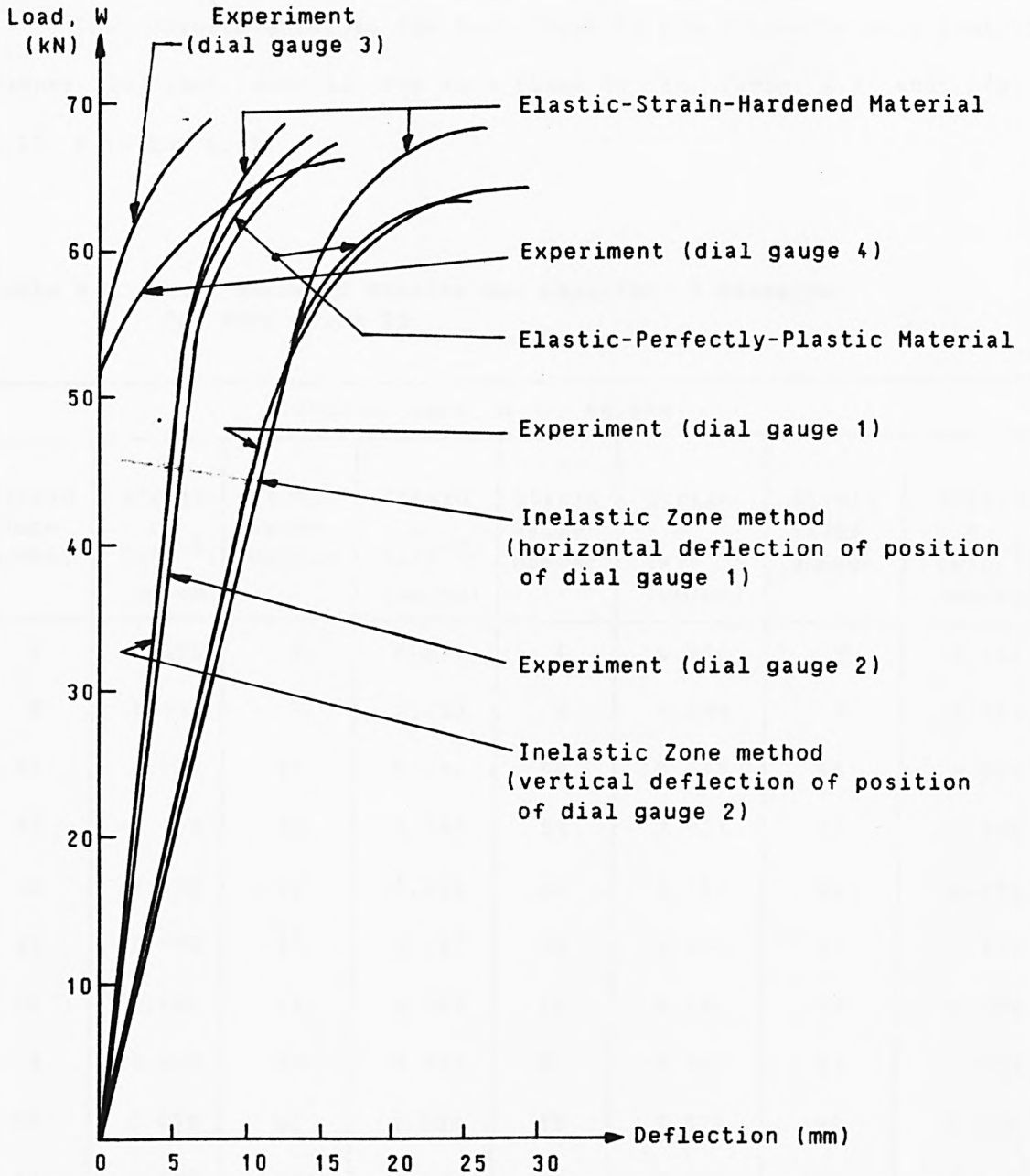


Fig. 6.12 The Equilibrium Paths For Test Frame T1

Results For Test Frame T2

The results obtained for test frame T2 are presented in a similar manner to that adopted for test frame T1 in Table 6.4 and Figs. 6.13, 6.14 and 6.15.

Table 6.4 Last Recorded Strains Not Less Than 0.001mm/mm For Test Frame T2

Vertical Load, W = 68.0kN							
Strain Gauge Number	Strain ϵ ($\times 10^{-2}$) (mm/mm)	Strain Gauge Number	Strain ϵ ($\times 10^{-2}$) (mm/mm)	Strain Gauge Number	Strain ϵ ($\times 10^{-2}$) (mm/mm)	Strain Gauge Number	Strain ϵ ($\times 10^{-2}$) (mm/mm)
0	0.356	3	0.233	4	0.200	5	0.325
6	0.279	7	0.202	8	0.230	9	0.311
51	0.105	54	0.134	55	0.117	56	0.588
57	-0.140	58	0.486	59	0.731	61	-0.544
62	2.132	63	-0.366	64	1.162	65	0.219
66	0.180	67	0.107	68	-0.207	71	1.912
72	-0.402	73	0.197	74	0.136	75	0.102
79	0.510	80	0.503	81	0.131	82	0.359
83	0.436	84	0.538	85	0.579	86	0.436
87	0.437	88	0.434	89	0.464	100	0.143
101	0.156	102	0.126	103	0.113	104	0.142
105	0.856						

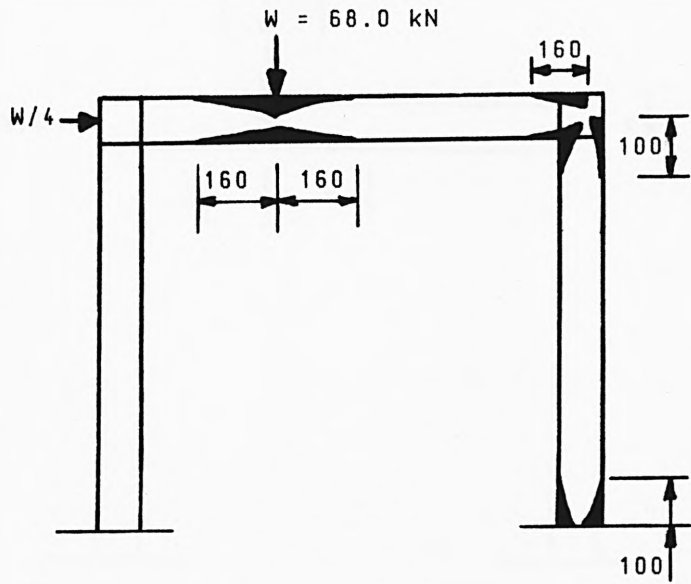
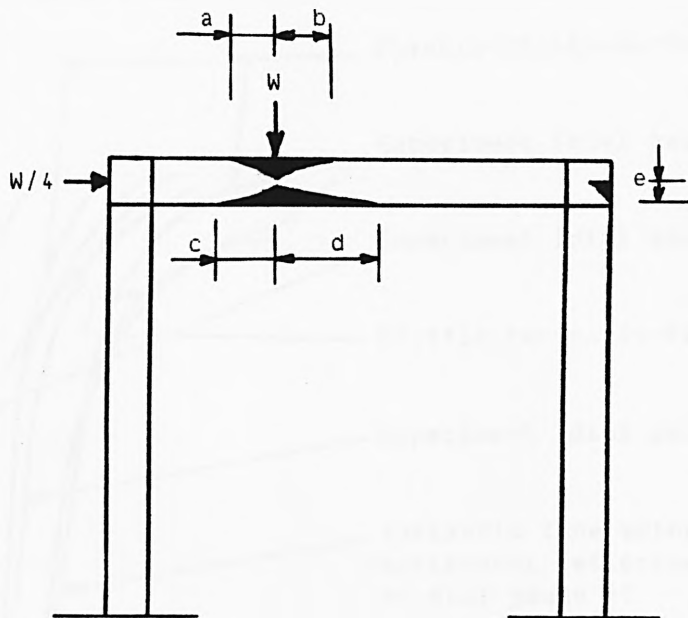


Fig. 6.13 The Inelastic Zones Near Failure Obtained By Experiment For Test Frame T2



For elastic-perfectly-plastic material,

$$a = 5 \text{ mm} ; b = 7 \text{ mm} ; c = 40 \text{ mm} ; d = 55 \text{ mm} ; e = 0$$

For elastic-strain-hardened material,

$$a = 50 \text{ mm} ; b = 70 \text{ mm} ; c = 84 \text{ mm} ; d = 117 \text{ mm} ; e = 17 \text{ mm}$$

$$W = 67.0 \text{ kN for elastic-perfectly-plastic material}$$

$$W = 72.0 \text{ kN for elastic-strain-hardened material}$$

Fig. 6.14 The Inelastic Zones Near Failure Obtained By The Inelastic Zone Method For Test Frame T2

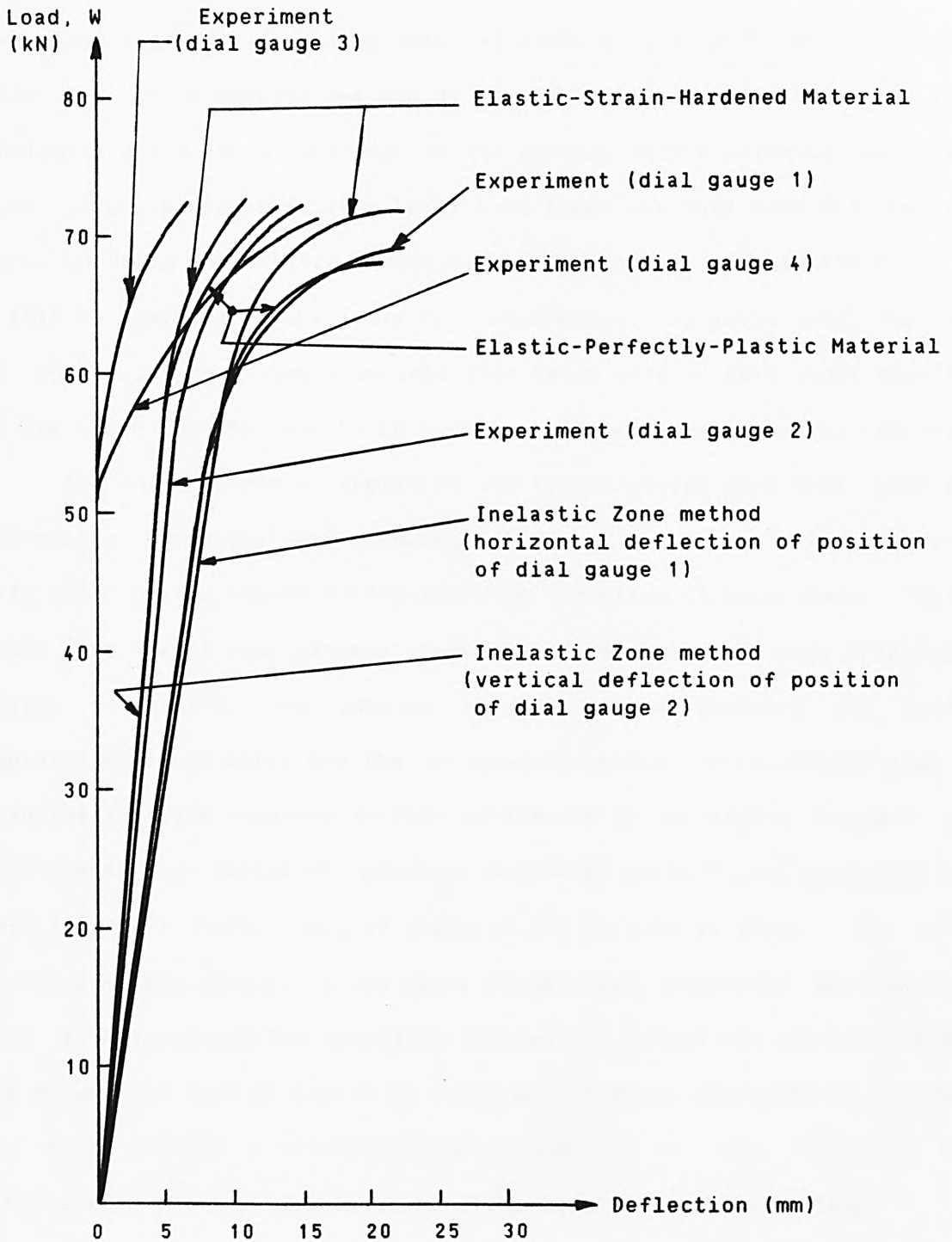


Fig. 6.15 The Equilibrium Paths For Test Frame T2

6.7 Remarks

The equilibrium paths obtained by the inelastic zone method for the elastic-perfectly-plastic material closely agree with those obtained from the tests despite the use of average material properties in the analyses while those obtained for the elastic-strain-hardened material gave slightly higher failure loads than those obtained from the tests. Thus, in using the elastic-strain-hardened material for mild steel for a stability analysis by the inelastic zone method, slightly lower values of the strain-hardening constants than those adopted here would need to be specified for the results to closely agree with experimental results.

The out-of-plane strengths of the frames tested were sufficient in preventing premature out-of-plane failure of the frames prior to the attainment of the theoretically-computed in-plane failure loads. Thus, while the use of less slender frames may be advocated in many practical design situations, the unusual nature of frame geometry and loads employed in these tests and the encouraging results obtained must give a structural frame designer greater confidence in specifying columns of high slenderness ratios for economic design of plane frames subjected to less stringent combinations of vertical and horizontal loads. The role of out-of-plane restraints for plane frames must, therefore, be seen not only as maintaining the specified slenderness ratios for the columns of the frames but also as improving frame out-of-plane strengths to account for such effects as eccentricities of loadings and non-uniformity of yield stress for the various plate elements of the cross-sections.

The results presented here confirm the presence of inelastic zones along frame members for frames loaded into the inelastic domain. The scatter of the inelastic zones determined from the tests, however, makes a reasonable analysis of the problem almost impossible to achieve.

Nevertheless, by adopting bilinear stress-strain relationships for the material, reasonable results have been obtained from stability analyses of the test frames by the inelastic zone method.

The comparisons made in this chapter further vindicate the inelastic zone method as an efficient analytical tool for investigating the stability of plane frames.

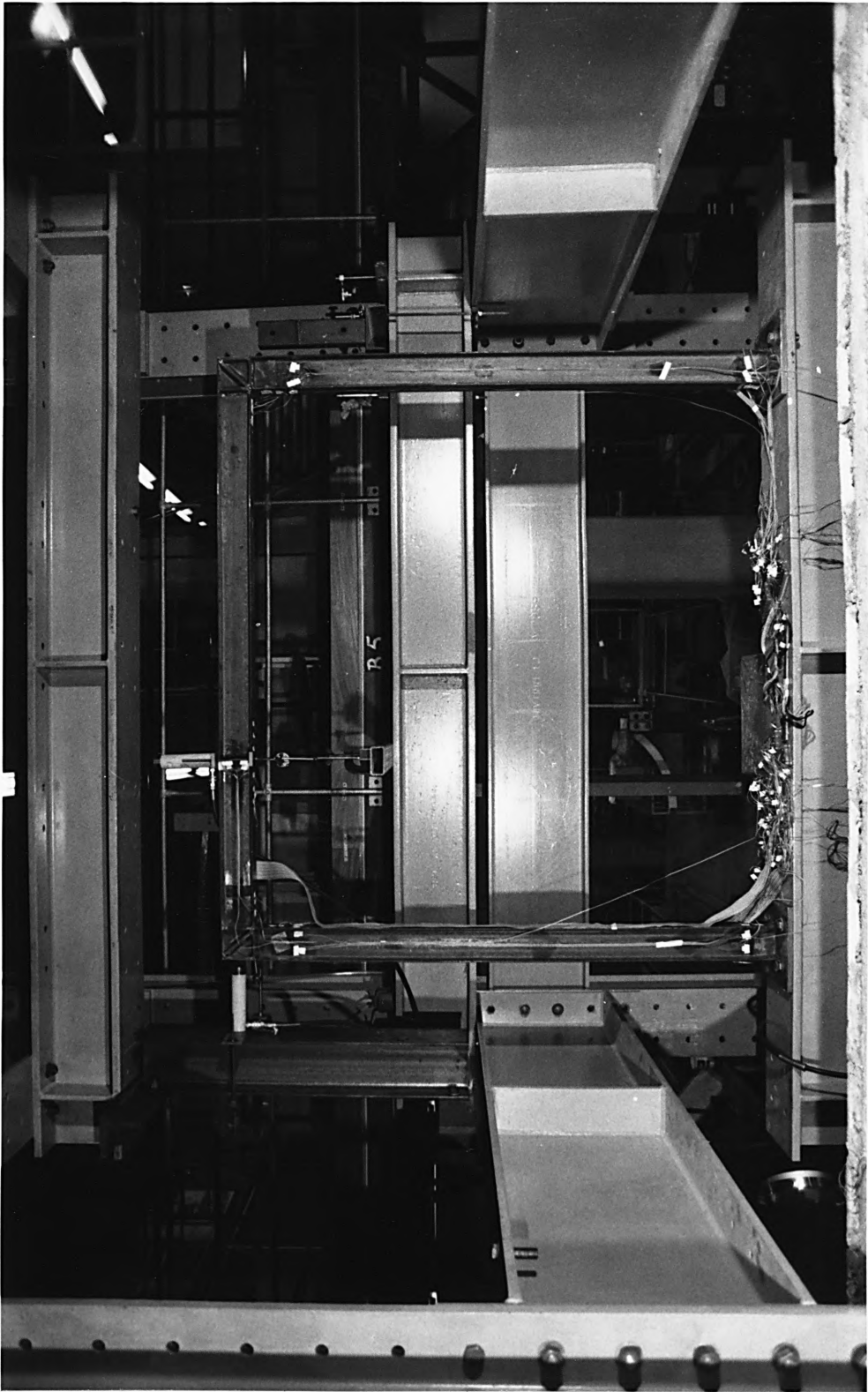


Fig. 6.16 Test Frame, Jacks And Strain Gauges

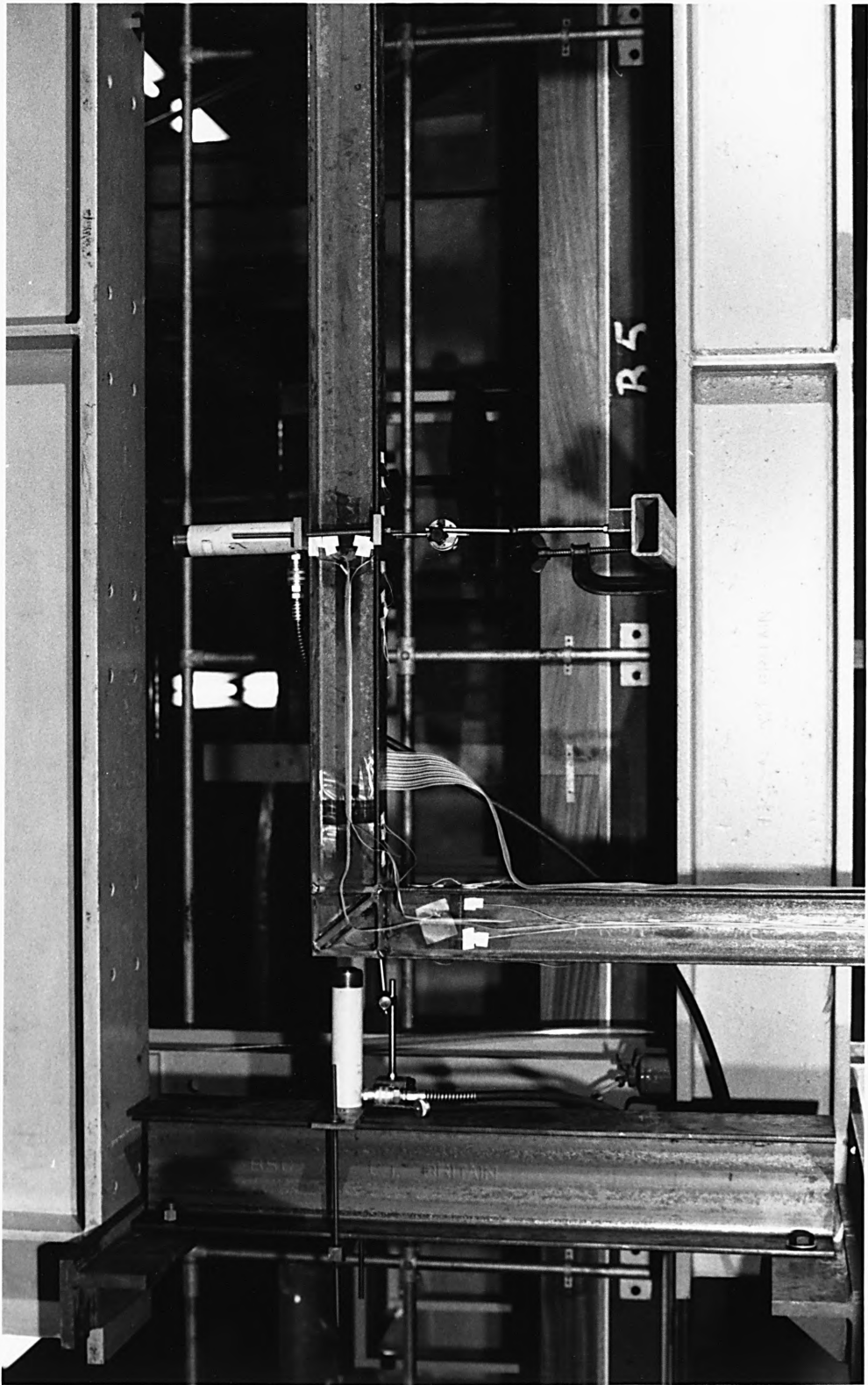


Fig. 6.17 Test Frame Knee Detail



Fig. 6.18 Stiffeners For Beam B2 (See Fig. 6.3)

CHAPTER 7

DESIGN RECOMMENDATIONS FOR METAL PLANE FRAMES

7.1 Introduction

In Chapters 5 and 6, results of frame stability analyses based on the proposed inelastic zone method were shown to agree well with available theoretical and experimental results for metal plane frames. In this chapter, the adequacy of the proposed method as a design tool will be examined. Recommendations for a satisfactory frame design and for the use of the inelastic zone method will be given. In addition, a new, simplified method for plane frame design, which avoids the computation of frame failure loads but considers only a non-linear, elastic analysis of the frame subjected only to the working loads, will be presented. This method considers the ultimate strength of a cross-section based on the formulae derived in Chapter 2. As stated in Chapter 1, design considerations will be confined to the selection of suitable section sizes for plane frame members assuming adequate connections and foundations.

7.2 General Procedures For Plane Frame Design

The design of a plane frame is a trial-and-process which depends not only on a structural analysis of the frame for a given set of loads but also on personal judgement, experience and intuition. During a design process, a constant re-appraisal of the various factors which affect the design is made and changes are made where necessary. Thus, a decision which is made at the beginning of a design process may be changed at a later stage. The various available techniques of structural

analysis and the variety of dimensions for rectangular and I-shaped cross-sections lead to further re-appraisal during a design process. The total cost of producing a design is also constantly reviewed during the design process and a seemingly satisfactory design may be dropped if it is considered to be expensive. Thus, an acceptable frame design cannot be achieved from structural considerations alone and more than one set of member section sizes can give a satisfactory frame design. Nevertheless, by following a specified set of design procedures, a constant standard of design can be maintained and a satisfactory frame design can be achieved.

The recommended procedures for plane frame design are described below under the following headings:

1. Design objectives
2. Means of achieving the design objectives.
3. Initial estimates of member section sizes.
4. Steps of analysis.

7.2.1 Design Objectives

The essential first step in a frame design process is to clearly identify the design objectives. These design objectives can be grouped under the following main headings:

1. Serviceability.
2. Ultimate strength.
3. Economy.
4. Balanced design.

The serviceability objective ensures that the displacements of the frame subjected to the working loads are within specified,

acceptable limits and that inelastic conditions are present or absent in the frame as may specified under these loads. The working loads should include loads which may be required to be supported by the frame at a future date and allowances for loads which may not (or cannot) be identified at the onset of the design process.

The ultimate strength objective ensures that the frame has a minimum factor of safety against failure. This objective is applied not only to the cross-section of each frame member but also to each frame member and to the entire frame as one unit.

The objective of economy ensures that the total design time (including computer time) and the total weight of frame lead to a total design cost which does not exceed the design budget.

A frame design is classified here as satisfactory if it satisfies the above design objectives. A satisfactory design which exactly satisfies the above design objectives is described here as a **balanced design**.

7.2.2 Means Of Achieving The Design Objectives

The second step in a frame design process is to identify the means of achieving the design objectives. Where inelastic conditions are not allowed under the working loads, a non-linear, elastic analysis of a plane frame is more appropriate for satisfying the serviceability objective than a linear, elastic analysis of the frame. Where inelastic conditions are allowed under the working loads, then a non-linear, inelastic analysis of the frame should be performed.

Any method of plane frame stability analysis which gives a lower-bound value of the frame failure load is more appropriate for satisfying the ultimate strength objective for the entire frame than any method

which gives an upper-bound value of this load. Limiting-stress (or interaction ratio) methods, in general, consider the ultimate strength of each member cross-section (based on assumed boundary conditions for each member) and do not compute frame failure loads. These methods cannot, therefore, be used to check the satisfaction of the ultimate strength objective for a frame.

In order to satisfy the objective of economy, consideration must be given not only to the method of structural analysis to be employed but also to the accuracy of the results that the method can give. Although a frame may fail by inelastic instability, the degree (or level) of inelasticity present at failure may be so low that many members in the frame remain elastic, causing uneconomic use of materials. Methods of analysis which allow the presence of several plastic hinges and inelastic zones under specified ultimate loads are particularly useful for achieving economy of weight of frame albeit at the expense of computer time which may be considered to be significant for design. Thus, in order to increase the number of plastic hinges and inelastic zones in a frame, it is essential to initially obtain a satisfactory design and to identify the extent of inelasticity present in the frame at failure. This is accomplished only from the bending moment distribution throughout the frame by establishing all points at which the first yield moments of the various member cross-sections have been exceeded. In general, it is best to avoid the development of significant inelastic zones in predominantly-axially-loaded members (such as columns) while allowing the development of significant inelastic zones in predominantly-transversely-loaded members (such as beams). This is because of the significant secondary bending moments

that can result as the column axial force acts through its displaced profile. Thus, the inelastic response of a given satisfactorily-designed plane frame can be improved by reducing the beam section sizes or increasing the column section sizes or by a combination of both activities. A re-analysis should, however, be undertaken to ensure that these changes do not lead to an unsatisfactory design. By applying the distributed inelasticity concept of structural behaviour without finite discretization of members and their cross-sections and by identifying the inelastic zones in a plane frame without the need to draw the bending moment diagrams, the inelastic zone method is directly suited to the easy achievement of this objective.

Notwithstanding the method of stability analysis employed for frame design, the equilibrium path for a frame is the best means of ascertaining the degree of departure of the design from the balanced design. Fig. 7.1 shows typical equilibrium paths for satisfactory,

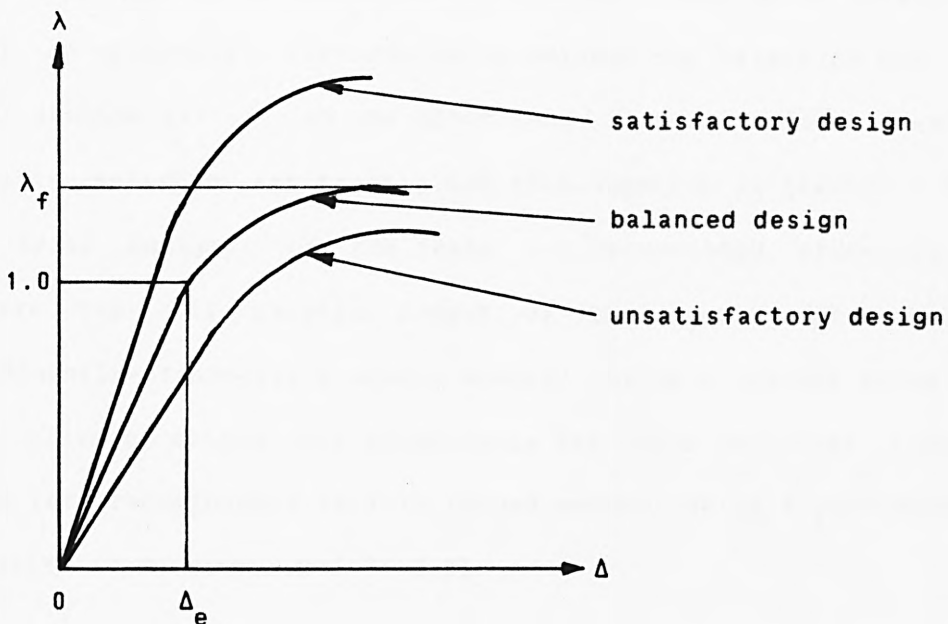


Fig. 7.1 Equilibrium Paths Obtained In Frame Design

balanced and unsatisfactory frame designs based on stability analyses of the entire frame. The failure load parameter and the maximum permissible horizontal and vertical deflections under the working loads (to the variable parts of which a unit load parameter is assigned) should be specified for the balanced design. It is also essential to specify whether or not inelastic conditions are permissible under the working loads. A balanced design is very difficult to achieve. Thus, a satisfactory design which is very close to the balanced design is the best that can be achieved in practice.

7.2.3 Initial Estimates Of Member Section Sizes

After choosing the appropriate method of analysis, it becomes necessary to select initial trial section sizes for the members before analysis can be commenced. Several analyses of the frame may be performed in which member sections sizes are revised before the final, satisfactory design is achieved. It is, therefore, quite unnecessary to engage in elaborate, time-consuming methods for selecting the initial member section sizes. On the other hand, member section sizes may be initially selected arbitrarily but this approach is likely to lead to many trial analyses of the frame. A recommended procedure is to estimate the full plastic moment of the section of a beam (or predominantly-transversely-loaded member) using a formula based on the rigid plastic method and to estimate the cross-sectional area of a column (or predominantly-axially-loaded member) using a specified squash load ratio (for example 0.2 to 0.3).

7.2.4 Steps Of Analysis

After selecting the initial section sizes for the frame members, the analysis of the frame for the given loads can be commenced. The recommended steps of analysis are as follows:

1. Group the working loads into load combinations.
2. Employ each working load combination in a linear or non-linear analysis as may be specified for satisfying the serviceability objective. Revise section sizes and repeat analysis where this objective is not satisfied. Go to the next step when this objective is satisfied.
3. From the acceptable results of Step 2, identify the most critical vertical load combination and the most critical combined load combination and employ each of these two load combinations in an analysis to satisfy the ultimate strength objective. Revise section sizes and re-analyse frame in each case when this objective is not satisfied. When this objective is satisfied, go to the next step.
4. If the design obtained gives an ultimate strength much greater than that specified or gives a maximum deflection much lower than that specified, reduce the section sizes for some members with a view to achieving a satisfactory design which is close to the balanced design and re-analyse frame. Then, check whether a satisfactory design is still maintained and re-analyse frame if necessary.
5. Terminate analysis and print results.

The above steps of analysis are summarized in the Flow Chart given in Fig. 7.2.

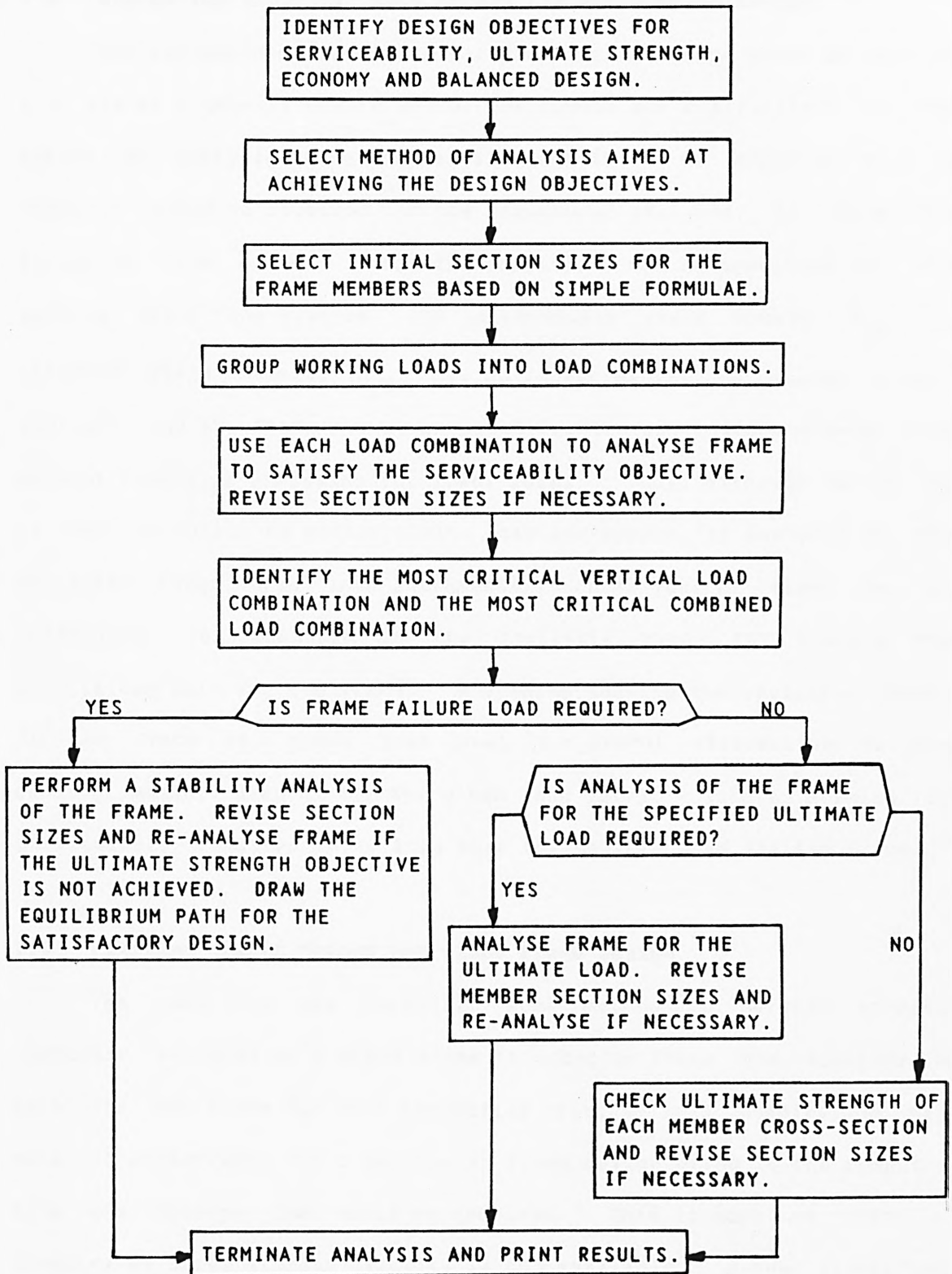


Fig. 7.2 A Flow Chart For Plane Frame Design

7.3 Use Of The Inelastic Zone Method For Plane Frame Design

The recommended procedures for plane frame design given in Section 7.2 are of a general nature and do not impose any restrictions on the method of analysis to be adopted although it can be expected that a computer would be required for the structural analyses. In using the inelastic zone method, inelastic conditions can be specified for the working loads (for example, the intermediate yield moment, M_{y2} , or ultimate yield moment, M_{y3} , may be specified for one member cross-section) and the frame may be analysed for the specified ultimate load without initially analysing for lower loads. Thus, although useful, it is not essential to employ finite load increments for analysis in the inelastic range. Few load increments (such as four or five) may be sufficient for analysis in the inelastic range for tracing the equilibrium path for the frame. A drawing showing the inelastic zones in the frame at a given load level is a useful alternative to the bending moment diagram for the given load level. Such a drawing is particularly required for a load near the failure load for the frame.

7.4 Limiting Moment Method For Plane Frame Design

The need for the inelastic zone method to perform several inelastic analyses of a plane frame in order to trace the equilibrium path for the frame for each identified critical load combination may make it undesirable for a particular frame design owing to the computer time and storage that would be required. This is more so where a computer of large storage capacity is not available. A new, simplified method which can be applied to any type of plane frame, can be used to satisfy serviceability and ultimate strength criteria for the frame and requires only one analysis of the frame subjected to one working load

combination is presented here as an alternative method. This method is called the **limiting moment method**.

In this method, inelastic zones are not required in the frame under the working loads. A non-linear, elastic analysis of the frame subjected to a working load combination is initially performed. The resulting member axial forces are multiplied by the specified failure load parameter (greater than unity which applies to the working load) for satisfying the ultimate strength objective for the loading being considered. This gives a factored axial load, P_u , for each member cross-section. This factored axial load is employed to obtain an ultimate yield moment, M_u , for the cross-section which is lower than that for the working load using the methods given in Chapter 2. The bending moment at the cross-section derived from the analysis is required not to exceed the **limiting moment**, M_{lw} , for the cross-section defined as

$$M_{lw} = M_u / \lambda_f \quad (7.1)$$

If the bending moment at a cross-section exceeds the limiting moment for the cross-section or if the serviceability objective is not satisfied, member section sizes are revised and a re-analysis of the frame is performed. Otherwise, the member section sizes are accepted for the working load combination being considered. This process is repeated for all working load combinations.

7.5 Design Examples

Three examples will now be given for designing regular and irregular plane frames using the proposed limiting moment method. The frames are for office buildings. The resulting satisfactory designs are required to be checked using the inelastic zone method. In each case, the following design specifications (which do not necessarily agree with those given in any Code of Practice) will apply:

1. The loading is proportional loading. All loads are applied as concentrated loads. External, vertical loads on each floor level include the weights of external, storey-height walls.
2. The material is structural steel of grade 43 ($E = 210\text{kN/mm}^2$ and $\sigma_y = 0.25\text{kN/mm}^2$) or grade 50 ($E = 210\text{kN/mm}^2$ and $\sigma_y = 0.35\text{kN/mm}^2$).
3. Ignore strain-hardening and initial member imperfections.
4. Requirements for serviceability:

Joint maximum horizontal deflection should not exceed height of frame above ground level/300.

Joint maximum vertical deflection should not exceed beam span/300.

5. Requirements for ultimate strength:

For vertical loading, ultimate load/working load = 1.50

For combined loading, ultimate load/working load = 1.20

Example 7.5.1

Design the five-storey, one-bay, regular frame loaded as shown in Fig. 7.3 which also shows the joint and member numbers (in brackets) used in the analyses.

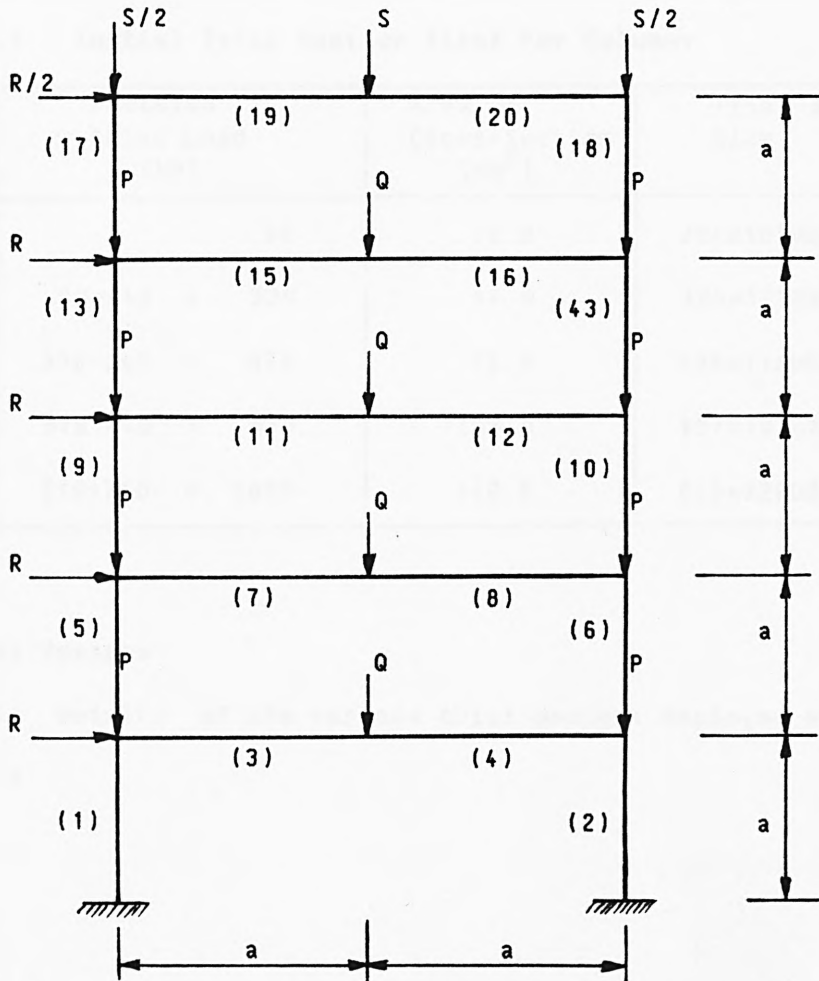
Try steel grade 43.

Try ultimate moment for beam to be given by

$$M_{y3} = \text{central load } \times \text{span} \times 1.5/6$$

Try cross-sectional area for column to be given by

$$A = \text{static axial load} \times 1.5 / (0.2 \times \text{yield stress})$$



$P = 100.0\text{kN}$; $Q = 120.0\text{kN}$; $R = 30.0\text{kN}$; $S = 60.0\text{kN}$; $a = 4000.0\text{mm}$

Fig. 7.3

Solution

1. Initial Estimates Of Member Section Sizes

(i) Floor Beam $M_{y3} = 1.5 \times 120 \times 8000 / 6 = 240000 \text{ kN.mm}$

Floor Beam Plastic Modulus = $240000 / (0.25 \times 1000) = 960 \text{ cm}^3$

Try 406x178UB60 kg/m

(ii) Roof Beam $M_{y3} = 1.5 \times 60 \times 8000 / 6 = 120000 \text{ kN.mm}$

Roof Beam Plastic Modulus = $120000 / (0.25 \times 1000) = 480 \text{ cm}^3$

Try 305x127UB42 kg/m

(iii) Column section sizes are given in Table 7.1.

Table 7.1 Initial Trial Section Sizes For Columns

Column Number	Factored Axial Load (kN)	Area Of Cross-Section (cm ²)	Trial Section Size
17	90	12.0	254x102UB22 kg/m
13	90+240 = 330	44.0	305x127UB42 kg/m
9	330+240 = 570	76.0	406x178UB67 kg/m
5	570+240 = 810	108.0	457x191UB98 kg/m
1	810+240 = 1050	140.0	610x229UB125 kg/m

2. Trial Designs

The details of the various trial designs employed are given in Table 7.2.

Table 7.2 Details Of Trial Designs

Trial	Loading	Member	Section Size	Remarks
1.	Combined	Each	As given on page 208	Unsatisfactory Design. Serviceability objective is not satisfied.
2.	Combined	As Trial 1 Except		Satisfactory design
		Floor Beam	457x191UB67 kg/m	
		Roof Beam	356x171UB51 kg/m	
		17	As member 13	
		9	As member 5	
3.	Vertical	As Trial 2		Satisfactory design

The load parameters obtained by the inelastic zone method for the satisfactory design are as follows:

For combined loading

$$\lambda_e = 1.18$$

$$\lambda_f = 2.35$$

and for vertical loading,

$$\lambda_e = 1.65$$

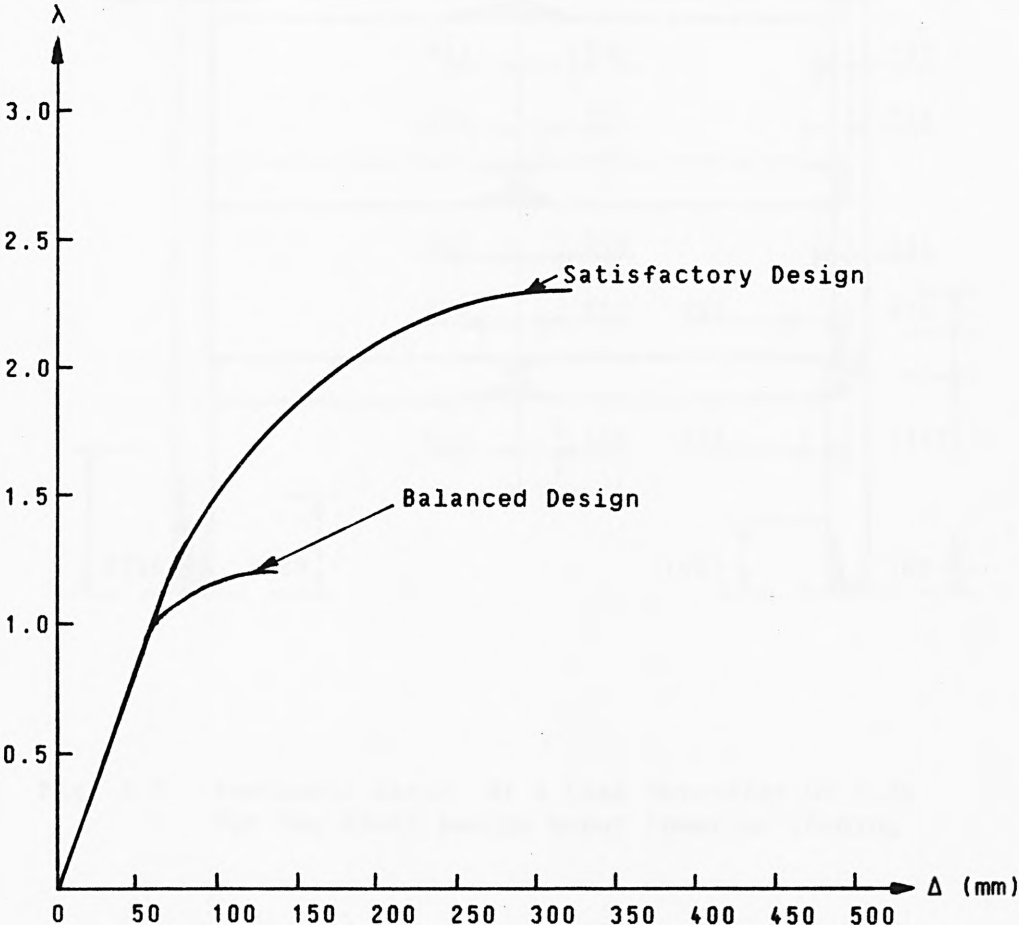
$$\lambda_f = 2.75$$

where λ_e is the load parameter for the end of elastic response.

Thus, the more critical design loading is combined loading and the equilibrium path for this loading is given in Fig. 7.4 while the corresponding inelastic zones near failure are given in Fig. 7.5.

It can be seen from Fig. 7.4 that the satisfactory design is governed by the serviceability objective while the ultimate strength

achieved after three trials is much greater than that required. Since the maximum deflection obtained for the working load is equal to the permissible deflection under this load and since the design is based on the limiting moment method, a re-design of the frame to approach a balanced design cannot be undertaken. It follows, therefore, that an inelastic analysis of the frame would be required in order to achieve a satisfactory design closer to the balanced design than that achieved by using the limiting moment method.



Δ = horizontal deflection of roof beam.

Fig. 7.4 Equilibrium Paths For Combined Loading

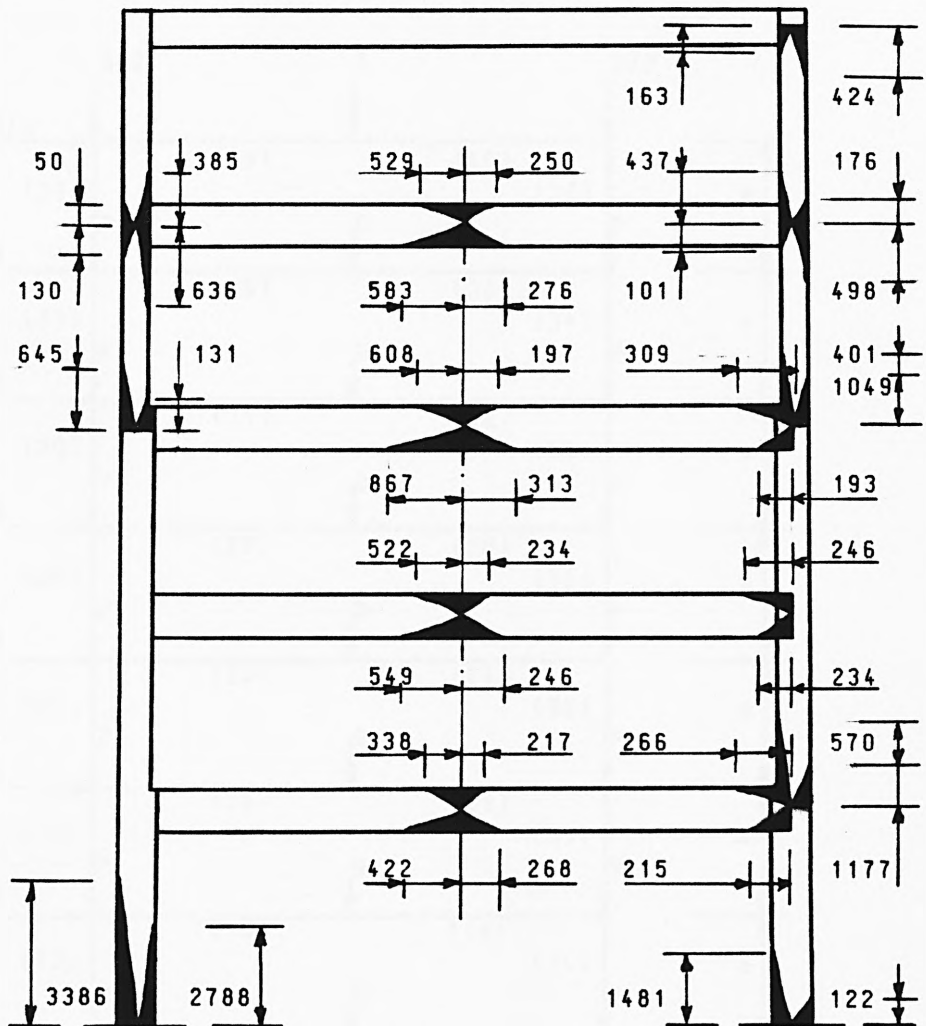


Fig. 7.5 Inelastic Zones At A Load Parameter Of 2.20 For The Final Design Under Combined Loading

Example 7.5.2

Design the ten-storey, one-bay, regular frame loaded as shown in Fig. 7.6 which also shows the joint and member numbers (in brackets)

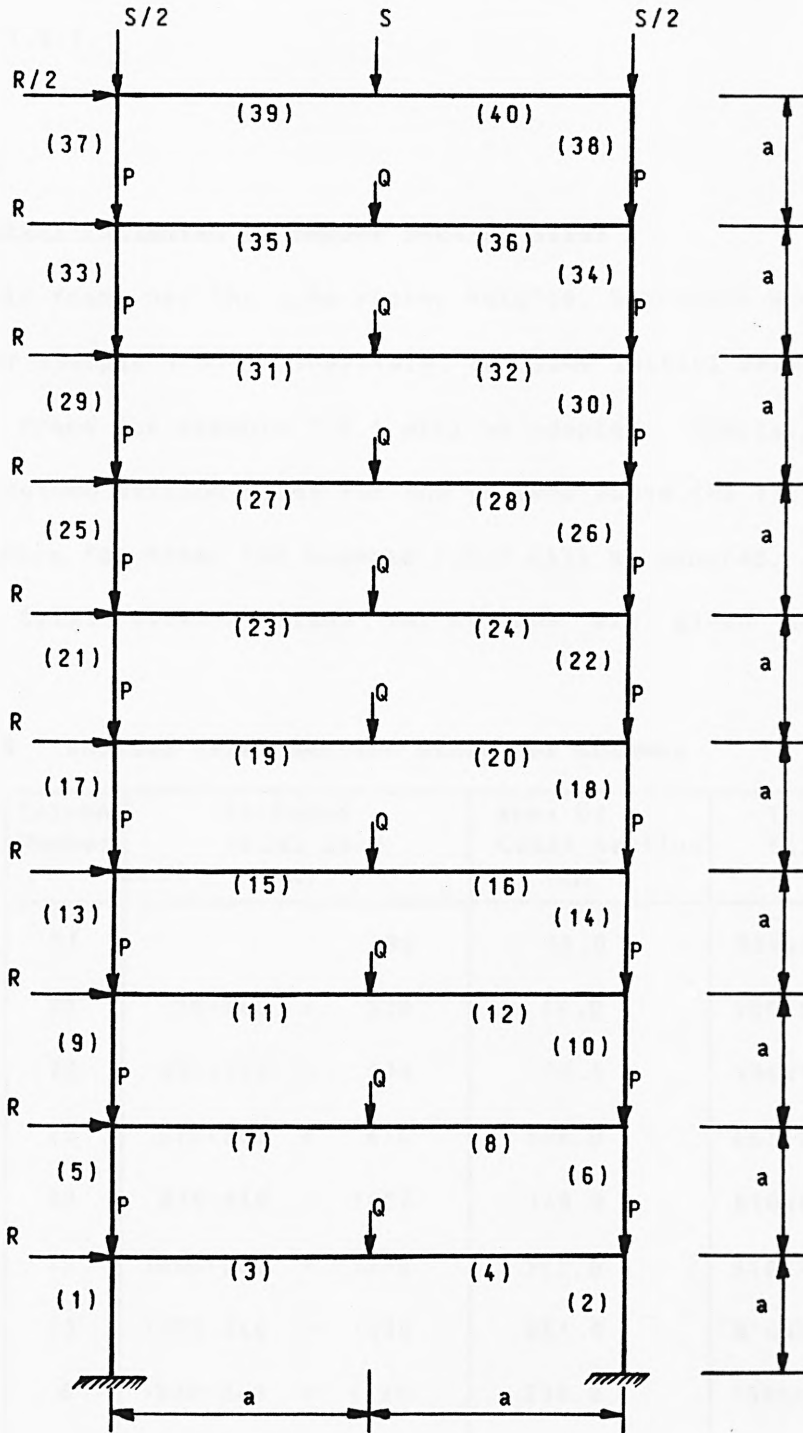


Fig. 7.6

used in the analyses. The values of a , P , Q , R , and S are the same as those for frame of example 7.5.1. Try steel grade 43 and use the simple formulae used to estimate the initial member section sizes for frame of example 7.5.1.

Solution

1. Initial Estimates Of Member Section Sizes

This frame has the same storey heights, bay-width and loads as the frame for example 7.5.1. Therefore, the same initial beam section sizes as for frame for example 7.5.1 will be adopted. Similarly, the same initial column section sizes for the columns above the fifth floor level as for those for frame for example 7.5.1 will be adopted. The complete initial trial section sizes for columns are given in Table 7.3.

Table 7.3 Initial Trial Section Sizes For Columns

Column Number	Factored Axial Load (kN)	Area Of Cross-Section (cm ²)	Trial Section Size
37	90	12.0	254x102UB22 kg/m
33	90+240 = 330	44.0	305x127UB42 kg/m
29	330+240 = 570	76.0	406x178UB67 kg/m
25	570+240 = 810	108.0	457x191UB98 kg/m
21	810+240 = 1050	140.0	610x229UB125 kg/m
17	1050+240 = 1290	172.0	610x305UB179 kg/m
13	1290+240 = 1530	204.0	610x305UB238 kg/m
9	1530+240 = 1770	236.0	838x292UB226 kg/m
5	1770+240 = 2010	268.0	914x305UB253 kg/m
1	2010+240 = 2250	300.0	914x305UB388 kg/m

2. Trial Designs

The details of the various trial designs employed are given in Table 7.4.

Table 7.4 Details Of Trial Designs

Trial	Loading	Member	Section Size	Remarks
1	Combined	Each	As given on page 213	Unsatisfactory Design. Serviceability Objective Is Not Satisfied.
2	Combined	As Trial 1 Except		Unsatisfactory Design. Serviceability Objective Is Not Satisfied.
		Floor Beam	457x191UB67 kg/m	
		Roof Beam	356x171UB51 kg/m	
		37, 33	356x171UB57 kg/m	
		29, 25	533x210UB101 kg/m	
		21	As member 17	
		13	As member 9	
3	Combined	As Trial 2 Except		Satisfactory design.
		37, 33	457x152UB60 kg/m	
		29, 25	533x210UB122 kg/m	
		21, 17	610x305UB238 kg/m	
		13	As member 9	
		5	As member 1	
4	Vertical	Each	As Trial 3	Satisfactory design.

The load parameters obtained by the inelastic zone method for the satisfactory design are as follows:

For combined loading

$$\lambda_e = 1.01$$

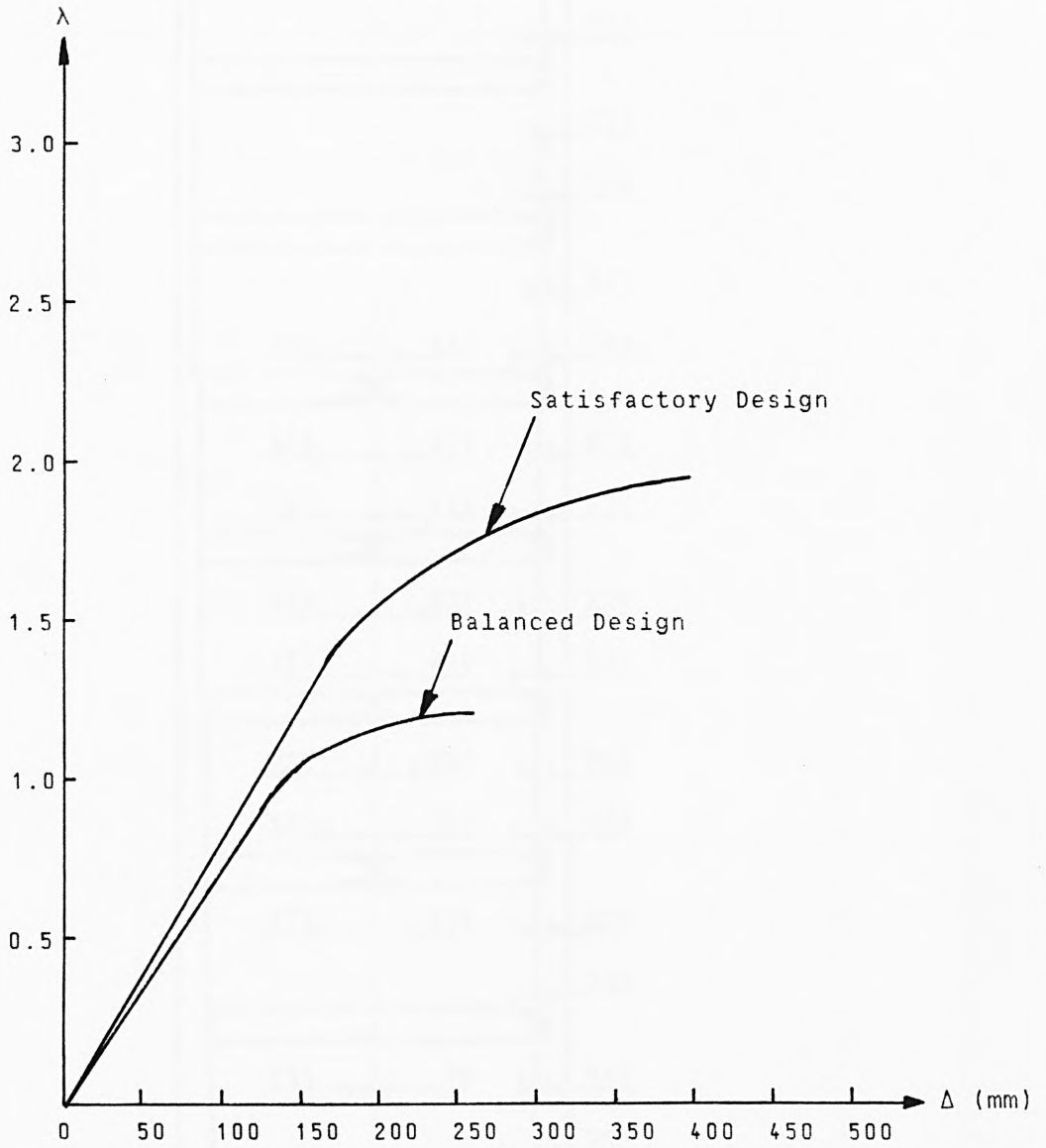
$$\lambda_f = 1.95$$

and for vertical loading

$$\lambda_e = 3.15$$

$$\lambda_f = 3.70$$

Thus, the more critical design loading is combined loading and the equilibrium path for this loading is given in Fig. 7.7 while the corresponding inelastic zones near failure are given in Fig. 7.8. Also, the serviceability objective governs the design of this frame. Since the design is based on the limiting moment method, member section sizes can be reduced and re-analyses performed until the maximum deflection under the working loads equals the permissible value of 133.33mm. However, an inelastic analysis of the frame would be required in order to achieve a satisfactory design closer to the balanced design than that achieved by using the limiting moment method.



Δ = horizontal deflection of roof beam.

Fig. 7.7 Equilibrium Paths For Combined Loading

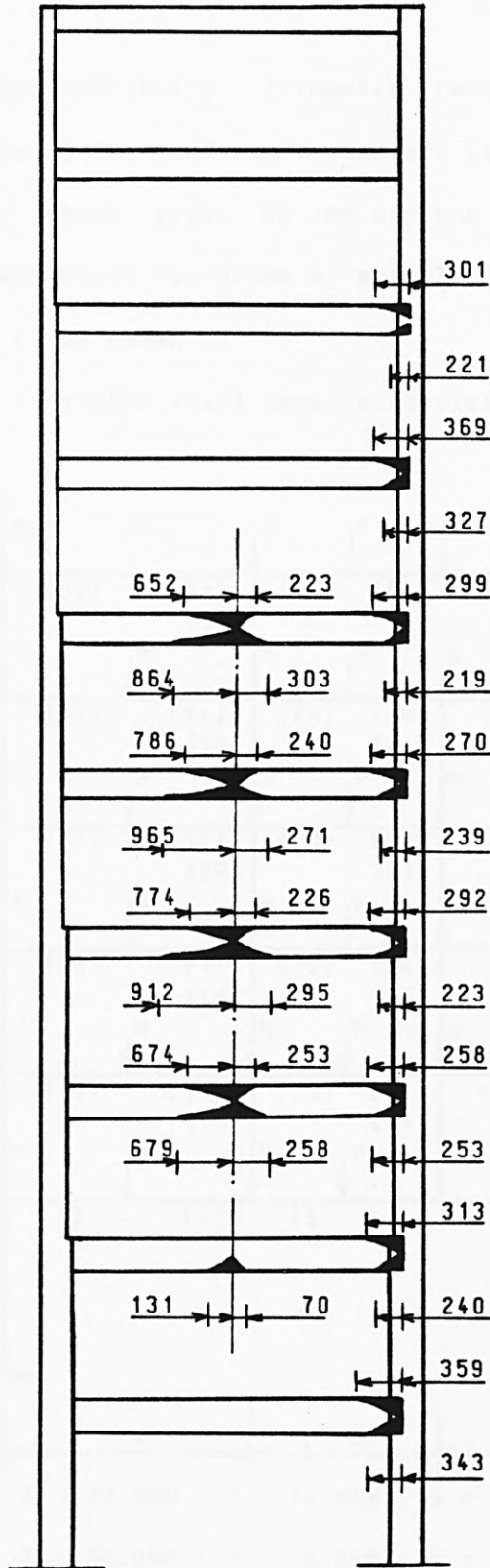


Fig. 7.8 Inelastic Zones At A Load Parameter Of 1.90 For Combined Loading

Solution

The first floor beam will be designed to be capable of spanning over 16m and its central deflection will be limited to span/600 instead of span/300. This is aimed at providing a relatively stiff support for the upper level beams.

Also, since the frame is irregular, both directions of wind will be considered in its design.

1. Initial Member Section Sizes

(i) Floor Beam M_{y3} (except first floor beam)

$$= 1.5 \times 100 \times 6000 / 6$$

$$= 150000 \text{ kN.mm}$$

$$\text{Required plastic modulus} = 150000 / (0.35 \times 1000)$$

$$= 428.6 \text{ cm}^3$$

Try 356x127UB33 kg/m.

(ii) Roof Beam $M_{y3} = 1.5 \times 75 \times 6000 / 6 = 112500 \text{ kN.mm}$

$$\text{Required plastic modulus} = 112500 / (0.35 \times 1000)$$

$$= 321.4 \text{ cm}^3$$

Try 305x102ub25 kg/m

(iii) Column section sizes are given in Table 7.5.

Table 7.5 Initial Trial Section Sizes For Columns

Column Number	Factored Axial Load (kN)	Area Of Cross-Section (cm ²)	Trial Section Size
49	112.5	12.9	305x127UB37 kg/m
39	112.5+225 = 337.5	38.6	305x127ub37 kg/m
29	337.5+225 = 562.5	64.3	457x152UB67 kg/m
19	562.5+225 = 787.5	90.0	457x152UB67 kg/m
9	787.5+225 = 1012.5	115.7	610x229UB101 kg/m
50	$(37.5+62.5+50 \times 5/7 + 65 \times 3/7) 1.5 = 245.4$	28.0	203x203UC46 kg/m
40	$245.4 + (50+83+33) 1.5 = 494.4$	56.5	203x203UC60 kg/m
30	494.4+249 = 743.4	85.0	254x254UC89 kg/m
20	743.4+249 = 992.4	113.4	305x305UC158 kg/m
10	992.4+249 = 1241.4	141.9	305x305UC158 kg/m
41	$(33+70.5+75 \times 1.5/4.5) = 192.8$	22.0	As member 40
31	192.8+249 = 441.8	50.5	As member 30
21	441.8+249 = 690.8	79.0	As member 20
11	690.8+249 = 939.8	107.4	AS member 10

Section sizes for members 51, 42, 32, 22 and 12 are same as for those for members 49, 39, 29, 19 and 9 respectively.

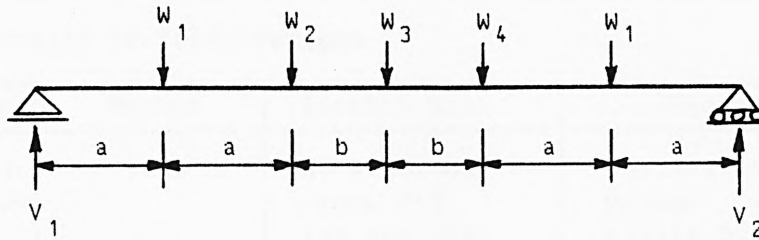
(iv) First floor beam

Fig. 7.10 shows the loading arrangement used in estimating the initial trial section size for the first floor beam based on the rigid-plastic method. The maximum bending moment occurs under the load of 910.6kN. Thus, with a unit vertical deflection imposed at the position of this load, the estimated full plastic moment of the section at this

load position is given by

$$M_p = [100 \times 0.5 + 910.6 + 66 \times 0.8 + 709.5 \times 0.6 + 100 \times 0.3] / [1/10000 + 1/6000]$$

$$= 5509125.0 \text{ kN.mm}$$



$$W_1 = 100.0 \text{ kN}$$

$$W_2 = 1241.4/1.5 + 83.0 = 910.6 \text{ kN}$$

$$W_3 = 66.0 \text{ kN}$$

$$W_4 = 939.8/1.5 + 83.0 = 709.5 \text{ kN}$$

$$a = 3000.0 \text{ mm}$$

$$b = 2000.0 \text{ mm}$$

Fig. 7.10

$$\text{Required plastic modulus} = 5509125 / (0.35 \times 1000) = 15740.4 \text{ cm}^3$$

Try 914x419UB388 kg/m.

(v) Ground floor columns

The section sizes for both columns will be made the same. Therefore, the estimate will be based on the factored axial load for column 1.

$$\text{From Fig. 7.10, } V_1 = 968.19 \text{ kN}$$

$$\begin{aligned} \text{Therefore, factored axial load on column 1} &= 1012.5 + 1.5 \times 968.19 \\ &= 2464.8 \text{ kN} \end{aligned}$$

$$\begin{aligned} \text{Required area of cross-section} &= 2464.8 / (0.25 \times 0.35 \times 100) \\ &= 281.7 \text{ cm}^2 \end{aligned}$$

Try 914x305UB289 kg/m.

2. Trial Designs

The details of the various designs employed are given in Table 7.6.

Table 7.6 Details Of Trial Designs

Trial	Loading	Member	Section Size	Remarks
1	Combined, Wind from Left.	Each	As given on pages 219, 220 and 221	Unsatisfactory Design. Serviceability Objective Is Not Satisfied.
2	As Trial 1	Floor Beams (except first)	457x191UB67 kg/m	Unsatisfactory Design. Serviceability Objective Is Not Satisfied.
		As Trial 1 Except		
		29, 19	457x152UB82 kg/m	
		9	610x229UB125kg/m	
3	As Trial 1	As Trial 2 Except		Satisfactory Design.
		Roof beam	457x152UB52kg/m	
		49, 51	406x152UB52kg/m	
4	Combined, Wind from Right.	As Trial 3		Unsatisfactory Design. Serviceability Objective Is Not Satisfied.
5	As Trial 4	As Trial 3 Except		Satisfactory Design.
		Roof beam	457x191UB67kg/m	
		49, 51	406x140UB46kg/m	
		50	203x203UC52kg/m	
6	Combined, Wind from Left	As Trial 5		Satisfactory Design.
		39, 42	As member 49	
7	Vertical	As Trial 5		Satisfactory Design.

The load parameters obtained by the inelastic zone method for the satisfactory design are as follows:

For combined loading with wind from left,

$$\lambda_e = 1.29$$

$$\lambda_f = 2.70$$

For combined loading with wind from right

$$\lambda_e = 1.27$$

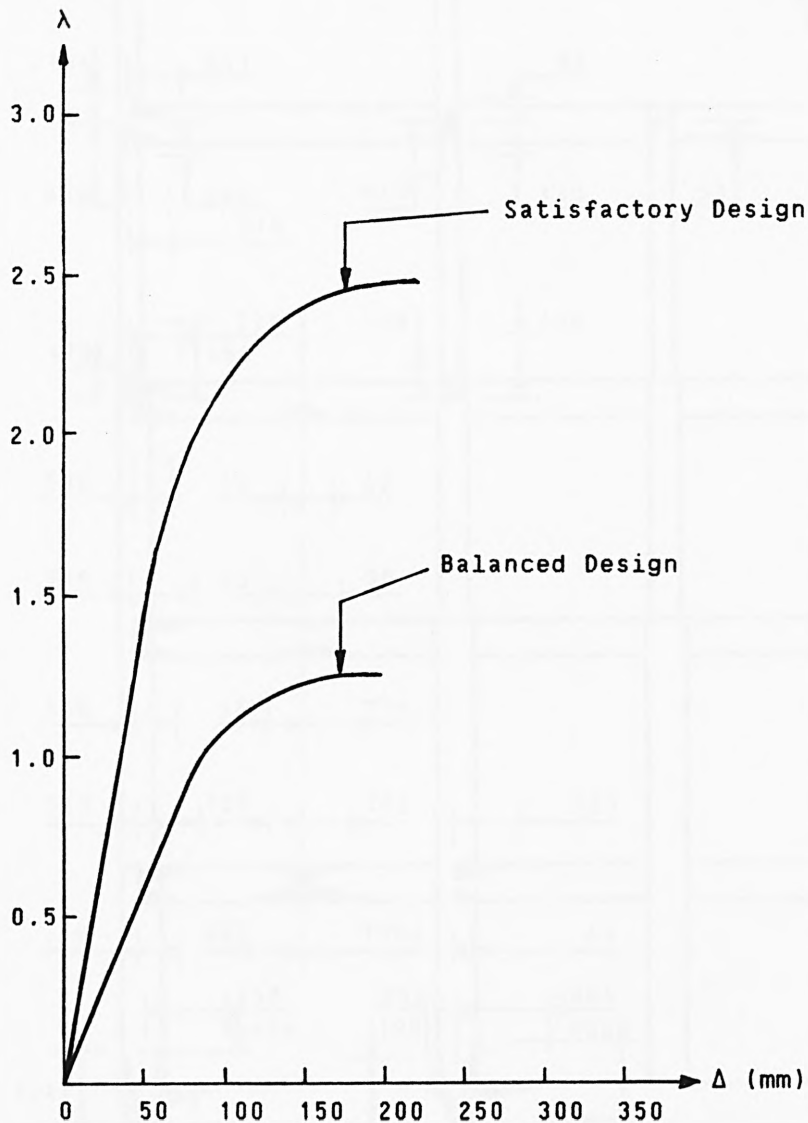
$$\lambda_f = 2.50$$

and for vertical loading

$$\lambda_e = 1.56$$

$$\lambda_f = 2.70$$

Thus, the most critical design loading is combined loading with wind acting from the right and the equilibrium path for this loading is given in Fig. 7.11 while the corresponding inelastic zones near failure are given in Fig. 7.12. The serviceability objective governs the design of this frame and an inelastic analysis of the frame would be required in order to obtain a satisfactory design closer to the balanced design than that achieved by the limiting moment method.



Δ = horizontal deflection of roof beam

Fig. 7.11 Equilibrium Paths For Combined Loading For Wind Acting From The Right

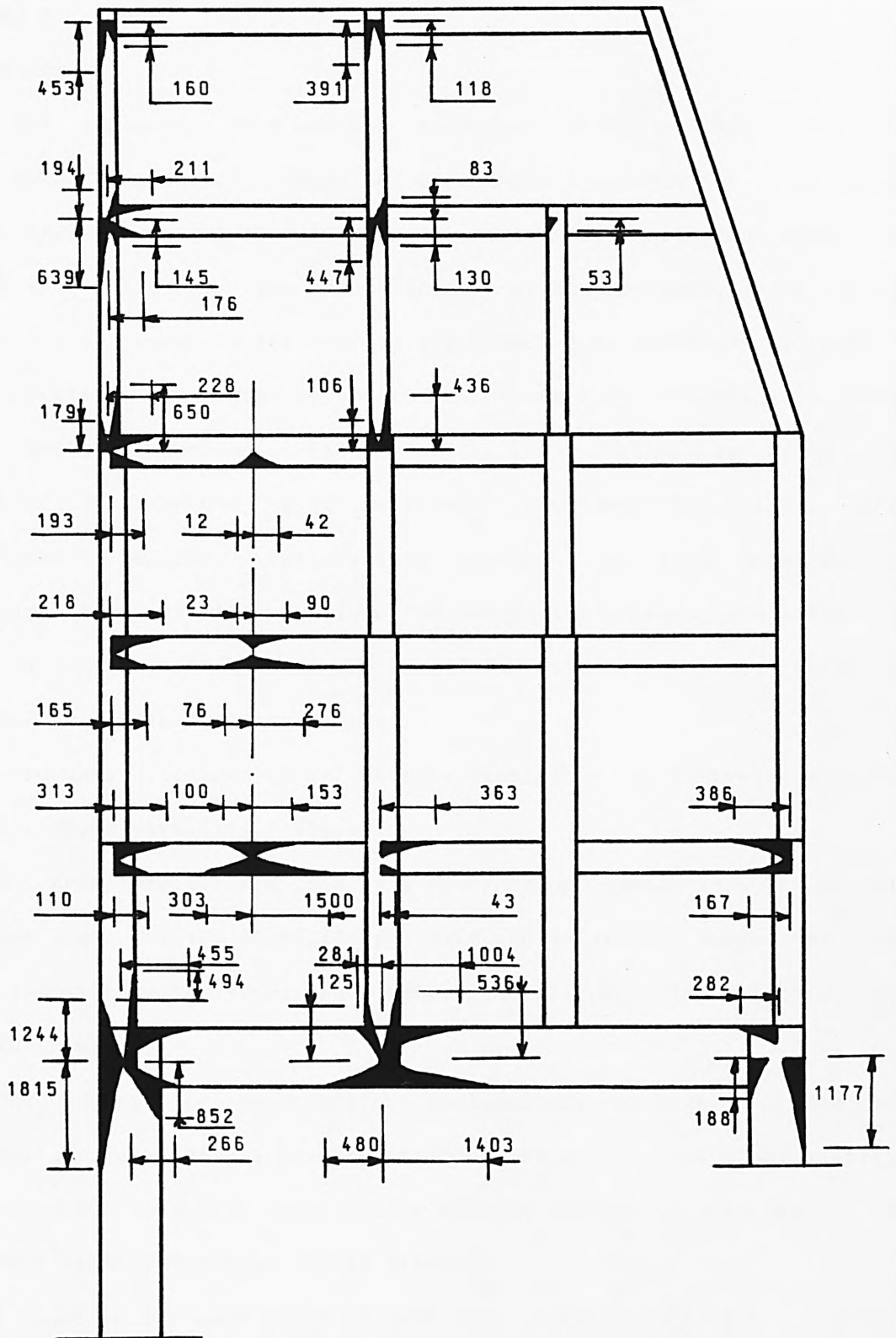


Fig. 7.12 Inelastic Zones At A Load Parameter Of 2.40 For Combined Loading With Wind Acting From The Right

CHAPTER 8

CONCLUSION

The inelastic zone method developed in this thesis uses the distributed inelasticity concept of structural behaviour for metal plane frame stability analysis and design. The method has two principal features. These are the identification of the inelastic zones in a plane frame loaded to failure and the adoption of solution procedures which increase in complexity only as the level of inelasticity in a frame member increases. Frame failure loads obtained by using the inelastic zone method agree well with published theoretical and experimental results. Satisfactory agreement was also obtained by comparing test results obtained for two portal frames subjected to vertical and horizontal loads and loaded to failure with those obtained by using the inelastic zone method.

The work described in this thesis highlights the following aspects of plane frame stability analysis:

1. The predicted failure load of a plane frame depends upon the method employed for the stability analysis and generally approaches the true value with increasing number of non-linear effects included in the analysis.
2. The concept of concentrated inelasticity for frames loaded to failure is a simplification of actual behaviour. The applicability of the distributed inelasticity concept adopted in this thesis is confirmed by tests on portal frames.
3. A bilinear representation of material stress-strain relationships is adequate and can be used to obtain direct formulae for computing the moment-curvature-axial force relationships for member cross-

sections without the need to sub-divide the cross-sections into smaller segments. These formulae are exact, subject to the shape of cross-section chosen and the characteristics of the stress-strain curve adopted.

4. The inelastic zone method is based on calculating tangent flexibility coefficients for a beam-column in a plane frame by using equations to represent the deflection curve for the beam-column. These equations take into account the displacements of all zone intersection points along the beam-column at any stage of analysis up to failure. The lengths of the elastic and inelastic zones are determined by satisfying equilibrium of moments and shear forces and compatibility of deflections and rotations at the zone intersection points.
5. For an elastic zone of a beam-column, an exact equation for the deflection curve is employed. For an inelastic zone of the beam-column, an approximate equation for the deflection curve is chosen which satisfies the curvature boundary conditions. The curvatures at the ends of an inelastic zone are obtained from the moment-curvature-axial force relationships for the cross-section.
6. The errors introduced in the values of deflection and rotation along an inelastic zone are small and diminish as the relative end displacement for the zone increases and as the length of the zone diminishes.
7. The errors introduced in the values of curvature along an inelastic zone depend entirely on the values of the bending moments and curvatures at the ends of the zone. For relatively small differences in these end values, satisfactory curvature distribution along the zone can be obtained. For relatively large

distribution of curvature along the zone may be introduced. In this case, improved curvature values can always be obtained by subdividing the inelastic zone into smaller segments at the expense of increased computational effort. It is worth noting that large errors in curvature distribution along an inelastic zone do not necessarily imply large errors in values of deflection and slope along the zone. Also, the deflection equation chosen in this thesis for an inelastic zone under-estimates curvature values along the zone when the origin of local member axes is at the end with the smaller bending moment and over-estimates curvature values along the zone when the origin is at the end with the larger bending moment.

8. The use of concentrated load simulations in a stability analysis of a plane frame for all distributed loads on the frame is adequate.

The foregoing remarks show that a realistic stability analysis of a plane frame can only be performed by using a computer. Early attempts to obtain frame failure loads aimed at economic, simplified manual methods. It was then necessary not only to ignore some of the factors which affect frame behaviour but also to adopt relatively large factors of safety for frame design. With the increased understanding of frame behaviour made possible by the use of computers, greater confidence is gained in designing taller, more slender and more irregular frames today than before. Thus, in choosing a method for plane frame stability analysis and design purposes, it is essential not only to consider economy of design time and weight of frame but also to consider the limitations of the method with regard to its treatment of non-linear effects and the desired level of accuracy which may necessitate the use

of a computer.

In order to increase the versatility of the inelastic zone method, it would be necessary to extend its application to other areas of structural stability analysis not considered in this thesis. Examples of these areas include the treatment of metal plane frames comprising members of hybrid cross-sections (fabricated from materials of different yield strengths), metal space frames comprising members of rectangular, I-shaped and tubular cross-sections, metal plates and reinforced concrete frames and slabs. Also, its extension to frames comprising members having composite sections of steel and reinforced concrete and to the dynamic stability analyses of frames would be desirable. It can be expected that any extension of the inelastic zone method to these and other areas of structural stability analysis would pose problems of analysis and can only be made possible by further research.

APPENDIX 1

FORMULAE FOR THE MOMENT-CURVATURE-AXIAL FORCE RELATIONSHIPS FOR A RECTANGULAR CROSS-SECTION OF AN ELASTIC-PERFECTLY-PLASTIC MATERIAL

Introduction

The relevant formulae can be derived directly from the general formulae for elastic-strain-hardened material presented in Chapter 2 by specifying a value slightly greater than unity (say 1.0001 or 1.001) for B_s and a large value tending to infinity (but not less than 30.0) for A_s . However, this approach will necessitate all the computational steps adopted in Sections 2.5 and 2.6 and will, therefore, make large demands on computer time and storage.

In this appendix, the relevant formulae are presented in simplified forms which altogether avoid the specification of the strain-hardening constants, A_s and B_s , and, therefore, make more economic use of the computer for the computations than when these constants are specified for this material. Reference should be made to Sections 2.5 and 2.6 for the symbols and figures relevant to this appendix.

Moment-Curvature-Axial Force Relationships For A Rectangular Cross-Section Subjected To The Primary Yield Stress Distribution

$$\psi_1 = \psi_2 = C_s = 0 \quad (\text{A1.1})$$

Hence substitution of Eqns. (2.8a) and (A1.1) into Eqn. (2.9a) gives

$$M_z = (P_s - P)(H/2 - a/3) \quad (\text{A1.2a})$$

$$\text{i.e. } a = 3[-M_z / (P_s - P) + H/2] \quad (\text{A1.2b})$$

Also, substitution of Eqns. (2.8a), (A1.2b) and (A1.1) into Eqn. (2.7e) gives

$$\psi = \alpha / [H(P_s - P) - 2M_z]^2 \quad (A1.3a)$$

$$\text{where } \alpha = 8(P_s - P)^3 / (9BE) \quad (A1.3b)$$

The value of the depth, a , of the elastic core which corresponds to σ_2 becoming equal to $-\sigma_y$ is obtained by substituting $-\sigma_y$ for σ in Eqn. (2.8a) thus:

$$a = H - P / (\sigma_y B) \quad (A1.4a)$$

The intermediate yield moment, M_{y2} , is determined by substituting Eqn. (A1.4a) into Eqn. (A1.2a) thus:

$$M_z = M_{y2} = R_a M_{y1} \quad (A1.4b)$$

$$\text{where } R_a = 1 + 2P / P_s \quad (A1.4c)$$

Moment-Curvature-Axial Force Relationships For A Rectangular Cross-Section Subjected To The Secondary Yield Stress Distribution

$$a_1 = [H - a_2 - P / (\sigma_y B)] / 2 \quad (A1.5a)$$

$$a_2 = \psi [M_p - M_z]^{0.5} \quad (A1.5b)$$

$$\psi = [12 / (\sigma_y B)]^{0.5} \quad (A1.5c)$$

$$M_p = [P_s^2 - P^2] / (4\sigma_y B) \quad (A1.5d)$$

APPENDIX 2

FORMULAE FOR THE MOMENT-CURVATURE-AXIAL FORCE RELATIONSHIPS FOR AN I-SHAPED CROSS-SECTION OF AN ELASTIC-PERFECTLY-PLASTIC MATERIAL.

Introduction

The formulae given in this appendix follow the procedure adopted for the rectangular cross-section in Appendix 1 and are based on the general formulae given in Sections 2.7 and 2.8.

Moment-Curvature-Axial Force Relationships For An I-Shaped Cross-Section Subjected To The Primary Yield Stress Distribution

For partial yielding of top flange, the depth, a , of the elastic core is determined from the following equation:

$$A_1 a^3 + A_2 a^2 + A_3 a + A_4 = 0 \quad (A2.1a)$$

$$\text{where } A_1 = -B/3 \quad (A2.1b)$$

$$A_2 = B(H/2 - G_1) \quad (A2.1c)$$

$$A_3 = -2G_1(2T - H)(B - t) \quad (A2.1d)$$

$$A_4 = G_2 - HG_1(H - 2T)(B - t) \quad (A2.1e)$$

$$G_1 = M_z / (P_s - P) \quad (A2.1f)$$

$$G_2 = BT^2(2T/3 - H/2) + \{t(H - 2T)^3 - B(T - H)^2(H - 4T)\} / 6 \quad (A2.1g)$$

by employing Newton's or similar method. Substitution of the resulting value of a into Eqn. (2.30a) gives the appropriate value for σ_2 from which n and ψ can be determined from Eqns. (2.7d) and (2.7e) respectively. If this value of a is within the limits

$$(H - T) \leq a \leq H$$

then it is accepted. Otherwise, it becomes necessary to consider the case of partial web yielding in the top of the cross-section.

The corresponding depth, a , of the elastic core for the determination of the intermediate yield moment is determined from the following equation

$$A_1 a^2 + A_2 a + A_3 = 0 \quad (A2.2a)$$

$$\text{where } A_1 = B \quad (A2.2b)$$

$$A_2 = 2(B-t)(2T-H) - (P_s - P)/\sigma_y \quad (A2.2c)$$

$$A_3 = H(H-2T)(B-t) \quad (A2.2d)$$

$$\text{from which } a = [-A_2 + \{A_2^2 - 4A_1A_3\}^{0.5}] / (2A_1) \quad (A2.2e)$$

If this value of a is within the limits

$$(H-T) \leq a \leq H$$

then its substitution and the substitution of $\sigma_2 = -\sigma_y$ into Eqn. (2.23a) gives the correct value for M_{y2} . Otherwise, it becomes necessary to consider the case of partial web yielding in the top of the cross-section.

For full yielding of top flange and partial yielding of web, the depth, a , of the elastic core for the determination of the curvature is determined from the following equation:

$$A_1 a^3 + A_2 a^2 + A_3 a + A_4 = 0 \quad (A2.3a)$$

$$\text{where } A_1 = -t/3 \quad (A2.3b)$$

$$A_2 = t(H/2 - G_1) \quad (A2.3c)$$

$$A_3 = T(B-t)(H-T-2G_1) \quad (A2.3d)$$

$$A_4 = T^2(B-t)(2T/3 - H/2 + G_1) \quad (A2.3e)$$

$$G_1 = M_z / (P_s - P) \quad (A2.3f)$$

by employing Newton's or similar method. Substitution of the resulting value of a into Eqn. (2.26a) gives the appropriate value for σ_2 from whence n and ψ can be determined from Eqns. (2.7d) and (2.7e) respectively.

The depth, a , of the elastic core for the determination of the intermediate yield moment is determined from the following equation:

$$B_1 a^2 + B_2 a + B_3 = 0 \quad (\text{A2.4a})$$

$$\text{where } B_1 = t \quad (\text{A2.4b})$$

$$B_2 = 2T(B-t) - (P_s - P) / \sigma_y \quad (\text{A2.4c})$$

$$B_3 = T^2(t-B) \quad (\text{A2.4d})$$

$$\text{from which } a = [-B_2 + \{B_2^2 - 4B_1B_3\}^{0.5}] / (2B_1) \quad (\text{A2.4e})$$

If this value of a is within the limits

$$T \leq a \leq (H-T) \quad (\text{A2.4f})$$

then its substitution and the substitution of $\sigma_2 = -\sigma_y$ into Eqn. (2.27a) the correct value for M_{y2} .

For $a = (H-T)$, the limiting axial force, P_{12} , is given by

$$P_{11} = P_s - \sigma_y [2(B-t)(2T-H)(H-T) + B(H-T)^2 + H(H-2T)(B-T)/(H-T)] \quad (\text{A2.5})$$

For $a = T$, the limiting axial force, is given by

$$P_{12} = P_s - \sigma_y BT = \sigma_y [BT + t(H-2T)] \quad (\text{A2.6})$$

Moment-Curvature-Axial Force Relationships For An I-Shaped Cross-Section Subjected To The Secondary Yield Stress Distribution

For full yielding of flange and partial yielding of web at both ends of cross-section, the relevant formulae for the depths a_1 and a_2 in Fig. 2.8 are given by

$$a_1 = (F - a_2) / 2 + T \quad (\text{A2.7a})$$

$$a_2 = \varphi (M_p - M_z)^{0.5} \quad (\text{A2.7b})$$

$$M_p = \sigma_y [Kt + BT(H-T)] \quad (\text{A2.7c})$$

$$K = F[2(H-2T) - F] / 4 \quad (\text{A2.7d})$$

$$F = (A - 2BT - P/\sigma_y)/t \quad (A2.7e)$$

$$\phi = [12/(\sigma_y t)]^{0.5} \quad (A2.7f)$$

Substitution of Eqns. (2.30a), (A2.7d) and (A2.7e) into Eqn. (A2.7c) gives

$$M_p = \sigma_y \{ [(H-2T)^2 - (P/(\sigma_y t))^2] / (4t) + BT(H-T) \} \quad (A2.7g)$$

The ultimate moment of resistance, M_{y3} , is evidently equal to the fully-plastic moment, M_p , for the curvature, ψ , determined by substituting Eqn. (A2.7b) into Eqn. (2.15e), to be infinite.

The formulae derived in this section are valid within the following limits:

$$a_1 \geq T \quad (A2.8a)$$

$$(a_1 + a_2) \leq (H - T) \quad (A2.8b)$$

If condition (A2.8b) is not satisfied, the axial force is very low and the approximate approach for case 1 in Section 2.7 should be adopted. The limiting axial force, P_{13} , above which these formulae are no longer applicable is derived from Eqn. (2.30a) by setting a_1 equal to T and a_2 equal to zero to obtain

$$P_{13} = P_s - 2\sigma_y BT \quad (A2.9a)$$

Substitution of Eqns. (2.22c) and (2.22d) into Eqn. (A2.9a) gives

$$P_{13} = \sigma_y t(H - 2T) \quad (A2.9b)$$

The corresponding limiting bending moment, M_{13} , is derived from Eqn. (2.31a) as

$$M_{13} = \sigma_y BT(H - T) \quad (A2.9c)$$

For full yielding of top flange and partial yielding of bottom flange and full or partial yielding of web, linear interpolation is employed as in Section 2.8.2 to determine the ultimate yield moment as follows:

$$M_{y3} = M_{13}R_c \quad (A2.10a)$$

where $R_c = (P_s - P) / (P_s - P_{13}) \quad (A2.10b)$

and $P_s > P > P_{13} \quad (A2.10c)$

APPENDIX 3

NEWTON'S METHOD OF SUCCESSIVE APPROXIMATIONS FOR SOLVING AN EQUATION OF ONE UNKNOWN

Let $f(x)$ be a function of x .

Let $f'(x)$ be the first derivative of $f(x)$.

We want to obtain the solution of the equation

$$f(x) = 0 \quad (\text{A3.1})$$

by trial-and-error. Let a first approximation for x be x_1 .

Then, the second approximation for x is given by

$$x_2 = x_1 - f(x_1)/f'(x_1) \quad (\text{A3.2})$$

It follows that the n th. approximation for x is given by

$$x_n = x_{n-1} - f(x_{n-1})/f'(x_{n-1}) \quad (\text{A3.3})$$

Iteration is continued by employing equation (A3.3) until the difference between x_n and x_{n-1} becomes very small or satisfies a convergence criterion. Then, the resulting value of x_n is chosen as the required value of x .

APPENDIX 4

FORMULAE FOR SOLVING TWO, THREE AND FOUR SIMULTANEOUS EQUATIONS

Introduction

In Chapter 3, solutions of two, three or four simultaneous equations were required to determine the deflection components due to curvature of the zone intersection points. Formulae for the explicit solutions of these equations are given in this appendix.

Formulae For Solving Two Simultaneous Equations

The matrix form of the relevant equations is given by

$$\begin{bmatrix} A_{11} & A_{12} \\ A_{12} & A_{22} \end{bmatrix} \begin{Bmatrix} X_1 \\ X_2 \end{Bmatrix} = \begin{Bmatrix} B_{11} \\ B_{22} \end{Bmatrix} \quad (\text{A4.1})$$

The required solution of Eqn. (A4.1) is given in matrix form as follows:

$$\begin{Bmatrix} X_1 \\ X_2 \end{Bmatrix} = \begin{bmatrix} 1/A_{11} & 0 \\ 0 & 1/F_{22} \end{bmatrix} \begin{Bmatrix} D_{11} \\ D_{22} \end{Bmatrix} \quad (\text{A4.2})$$

where $f_1 = A_{12}/A_{11}$

$$F_{22} = A_{22} - f_1 A_{12}$$

$$g_1 = A_{12}/F_{22}$$

$$D_{11} = B_{11} Q_{11} + B_{22} Q_{12}$$

$$D_{22} = B_{11} Q_{21} + B_{22} Q_{22}$$

$$Q_{11} = 1 + f_1 g_1$$

$$Q_{12} = -g_1$$

$$Q_{21} = -f_1$$

(A4.3)

Formulae For Solving Three Simultaneous Equations

The matrix form of the relevant equations is given by

$$\begin{bmatrix} A_{11} & A_{12} & 0 \\ A_{12} & A_{22} & A_{23} \\ 0 & A_{23} & A_{33} \end{bmatrix} \begin{Bmatrix} X_1 \\ X_2 \\ X_3 \end{Bmatrix} = \begin{Bmatrix} B_{11} \\ B_{22} \\ B_{33} \end{Bmatrix} \quad (\text{A4.4})$$

The required solution of Eqn. (A4.4) is given in matrix form as follows:

$$\begin{Bmatrix} X_1 \\ X_2 \\ X_3 \end{Bmatrix} = \begin{bmatrix} 1/A_{11} & 0 & 0 \\ 0 & 1/F_{22} & 0 \\ 0 & 0 & 1/F_{33} \end{bmatrix} \begin{Bmatrix} D_{11} \\ D_{22} \\ D_{33} \end{Bmatrix} \quad (\text{A4.5})$$

where

$$\begin{aligned} f_1 &= A_{12}/A_{11} \\ F_{22} &= A_{22} - f_1 A_{12} \\ f_2 &= A_{23}/F_{22} \\ F_{33} &= A_{33} - f_2 A_{23} \\ g_1 &= A_{23}/F_{33} \\ g_2 &= A_{12}/C_{22} \\ D_{11} &= B_{11} Q_{11} + B_{22} Q_{12} + B_{33} Q_{13} \\ D_{22} &= B_{11} Q_{21} + B_{22} Q_{22} + B_{33} Q_{23} \\ D_{33} &= B_{11} Q_{31} + B_{22} Q_{32} + B_{33} \\ Q_{11} &= 1 + f_1 g_2 (1 + f_2 g_1) \\ Q_{12} &= -g_2 (1 + f_2 g_1) \\ Q_{13} &= g_1 g_2 \\ Q_{21} &= -f_1 (1 + f_2 g_1) \\ Q_{22} &= 1 + f_2 g_1 \\ Q_{23} &= -g_1 \\ Q_{31} &= f_1 f_2 \\ Q_{32} &= -f_2 \end{aligned} \quad (\text{A4.6})$$

Formulae For Solving Four Simultaneous Equations

The matrix form of the relevant equations is given by

$$\begin{bmatrix} A_{11} & A_{12} & 0 & 0 \\ A_{12} & A_{22} & A_{23} & 0 \\ 0 & A_{23} & A_{33} & A_{34} \\ 0 & 0 & A_{34} & A_{44} \end{bmatrix} \begin{Bmatrix} X_1 \\ X_2 \\ X_3 \\ X_4 \end{Bmatrix} = \begin{Bmatrix} B_{11} \\ B_{22} \\ B_{33} \\ B_{44} \end{Bmatrix} \quad (\text{A4.7})$$

The required solution of Eqn. (A4.7) is given in matrix form as follows:

$$\begin{Bmatrix} X_1 \\ X_2 \\ X_3 \\ X_4 \end{Bmatrix} = \begin{bmatrix} 1/A_{11} & 0 & 0 & 0 \\ 0 & 1/F_{22} & 0 & 0 \\ 0 & 0 & 1/F_{33} & 0 \\ 0 & 0 & 0 & 1/F_{44} \end{bmatrix} \begin{Bmatrix} D_{11} \\ D_{22} \\ D_{33} \\ D_{44} \end{Bmatrix} \quad (\text{A4.8})$$

$$\text{where } f_1 = A_{12}/A_{11}$$

$$F_{22} = A_{22} - f_1 A_{12}$$

$$f_2 = A_{23}/F_{22}$$

$$F_{33} = A_{33} - f_2 A_{23}$$

$$f_3 = A_{34}/F_{33}$$

$$F_{44} = A_{44} - f_3 A_{34}$$

$$g_1 = A_{34}/F_{44}$$

$$g_2 = A_{23}/F_{33}$$

$$g_3 = A_{12}/F_{22}$$

(A4.9)

$$D_{11} = B_{11} Q_{11} + B_{22} Q_{12} + B_{33} Q_{13} + B_{44} Q_{14}$$

$$D_{22} = B_{11} Q_{21} + B_{22} Q_{22} + B_{33} Q_{23} + B_{44} Q_{24}$$

$$D_{33} = B_{11} Q_{31} + B_{22} Q_{32} + B_{33} Q_{33} + B_{44} Q_{34}$$

$$D_{44} = B_{11} Q_{41} + B_{22} Q_{42} + B_{33} Q_{43} + B_{44}$$

$$Q_{11} = 1 + f_1 g_3 (1 + f_2 g_2 (1 + f_3 g_1))$$

$$Q_{12} = -g_3 (1 + f_2 g_2 (1 + f_3 g_1))$$

$$\begin{aligned}
Q_{13} &= g_2 g_3 (1 + f_3 g_1) \\
Q_{14} &= -g_1 g_2 g_3 \\
Q_{21} &= -f_1 (1 + f_2 g_2 (1 + f_3 g_1)) \\
Q_{22} &= 1 + f_2 g_2 (1 + f_3 g_1) \\
Q_{23} &= -g_2 (1 + f_3) \\
Q_{24} &= g_1 g_2 \\
Q_{31} &= f_1 f_2 (1 + f_3 g_1) \\
Q_{32} &= -f_2 (1 + f_3 g_1) \\
Q_{33} &= 1 + f_3 g_1 \\
Q_{34} &= -g_1 \\
Q_{41} &= -f_1 f_2 f_3 \\
Q_{42} &= f_2 f_3 \\
Q_{43} &= -f_3
\end{aligned}$$

(A4.9 continued)

APPENDIX 5

A PARAMETRIC STUDY OF THE PROPOSED DEFLECTION CURVE FOR AN INELASTIC ZONE OF A BEAM-COLUMN

Introduction

Eqn. (3.17), reproduced here as Eqn. (A5.1a), defines the proposed deflection curve for an inelastic zone, 1-2, of a beam-column.

$$y = A\cos(m_1x) + B\sin(q_1x) - M_1[1-x/B_1]/P - M_2[x/B_1]/P + \Delta_1[1-x/B_1] + \Delta_2[x/B_1] \quad (\text{A5.1a})$$

In this equation, the origin of Cartesian co-ordinates is at the end with the bending moment, M_1 . This equation was chosen by comparison with the exact, well-known equation for the deflection curve for an elastic beam-column so that the tangent flexibility coefficients for the entire beam-column comprising a number of elastic and inelastic zones can be easily determined by assigning appropriate values to the arbitrary constants, A , B , m_1 and q_1 . The slope and curvature equations derived from Eqn. (A5.1a) are as follows:

$$y' = -Am_1\sin(m_1x) + Bq_1\cos(q_1x) + [(M_1 - M_2)/P + \Delta_2 - \Delta_1]/B_1 \quad (\text{A5.1b})$$

$$y'' = -[Am_1^2\cos(m_1x) + Bq_1^2\sin(q_1x)] \quad (\text{A5.1c})$$

For an inelastic zone, however, the depths of the elastic core vary with length and Eqns. (A5.1) may not give identical results with those obtained by inter-changing the end bending moments or by placing the origin of Cartesian co-ordinates at the end with the bending moment, M_2 .

The main aims of this Parametric Study are to ascertain the significance of these differences and to highlight any of the limitations of Eqns. (A5.1).

The Parameters

Curve 1 of Fig. A5.1 represents the deflected shape of an inelastic zone, 1-5, subjected to an axial force, P , and end bending moments, M_1 and M_5 . The relative displacement of the ends of the zone is Δ and the yielding spreads from end 1 to end 5 so that the values of bending moment and curvature at end 1 are greater than the corresponding values at end 5. Curve 2 of Fig. A5.1 is a mirror-image of Curve 1 except that the origin of Cartesian co-ordinates is at end 1 for Curve 1 and at end 5 for Curve 2.

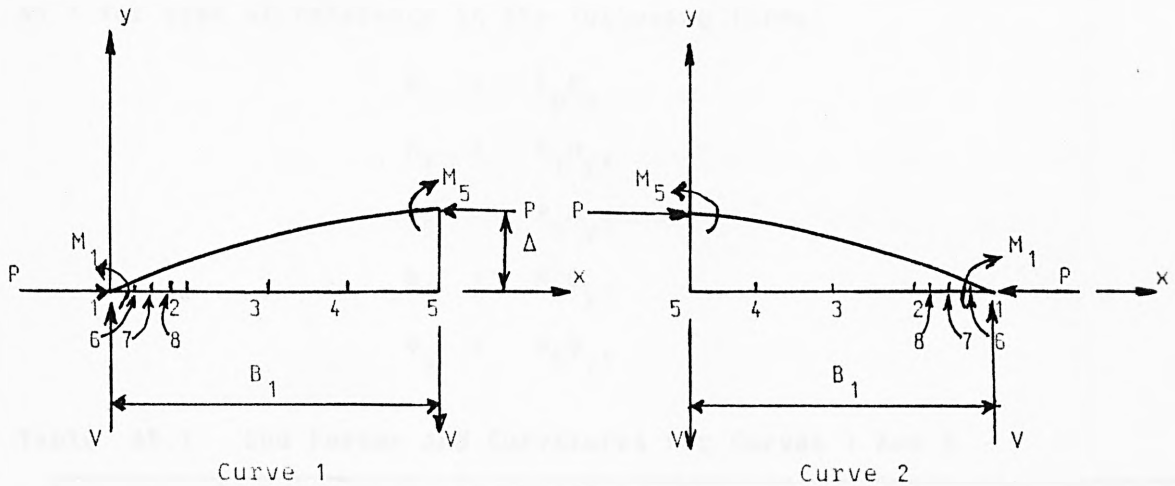


Fig. A5.1

This Parametric Study will be carried out by selecting values for the parameters, P , B_1 and Δ and calculating the moment, deflection, rotation and curvature variation at intermediate points along the zone for the two curves shown in Fig. A5.1. The values of the parameters are as follows:

values for P are $0.001P_s$ and $0.2P_s$.

values for B_1 are 50.0mm and 200.0mm and

values for Δ are 1.0mm and 20.0mm.

Also, two types of inelastic zone will be studied, namely the zone for which $M_1 = M_{y2}$ and $M_5 = M_{y1}$ and the zone for which $M_1 = M_{y3}$ and $M_5 = M_{y2}$

where the bending moments are determined for the chosen values of the axial force.

The I-shaped cross-section (that is 305x127UB48kg/m), yield stress and modulus of elasticity employed in Example 2.1 for an elastic-perfectly-plastic material will be employed here. Thus, the values of axial force and the corresponding values of the bending moments are given in Table 2.1. The curvature values corresponding to the chosen axial force and bending moment values are derived from Fig. 2.10. The values of axial force, bending moments and curvatures are given in Table A5.1 for ease of reference in the following forms:

$$\begin{aligned}
 P &= C_p P_s \\
 M_1 &= R_1 M_{y1} \\
 M_5 &= R_5 M_{y1} \\
 \psi_1 &= N_1 \psi_{y1} \\
 \psi_5 &= N_5 \psi_{y1}
 \end{aligned}$$

Table A5.1 End Forces And Curvatures For Curves 1 And 2

Parameter	Value			
C_p	0.001		0.2	
P	1.505 kN		301.0 kN	
M_{y1}	151000.0 kN.mm		121000.0 kN.mm	
ψ_{y1}	0.00000766 mm ⁻¹		0.00000614 mm ⁻¹	
	Zone With $M_1 = M_{y2}$ And $M_2 = M_{y1}$	Zone With $M_1 = M_{y3}$ And $M_2 = M_{y2}$	Zone With $M_1 = M_{y2}$ And $M_2 = M_{y1}$	Zone With $M_1 = M_{y3}$ And $M_2 = M_{y2}$
R_1	1.002	1.155	1.283	1.358
R_5	1.000	1.002	1.000	1.283
N_1	1.002	5.000	4.000	5.000
N_5	1.000	1.002	1.000	4.000

The results of this Parametric Study are summarized in Tables A5.2 to A5.11 inclusive and in Figs. A5.2 to A5.5 inclusive. The results are given for quarter points along the zones and for quarter points along the end segments of the zones, each segment being of length one-quarter that of the zone.

The following notations are used in the Tables and Figures:

$$C_1 = m_1/q_1$$

$$R_i = M_i/M_{y1}$$

$$N_i = \psi_i/\psi_{y1}$$

Δ_i = deflection of point i

θ_i = rotation of point i

EQ. = curvature value determined from Eqn. (A5.1c)

FG. = curvature value determined from Fig. 2.10

Zone	Point 1		Point 2		Point 3		Point 4	
	EQ.	FG.	EQ.	FG.	EQ.	FG.	EQ.	FG.
Z_1	0.0000	0.0000	0.0000	0.0000	0.0000	0.0000	0.0000	0.0000
Z_2	0.0000	0.0000	0.0000	0.0000	0.0000	0.0000	0.0000	0.0000
Z_3	0.0000	0.0000	0.0000	0.0000	0.0000	0.0000	0.0000	0.0000
Z_4	0.0000	0.0000	0.0000	0.0000	0.0000	0.0000	0.0000	0.0000
Z_5	0.0000	0.0000	0.0000	0.0000	0.0000	0.0000	0.0000	0.0000
Z_6	0.0000	0.0000	0.0000	0.0000	0.0000	0.0000	0.0000	0.0000
Z_7	0.0000	0.0000	0.0000	0.0000	0.0000	0.0000	0.0000	0.0000
Z_8	0.0000	0.0000	0.0000	0.0000	0.0000	0.0000	0.0000	0.0000
Z_9	0.0000	0.0000	0.0000	0.0000	0.0000	0.0000	0.0000	0.0000
Z_{10}	0.0000	0.0000	0.0000	0.0000	0.0000	0.0000	0.0000	0.0000
Z_{11}	0.0000	0.0000	0.0000	0.0000	0.0000	0.0000	0.0000	0.0000
Z_{12}	0.0000	0.0000	0.0000	0.0000	0.0000	0.0000	0.0000	0.0000
Z_{13}	0.0000	0.0000	0.0000	0.0000	0.0000	0.0000	0.0000	0.0000
Z_{14}	0.0000	0.0000	0.0000	0.0000	0.0000	0.0000	0.0000	0.0000
Z_{15}	0.0000	0.0000	0.0000	0.0000	0.0000	0.0000	0.0000	0.0000

Table A5.2 Results For Inelastic Zone 1-5

Parameter		Value							
C_p		0.001				0.001			
R_1		1.002				1.002			
R_5		1.000				1.000			
N_1		1.002				1.002			
N_5		1.000				1.000			
B_1		50.0				200.0			
Δ_1		0.0				0.0			
Δ_5		1.0				1.0			
Result	Curve 1		Curve 2		Curve 1		Curve 2		
R_2	1.0015		1.0015		1.0015		1.0015		
R_3	1.0010		1.0010		1.0010		1.0010		
R_4	1.0005		1.0005		1.0005		1.0005		
Δ_2	0.25185		0.25185		0.27875		0.27875		
Δ_3	0.50246		0.50246		0.53836		0.53836		
Δ_4	0.75177		0.75177		0.77877		0.77877		
θ_1	0.020192		-0.020192		0.005767		-0.005767		
θ_2	0.020095		-0.020095		0.005383		-0.005383		
θ_3	0.020000		-0.020000		0.005000		-0.005000		
θ_4	0.019904		-0.019904		0.004616		-0.004616		
θ_5	0.019808		-0.019808		0.004234		-0.004234		
N_2	EQ.	FG.	EQ.	FG.	EQ.	FG.	EQ.	FG.	
	1.0015	1.0015	1.0015	1.0015	1.0015	1.0015	1.0015	1.0015	
	1.0010	1.0010	1.0010	1.0010	1.0010	1.0010	1.0010	1.0010	
	1.0005	1.0005	1.0005	1.0005	1.0005	1.0005	1.0005	1.0005	
C_1	1.000								

Table A5.3 Results For Inelastic Zone 1-5

Parameter		Value							
C_p		0.001				0.001			
R_1		1.002				1.002			
R_5		1.000				1.000			
N_1		1.002				1.002			
N_5		1.000				1.000			
B_1		50.0				200.0			
Δ_1		0.0				0.0			
Δ_5		20.0				20.0			
Result		Curve 1		Curve 2		Curve 1		Curve 2	
R_2		1.0015		1.0015		1.0015		1.0015	
R_3		1.0010		1.0010		1.0010		1.0010	
R_4		1.0005		1.0005		1.0005		1.0005	
Δ_2		5.00185		5.00185		5.02875		5.02875	
Δ_3		10.00246		10.00246		10.03836		10.03836	
Δ_4		15.00177		15.00177		15.02877		15.02877	
θ_1		0.400192		-0.400192		0.100767		-0.100767	
θ_2		0.400095		-0.400095		0.100383		-0.100383	
θ_3		0.400000		-0.400000		0.100000		-0.100000	
θ_4		0.399040		-0.399040		0.099616		-0.099616	
θ_5		0.399808		-0.399808		0.090233		-0.090233	
		EQ.	FG.	EQ.	FG.	EQ.	FG.	EQ.	FG.
N_2		1.0015	1.0015	1.0015	1.0015	1.0015	1.0015	1.0015	1.0015
N_3		1.0010	1.0010	1.0010	1.0010	1.0010	1.0010	1.0010	1.0010
N_4		1.0005	1.0005	1.0005	1.0005	1.0005	1.0005	1.0005	1.0005
C_1		1.000							

Table A5.4 Results For Inelastic Zone 1-5

Parameter	Value							
C_p	0.2				0.2			
R_1	1.283				1.283			
R_5	1.0				1.0			
N_1	4.0				4.0			
N_5	1.0				1.0			
B_1	50.0				200.0			
Δ_1	0.0				0.0			
Δ_5	1.0				1.0			
Result	Curve 1		Curve 2		Curve 1		Curve 2	
R_2	1.2123		1.2123		1.2124		1.2123	
R_3	1.1415		1.1415		1.1416		1.1415	
R_4	1.0708		1.0708		1.0709		1.0708	
Δ_2	0.255587		0.25218		0.339377		0.284888	
Δ_3	0.507404		0.502765		0.61844		0.544258	
Δ_4	0.75519		0.751968		0.838281		0.781499	
θ_1	0.0206		-0.020244		0.007398		-0.005975	
θ_2	0.020295		-0.0220108		0.006181		-0.005431	
θ_3	0.019996		-0.019989		0.004985		-0.004955	
θ_4	0.019703		-0.019887		0.003812		-0.004546	
θ_5	0.019415		-0.019801		0.002661		-0.004205	
	EQ.	FG.	EQ.	FG.	EQ.	FG.	EQ.	FG.
N_2	3.9293	3.5000	1.6618	3.5000	3.9293	3.5000	1.6624	3.5000
N_3	3.8585	2.5000	1.4412	2.5000	3.8582	2.5000	1.4417	2.5000
N_4	3.7877	1.5000	1.2206	1.5000	3.7865	1.5000	1.2209	1.5000
C_1	1.766							

Table A5.5 Results For Inelastic Zone 1-5

Parameter	Value							
C_p	0.2				0.2			
R_1	1.283				1.283			
R_5	1.000				1.000			
N_1	4.0				4.0			
N_5	1.0				1.0			
B_1	50.0				200.0			
Δ_1	0.0				0.0			
Δ_5	20.0				20.0			
Result	Curve 1		Curve 2		Curve 1		Curve 2	
R_2	1.2123		1.2123		1.2124		1.2123	
R_3	1.1415		1.1415		1.1416		1.1415	
R_4	1.0708		1.0708		1.0709		1.0708	
Δ_2	5.005587		5.00218		5.089377		5.034888	
Δ_3	10.007404		10.002765		10.11844		10.044258	
Δ_4	15.005519		15.001968		15.088281		15.031499	
θ_1	0.40060		-0.400244		0.102398		-0.100976	
θ_2	0.400295		-0.400108		0.101181		-0.100431	
θ_3	0.399996		-0.399989		0.099985		-0.099955	
θ_4	0.399703		-0.399887		0.098812		-0.099546	
θ_5	0.399415		-0.399801		0.097661		-0.099205	
	EQ.	FG.	EQ.	FG.	EQ.	FG.	EQ.	FG.
N_2	3.9293	3.5000	1.6618	3.5000	3.9293	3.5000	1.6624	3.5000
N_3	3.8585	2.5000	1.4412	2.5000	3.8582	2.5000	1.4417	2.5000
N_4	3.7877	1.5000	1.2206	1.5000	3.7865	1.5000	1.2209	1.5000
C_1	1.766							

Table A5.6 Results For Inelastic Zone 1-5

Parameter	Value							
C_p	0.001				0.001			
R_1	1.155				1.155			
R_5	1.002				1.002			
N_1	5.0				5.0			
N_5	1.002				1.002			
B_1	50.0				200.0			
Δ_1	0.0				0.0			
Δ_5	1.0				1.0			
Result	Curve 1		Curve 2		Curve 1		Curve 2	
R_2	1.1168		1.1168		1.1168		1.1168	
R_3	1.0785		1.0785		1.0785		1.0785	
R_4	1.0403		1.0403		1.0403		1.0403	
Δ_2	0.25882		0.25251		0.39172		0.28991	
Δ_3	0.51176		0.50325		0.68856		0.55105	
Δ_4	0.7588		0.7523		0.8910		0.7867	
θ_1	0.020949		-0.020277		0.008791		-0.006106	
θ_2	0.02047		-0.020125		0.006883		-0.0055	
θ_3	0.019997		-0.019990		0.00499		-0.004958	
θ_4	0.019527		-0.01987		0.003112		-0.004479	
θ_5	0.019062		-0.019766		0.001248		-0.004063	
	EQ.	FG.	EQ.	FG.	EQ.	FG.	EQ.	FG.
N_2	4.9618	3.8000	1.4988	3.8000	4.9618	3.8000	1.4988	3.8000
N_3	4.9235	3.0000	1.3332	3.0000	4.9235	3.0000	1.3332	3.0000
N_4	4.8853	2.4000	1.1678	2.4000	4.8853	2.4000	1.1678	2.4000
C_1	2.081							

Table A5.7 Results For Inelastic Zone 1-5

Parameter		Value							
C_p		0.001				0.001			
R_1		1.155				1.155			
R_5		1.002				1.002			
N_1		5.0				5.0			
N_5		1.002				1.002			
B_1		50.0				200.0			
Δ_1		0.0				0.0			
Δ_5		20.0				20.0			
Result		Curve 1		Curve 2		Curve 1		Curve 2	
R_2		1.1168		1.1168		1.1168		1.1168	
R_3		1.0785		1.0785		1.0785		1.0785	
R_4		1.0403		1.0403		1.0403		1.0403	
Δ_2		5.00882		5.00251		5.14172		5.03991	
Δ_3		10.01176		10.00325		10.18856		10.05105	
Δ_4		15.0088		15.0023		15.141		15.0367	
θ_1		0.400949		-0.400277		0.103791		-0.101106	
θ_2		0.400470		-0.400125		0.101883		-0.100500	
θ_3		0.399997		-0.399990		0.099990		-0.099958	
θ_4		0.399527		-0.399870		0.098112		-0.099479	
θ_5		0.399062		-0.399766		0.096248		-0.099063	
		EQ.	FG.	EQ.	FG.	EQ.	FG.	EQ.	FG.
N_2		4.9618	3.8000	1.4988	3.8000	4.9618	3.8000	1.4988	3.8000
N_3		4.9235	3.0000	1.3332	3.0000	4.9235	3.0000	1.3332	3.0000
N_4		4.8853	2.4000	1.1678	2.4000	4.8853	2.4000	1.1678	2.4000
C_1		2.081							

Table A5.8 Results For Inelastic Zone 1-5

Parameter		Value							
C_p		0.2				0.2			
R_1		1.358				1.358			
R_5		1.283				1.283			
N_1		5.0				5.0			
N_5		4.0				4.0			
B_1		50.0				200.0			
Δ_1		0.0				0.0			
Δ_5		1.0				1.0			
Result	Curve 1		Curve 2		Curve 1		Curve 2		
R_2	1.3393		1.3393		1.3395		1.3395		
R_3	1.3205		1.3205		1.3205		1.3205		
R_4	1.3018		1.3018		1.3020		1.3020		
Δ_2	0.257055		0.255988		0.352899		0.345836		
Δ_3	0.509369		0.507940		0.639933		0.627075		
Δ_4	0.756999		0.755922		0.851990		0.844774		
θ_1	0.020756		-0.020642		0.008023		-0.007570		
θ_2	0.020374		-0.020317		0.006496		-0.006267		
θ_3	0.019997		-0.019996		0.004988		-0.004986		
θ_4	0.019624		-0.019682		0.003498		-0.003726		
θ_5	0.019256		-0.019372		0.002026		-0.002487		
	EQ.	FG.	EQ.	FG.	EQ.	FG.	EQ.	FG.	
N_2	4.9416	4.9000	4.2072	4.9000	4.9424	4.9000	4.2084	4.9000	
N_3	4.8832	4.8500	4.1382	4.8500	4.8840	4.8500	4.1394	4.8500	
N_4	4.8247	4.8000	4.0691	4.8000	4.8250	4.8000	4.0700	4.8000	
C_1	1.087								

Table A5.9 Results For Inelastic Zone 1-5

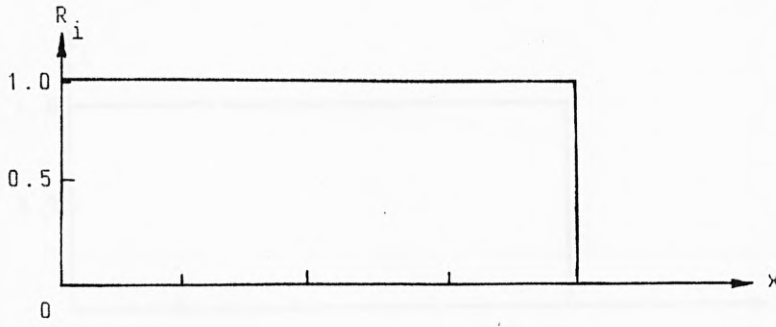
Parameter	Value								
C_p	0.2				0.2				
R_1	1.358				1.358				
R_5	1.283				1.283				
N_1	5.0				5.0				
N_5	4.0				4.0				
B_1	50.0				200.0				
Δ_1	0.0				0.0				
Δ_5	20.0				20.0				
Result	Curve 1		Curve 2		Curve 1		Curve 2		
R_2	1.3393		1.3393		1.3395		1.3395		
R_3	1.3205		1.3205		1.3208		1.3208		
R_4	1.3018		1.3018		1.3020		1.3020		
Δ_2	5.007055		5.005988		5.112899		5.095836		
Δ_3	10.009369		10.00794		10.149933		10.127075		
Δ_4	15.006999		15.005922		15.111998		15.094774		
θ_1	0.400756		-0.400642		0.103023		-0.102570		
θ_2	0.400374		-0.400317		0.101496		-0.101267		
θ_3	0.399997		-0.399996		0.099988		-0.099986		
θ_4	0.399624		-0.399682		0.098498		-0.098726		
θ_5	0.399256		-0.399372		0.097026		-0.097487		
N_2	EQ.	FG.	EQ.	FG.	EQ.	FG.	EQ.	FG.	
	4.9416	4.9000	4.2072	4.9000	4.9424	4.9000	4.2084	4.9000	
	N_3	4.8832	4.8500	4.1382	4.8500	4.8840	4.8500	4.1394	4.8500
	N_4	4.8847	4.8000	4.0691	4.8000	4.8250	4.8000	4.0700	4.8000
C_1	1.087								

Table A5.10 Results For End Segment 1-2 For Inelastic Zone 1-5 Considered In Table A5.4

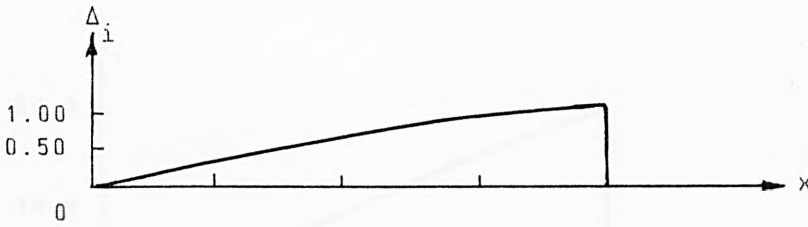
Parameter	Value							
C_p	0.2				0.2			
R_1	1.283				1.283			
R_2	1.2123				1.2123			
N_1	4.0				4.0			
N_2	3.5				3.5			
$B_1/4$	12.5				50.0			
Δ_1	0.0				0.0			
Δ_2	0.255587				0.339377			
Result	Curve 1		Curve 2		Curve 1		Curve 2	
R_6	1.2653		1.2653		1.2653		1.2653	
R_7	1.2476		1.2476		1.2476		1.2476	
R_8	1.2300		1.2300		1.2300		1.2300	
Δ_6	0.064249		0.064223		0.090278		0.090066	
Δ_7	0.128261		0.128227		0.177168		0.177016	
Δ_8	0.192039		0.192013		0.260118		0.259702	
θ_1	0.020598		-0.020587		0.007391		-0.007347	
θ_6	0.020522		-0.020516		0.007086		-0.007064	
θ_7	0.020446		-0.020446		0.006785		-0.006785	
θ_8	0.020372		-0.020377		0.006488		-0.006510	
θ_2	0.020299		-0.02031		0.006194		-0.006239	
	EQ.	FG.	EQ.	FG.	EQ.	FG.	EQ.	FG.
N_6	3.9490	3.9500	3.6654	3.9500	3.9490	3.9500	3.6654	3.9500
N_7	3.8979	3.8500	3.6103	3.8500	3.8979	3.8500	3.6103	3.8500
N_8	3.8468	3.7500	3.5551	3.7500	3.8468	3.7500	3.5551	3.7000
C_1	1.039							

Table A5.11 Results For End Segment 1-2 Of Inelastic Zone 1-5 Considered In Table A5.6

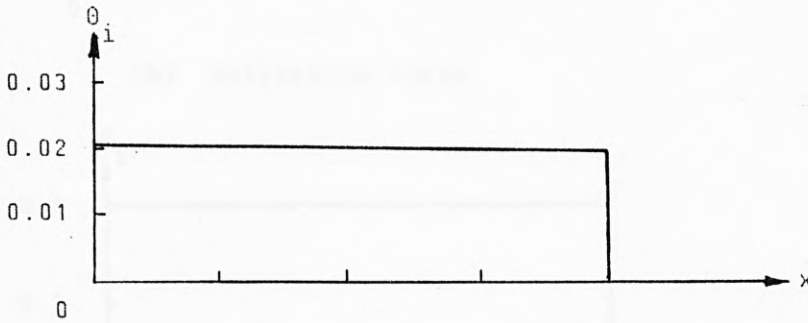
Parameter	Value							
C_p	0.001				0.001			
R_1	1.155				1.155			
R_2	1.1168				1.1168			
N_1	5.0				5.0			
N_2	3.8				3.8			
$B_1/4$	12.5				50.0			
Δ_1	0.0				0.0			
Δ_2	0.25882				0.39172			
Result	Curve 1		Curve 2		Curve 1		Curve 2	
R_6	1.1454		1.1454		1.1454		1.1454	
R_7	1.1359		1.1359		1.1359		1.1359	
R_8	1.1263		1.1263		1.1263		1.1263	
Δ_6	0.065195		0.065085		0.10582		0.10491	
Δ_7	0.13011		0.13000		0.20656		0.20515	
Δ_8	0.194615		0.19460		0.30159		0.30069	
θ_1	0.020946		-0.020894		0.008783		-0.008583	
θ_6	0.020823		-0.020800		0.008306		-0.008205	
θ_7	0.020705		-0.020706		0.007832		-0.007831	
θ_8	0.020587		-0.020614		0.007361		-0.007461	
θ_2	0.020473		-0.020522		0.006893		-0.007096	
	EQ.	FG.	EQ.	FG.	EQ.	FG.	EQ.	FG.
N_6	4.9675	4.7000	3.9242	4.7000	4.9675	4.7000	3.9242	4.7000
N_7	4.9349	4.4000	3.8830	4.4000	4.9349	4.4000	3.8830	4.4000
N_8	4.9024	4.1000	3.8414	4.1000	4.9024	4.1000	3.8414	4.1000
C_1	1.128							



(a) Moment Distribution Diagram

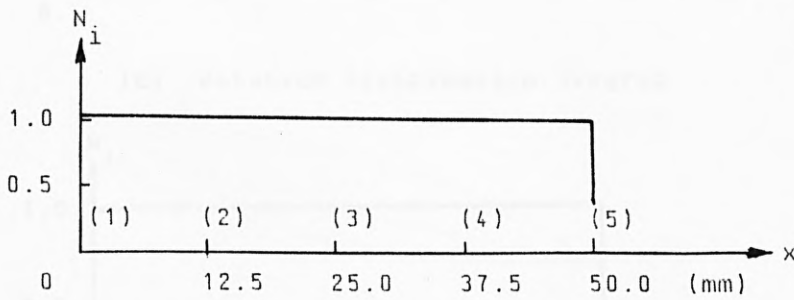


(b) Deflection Curve



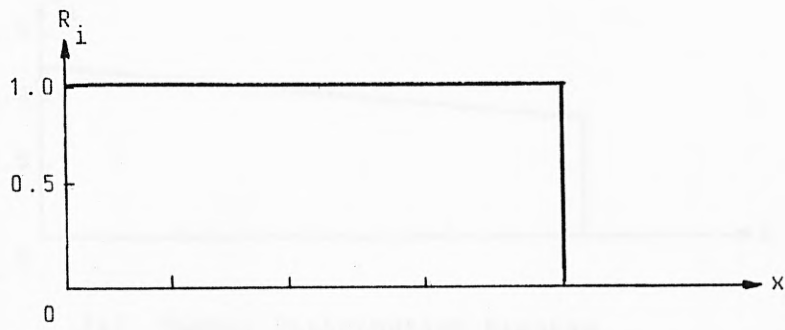
(c) Rotation Distribution Diagram

$C_1 = 1.000$

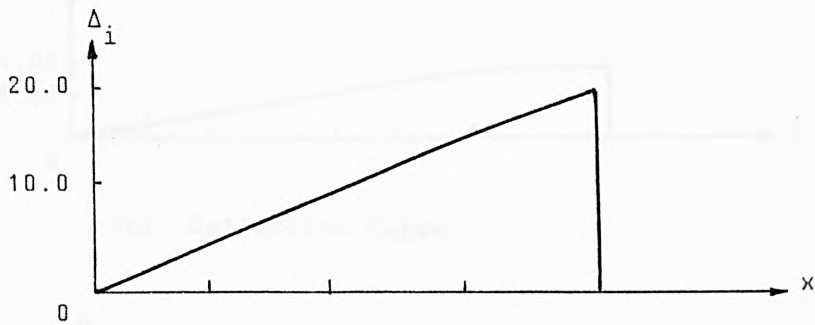


(d) Curvature Distribution Diagram

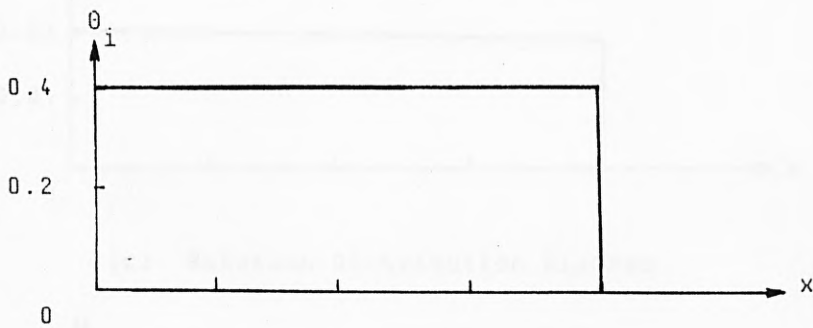
Fig. A5.2 Deflection Curve And Moment, Rotation And Curvature Distribution Diagrams For Curves 1 And 2 For Inelastic Zone Of Length 50.0mm Considered In Table A5.2



(a) Moment Distribution Diagram

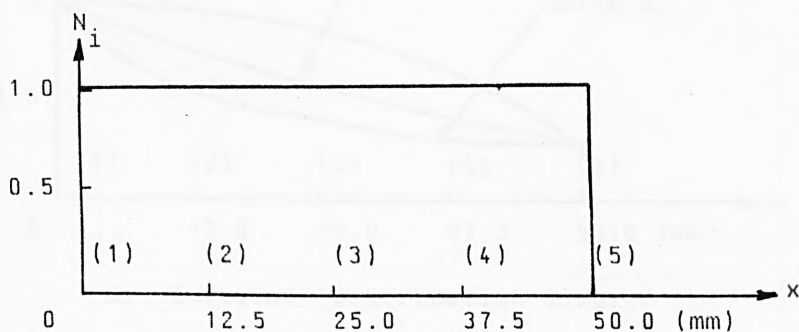


(b) Deflection Curve



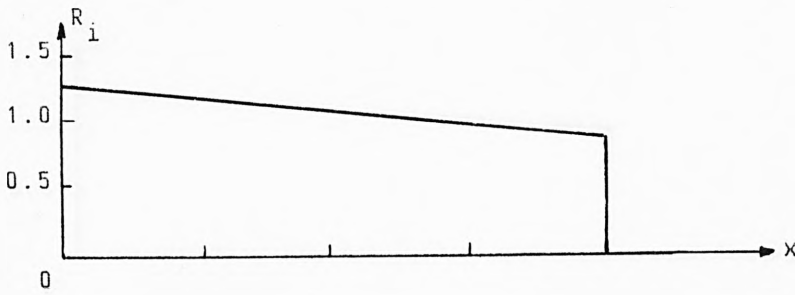
(c) Rotation Distribution Diagram

$C_1 = 1.000$

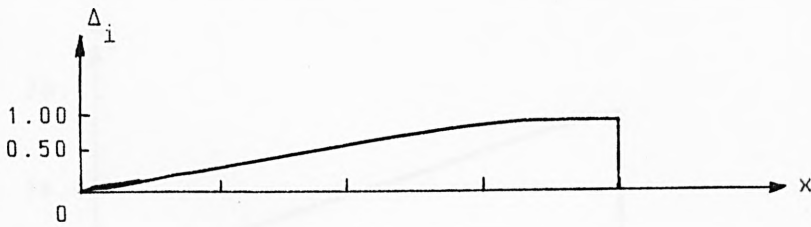


(d) Curvature Distribution Diagram

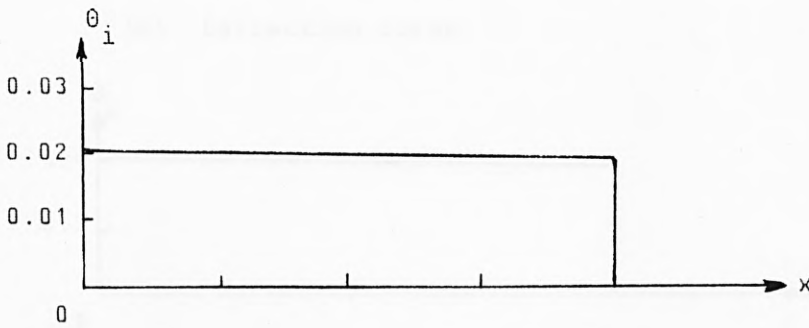
Fig. A5.3 Deflection Curve And Moment, Rotation And Curvature Distribution Diagrams For Curves 1 And 2 For Inelastic Zone Of Length 50.0mm Considered In Table A5.3



(a) Moment Distribution Diagram

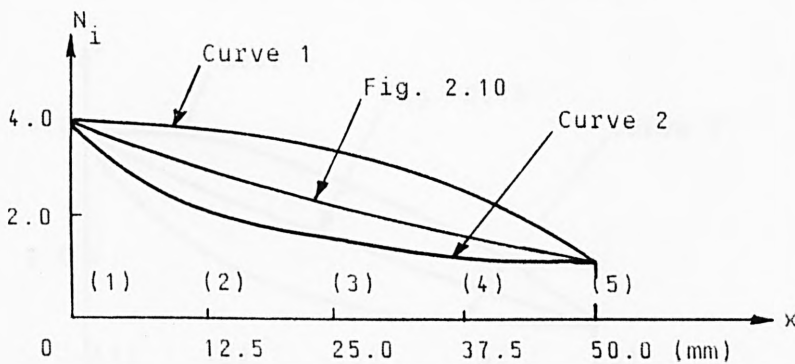


(b) Deflection Curve



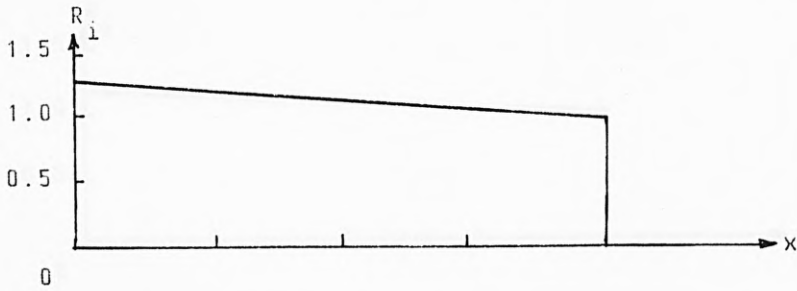
(c) Rotation Distribution Diagram

$C_1 = 1.766$



(d) Curvature Distribution Diagram

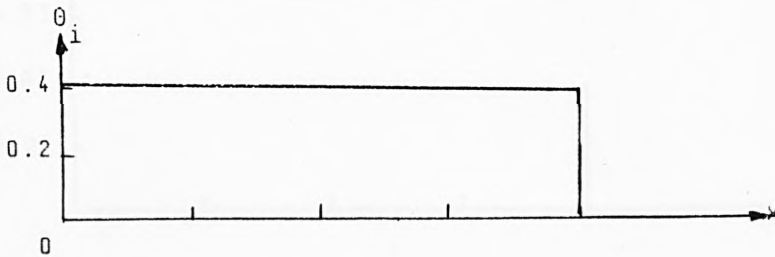
Fig. A5.4 Deflection Curve And Moment, Rotation And Curvature Distribution Diagrams For Curves 1 And 2 For Inelastic Zone Of Length 50.0mm Considered In Table A5.4



(a) Moment Distribution Diagram

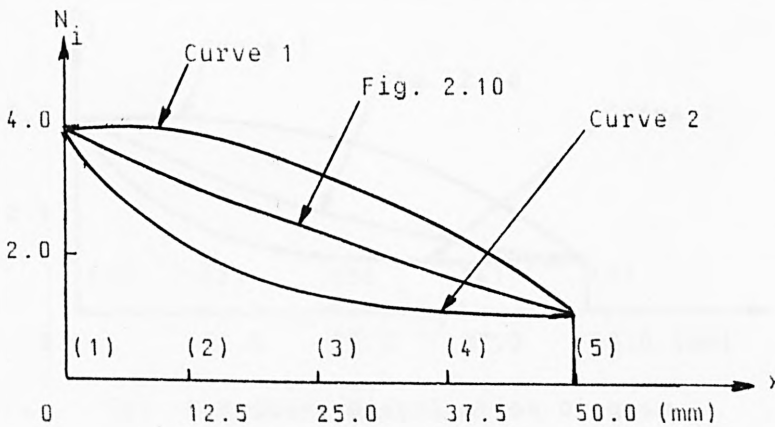


(b) Deflection Curve



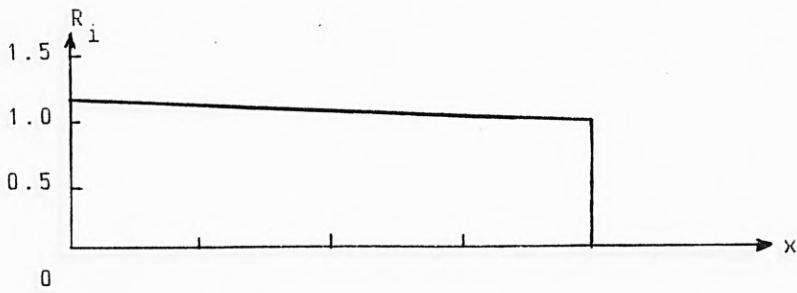
(c) Rotation Distribution Diagram

$C_1 = 1.766$

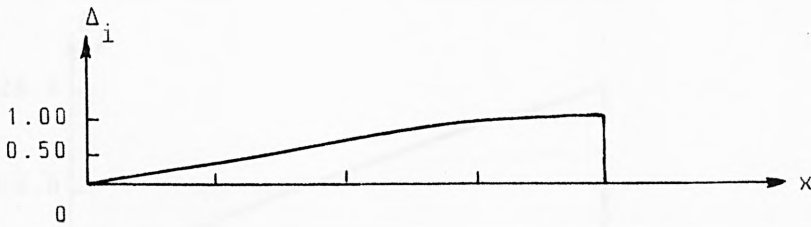


(d) Curvature Distribution Diagram

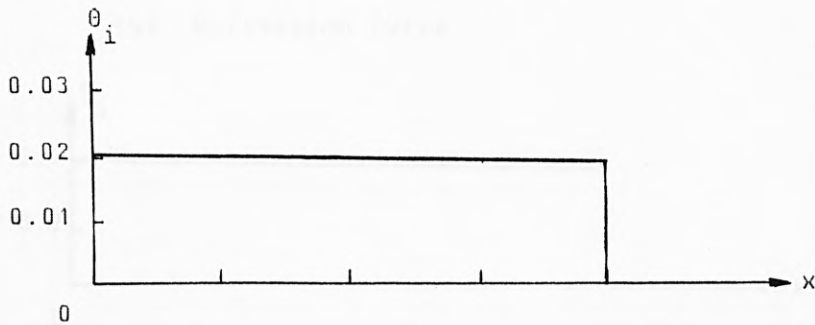
Fig. A5.5 Deflection Curve And Moment, Rotation And Curvature Distribution Diagrams For Curves 1 And 2 For Inelastic Zone Of Length 50.0mm Considered In Table A5.5



(a) Moment Distribution Diagram

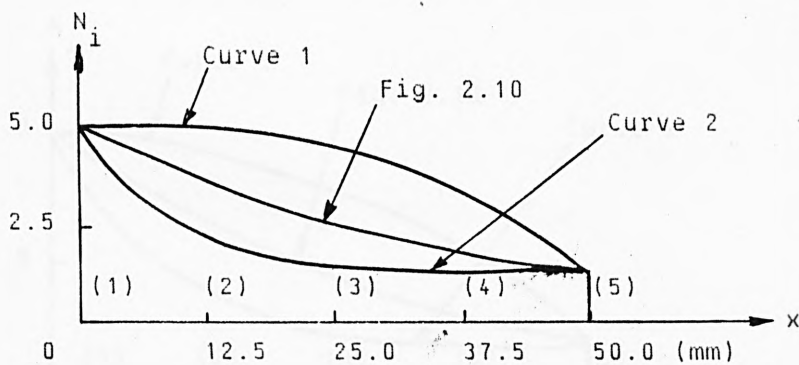


(b) Deflection Curve



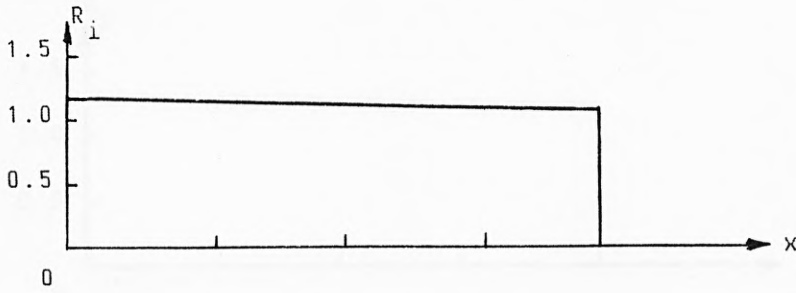
(c) Rotation Distribution Diagram

$C_1 = 2.081$

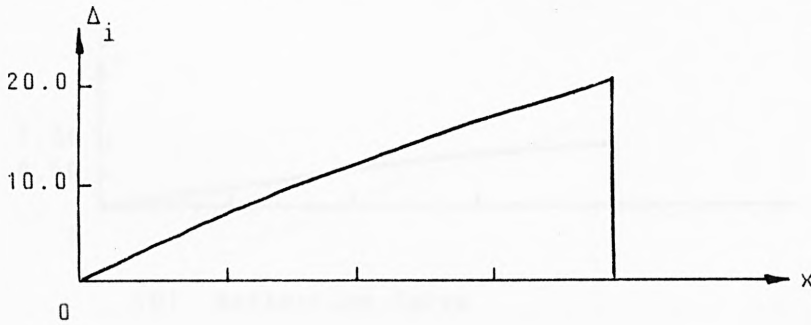


(d) Curvature Distribution Diagram

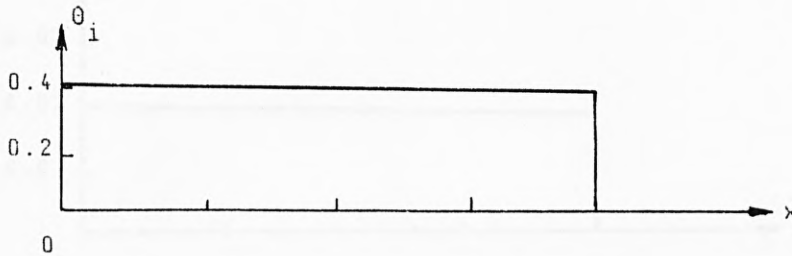
Fig. A5.6 Deflection Curve And Moment, Rotation And Curvature Distribution Diagrams For Curves 1 And 2 For Inelastic Zone Of Length 50.0mm Considered In Table A5.6



(a) Moment Distribution Diagram

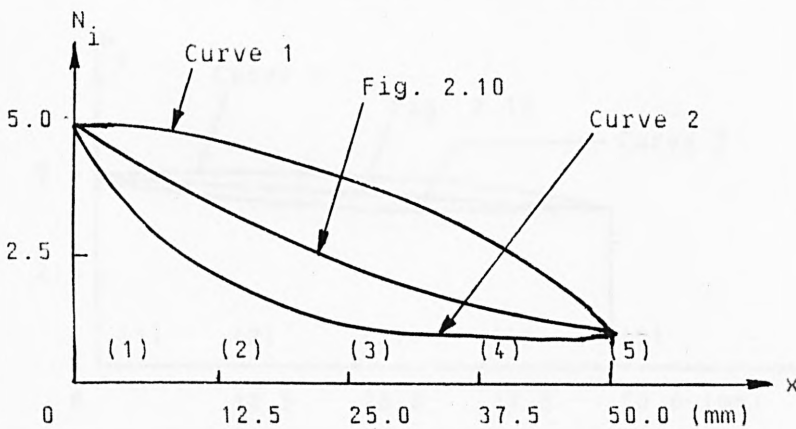


(b) Deflection Curve



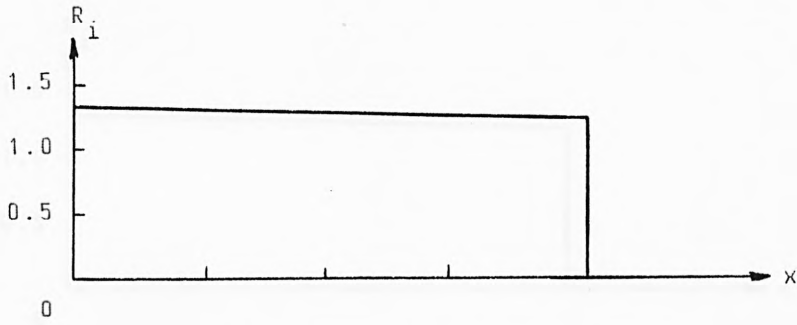
(c) Rotation Distribution Diagram

$C_1 = 2.081$

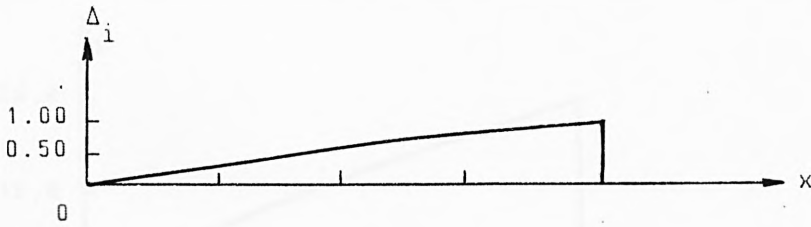


(d) Curvature Distribution Diagram

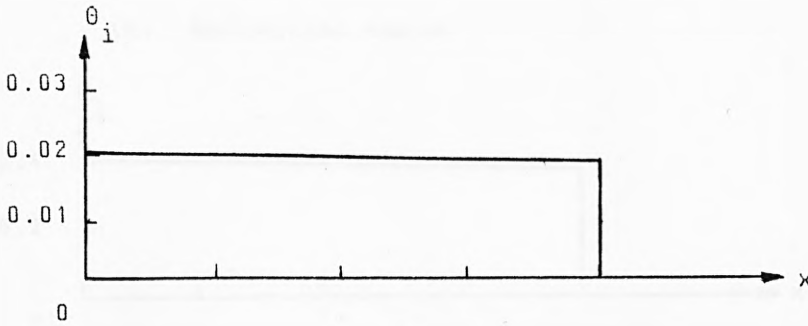
Fig. A5.7 Deflection Curve And Moment, Rotation And Curvature Distribution Diagrams For Curves 1 And 2 For Inelastic Zone Of Length 50.0mm Considered In Table A5.7



(a) Moment Distribution Diagram



(b) Deflection Curve



(c) Rotation Distribution Diagram

$C_1 = 1.087$

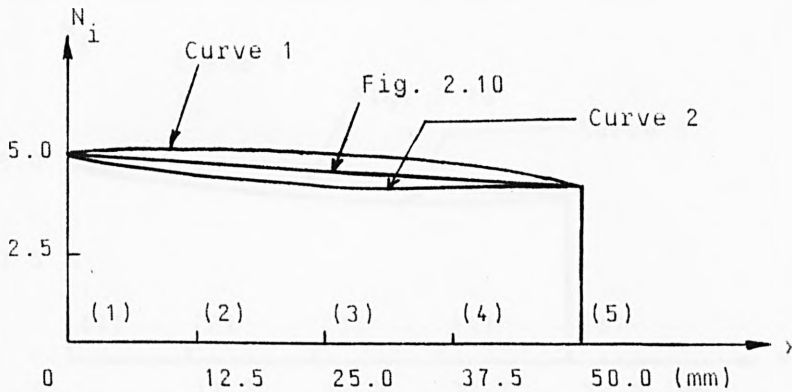
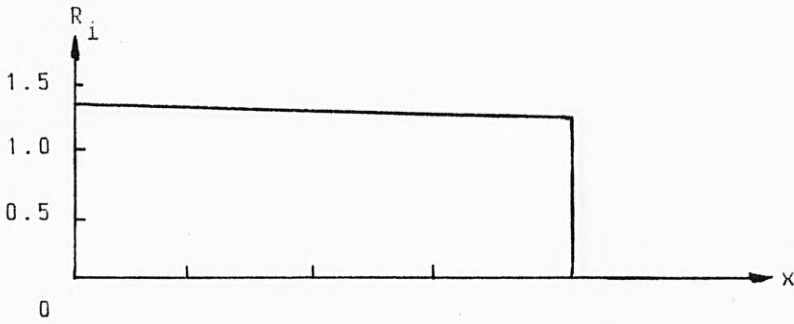
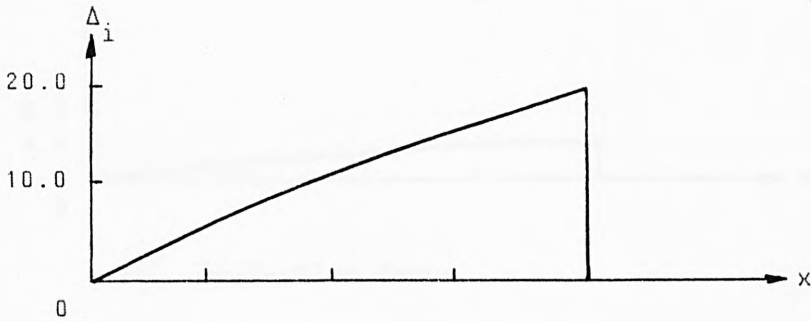


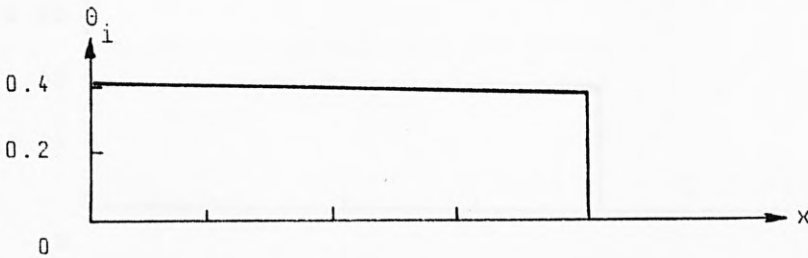
Fig. A5.8 Deflection Curve And Moment, Rotation And Curvature Distribution Diagrams For Curves 1 And 2 For Inelastic Zone Of Length 50.0mm Considered In Table A5.8



(a) Moment Distribution Diagram

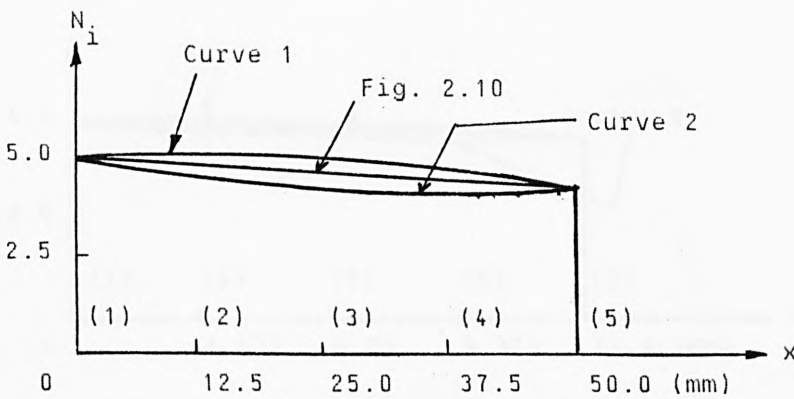


(b) Deflection Curve



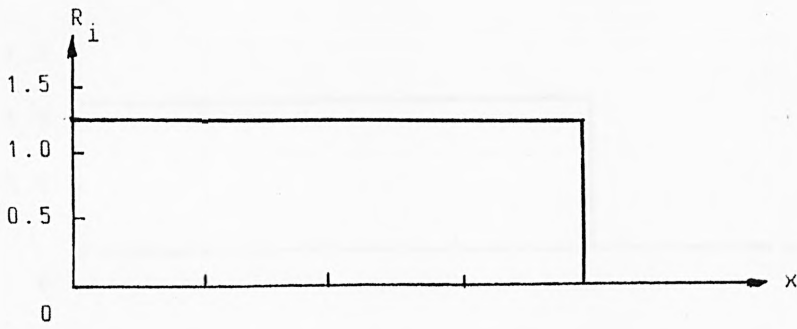
(c) Rotation Distribution Diagram

$C_1 = 1.087$

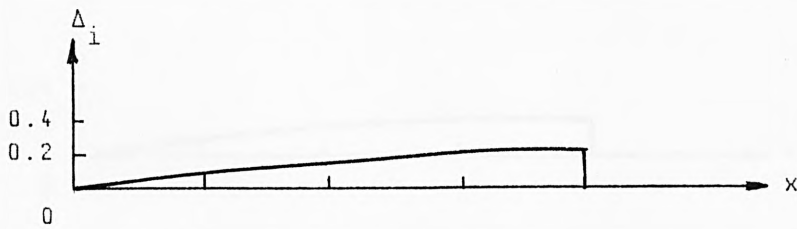


(d) Curvature Distribution Diagram

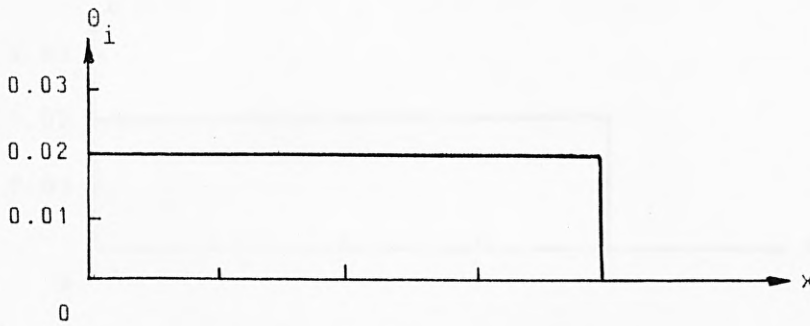
Fig. A5.9 Deflection Curve And Moment, Rotation And Curvature Distribution Diagrams For Curves 1 And 2 For Inelastic Zone Of Length 12.5mm Considered In Table A5.9



(a) Moment Distribution Diagram

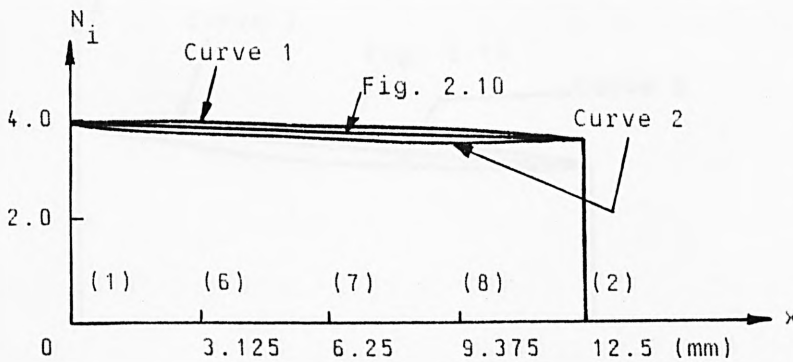


(b) Deflection Curve



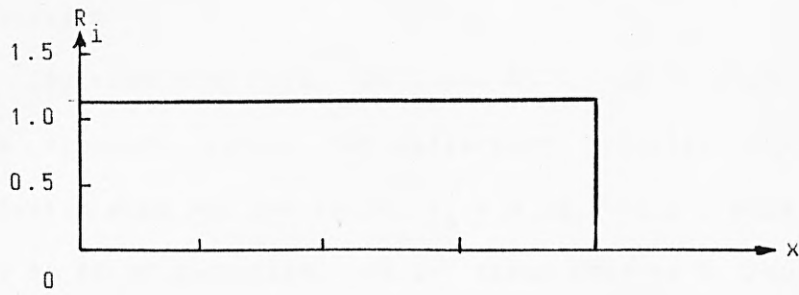
(c) Rotation Distribution Diagram

$C_1 = 1.039$

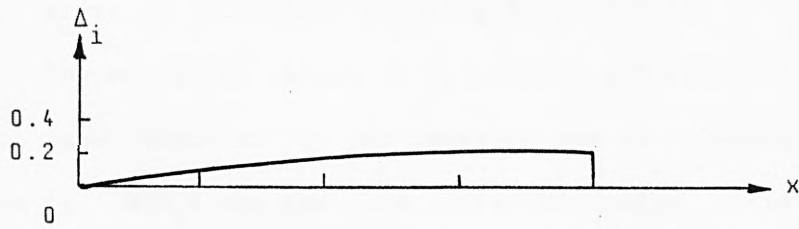


(d) Curvature Distribution Diagram

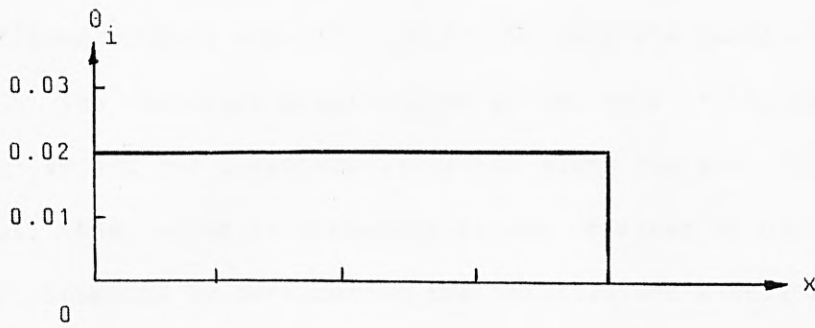
Fig. A5.10 Deflection Curve And Moment, Rotation And Curvature Distribution Diagrams For Curves 1 And 2 For Inelastic Segment Of Length 12.5mm Considered In Table A5.10



(a) Moment Distribution Diagram

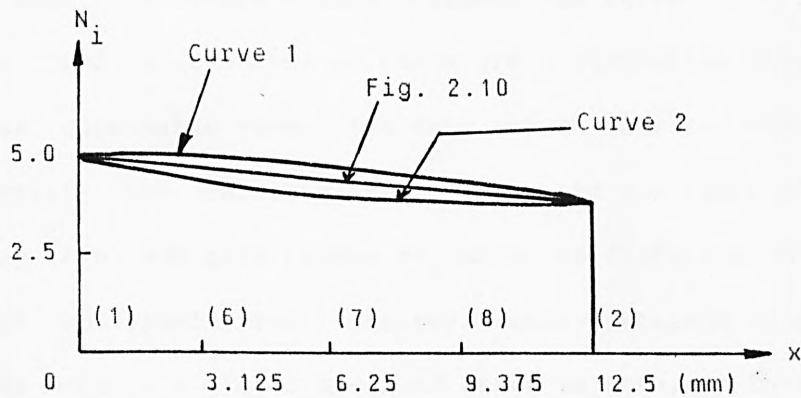


(b) Deflection Curve



(c) Rotation Distribution Diagram

$C_1 = 1.128$



(d) Curvature Distribution Diagram

Fig. A5.11 Deflection Curve And Moment, Rotation And Curvature Distribution Diagrams For Curves 1 And 2 For Inelastic Segment Of Length 12.5mm Considered In Table A5.11

Discussion

By examining Figs. A5.2 and A5.3, it is clear that Eqns. (A5.1) give accurate values for deflection, rotation and curvature for an inelastic zone for the ratio, $C_1 = m_1/q_1 = 1.0$. Also by examining Figs. A5.4 to A5.11 inclusive, it is clear that as C_1 increases above unity, due to large differences of either end moments or end curvatures for the zone, error is introduced by using Eqns. (A5.1).

The errors in values of deflection and rotation along the zone are small and diminish as the rotation due to relative end displacement (that is, Δ/B_1) for the zone increases. Also, while improved values of deflection and rotation can be obtained by sub-dividing the zone into four equal parts, the differences between these values and those obtained without sub-division of the zone are small and acceptable.

The relative displacement of the ends of the inelastic zone does not affect the curvature variation along the zone (See Eqn. (A5.1c)). Thus, the error in curvature values obtained by using Eqn. (A5.1c) is not minimized by considering the relative end displacement for the zone. The nature of this error is such that at a given cross-section within the zone, curvature values obtained for Curve 1 of Fig. A5.1 are higher than, and give shapes of curvature distribution diagram different from those obtainable from, the true values obtained from Fig. 2.10. By contrast, the curvature values obtained for Curve 2 of Fig. A5.1 are lower than, and give shapes of curvature distribution diagram similar to those obtainable from, the true values obtained from Fig. 2.10. In other words, a higher level of error is obtained by using Curve 1 than by using Curve 2 of Fig. A5.1. In general, for values of C_1 between 1.0 and 1.2, the curvature values for Curves 1 and 2 are reasonably close to the true values given in Fig. 2.10. For values of C_1 greater than 1.2,

improved curvature values can be obtained by sub-dividing the inelastic zone into smaller segments. Such a refinement of analysis is undertaken at the expense of much computational effort. In all cases of analysis, however, the curvature values for the ends of any inelastic zone are selected from the moment-curvature-axial force relationships for the cross-section.

Although this Parametric Study shows differences in curvature values in certain cases, these do not necessarily translate into significant errors in deflections, rotations and tangent flexibility coefficients for an inelastic beam-column. This is due to the use of exact deflection curve for an elastic zone and to adequate account being taken of the deflections of all zone intersection points along the beam-column at all stages of analysis.

APPENDIX 6

CONVERSION TABLE

Imperial Unit	Equivalent Metric Unit
1 in	25.4 mm
1 ft	0.3048 m
1 lbf	4.448 N
1 tonf	9.964 kN
1 lbf/ft	14.59 N/m
1 tonf/ft	32.69 kN/m
1 lbf/in ²	0.006895 N/mm ²
1 lbf/ft ²	47.88 N/m ²
1 tonf/in ²	15.44 N/mm ²
1 tonf/ft ²	0.1073 N/mm ²
1 lbf/ft ³	157.1 N/m ³
1 tonf/ft ³	351.9 kN/m ³
1 lbf-ft	1.356 N.m

Other Useful Conversions.

1kgf	=	9.807N
1kN	=	0.2248kips
1kip	=	1000.0lbf
1kgf/m ³	=	0.0624lbf/ft ³

REFERENCES

1. Euler, L., "Sur la Force des Colonnes", Memoires de l'Academie Royale des Sciences et Belles Lettres de Berlin, Vol. 13, 1759. English translation by J.A. Van den Broek, Am. Jnl. of Phy., Vol. 15, 1947.
2. Johnston, B.G., "Guide To Design Criteria For Metal Compression Members", Second Edition, Column Research Council, John Wiley and Sons., Inc., 3rd. Ed. 1976.
3. Galambos, T.V., "Structural Members And Frames", Prentice Hall, New Jersey, 1968.
4. Chajes, A., "Principles Of Structural Stability Theory", Prentice Hall, New Jersey, 1974.
5. Heyman, J. "An Approach To The Design Of Tall Steel Buildings", Proc. I.C.E., Vol. 17, December, 1960.
6. Horne, M.R. And Merchant, W., "The Stability Of Frames", Pergamon Press, 1965.
7. Lu, L.W., "A Survey Of Literature On The Stability Of Frames", Fritz Engineering Laboratory Bulletin, Welding Research Council, September, 1962.
8. Zweig, A. And Kahn, A., "Buckling Analysis Of One-Storey Frames", Journal of the Structural Division, A.S.C.E., Vol. 94, No. ST9, September, 1968.
9. Gregory, M.S., "Framed Structures: The Instability Problem", Proceedings I.C.E., London, November, 1966.
10. Gregory, M.S., "Elastic Instability", E. and F.N. Spon Ltd., London, 1967.

11. Coates, R.C., Coutie, M.G. And Kong, F.K., "Structural Analysis", Thomas Nelson and Sons, 1972.
12. Kirby, P.A. And Nethercot, D.A., "Design For Structural Stability", Crosby Lockwood Staples, Granada Publishing, 1979.
13. Allen, H.G. And Bulson, P.S., "Background To Buckling", McGraw-Hill Book Company, 1980.
14. Livesley, R.K. And Chandler, D.B., "Stability Functions for Structural Frameworks", Manchester University Press, 1962.
15. Timoshenko, S.P. And Gere, J.M., "Theory Of Elastic Stability", McGraw-Hill Book Company, New York, 1961.
16. Brebbia, C.A. and Connor, J.J., "Fundamentals Of Finite Element Techniques", Butterworths, London, 1973.
17. Livesley, R.K., "Matrix Methods Of Structural Analysis", Pergamon Press, 1964.
18. Birnstiel, C. and Iffland, J.S.B., "Factors Influencing Frame Stability", Journal of the Structural Division, A.S.C.E., February, 1980.
19. Baker, J.F., Horne, M.R. and Heyman, J., "The Steel Skeleton, Vol. 2", Cambridge University Press, 1956.
20. Salem, A., "Structural Frameworks", Ph.D. Thesis, University Of Manchester, 1958.
21. Ariaratnam, S.T., "The Collapse Load Of Elastic-Plastic Structures", Ph.D. Thesis, Cambridge University, 1959.
22. Davies, J.M., "The Stability Of Plane Frameworks Under Static and Repeated Loading", Ph.D. Thesis, University Of Manchester, 1965.
23. Harung, H.S., "Elastic-Plastic Failure Analysis Of Three-Dimensional Skeletal Frames", Ph.D. Thesis, Victoria University Of Manchester, 1973.

24. Beedle, L.S., "Plastic Design Of Steel Frames", John Wiley and Sons, 1958.
25. Neal, B.G., "The Plastic Methods Of Structural Analysis", Chapman and Hall, London, 1965.
26. Burnett, N., Johnson, L.G., Morris, L.J., Randall, A.L. and Thompson, C.P., "Plastic Design", B.C.S.A., 1965.
27. Horne, M.R. and Chin, M.W., "Plastic Design Of Portal Frames In Steel To B.S. 968", B.C.S.A., 1966.
28. Horne, M.R., "Plastic Theory Of Structures", First Edition, Nelson, London, 1971; Second Edition, Pergamon Press, Oxford, 1979.
29. CONSTRADO, "Steel Designers' Manual", Crosby Lockwood Staples, London, Fourth Edition, 1972.
30. Medland, I.C., "Strain-Hardening And The Collapse Load Of Steel Frameworks", Ph.D. Thesis, University Of Manchester, 1963.
31. Horne, M.R. and Medland, I.C., "Collapse Loads Of Steel Frameworks Allowing For The Effect Of Strain-Hardening", Proc. I.C.E., London, Vol. 33, March, 1966.
32. Anderson, D. and Lok, T.S., "Design Studies On Unbraced, Multi-Storey Steel Frames", The Structural Engineer, Vol. 61B, June, 1983.
33. Lyon, J.R., "The Incremental Collapse Of Ductile Structures", Ph.D. Thesis, Cambridge University, 1962.
34. Davies, J.M., "Collapse and Shakedown Loads Of Plane Frames", Journal of the Structural Division, A.S.C.E., June, 1967.
35. Davies, J.M., "Variable Repeated Loading and the Plastic Design Of Structures", The Structural Engineer, May, 1970.

36. Majid, K.I., "Elastic-Plastic Structural Analysis", Ph.D. Thesis, University Of Manchester Institute of Science and Technology, 1963.
37. Moses, F., "Stability Of Inelastic Frames", Ph.D. Thesis, Cornell University, 1963.
38. Anderson, D. and Lok, T.S., "An Elasto-Plastic Hand Method for Unbraced Rigid-Jointed Steel Frames", Proceedings of the Michael R. Horne Conference on "Instability and Plastic Collapse of Steel Structures" edited by Morris, L.J., Granada, 1983.
39. Kassimali, A., "Large Deformation Analysis Of Elastic-Plastic Frames", Journal of the Structural Division, A.S.C.E., August, 1983.
40. Horne, M.R. and Majid, K.I., "Elastic-Plastic Design Of Rigid-Jointed Sway Frames By Computer", First Report, Study Of Analytical and Design Procedures for Elastic and Elastic-Plastic Structures, University of Manchester Institute of Science and Technology, 1966.
41. Jennings, A. and Majid, K.I., "An Elastic-Plastic Analysis for Framed Structures Loaded up to Collapse", The Structural Engineer, 43, No. 12, December, 1965.
42. Morris, G.A. and Fenves, S.J., "Elastic-Plastic Analysis of Frameworks", Journal of the Structural Division, A.S.C.E., Vol.96, No. ST5, May, 1970.
43. Korn, A. and Galambos, T.V., "Behaviour of Elastic-Plastic Frames", Journal of the Structural Division, A.S.C.E., Vol.94, May, 1968.
44. Majid, K.I., "Non-linear Structures", Butterworths, 1972.

45. Anderson, D., "Investigations Into The Design Of Plane Structural Frames", Ph.D. Thesis, Victoria University of Manchester, 1969.
46. Korn, A., "The Elastic-Plastic Behaviour Of Multi-Storey, Unbraced Planar Frames", D.Sc. Dissertation, Washington University, 1967.
47. Majid, K.I. and Anderson, D., "Elastic-Plastic Design Of Sway Frames By Computer", Proc. I.C.E., 41, December, 1968.
48. Lu, L.W., "Stability of Elastic and Partially-Plastic Frames", Ph.D. Thesis, Lehigh University, 1960.
49. Masur, E.F., Chang, I.C. and Donnell, L.H., "Stability of Frames in the Presence of Primary Bending Moments", Journal of the Engineering Mechanics Division, A.S.C.E., Vol.87, 1961.
50. Yen, Y.C., Lu, L.W. and Driscoll, G.C.Jr., "Tests on the Stability of Welded Steel Frames", Fritz Engineering Laboratory Bulletin, Welding Research Council, September, 1962.
51. Lu, L.W., "Stability of Frames under Primary Bending Moments", Journal of the Structural Division, A.S.C.E., Vol. 89, No. ST3, 1963.
52. Bleich, F., "Buckling Strength of Metal Structures", McGraw-Hill Book Company, 1952.
53. Zienkiewicz, O.C., "The Finite Element Method in Engineering Science", McGraw-Hill Book Company, London, 1971.
54. Zienkiewicz, O.C. and Cheung, Y.K., "The Finite Element Method in Structural and Continuum Mechanics", McGraw-Hill Book Company, 1967.
55. Moses, F., "Inelastic Frame Buckling" Journal of the Structural Division, A.S.C.E., December, 1964.

56. Vinnakota, S., "Flambage des Cardes dans le Domaine Elasto-Plastique", Ph.D. Thesis, l'Ecole Polytechnique Federale de Lausanne, Switzerland, 1967.
57. Seniwongse, M., "The Deformation of Reinforced Concrete Beams and Frames up to Failure", The Structural Engineer, Vol. B., December, 1979.
58. Kang, Y.J. and Scordelis, A.C., "Non-linear Analysis of Prestressed Concrete Frames", Journal of the Structural Division, A.S.C.E., February, 1980.
59. El-Zanaty, M.H. and Murray, D.W., "Non-linear Finite Element Analysis of Steel Frames", Journal of the Structural Division, A.S.C.E., February, 1983.
60. Smith, J.O. and Sidebottom, O.M., "Inelastic Behaviour of Load-Carrying Members", John Wiley and Sons, New York, 1965.
61. Andreaus, U. and D'Asdia, P., "Analysis of Elastic-Plastic Frames at Large Displacement Range Accounting For Finite Spread of Yielding Zones", Proceedings of the Michael R. Horne Conference on "Instability and Plastic Collapse of Steel Structures", edited by Morris, L.J., Granada, 1983.
62. Martin, H.C., "Introduction To Matrix Methods Of Structural Analysis", McGraw-Hill Book Company, 1966.
63. Sherman, D.R., Erzurumlu, H. and Mueller, W.H., "Behavioural Study of Circular Tubular Beam-Columns", Journal of the Structural Division, A.S.C.E., June, 1979.
64. Stringer, D.C., "The Elastic-Plastic Behaviour Of Restrained Columns", Ph.D. Thesis, University Of Manchester, 1972.
65. Hutchings, R., "The Elastic-Plastic Behaviour Of Columns Under Biaxial Loading", Ph.D. Thesis, University Of Manchester, 1973.

66. Viridi, K.S., "Inelastic Column Behaviour - Its Application To Composite Columns In Biaxial Bending and Stiffened Plates In Compression", Ph.D. Thesis, University of London, 1973.
67. Viridi, K.S. and Dowling, P.J., "The Ultimate Strength Of Biaxially-Restrained Columns", Proc. I.C.E., Part 2, 1976.
68. Viridi, K.S. and Sen, K., "Torsion and Computed Ultimate Loads Of H-Columns", Journal of the Structural Division, A.S.C.E., February, 1981.
69. Vinnakota, S. and Badoux, J.C., "Strength of Laterally-Loaded Restrained Beam-Columns", The Institution Of Engineers, Australia, October, 1970.
70. Vinnakota, S. and Badoux, J.C., "Strength of Laterally-Loaded Inelastically-Restrained Beam-Columns", Civil Engineering Transaction, October, 1971.
71. Chen, W.F. and Atsuta, T., "Theory of Beam-Columns, Vols. 1 and 2", McGraw-Hill Book Company, Vol. 1, 1976, Vol. 2, 1977.
72. Wood, R.H., "A New Approach To Column Design", Building Research Establishment Report, H.M.S.O., 1974.
73. Chen, W.F., "End Restraint and Column Stability", Journal of the Structural Division, A.S.C.E., November, 1980.
74. Bresler, B., Lin, T.Y. and Scalzi, J.B., "Design of Steel Structures", John Wiley and Sons, Second Edition, 1968.
75. American Institute of Steel Construction, "Manual of Steel Construction", Seventh Edition, 1973.
76. British Standard Institution, "Draft Standard Specification for the Structural Use of Steelwork in Building: Part 1: Simple Construction and Continuous Construction", B.S.I., 13908DC, 1977.

77. Wood, R.H., "Effective Lengths of Columns in Multi-Storey Buildings", *The Structural Engineer*, July to September, 1974.
78. Moy, F.C.S. and Downs, T., "New Interaction Equation for Steel Beam-Columns", *Journal of the Structural Division, A.S.C.E.*, May, 1980.
79. Saka, M.P., "Optimum Design Of Structures", Ph.D. Thesis, University of Aston in Birmingham, 1980.
80. Okdey, S., "Design of Sway Frames", Ph.D. Thesis, University of Aston in Birmingham, 1980.
81. Grierson, D.E. and Lee, W.H., "Discrete Optimization of Frameworks under Elastic and Plastic Performance Constraints", *Proceedings of the Michael R. Horne Conference on "Instability and Plastic Collapse of Steel Structures"*, edited by Morris, L.J., Granada, 1983.
82. Hays, C.O.Jr. and Santhanam, T.K., "Inelastic Section Response By Tangent Stiffness", *Journal of the Structural Division, A.S.C.E.*, July, 1979.
83. Viridi, K.S. and Dowling, P.J., "Composite Columns in Biaxial Bending", Paper in "Axially-Compressed Structures-Stability and Strength", edited by Narayanan, R., 1982.
84. Heyman, J., "The Development of Plastic Theory 1936-48: Some Notes for A Historical Sketch", *Proceedings of the Michael R. Horne Conference on "Instability and Plastic Collapse of Steel Structures"* edited by Morris, L.J., Granada, 1983.
85. Scholz, H., "A Multi-Curve Interaction Method for the Plastic Analysis and Design of Unbraced and Partially-Braced Frames", Ph.D. Thesis, University of the Witwatersrand, Johannesburg, 1981.

86. Scholz, H., "A New Multi-Curve Interaction Version of the Merchant-Rankine Approach", Proceedings of the Michael R. Horne Conference on "Instability and Plastic Collapse of Steel Structures", edited by Morris, L.J., Granada, 1983.
87. Scholz, H.E., "Simplified Interaction Method for Sway Frames", Journal of Structural Engineering, A.S.C.E., Vol. 110, No. 5, May, 1984.
88. Erbatur, F., "Computer Shakedown Analysis Of Planar Structures", Computers & Structures, Vol. 18, No. 6, 1984.
89. British Standards Institution, "BS 18: Methods For Tensile Testing Of Metals, Part 2, Steel (General), 1971."